

Sheffield Hallam University

Impact sound insulation of flooring systems with polyurethane foam on concrete floors

HALL, Robin

Available from the Sheffield Hallam University Research Archive (SHURA) at:

<http://shura.shu.ac.uk/3135/>

A Sheffield Hallam University thesis

This thesis is protected by copyright which belongs to the author.

The content must not be changed in any way or sold commercially in any format or medium without the formal permission of the author.

When referring to this work, full bibliographic details including the author, title, awarding institution and date of the thesis must be given.

Please visit <http://shura.shu.ac.uk/3135/> and <http://shura.shu.ac.uk/information.html> for further details about copyright and re-use permissions.

CITY CAMPUS, POND STREET,
SHEFFIELD, S1 1TB.

101 610 897 4



REFERENCE

ProQuest Number: 10697045

All rights reserved

INFORMATION TO ALL USERS

The quality of this reproduction is dependent upon the quality of the copy submitted.

In the unlikely event that the author did not send a complete manuscript and there are missing pages, these will be noted. Also, if material had to be removed, a note will indicate the deletion.



ProQuest 10697045

Published by ProQuest LLC (2017). Copyright of the Dissertation is held by the Author.

All rights reserved.

This work is protected against unauthorized copying under Title 17, United States Code
Microform Edition © ProQuest LLC.

ProQuest LLC.
789 East Eisenhower Parkway
P.O. Box 1346
Ann Arbor, MI 48106 – 1346

**Impact Sound Insulation of Flooring Systems with
Polyurethane Foam on Concrete Floors**

Robin Hall

A thesis submitted in partial fulfilment of the requirements
of
Sheffield Hallam University
for the degree of Doctor of Philosophy

March 1999





LEVEL 1

ABSTRACT

The problem of unwanted noise in buildings has grown continuously over the last twenty years and impact noise through separating floors has been identified as a particularly important problem. One accepted method for improving impact sound insulation is to use floating floors in which the walking surfaces are isolated from the supporting structure by a resilient layer. Traditionally the resilient layers comprise mineral or glass fibre quilts but other materials such as flooring grade polystyrene are increasingly used. Recently, shallow profile floating floors comprising flexible open cell polyurethane foam resilient layers have been developed. These systems are attractive for refurbishment projects since they can simply be placed on existing floors in order to improve their impact sound insulation whilst raising the existing floor level less than systems comprising fibre quilts. Shallow profile floating floors with thin layers of flexible open cell polyurethane foam are the subject of investigation as part of this research work.

This thesis reviews the previous research on polyurethane foams and evaluates the usefulness of the Standard Tests on these materials for assisting in the selection of foam for use as resilient layers under lightweight floors. Both the static and dynamic behaviour of flexible open cell polyurethane foam are investigated and recycled polyurethane foam is shown to be particularly useful for use under floating floors. Its characteristic behaviour under compressive strain is described for the first time.

This thesis shows that by modifying the Standard Method for the determination of the dynamic stiffness of resilient layers under floating floors (BS EN 29052-1), the effect of the air contained in the open cell foam specimens can be included in the Standard laboratory test. The modification makes it possible to evaluate the dynamic stiffness of low airflow resistivity resilient polyurethane resilient layers using the apparatus described in BS EN 29052-1 for the first time.

Field measurements of impact sound pressure level conducted using sections of lightweight shallow profile floating floor on a concrete supporting floor are described. The measured improvements in impact sound insulation achieved by using the sections of floating floor are compared with the improvements predicted using the results from the modified Standard laboratory tests on the foams used as resilient layers. It is shown that by compensating for the mass impedance of the Standard tapping machine hammers good correlation between predicted and measured data is achieved. A simple method for predicting the weighted standardised impact sound pressure level ($L'_{nT,w}$) in the receiving room is proposed which shows excellent correlation with $L'_{nT,w}$ obtained from the measured data. The work shows that BS EN 29052-1 is more widely applicable than the Standard itself states and for the first time identifies a method of predicting the performance of lightweight shallow profile floating floors with polyurethane foam resilient layers.

Finally the use of the ISO tapping machine for assessing the impact sound insulation of the very lightweight floating floors of interest to this research is considered. Different methods of correlating perceived and measured the impact sound insulation of floors are reviewed. Experimental results conducted in this research programme, along with searches of the literature confirm that the tapping machine is a suitable source for measuring the impact sound insulation of these floors.

CONTENTS

Abstract	ii
Contents	iii
List of figures	vi
List of tables	ix
Acknowledgements	x
Dedication	xi

CHAPTER 1.

IMPACT NOISE IN BUILDINGS

1.1	Background	1
1.2	Impact noise and floating floors	1
1.3	Shallow profile floating floors	4
1.4	Dynamic stiffness	7
1.5	The way forward	8
1.6	References	11

CHAPTER 2.

POLYURETHANE FOAM

2.1	Introduction	13
2.2	Background	13
2.3	Manufacture of polyurethane foam	14
	2.3.1 Virgin foam	14
	2.3.2 Recycled polyurethane foam: rebond	15
2.4	Literature review: work on polyurethane foam	17
	2.4.1 Static behaviour	17
	2.4.2 Dynamic behaviour	24
	2.4.3 Resilient layers for isolation in floors	26
	2.4.4 Composite flooring systems	28
	2.4.5 Mackenzie's work	29
	2.4.6 Standard tests on polyurethane foam	30
2.5	Summary of the literature review	31
2.6	Conclusions	33
2.7	References	36

CHAPTER 3

STATIC BEHAVIOUR OF FLEXIBLE POLYURETHANE FOAMS

3.1	Introduction	40
3.2	Background	40
3.3	Testing method	41
3.4	Results	44
3.5	Discussion	52
3.6	Conclusions	56
3.7	References	57

CHAPTER 4

DYNAMIC BEHAVIOUR OF FLEXIBLE POLYURETHANE FOAM

4.1	Introduction	59
4.2	Background	59

4.2.1	BS EN 29052-1	62
4.2.2	Resonant frequency	62
4.2.3	Damping	64
4.3.	Test method	66
4.3.1	Calibration	66
4.3.2	Laboratory experiments	67
4.4	Results	69
4.5	Discussion	81
4.6	Conclusions	87
4.7	References	89
CHAPTER 5		
AIRFLOW RESISTIVITY		
5.1	Introduction	91
5.2	Background	91
5.2.1	Measurement of airflow resistivity	93
5.3	Test method	94
5.4	Results	96
5.5	Discussion	97
5.6	Conclusions	102
5.7	References	104
CHAPTER 6		
FIELD MEASUREMENTS OF IMPACT SOUND		
6.1	Introduction	105
6.2	Background: development programme	105
6.3	Testing method	109
6.4	Results	110
6.5	Discussion	115
6.6	Conclusions	116
6.7	References	118
CHAPTER 7		
A NEW METHOD FOR MEASURING THE DYNAMIC STIFFNESS OF RESILIENT LAYERS		
7.1	Introduction	119
7.2	Testing method	120
7.3	Results	122
7.4	Discussion	128
7.5	Conclusions	133
7.6	References	135
CHAPTER 8		
IMPACT SOUND INSULATION OF FLOATING FLOORS		
8.1	Introduction	137
8.2	Background	137
8.3	The prediction of impact sound insulation with floating floors	139
8.3.1	Locally reacting floating floors	139
8.3.2	Resonantly reacting floating floors	145
8.3.3	The resilient layer as a wave medium	150
8.4	Discussion of the prediction models	154

8.5	Conclusions	156
8.6	References	157

CHAPTER 9

PREDICTING IMPACT SOUND INSULATION

9.1	Introduction	158
9.2	Predicting the impact sound insulation of floating floors	158
9.3	Driving point impedance of mdf	159
9.4	Prediction of $L'_{nT,w}$	160
9.5	Results	160
	9.5.1 Longitudinal wavespeed in mdf	160
	9.5.2 Prediction of ΔL	161
9.6	Discussion	174
9.7	Conclusions	177
9.8	References	179

CHAPTER 10

TESTING SMALL SECTIONS OF FLOATING FLOOR

10.1	Introduction	180
10.2	background	181
10.3	Experimental method	182
10.4	Results	184
10.5	Discussion	187
10.6	Conclusions	189
10.7	References	191

CHAPTER 11

THE RATING OF FLOORS WITH THE ISO TAPPING MACHINE

11.1	Introduction	192
11.2	Review of measurement of impact sound insulation	192
11.3	Rating of floors	194
11.4	Lightweight floating floors	196
11.5	Experimental method	198
	11.5.1 Tapping machine hammers on mdf and concrete	198
	11.5.2 The deflection of lightweight floating floors under walking	198
11.6	Results	199
11.7	Discussion	201
11.8	Conclusions	204
11.9	References	205

CHAPTER 12

SUMMARY AND CONCLUSIONS

12.1	Introduction	208
12.2	Noise in buildings and floating floors	208
12.3	Summary of main findings	210
12.4	Final comments	214
12.5	Recommendations for further research	215
12.6	Concluding remarks	217
12.7	References	219

APPENDICES

APPENDIX A1

Results of field measurements not presented in thesis

A1

APPENDIX A2

The modified method for the dynamic stiffness of resilient layers

A11

APPENDIX A3

Published work arising from this research

A15

LIST OF FIGURES

Figure Number	Description	Page Number
1.1	Concrete base with floating layer	3
1.2	Wooden base with floating layer	3
1.3	Batten with resilient strip	5
1.4	system with open and closed cell polyurethane foam in parallel	5
2.1	Rebond manufacturing process	16
2.2	Typical stress-strain curve for open cell polyurethane foam	18
2.3	redrawing of the Gibson and Ashby model of the open polyurethane foam cell	20
2.4	example of energy absorption curve approach to foam optimisation	23
3.1	arrangement for compression tests	43
3.2	final loading curves for rebond open cell foams	44
3.3	final loading curves for virgin open cell foams	44
3.4	initial loading and final loading and unloading curves for reconstituted foam (78 kg/m^3)	46
3.5	initial loading and final loading and unloading curves for virgin foam (28 kg/m^3)	47
3.6	initial loading and final loading and unloading curves for virgin foam (62 kg/m^3)	47
3.7	comparison of final loading strokes for reconditioned and virgin open cell foam	49
3.8	initial loading curves for 78 kg/m^3 reconstituted foam compressed parallel and perpendicular to the direction of compression in forming	50
3.9	initial loading curves for single density reconstituted foam compressed parallel and perpendicular to the direction of compression in forming	51
3.10	loading and unloading curves for single density polyurethane crumb	51
4.1	Kennedy and Pancu method for damping	66
4.2	force transducer calibration	67
4.3	apparatus for measuring resonant frequency	69
4.4	accelerometer calibration curve	70
4.5	force transducer calibration curve	71
4.6	acceleration response from tests with and without plaster of Paris	71
4.7	input-output phase difference with and without plaster of Paris	72
4.8	accelerance and input force for 144 kg/m^2 rebond foam; 1V input	72
4.9	accelerance and input force for 144 kg/m^2 rebond foam; 2V input	73
4.10	accelerance and input force for 144 kg/m^2 rebond foam; 3V input	73
4.11	system response with a 28 kg/m^3 virgin foam specimen, 16.2 mm thick	75
4.12	system response with a 144 kg/m^3 rebond foam specimen, 13.2 mm thick	75
4.13	system response with a 64 kg/m^3 rebond foam specimen, 12.6 mm thick	76
4.14	system response with a 78 kg/m^3 (measured 69 kg/m^3) rebond foam specimen, 13.2 mm thick	76

4.15	system response with a 62 kg/m ³ (measured 69 kg/m ³) virgin foam specimen, 9.6 mm thick	77
4.16	test system resonant frequency with specimens of different types and thicknesses of foam	78
4.17	system response with a 64 kg/m ³ rebond foam specimen, 12.6 mm thick, Kennedy and Pancu method	78
4.18	first loading strokes for 62 and 28 kg/m ³ virgin foam	83
4.19	dynamic versus static stiffness for rebond foam	85
4.20	dynamic versus static stiffness for virgin foam	85
5.1	apparatus for measuring airflow resistivity	95
5.2	cutting required thickness from block	98
5.3	micrograph of 28 kg/m ³ virgin foam, taken perpendicular to the rise direction	100
5.4	micrograph of 28 kg/m ³ virgin foam, taken in the rise direction	100
5.5	micrograph showing 78 kg/m ³ rebond foam, taken perpendicular to the forming compression	101
5.6	micrograph showing 144 kg/m ³ rebond foam, taken perpendicular to the forming compression	101
5.7	micrograph showing 144 kg/m ³ rebond foam, taken parallel to the forming compression	102
6.1	concrete floor before and after treatment with mdf system	106
6.2	wooden floor before and after treatment with mdf flooring	107
6.3	concrete floor before and after treatment with chipboard system	107
6.4	wooden floor before and after treatment with chipboard system	108
6.5	L' _{nT} for different thicknesses of 78 kg/m ³ rebond	111
6.6	L' _{nT} for different resilient layers	114
6.7	comparison of different sized samples with 78 kg/m ³ rebond resilient layer	114
6.8	L' _{nT,w} versus thickness for 78 kg/m ³ rebond foam layers	116
7.1	specimens cut from floating floor resilient layer	121
7.2	petroleum jelly sealing the edges of the test specimen	122
7.3	test system with 78 kg/m ³ rebond; unsealed specimen	125
7.4	test system with 78 kg/m ³ rebond; sealed specimen	125
7.5	test system with 128 kg/m ³ rebond; unsealed specimen	126
7.6	test system with 128 kg/m ³ rebond; sealed specimen	126
7.7	test system with 28 kg/m ³ virgin foam; unsealed specimen	127
7.8	test system with 28 kg/m ³ virgin foam; sealed specimen	127
7.9	Kennedy and Pancu construction for η	133
8.1	linear four pole mechanical system	151
9.1	ΔL for 6 mm thick 78 kg/m ³ rebond	164
9.2	ΔL for 12 mm thick 78 kg/m ³ rebond	164
9.3	ΔL for 14 mm thick 78 kg/m ³ rebond	165
9.4	ΔL for 16 mm thick 78 kg/m ³ rebond	165
9.5	ΔL for 10 mm thick 64 kg/m ³ rebond	166
9.6	ΔL for 11.5 mm thick 96 kg/m ³ rebond	166
9.7	ΔL for 9 mm thick 128 kg/m ³ rebond	167
9.8	ΔL for 11 mm thick 144 kg/m ³ rebond	167
9.9	ΔL for 28 kg/m ³ virgin foam	168
9.10	ΔL for 15.1 m ² floating floor with 8 mm thick 78 kg/m ³ rebond	168
9.11	L' _{nT} for 6 mm thick 78 kg/m ³ rebond	169

9.12	L'_{nT} for 12 mm thick 78 kg/m ³ rebond	169
9.13	L'_{nT} for 14 mm thick 78 kg/m ³ rebond	170
9.14	L'_{nT} for 16 mm thick 78 kg/m ³ rebond	170
9.15	L'_{nT} for 10 mm thick 64 kg/m ³ rebond	171
9.16	L'_{nT} for 11.5 mm thick 96 kg/m ³ rebond	171
9.17	L'_{nT} for 9 mm thick 128 kg/m ³ rebond	172
9.18	L'_{nT} for 11 mm thick 144 kg/m ³ rebond	172
9.19	L'_{nT} for 8 mm thick 28 kg/m ³ virgin foam	173
9.20	L'_{nT} for 15.1 m ² section of mdf flooring with 6 mm 78 kg/m ³ resilient layer	173
9.21	L'_{nT} for refurbished floor in council flat	174
10.1	arrangement of floating floor sections for mobility tests	183
10.2	arrangement of flooring sections for impact sound insulation test	184
10.3	average driving point mobility for single boards and for boards attached to others	185
10.4	average driving point mobility for single boards and for boards attached to others, 100 Hz to 1000 Hz	186
10.5	average driving point mobility for single boards and for boards attached to others, 1000 Hz to 10000 Hz	186
10.6	ΔL with single sections and larger section of floating floor	187
11.1	circuit for measuring hammer contact time	199
11.2	tapping machine hammer on mdf	200
11.3	tapping machine hammer on concrete	200
11.4	deflection of lightweight flooring with 78 kg/m ³ polyurethane rebond resilient layer due to walking and stepping heavily	201

LIST OF TABLES

Table Number	Description	Page Number
3.1	Young's modulus for the foams tested	45
3.2	the effect of conditioning on Young's modulus	48
3.3	Energy involved in loading and unloading cycles	48
4.1	comparison of static and dynamic stiffness and loss factor for different types and thicknesses of foam specimen	80
4.2	comparison of static and dynamic stiffness using data from the first compression in the static tests	84
5.1	Airflow resistivity for rebond foam	96
5.2	Airflow resistivity for virgin foam	96
5.3	Comparison of sample stiffness and air stiffness for different thicknesses of rebond foam	99
6.1	impact sound pressure level for systems with different thicknesses of 78 kg/m^3 rebond foam layers	112
6.2	impact sound pressure levels for systems with different resilient layers	113
7.1	resonant frequency and dynamic stiffness for the test system with different foam specimens	123
7.2	loss factors for the tests systems	124
7.3	difference in the values of resilient layer dynamic stiffness produced by the two methods of including the air stiffness	129
9.1	longitudinal wavespeed	162
9.2	comparison of predicted and measured $L'_{nT,w}$	163

ACKNOWLEDGEMENTS

I should like to acknowledge the contribution of Professor Robin K. Mackenzie who initiated this programme of research and whose earlier work made it possible.

The contribution of Doctor Hocine Boudah who inherited the supervision of a project outside his area of expertise must be acknowledged. His advice and support during my time at Sheffield were much valued.

I am grateful to Carl Hopkins, of BRE, for the interest he has shown in my work and am pleased to be able to thank him formally for his constructive criticism during our discussions. Carl's advice was particularly helpful during the final stages of this research.

I owe thanks to Madeline for her support and her belief that I would successfully complete this project.

DEDICATION

This work is dedicated to my parents, Laurence and Myrtle Hall who have had to wait twenty years too long to see it.

It is also dedicated to my children Sam and Rowan who have missed the chance to be brought up middle class.

CHAPTER 1

IMPACT NOISE IN BUILDINGS

1.1 Background

The problem of unwanted noise in buildings is increasingly becoming a source of complaint and of growing interest to all with responsibility for the built environment. In 1982 investigations demonstrated that poor sound insulation was the most commonly cited defect with new houses¹ In 1984 The Avon, Gloucestershire and Somerset Environmental Health Monitoring Committee showed that 61% of all complaints received concerned domestic noise². The Building Research Establishment (BRE) stated in 1988 that complaints to Environmental Health Officers about noise from domestic premises had increased by around 800% over the previous ten years³ and the 1993/94 annual report by the Chartered Institute of Environmental Health found an increase of 10.5% in the number of complaints about noise over the previous year⁴. In a survey of the subjective response of the occupants of conversion flats Raw and Oseland⁵ found that noise from the flat above through the separating floor was particularly disturbing due to the component of impact noise and its unpredictable nature. The reduction of this type of noise is therefore an important part in alleviating a problem which has steadily increased over the last twenty years.

1.2 Impact noise and floating floors

Approved Document E of the Building Regulations⁶ describes several widely used floor constructions which have been shown to give acceptable sound insulation between dwellings. One recommended method of achieving acceptable impact sound insulation is to install a floating floor in which the walking surface is decoupled from the rest of the structure by a resilient layer. Floating floors can be used on both concrete and wooden supporting floors and their effectiveness in reducing impact noise depends mainly on the resilient layer used⁶. Examples of floating floors from the Approved Document are shown in Figure 1.1 and Figure 1.2.

Figure 1.1a shows a 55 mm thick cement sand screed over a resilient layer supported by a concrete slab. A mineral fibre quilt 25 mm thick and with a density of 36 kg/m^3 is specified for the resilient layer but 13 mm pre-compressed expanded polystyrene or 5 mm extruded polyethylene closed cell foam are also used. Figure 1.1b shows a tongued and grooved chipboard timber raft supported by timber battens lain on the resilient layer. 13 mm thick mineral fibre can be used if the battens have an integral closed cell resilient foam strip⁶.

Figure 1.2 shows a floating floor supported by a timber floor. The pugging adds mass to the floor and therefore improves the insulation against airborne sound. The resilient layer is 25 mm thick mineral fibre with a density of $80\text{-}100 \text{ kg/m}^3$ which supports an 18 mm thick tongued and grooved chipboard walking surface. Acoustically, the main problem with all resilient layers is that if they are sufficiently stiff to give a floor good stability they are less capable of providing a high degree of isolation and a balance has to be struck between the mechanical and acoustic properties^{7,8}.

For many refurbishment projects the simplest way to improve the impact sound insulation of a separating floor is simply to lay a floating floor with a chipboard or medium density fibreboard (mdf) platform on top of the existing floor. The advantage of this approach is that it does not involve modifications to the ceiling of the room below where there may be features, such as ornate cornices and covings, that need to be retained. A disadvantage of this approach is that it involves raising the level of the existing walking surface. These increases need to be kept to a minimum in order to avoid unacceptably large steps up into rooms or reduced door height.

If mineral fibre quilts are used as resilient layers then they must be no less than the 25 mm thickness specified in the Building Regulations Part E or the stiffness of the air enclosed in the material dominates⁹ and the effectiveness of the quilt as an isolator becomes increasingly reduced. Using a mineral fibre quilt therefore results in an increase in floor level of 25 mm plus the thickness of the walking platform (often 18 mm chipboard) which is unacceptable to many architects and building control authorities¹⁰. For refurbishment projects especially then there is a need for low profile floating floor systems which are easy to fit and which minimise increases in floor level whilst providing good impact sound insulation.

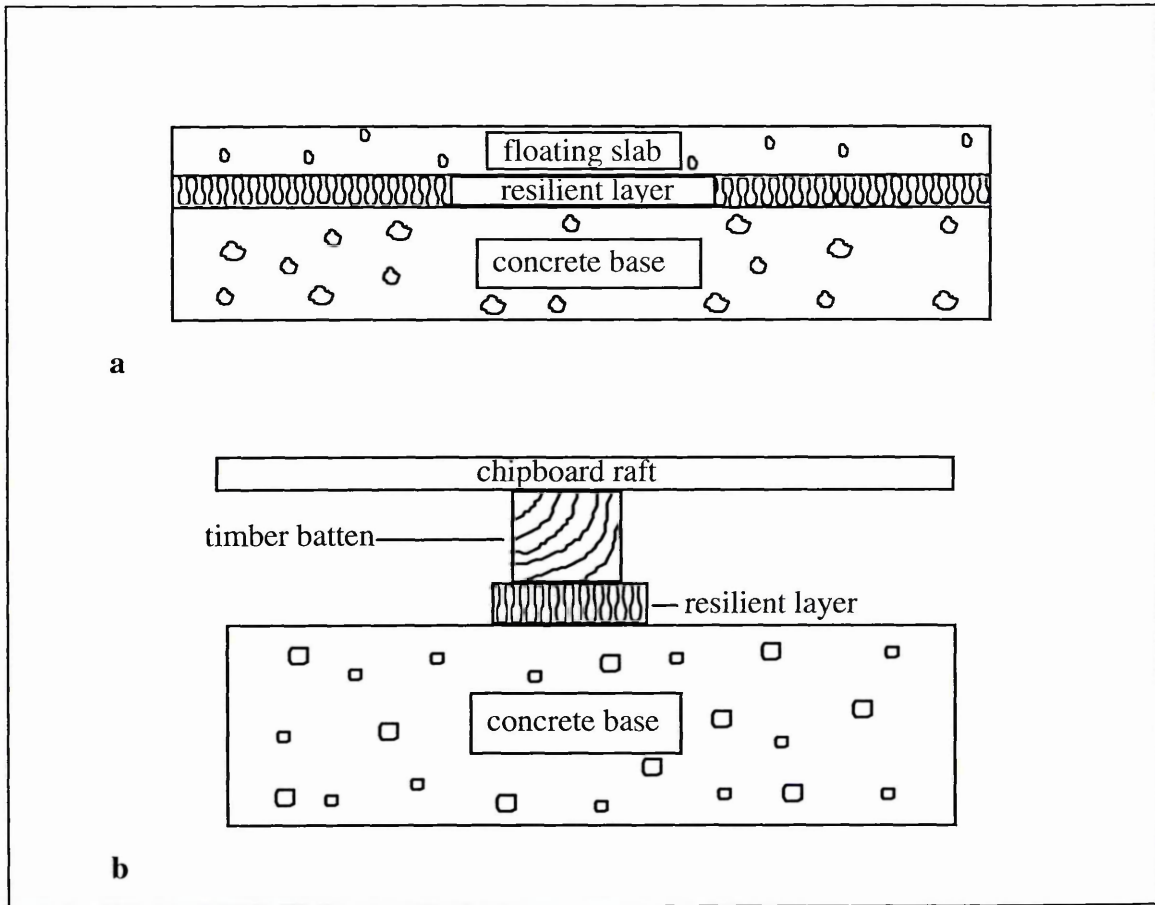


Figure 1.1: Concrete base with floating floor.

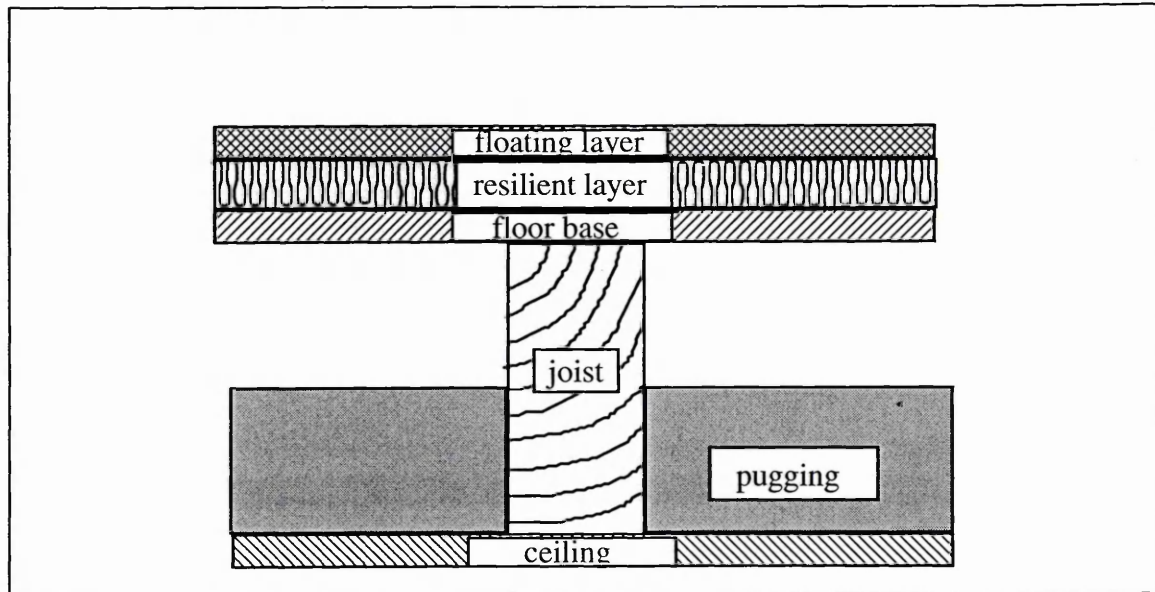


Figure 1.2: Wooden base with floating floor

1.3 Shallow profile floating floors

The need for shallow profile floating floors has led to research into materials other than mineral fibre or fibre glass for use as resilient layers in floating floor systems. Early proprietary flooring systems such as those developed by Cullum¹¹ and Hofbauer¹² preferred cork as the resilient material. The subsequent development of flexible polymers has led to the availability of many more materials with the potential for providing good vibration isolation and an increase in the choice of materials as resilient layers under floors. Research into the use of polymer foams as isolators by Mackenzie led to the conclusion that low density flexible open cell polyether urethane (henceforth the generic term polyurethane will be used) foam provided the most cost effective alternative to mineral fibre quilts¹³.

Mackenzie's research into the use of flexible polyurethane foams began in 1984 following investigations by the Scottish Special Housing Association into the failure of fibre quilt resilient layers in the floors of dwellings constructed in the 1970s. Floor inspections revealed that in many cases the brittle fibres of the quilts between the battens and the surface of the structural floor had been ground to dust¹⁴. Water penetration into kitchen and bathroom floors was another cause of mineral fibre quilt failure. Resilient polyurethane foams do not fail in such a manner in these circumstances. In addition they are more pleasant (and easier) to handle than mineral fibre quilts, do not pose the problem of potentially harmful airborne fibres associated with mineral fibre quilts and often have better long term performance¹⁵.

This research led to the development of several proprietary systems incorporating flexible open cell polyurethane foam for isolating floating floors. Some used strips of open and closed cell polyurethane foam in series to isolate the walking surface^{16,17,18,19}, as shown in Figure 1.3 and another²⁰, comprised tongued and grooved interlocking sections of chipboard flooring beneath which open cell polyurethane foam was glued. This system also used strips of closed cell polyurethane foam, but in parallel with the open cell foam, to reinforce the tongued and grooved joints as shown in Figure 1.4.

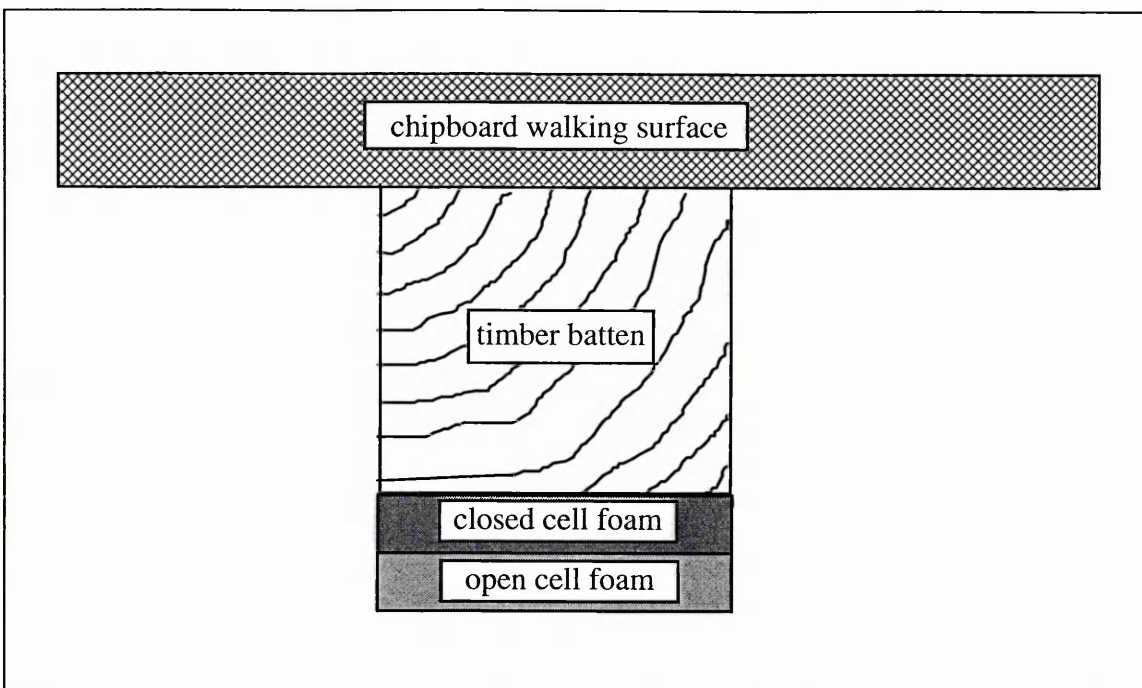


Figure 1.3: Batten with resilient strip.

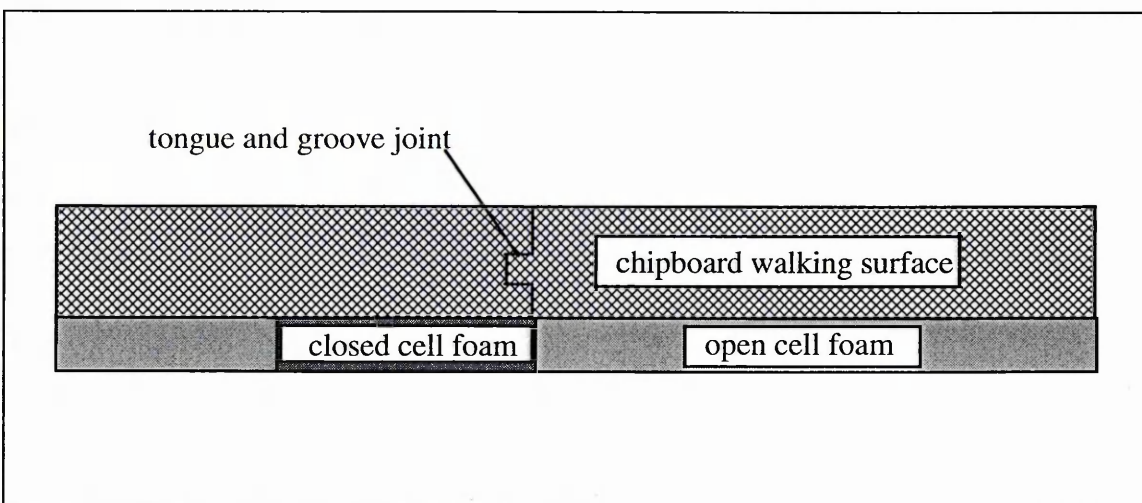


Figure 1.4: system with open and closed cell polyurethane foam in parallel.

The industry still had a need for a shallow profile floating floor system which raised the existing floor level less than 20 mm, especially for refurbishment projects. Following on from the above research, Mackenzie developed a shallow profile flooring system comprising interlocking tongued and grooved 9 mm thick mdf boards to which a resilient layer of low density (28 kg/m^3) virgin open cell foam was attached²¹. The resilient foam layer was 8 mm thick resulting in the first floating floor system comprising open cell polyurethane foam having a thickness less than 20 mm. This

system also reinforced the tongued and grooved joints with a closed cell polyurethane foam strip in parallel with the open cell foam.

The closed cell foam strip is necessary because flooring systems comprising low density virgin open cell foam as the resilient layer can exhibit discernible movement as they are walked upon²². This can cause problems of fatigue along the joints. The closed cell foam is much stiffer than the open cell foam due the pneumatic effect of air enclosed in the cells and so excessive movement, and therefore the possibility of fatigue along the joint, is considerably reduced.

According to the manufacturers of the system, laboratory tests, carried out at Heriot Watt University Edinburgh, showed an improvement 10 of dB in the Weighted Standardised Impact Sound Level ($L'_{nT,w}$) from fitting the system on a timber floor. On a concrete floor the improvement was 18 dB²³. A shallow profile floating floor system, especially suitable for refurbishment projects, providing good acoustic performance and walking stability appeared to have been developed.

More recently work at Sheffield Hallam university has identified that reconstituted foam has compression characteristics which make it more suitable for use as a resilient layer than virgin foam²². Field tests according to the method of BS 2750 Part 7²⁴ on tongued and grooved systems comprising 18 mm thick chipboard with reconstituted foam showed improvements in $L'_{nT,w}$ of 21 dB and 6 dB and for 9 mm thick mdf with reconstituted foam 20 dB and 5 dB on concrete and wooden floors respectively²⁵. The resilient layer of reconstituted foam was nominally 8 mm thick for all the different situations and the floors were rated according to BS 5821 Part 2²⁶. These flooring systems are now available commercially²⁵.

For architects and designers charged with the task of improving the impact sound insulation of floors it is desirable to be able to predict the likely acoustic performance offered by different treatments. Despite the growing interest in shallow profile floating floors comprising polyurethane foam, especially for refurbishment projects, no method has been identified which allows the prediction of the improvement impact sound insulation when they are used in the field from the properties of their component parts.

1.4 Dynamic stiffness

With floating floors the resilient layer has the greatest effect on the impact sound insulation of the flooring system as a whole⁶ and it is the dynamic stiffness of the layer which determines how effective an insulator against impact sound the floor will be. The Standard method for determining the dynamic stiffness of materials used under floating floors is BS EN 29052-1²⁷ and the search for alternatives to resilient layers made from quilts is likely to make this Standard increasingly important.

Flooring grade polystyrene for example is made from expanded polystyrene which has been crushed by as much as 70% by passing it between rollers thus rupturing closed cell walls and rendering the material more flexible. There is currently no Standard governing the amount of compression to which polystyrene sheet is subjected in the production of flooring grade polystyrene. It is therefore probable that the dynamic stiffnesses of the same thickness and density flooring grade polystyrene from different manufacturers will vary. If designers are to be able to predict the likely performance of this material as a resilient layer then the dynamic stiffness of the product must be determined by the Standard Method²⁷.

Unfortunately BS EN 29052-1 cannot be used to determine the dynamic stiffness of all resilient layers under floating floors. The Standard states: it does not apply to loadings lower than 0.4 kPa or greater than 4 kPa or to materials having low airflow resistivity (less than 10 kPa.s/m²). The density of the mdf decking used in the shallow profile floors is around 790 kg/m³ which means that it imposes a static load of around 0.07 kPa on the resilient layer. It appeared that BS EN 29052-1 could not be used to determine the dynamic stiffness of the thin layers of polyurethane foam used under the shallow profile floating floors of interest.

Despite this, the method described in BS EN 29052-1 was adopted as the means of determining the dynamic stiffness of the test samples of the polyurethane foams of interest in this research. Similar methods are available but that described in the Standard is simple and as legitimate as any other. Further justification for adopting this Standard Method is given in Chapter 2.

1.5 The way forward

This thesis is concerned with the use of flexible open cell polyurethane foam as the resilient layer in lightweight floating floors. The objective is to develop a method for predicting the acoustic performance of lightweight shallow profile floating floors from the properties of their flexible polyurethane foam resilient layers. A method for relating the performance of laboratory samples of foam to that of the material when used under a floor must therefore be identified. When this is achieved this will be possible to develop a method for predicting the improvement in impact sound insulation obtained by placing such lightweight floating floors on supporting floors.

The usefulness of the current standard tests on these materials for predicting their suitability as resilient layers under floors will be reviewed. It will examine the dynamic behaviour of thin layers of flexible polyurethane foam, in particular recycled foam. It is noted that there is currently no standard laboratory method for determining the dynamic stiffness of low airflow resistivity polyurethane foam layers under floating floors. Nor is there a standard method for determining the dynamic stiffness of resilient layers under lightweight floating floors.

Chapter 2 contains a review of the literature on flexible polyurethane foams and the manufacture of both virgin and recycled flexible polyurethane foam is described. The most commonly used Standard Methods for testing these materials are summarised and their relevance to this research programme is discussed. Recent research into the use of flexible polymer foams in floors is discussed in particular and from this the methodology adopted in this research programme is both determined and justified.

Chapter 3 describes the results from static tests on polyurethane foams carried out in the laboratory in order to assess their load bearing characteristics. In particular it describes the behaviour of recycled polyurethane foam under compression. Searches of the database held by Rapra Technology Ltd., the largest available on polymer foams, and discussions with representatives of the plastics industry in the UK, Europe and the USA have failed to find any reference to this. It is therefore believed that the characteristic behaviour of recycled polyurethane foam under compression is described for the first time as a result of this research.

The load bearing characteristics of resilient layers in floors are of primary importance since no floor treatment can be specified if it provides insufficient stability. The impact sound insulation of such floors however is governed by the dynamic properties of these layers and Chapter 4 describes the laboratory tests to compare the dynamic stiffnesses of different standard polyurethane foam specimens. BS EN 29052-1 states that the relationship between the dynamic stiffnesses of the laboratory specimens and the dynamic stiffnesses of resilient layers under floating floors depends on the airflow resistivity of the resilient material. Experiments to determine the airflow resistivity are therefore described in Chapter 5 and the results are presented.

Field tests to measure the standardised impact sound pressure level (L'_{nT}) with samples of different types of shallow profile floating floor comprising flexible polyurethane foam on a concrete supporting floor are described in Chapter 6. Results from tests on full floors carried out as part of a development programme for a manufacturer of flooring systems are also described. The measurements described in Chapter 5 showed that the airflow resistivity of the foam adopted for use in a (now) commercially available flooring system is so low that, according to BS EN 29052-1, the dynamic stiffness of the laboratory specimens cannot be related to that of a resilient layer comprising this material under a floor.

Chapter 7 describes a novel modification to the Standard Method designed to include the effect of the air in the laboratory specimens. The modification, for the first time, allows the results from laboratory tests to be used to determine the dynamic stiffness of low airflow resistivity resilient layers under floors. It also means that the dynamic stiffness of a specimen in the modified test method can be taken to be the same as the stiffness of the material when used as a resilient layer under a floating floor.

A method for predicting the improvement in impact sound insulation from lightweight floating floors on concrete supporting floors is described in Chapter 8. This method uses data from the modified Standard Test²⁷ described in the previous chapter. The prediction is made possible by compensating for the significant effect of the hammers of the Standard Impact Noise Source on the lightweight walking surface. The approach has been described previously²⁸ but its adoption in this research means that the range of application of BS EN 29052-1 has been extended considerably. In particular the

acoustic performance of novel lightweight shallow profile floating floor systems on concrete supporting floors can be predicted for the first time.

The predicted improvements are compared with the results from the field tests described in Chapter 6. Good correlation over a range of improvement in impact sound insulation up to 40 dB is demonstrated. It is shown that this good correlation occurs over the most significant frequency range for floating floors on concrete supporting floors when the Standard Method for rating the impact sound insulation of floors²⁶ is used. A novel treatment of the data is described which allows the prediction of $L'_{nT,w}$ for the samples of lightweight shallow profile floating floor used in the field tests. Chapter 9 considers whether the field tests on small sections of floating floor can justifiably be used to give an indication of the performance of complete floating floors.

The debate as to the suitability of the ISO tapping machine for testing the lightweight shallow profile floating floors of interest to this research is joined in Chapter 10. This chapter begins with a brief review of the development of the tapping machine. A review of the literature concerning the usefulness of the tapping machine for assessing the impact sound insulation of floors is then presented. It is concluded that the use of the ISO tapping machine is justified. Experimental results are then presented which demonstrate that the tapping machine can legitimately be used for testing the lightweight shallow profile floating floors

Finally, in Chapter 12, a general discussion of the main findings of the thesis is presented together with recommendations for further research and concluding remarks.

1.6 References

- 1 LANGDON F.J., BULLER I.B., SCHOLLES W.E., *Noise from neighbours and sound insulation of party walls in houses*, BRE Information Paper, 1982, IP 13/82.
- 2 Avon, Gloucestershire and Somerset Environmental Health Monitoring Committee *Domestic noise - a guide for environmental health officers*, 1984.
- 3 BUILDING RESEARCH ESTABLISHMENT, *sound insulation between dwellings*, 1988, BRE Literature Package.
- 4 Chartered Surveyor Monthly, March, 1996
- 5 RAW G.J., OSELAND N.A, Subjective response to noise through party walls in conversion flats, *Applied Acoustics.*, 1991, Vol. 32, 215-231.
- 6 DEPARTMENT OF THE ENVIRONMENT AND THE WELSH OFFICE, The Building Regulations, *Resistance to the passage of sound*, 1991, Approved Document E.
- 7 MACNEIL J, Making the peace, *Building*, 13 March., 1992.
- 8 UTLEY W.A., CAPPELIN P, The sound insulation of wood joist floors in timber frame constructions, *Applied Acoustics*, 1978, 11, 147-164.
- 9 JOHANSSON C., ANGREN A., Development of a lightweight wooden joist floor, *Applied Acoustics*, 1994, 43, 67-79.
- 10 MACKENZIE R.K, Upgrading of floors in refurbishment projects, *Proc. IOA.*, 1993, Vol. 15, Part 15, 301-309.
- 11 CULLUM D.J., UK Patent No 14468, *Improvements in the construction of floors*, Filing Date 17 May 1935.
- 12 HOFBAUER G., German Patent No 714399, *Scall and warmedammende verbindung von im abstand voneinander angeordneten bauteilen*, Filing Date 17 December 1935.
- 13 MACKENZIE R.K, Improvement of sound insulation of timber floors: a study of the relative significance of mass, resonance and resilience in the system, *Proc. IOA.*, 1986, Vol. 8, 79-89.
- 14 MACKENZIE R.K., HALL R, Developments in the application of flexible open-cell polymer foams, *Proc. IOA.*, 1996, Vol. 18 (3), 29-38.

-
- 15 MACKENZIE R.K., Development of a sound absorbing flooring system, *Proc. IOA.*, 1986, Vol. 8, 169-174.
 - 16 MACKENZIE R.K., UK Patent No 2259131, *Sound deadening in floor construction*, Filing Date 21 August 1992.
 - 17 MACKENZIE R.K., UK Patent No 2192913, *Sound attenuating floor construction using an open-cell foam strip*, Filing Date 24 June 1986.
 - 18 MACKENZIE R.K., UK Patent No 2196356, *Sound attenuating floor construction using a laminated open and closed cell foam strip*, Filing Date 25 June 1986.
 - 19 MACKENZIE R.K., UK Patent No 2214537, *Improvements in sound attenuating floor construction*, Filing Date 25 January 1988.
 - 20 MACKENZIE R.K., UK Patent No 0536161, *Floor construction involving resilient strip*, Filing Date 23 May 1991.
 - 21 MACKENZIE R.K., European Patent Application No 949154618.6, *Floor construction involving shallow profile deck*, Filing Date 19 May 1994
 - 22 HALL R., MACKENZIE R.K., Reconstituted versus virgin open cell foams in floating floors, *Building Acoustics*, 1995, Vol. 2, No 2, 419-436.
 - 23 MACKENZIE R.K., HALL R., The use of low density polymer foams as resilient layers in floors, *Proc. IOA*, 1994, Vol. 16 Part 2, 381-391.
 - 24 BS 2750, 1980, *Measurement of Sound Insulation in Buildings and of Building Elements, part 7, Field Measurements of Impact Sound Insulation of Floors*.
 - 25 BOUGDAH H., HALL R., Impact sound insulation of floors using recycled polyurethane foam, *Proc. Clima 2000*, 1997, International Conference, Brussels, Belgium.
 - 26 BS 5821, 1984, *Rating the sound insulation in buildings and of building elements, part 2, method for rating the impact sound insulation*.
 - 27 BS EN 29052-1, 1992, *Acoustics - materials for acoustical applications - materials used under floating floors in dwellings*.
 - 28 CREMER L., HECKL M., UNGAR E.E., *Structure-borne sound, 2nd ed.*, Publ. Springer-Verlag, 1988.

CHAPTER 2

POLYURETHANE FOAM

2.1 Introduction

This chapter contains a review of the literature on flexible polyurethane foams. It describes their nature and briefly describes the manufacture of both virgin and recycled flexible polyurethane foams. The most important studies carried out into the static and dynamic behaviour of polyurethane foams are examined and this research is put into the context of the requirements of industry. A review of the different approaches to modelling the behaviour of flexible polyurethane foam is included. In particular research into the use of flexible polyurethane foams under floors and in composite flooring systems is discussed

After the Standard Tests on flexible polyurethane foam most relevant for this research are described the literature review is summarised. Finally conclusions are drawn which justify the experimental approach adopted in this research programme.

2.2 Background

Flexible polyurethane foam is a particular form of cellular plastic material whose properties are determined partly by the base polymer from which it is constructed but more so by the density of the foam and the form of the cells within the material. Cellular structures are common in nature because they combine high strength with lightness: wood and cancellous bone are just two examples although the example which perhaps springs first to mind is the honeycomb.

Not only can cellular structures provide high strength but some also provide flexibility and resilience. Cork and sponge are naturally occurring examples of this and their structures were the subject of study by Hooke after perfecting his microscope. According to Gibson and Ashby¹ it was Hooke who first used the term cell (derived

from the Latin cella; a small room or chamber) and published drawings of the structures of cork and sponge as long ago as 1664².

Cork has long been recognised as a material useful for reducing the transmission of unwanted vibrations, it was the preferred resilient layer in the earliest proprietary sound reducing flooring systems^{3,4} identified in this research and is still cited as a vibration isolator⁵. The development of polymer science however has led to the availability of many more materials for vibration isolation. One of these materials is flexible polyurethane foam.

The foams of interest to this research programme are flexible open cell polyurethane foams. These foams are extensively used as cushioning in furnishing and in packaging due to their load bearing characteristics and ease of moulding and forming. The cutting and forming process for producing the required products can be very wasteful however. Boatz⁶ et al state that up to 25% of slabstock foam can become scrap in the forming process and the Polyurethane Foam Association (USA) claims⁷ that this figure can be as high as 30%. Such high levels of waste can pose expensive disposal problems but fortunately flexible polyurethane scrap can be recycled⁸ to make reconstituted (or rebond, the industry's term for the material) foam. Given the growing importance of recycling and therefore energy saving, rebond polyurethane foam was studied in this research programme and its manufacture is described in the next section of this chapter.

2.3 Manufacture of polyurethane foam

2.3.1 Virgin foam

Polyurethane foam can have open cells, rendering the foam porous, or closed cells where the cells are separated from each other by a membrane making the foam impervious to the passage of air. Slabstock polyurethane foams are made by using a "blowing agent" to expand a fluid polymer phase to a low density polymer state and then freezing this state⁹. In the case of polyurethane foams the blowing agent is usually water which reacts with the isocyanate in the fluid to produce carbon dioxide gas (CO₂). The CO₂ produced migrates to the air bubbles which are mixed in the fluid and which act as nucleation sites so the gas bubbles in the liquid polymer mixture expand and the mixture begins to take on a cellular form. Between 100 and 200 seconds after mixing

the reagents together, the blowing reaction ceases but the reaction which forms the long chain polymer networks (the gelling reaction) in the end product continues thus strengthening the cell struts.

During the forming process surface tension can draw the polymer material to the cell edges leaving only a thin membrane. With an open cell foam these thin membranes between the cells burst once the expansion of the polymer mixture has finished allowing the gas contained to escape to leave a lightweight, flexible, porous material. In closed cell foams the membranes are much more substantial and contain a significant fraction of the solid polymer. With these foams the cell walls remain intact and contribute to the strength of the resulting polyurethane foam¹. In addition, the gas within the cells adds strength to the material due to pneumatic effects.

2.3.2 Recycled polyurethane foam: rebond

The need for recovered scrap polyurethane foam is particularly high in the USA where much of the carpet underlay produced comprises recycled foam. The demand far outstrips the supply and scrap polyurethane foam is exported from Europe to the USA in an effort to meet the industry's needs. The Polyurethanes Recycle and Recovery Council (PURRC), a unit of the Polyurethane Division of The Society of the Plastics Industry, predict⁷ that the demand for recovered polyurethane foam will increase in the USA and also in Europe where the interest in recycling scrap foam is growing.

Such was the demand for scrap foam in the UK in 1996 that it was possible for manufacturers to make more profit by simply selling on their stockpiles of recovered foam rather than producing and selling other products from the material¹⁰. Apart from carpet underlay the main use for recycled polyurethane foam is in cushioning for furnishing and vehicle seats although it is also used in sports floors, for example in gymnasiums¹¹ and in indoor bowling greens¹².

Rebond is a moulded product made from pieces of flexible polyurethane foam which have been shredded to produce chips of a reasonably uniform size which are held together with a binder. The manufacturing process is illustrated schematically in Figure 2.1. The scrap foam is put into a shredder where polyurethane foam chips are produced.

The chips are screened and passed on to the storage hopper where they are held prior to mixing. The chips are mixed with the polymer binder in the blend tank from where the, now polymer coated, chips are passed to the mould. Here the rebond is formed by compressing the chips, mixed with steam, to the thickness needed to give rebond of the required density¹³. The required thicknesses of the rebond foam are then cut from the blocks produced in the mould. Typically the range of densities produced is 60-200 kg/m³. Although the density can be controlled by compressing the mixture of chips to a greater or lesser degree, if high density rebond is required then higher density scrap is used in the process and scrap rebond is recycled again in order to increase the average density of the constituents. The quality of the rebond is controlled by¹³:

- The type of scrap foam used
- The chip size and uniformity of the constituents
- The density
- The quality of the binder
- The binder/foam ratio

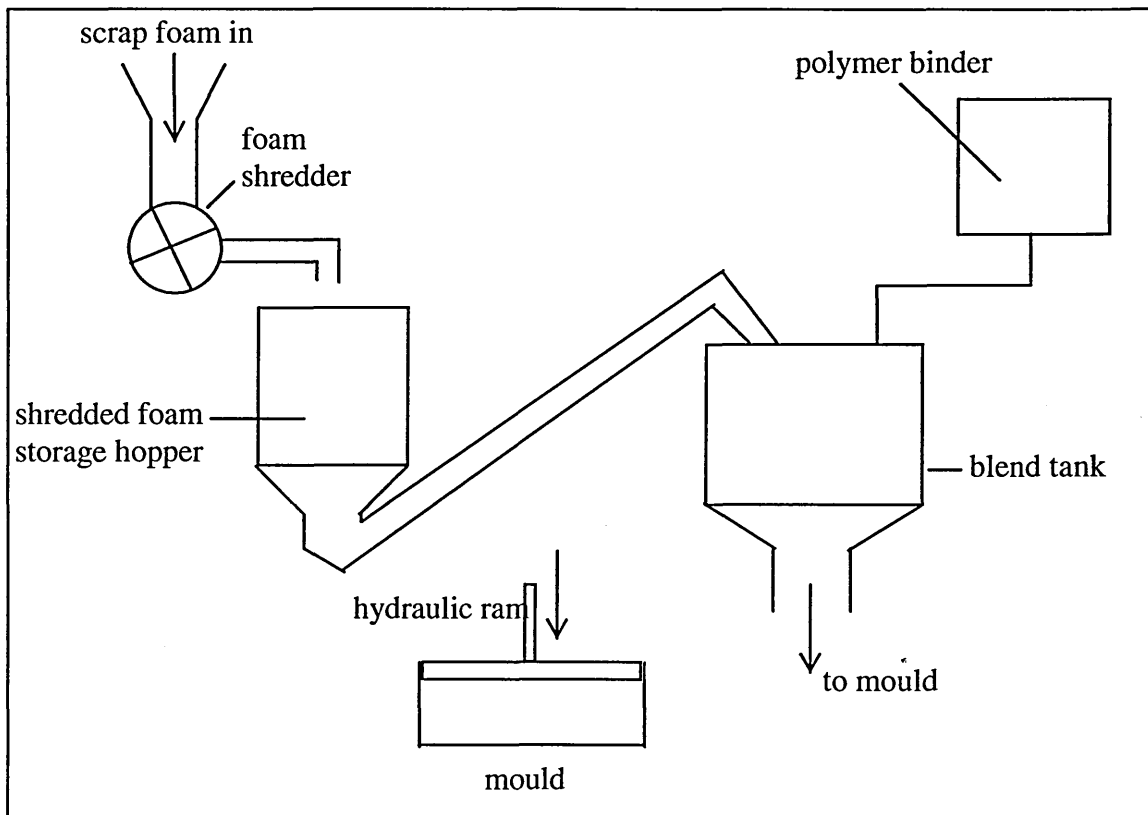


Figure 2.1: Rebond manufacturing process

2.4 Review of work on polyurethane foam

2.4.1 Static behaviour

The behaviour of virgin polyurethane foam is governed partly by the base polymer from which the material is made but more so by the shape of the individual cells in the foam and whether the foam has open or closed cells. Since this thesis is concerned with the use of flexible open cell polyurethane foams in floors detailed discussion of the behaviour and properties of foams will be restricted to these. The most successful attempts to model the behaviour of these materials will be described in some detail later in this chapter but an example of the behaviour of low density flexible polyurethane foam under compression is included here as an introduction to a review of the work already carried out in this field.

Figure 2.2 shows a stress-strain curve for a compression cycle on a 12 mm thick sample of low density (20 kg/m^3) virgin open cell foam, compressed at a strain rate of 0.14 s^{-1} , which is typical of the response of this type of foam. It can be seen that, after the initial small strain, the loading curve is highly non-linear and that the unloading curve does not return along the same path when the compressive force is removed at the same rate. Energy is therefore dissipated over the cycle. It can also be seen that the foam does not quite return to its original thickness in the time taken to remove the load: there is a pseudo set.

The cells in open cell foam can be considered to be made from beams or struts of solid polymer interconnected with their neighbouring cells. This approach allows easy explanation of the shape of the curve shown in Figure 2.2. The linear relationship between stress and strain in the initial portion of the curve, up to the clearly defined yield point, is due to the elastic bending of the cell beams or struts. The “plateau” region after the yield point is due to the non linear elastic buckling of the beams and the steeply rising portion of the curve is due to “densification” where the buckled beams begin to touch and interact with each other. As compression continues the voids in the foam are reduced more and more and the foam begins to act like the solid polymer from which it is made.

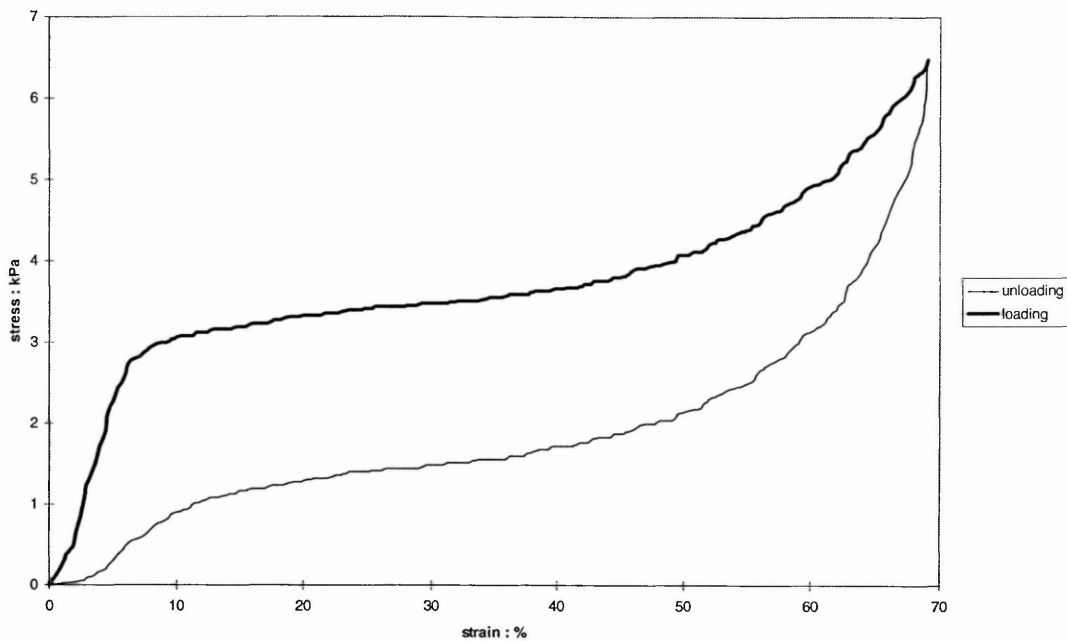


Figure 2.2: Typical stress-strain curve for open cell polyurethane foam

According to Suh⁹ the first commercial cellular polymer was sponge rubber which was introduced between 1910 and 1920 since which time there has been considerable research into these materials. Much work has been directed towards the development of mathematical models to describe the behaviour illustrated in Figure 2.2.

The nature of the research into the behaviour of polyurethane foams has been, to a large extent, driven by the demands of industry who use them primarily as packaging material or as cushioning in furniture. For furnishing the key requirements are to provide adequate support and comfort and to resist fatigue. When designing packaging, or say car headrests, fragile objects need to be protected from the damaging decelerations encountered in impacts. Knowledge of the energy absorption for a given compressive deformation afforded by a particular foam is required, as is the maximum deceleration suffered by an object of given shape and mass impacting upon it. Much of the modelling of polyurethane foam behaviour has therefore been aimed at producing useful tools for optimising their use in packaging.

The complexity of polyurethane foam structure meant that the most successful early attempts to model their stress-strain behaviour under compression used empirical models to relate stress and strain. This work has been reviewed by Hilyard^{14,15}, Collier¹⁶

and Gibson and Ashby¹ who considered the most widely useful approach to be that of Rusch whose work followed that of Gent and Thomas. Gent and Thomas were the first to relate the effective Young's modulus of an open cell foam to the volume fraction of solid polymer in the material^{17,18}.

Rusch described the stress-strain curve in terms of an empirical shape factor ($\Psi(\epsilon)$) where¹⁹

$$\sigma(\epsilon) = E_f \Psi(\epsilon) \epsilon \quad \text{N / m}^2$$

Equation 2.1

$$\sigma = \text{stress N/m}^2$$

$$\epsilon = \text{strain}$$

E_f = Young's modulus for the foam N/m^2 given by

$$E_f = E_p \left(\frac{\Phi_o}{12} \right) (2 + 7\Phi_o + 3\Phi_o^2) \quad \text{N/m}^2$$

Equation 2.2

where

E_p = Young's modulus for the solid polymer from which the foam is made N/m^2

Φ_o = the volume fraction of polymer in the foam; $\left(\frac{\text{volume of polymer}}{\text{volume of foam}} \right)$

$\Psi(\epsilon)$ is given by

$$\Psi(\epsilon) = a\epsilon^{-p} + b\epsilon^q$$

Equation 2.3

a, b, p and q are empirically determined curve fitting constants.

It can be seen from Equation 2.2 that when $\Phi_o = 1$, $E_f = E_p$.

Both the maximum deceleration suffered by an object packaged in foam and the impact energy per unit volume absorbed by a foam can be related to the stress-strain behaviour of the foam through Rusch's shape factor. This then was a method for optimising foams

for a particular situation but, as Gibson and Ashby observe, it is an entirely empirical approach and lacks any mechanistic basis¹.

Gibson and Ashby combined empiricism with physical modelling in their approach to optimising foam for a particular application. Their modelling of the behaviour of polyurethane foam is supported by impressive correlation with experimental data and is particularly elegant in its simplicity. Their simplest model of the single cellular unit in an open cell foam is a cube constructed of vertical and horizontal beams of the solid polymer with length (l) and thickness (t) which are connected to other cells by other beams in their centres. The model is shown in Figure 2.3.

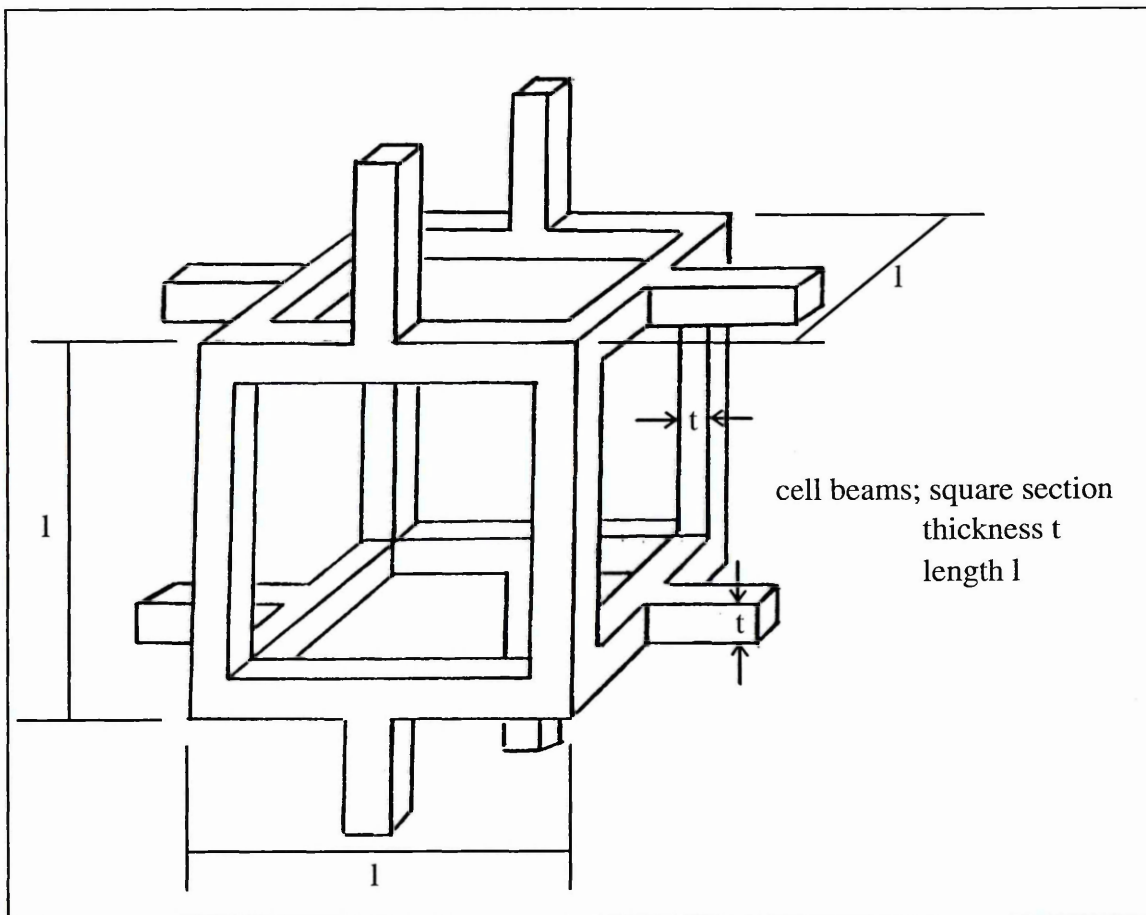


Figure 2.3: redrawing of the Gibson and Ashby model of the open polyurethane foam cell.

The relative density of the cell (ρ_f/ρ_s) and the second moment of area (I) are related to t and l by¹

$$\frac{\rho_f}{\rho_s} \propto \left(\frac{t}{l}\right)^2$$

Equation 2.4

and

$$I \propto t^4 \text{ m}^4$$

Equation 2.5

where ρ_f and ρ_s are the densities of the foam and the solid polymer respectively.

The Young's modulus for the foam is calculated from the linear elastic deflection of a beam of length (l) loaded at its mid point by a force (F). Using standard beam theory²⁰, Gibson and Ashby deduce the linear elastic deflection (δ) of the beam to be given by

$$\delta \propto \frac{Fl^3}{E_p I} \text{ m}$$

Equation 2.6

and Young's modulus for the foam to be

$$E_f = \frac{\sigma}{\epsilon} = \frac{C_1 E_p I}{l^4} \text{ N / m}^2$$

Equation 2.7

Using Equations 2.4 and 2.5 Gibson and Ashby derive:

$$E_f = \frac{\sigma}{\epsilon} = C_1 E_p \left(\frac{\rho_f}{\rho_s}\right)^2 \text{ N / m}^2$$

Equation 2.8

C_1 is a constant, found to be¹ ≈ 1 . E_f , E_p are the Young's moduli of the foam and the solid polymer respectively.

The yield stress (σ_{el}) at which the horizontal beams begin to deform by elastic buckling is given by¹:

$$\sigma_{el} = C_2 E_p \left(\frac{\rho_f}{\rho_s} \right)^2 \text{ N / m}^2$$

Equation 2.9

C_2 is a constant found to be¹ ≈ 0.05 .

A refinement of this simplest model uses a cell in which the vertical beams are longer than the horizontal beams which is closer to the situation in real foams since the cells are slightly elongated in the rise direction. Since the horizontal beams are now shorter than the vertical beams Equation 2.6 states that the foam will deflect less for a given compressive force in the vertical direction than in the horizontal direction. This mirrors the real situation where virgin open cell polyurethane foams are most stiff in their rise direction, due to the elongation of the cells in this direction caused by the blowing process.

Gibson and Ashby describe the construction of energy absorption diagrams to enable optimisation of a foam for a particular shock absorbing application¹. The area under the loading curve shown in Figure 2.2 up to the onset of densification is equal to the energy per unit volume (W) absorbed by the foam in being strained up to this point, if the horizontal axis shows decimal strain. The stress at this point is termed the peak stress (σ_p) and the foam which absorbs most energy up to the maximum permitted stress is the best for the particular application.

The energy absorption diagrams are particularly useful because they allow comparison of different types of foam on the same axes. A foam specimen is compressed to produce a stress-strain curve like that shown in Figure 2.2 and the energy absorbed per unit volume up to a particular strain is determined from the compression data. The energy absorbed per unit volume up to a particular strain is plotted against the peak stress at that particular strain. The process is then repeated at different strain rates and with different foam specimens. Both axes are normalised by the Young's modulus of the polymer from which the foam specimen is made which allows foams made from different polymers to be compared on the same graph. In this way a series of curves is plotted and a line drawn which just touches the point on the curve corresponding to the

onset of densification. Figure 2.4 illustrates the procedure using stress-strain data from just two different foams compressed at the same rate of strain whose stress-strain curves can be seen in Figures 3.5 and 3.6, the Young's modulus for the polymer is taken¹ to be 45 MN/m².

The best foam for a particular application is the one which absorbs the required amount of energy up to the onset of densification at the required strain rate. The heavy straight line in Figure 2.4 just touches both the curves and illustrates how the “envelope” of optimum foam density is obtained at the specified strain rate.

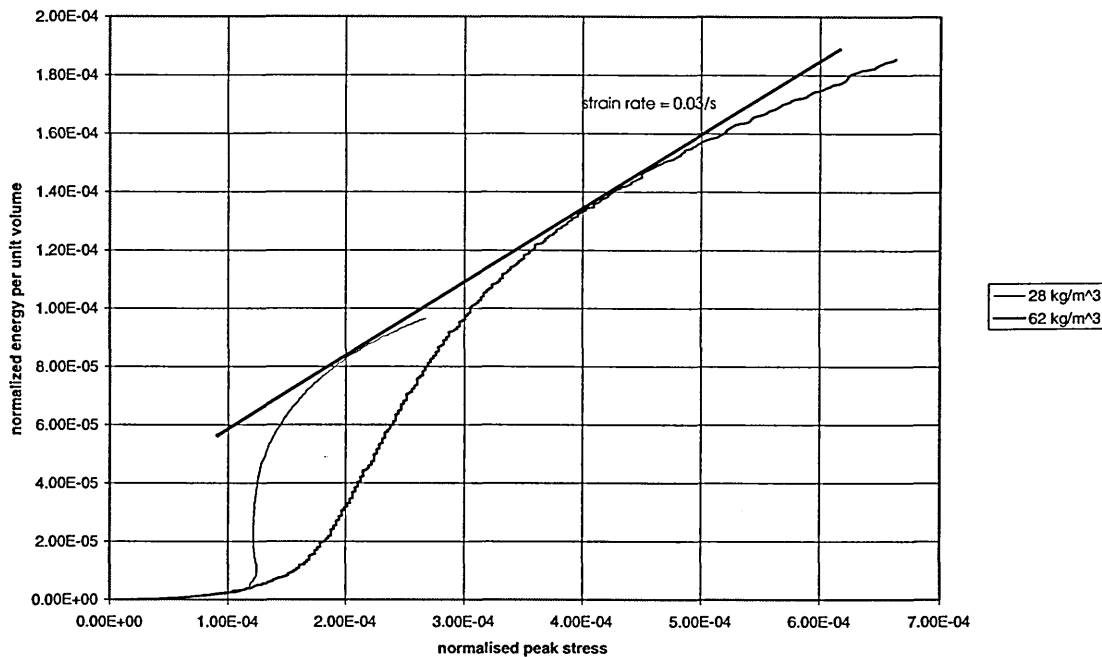


Figure 2.4: example of energy absorption curve approach to foam optimisation

The approaches of Rusch and Gibson and Ashby both require considerable experimentation in order to allow the optimum choice of foam for a particular application. Models based on the shape and size of the struts forming the cells making up the foam would avoid this and so, despite the complexity of polyurethane foams, these have been sought. Dementev and Tarakanov^{21,22} managed to relate the stress-strain behaviour of polyurethane foams at small strains, in the approximately Hookean part of the stress-strain curve, to the dimensions of the Struts forming the cellular structure. More recently Kraynik and Warren²³ have succeeded in relating foam

behaviour under large compression to the dimensions of the elements making up the individual cells and there are now software packages available for modelling the compressive behaviour of polyurethane foams, e.g. ABAQUS²⁴.

Probably the most important point of the stress-strain curve shown in Figure 2.2, for resilient layers under floors, is that at which the struts forming the cells begin to collapse elastically, which is where linear relationship between stress and strain breaks down. Once the yield stress is exceeded the cellular structure collapses rapidly for little increase in stress and such rapid and relatively large deflections are easily discernible as floors are walked on. The first requirement from a floor is that it gives acceptable stability: designers and architects are unlikely to specify a floor that does not satisfy this requirement no matter how good the sound insulation offered.

2.4.2 Dynamic behaviour

Polymer foams are complex materials and their complex modulus is described by²⁵

$$E^* = E' + jE''$$

Equation 2.10

or

$$E^* = E'(1 + j\eta)$$

Equation 2.11

where E^* = dynamic Young's modulus N/m^2

$$j = \sqrt{-1}$$

E' = storage modulus: associated with elastic processes in phase with the applied strain. (related to energy stored)

E'' = loss modulus: associated with viscous loss processes and 90° out of phase with the applied strain. (related to energy dissipated)

$$\eta = \frac{E''}{E'} : \text{the loss factor.}$$

The storage modulus of low density flexible polyurethane foams has been shown to highly dependent on quiescent strain¹⁶, first falling and then rising again after a minimum around 20% strain.

The need to be able to predict the energy absorption of polyurethane foams has been discussed. The dynamic behaviour of these materials which appears to be of most interest to industry is its ability to withstand dynamic fatigue when subjected to the forces experienced in, say, loaded vehicle seats or carpet underlay when walked upon. Indeed when Shestopol and Chilcott²⁶ researched the vibration isolation properties of flexible urethane foams in the late eighties they found only one reference on the subject²⁷.

It is certainly true that there are relatively few references in the literature on this aspect of the properties of polyurethane foam although in 1965 a design guide for polyurethane foam isolation systems was published²⁸. This work came about due to the need to protect sensitive equipment from damaging vibrations and forces in the confined spaces of US military aircraft. Polyurethane foams were considered particularly attractive for this application because of their inherent damping properties and because their non linear behaviour meant energy could be absorbed with much smaller deflections than with linear isolators without subjecting sensitive equipment to unacceptable decelerations.

Collier's work¹⁶ also dealt with the use of polyurethane foams as isolators: in particular with their performance at the high levels of strain experienced in car seats for which he developed a mathematical model. Collier's research is the only work identified which proposes a correlation between information obtained from static stress-strain curves and the dynamic performance of foams. Collier investigated the performance of foams at high quiescent strains: he proposed that the effective Young's modulus under dynamic loading at a particular quiescent strain is dominated by the gradient of the unloading curve at that strain (at the point of testing machine cross head reversal) when determined using the usual static method. A method for determining the gradient at this point more easily was later proposed by Hilyard et al²⁹.

The more recent work on the ability of polyurethane foams to resist fatigue has, to no small extent, been driven by problems of the fatigue failure of carpet underlay in the USA. Stevens et al³⁰ compared methods for obtaining the dynamic fatigue performance of carpet underlay foams. They point out that this is important for the foam manufacturing industry since claims of performance and longevity for products have too

frequently failed to be realised in the field resulting in manufacturers having to bear the expense of replacement. One of their conclusions was that a fatigue test method which effectively predicts the fatigue performance of carpet underlay in use should be adopted by industry. Hager and Craig³¹, however, point out that laboratory tests involving accelerated durability tests can give an incomplete and sometimes inaccurate picture of how a material might perform in the field.

As a consequence of the difficulty in predicting the performance of carpet underlay, the industry in the USA along with the Polyurethane Foam Association and the Georgia Institute of Technology worked on developing a standard test which would give meaningful data from which realistic conclusions could be drawn. Their solution³² was to employ people of different weights to walk up and down a narrow corridor of carpet covered underlay a specified number of times. When the walking is over, small samples are cut from the underlay and taken to a laboratory for fatigue testing.

2.4.3 Resilient layers for isolation in floors

The research carried out into the performance of polymer foams used under floating floors almost all involves the investigation of closed cell foams. Flooring grade polystyrene is a special case of a closed cell foam in that it is a rigid foam which has been compressed, thus rupturing some of the cell walls and rendering the material flexible. Pritz investigated polystyrene and polyethylene closed cell foams³³ used under floors having failed to find any references to their dynamic moduli or damping properties in the literature. The methods used in his research had been developed over a series of investigations into the dynamic properties of mineral and glass wool materials^{34,35,36} as well as polyurethane foam and rubber³⁷.

Measurements were made³³ on both long thin samples excited from above and on shorter prismatic samples excited from below and supporting a load mass so that the variables of interest could be measured as functions of frequency and amplitude respectively. The measurements on the long polystyrene specimens were carried out under vacuum so that the dynamic Young's modulus and loss factor could be solely attributed to the frame material of the foams investigated, other samples could be tested in air. Measurements were made over a frequency range from 100 to 3000 Hz.

The loss factors for both foams were low and increased with frequency but the increases were found to be insignificant for practical applications. The frame dynamic modulus for both the polystyrene and polyethylene foams was found to increase with frequency but the increase was insignificant for practical applications in floating floors. Neither the Young's modulus nor the loss factor of the foams was found to depend on the strain amplitude if it were less than 10^{-3} . At greater amplitudes than this the Young's modulus increased whilst the loss factor decreased with increasing strain. These results are in agreement with those from an earlier investigation³⁷ using polyurethane foam which also found little significant increase in Young's modulus or loss factor over a similar frequency range.

Pritz's work on glass fibre materials used under floating floors followed that of Ver³⁸ who had studied the dynamic performance of this and other materials used for vibration isolation. Cork, fibre glass and neoprene were investigated in this study and Ver too found that the loss factor of the materials was independent of frequency between 10 and 2000 Hz. The dynamic stiffness of the materials was found to be constant below the resonant frequency of the test system and was found to increase with increasing static load. Ver found that the dynamic stiffness of the materials could not be determined from the static load deflection curves. He states that correlation between the static and dynamic stiffnesses could be found only by using the initial slope, taken at small deflections, of the static load deflection curve. Here, the stiffness evaluated from the initial slope was two to three times smaller than the measured dynamic stiffness.

The conclusions from Pritz's research with polymer foams, that there was no significant increase in either the dynamic Young's modulus or the loss factor with frequency, are in agreement with the findings of Sim and Kim³⁹. Here the variables were studied over a frequency range of 200 to 10000 Hz with several polyurethane blocks. Unfortunately the blocks are described only in terms of their shape factor (the ratio of the cross-sectional area to the total area of the stress free surfaces for the specimen³⁹) but from comparison with values for Young's modulus and loss factor measured for rubber and polyurethane foam³⁷ the blocks must be solid polyurethane.

2.4.4 Composite flooring systems

Recently much work has been carried out on flooring systems incorporating flexible polyurethane foam in Japan where the need for good impact noise insulation in lightweight multiple occupation buildings is of increasing importance. Sueyoshi and others have been investigating the performance of lightweight composite flooring systems comprising polymer foam resilient layers for several years. Early experiments were carried out using small samples comprising different types and thicknesses of wood fastened to different resilient damping layers⁴⁰. The samples were placed on a solid base and impacted with a hammer with an integral force transducer which was hinged so that it dropped from a constant height throughout the tests. It was shown that the vibration of wood strips at their natural frequencies can be reduced significantly by attaching them to strips of rubber sheeting, even if the sheeting is relatively light and flexible.

Their approach involves the use of Fast Fourier Transform (FFT) techniques and later work⁴¹, again on small laboratory samples, investigated the dynamic behaviour of wood/foam rubber composites subjected to random vibration excitation from an electromagnetic shaker. FFT analysis made it possible to measure the dynamic stiffness and mechanical impedance at the driving point of the sample. Here again the thickness of the wood was varied in order to determine the thickness at which the system ceased to behave as a single degree of freedom system.

The experimentation described above was part of a programme designed to develop laboratory tests which would give an indication of the impact sound insulating qualities of composite flooring systems. The two experimental techniques briefly described above were combined to investigate 27 different types of composite wood flooring⁴² each having more than two layers. The dynamic stiffness of the composites at the driving point was measured using the FFT techniques⁴¹ and the magnitude of the dynamic stiffness for these multi degree of freedom systems was taken to be the sum of the equivalent stiffnesses at each mode.

The dynamic stiffness was then compared with the maximum impact force on the composites due to a 500 g hammer, with integral force transducer, being dropped from a

height of 4 cm. The authors of this work demonstrate close correlation between equivalent stiffness and maximum impact force and therefore state that the equivalent stiffness of the flooring composites is one of the indices of shock absorbing performance for a light impact load.

It should be noted however that all the composite systems tested by Sueyoshi et al comprised foam with closed cells and that correlation between the indices measured in the laboratory and the acoustic performance of the composite systems in the field, or laboratory, has not been demonstrated. No research has been identified which is specifically aimed at relating laboratory tests to the acoustic performance of lightweight flooring systems comprising open cell polyurethane foams in the field. The only references identified which have examined the acoustic performance of light weight floating floors comprising flexible open cell polyurethane foam have been those of Mackenzie⁴³.

2.4.5 Mackenzie's work

The reasons for the development of the first lightweight shallow profile floating floor system were outlined in Chapter 1. Mackenzie's approach was to construct and test flooring systems by measuring the standardised impact sound pressure level in a receiving room in tests conducted according to BS 2750 Part 7. Several different polymer foams were used as resilient layers and their performance was compared with the more traditional fibre quilts⁴³. After much experimentation an open cell flexible virgin polyurethane foam was decided upon for the shallow profile flooring systems.

The acoustic performance of any sound reducing flooring system is the measure of its success or failure. It was clear that linking the acoustic performance of the floating floors to the performance of laboratory specimens made from their resilient layers would be a major contribution to their development. Mackenzie⁴³ compared the natural frequencies of several systems which were calculated from static load-deflection tests. This was done since a low natural frequency usually corresponds to improvements in vibration isolation beginning at relatively low frequency⁴⁴. He states⁴³ that these natural frequencies may be up to 20% too low because the dynamic stiffness of polymers is greater than their static stiffness. It was clear that the dynamic stiffness of the resilient

layers must be measured if correlation between the acoustic performance of flooring systems and laboratory tests were to be identified.

2.4.6 Standard tests on polyurethane foam

The gamut of the usual Standard Tests carried out on flexible polyurethane foams is found in BS 4443⁴⁵. This Standard contains static, or quasi-static, and dynamic mechanical tests carried out on cellular foams as well as tests to determine the effect of solvents and of temperature and humidity on them although these latter effects are beyond the scope of this research. Many of the procedures described in the Standard are designed to assess the usefulness of polyurethane foams for cushioning or packaging. None is specifically designed for assessing the usefulness of foam used to support a floating floor.

For the application under discussion in this thesis the behaviour of foam under compression is of prime importance although tear strength and tensile strength may be relevant to the practicalities of cutting the foam to the required thickness and bonding it to other materials. The static and quasi-static tests described in the above Standard all take account of the effect of conditioning on samples. Method 5a⁴⁶ describes the method for obtaining the compressive stress-strain characteristics of flexible polyurethane foams and also the required pre-conditioning of tests samples before these can be obtained experimentally. This method is described in detail in Chapter 3.

BS 4443 Part 2 Method 7 describes the way in which the indentation hardness of foams is obtained. This procedure requires a 200 mm diameter indenter to be pressed into a 50 mm thick square specimen (of side $[390\pm 10]$ mm) to a depth of 70% of the original thickness at a specified rate of 100 mm per minute. This is repeated twice more and then the sample indented to 40% of its thickness, this indentation is maintained for 30 s and then the force is measured. The test is useful for assessing the behaviour of the material when it is used as a cushion or as packaging but provides no information for this application that cannot be derived from the stress-strain characteristics of the material. Indeed, under the flooring systems of interest, the load on the foam is not localised as in this test but spread by the supported walking surface.

BS 4443 Part 3 Section 3 Method 9 (replaced by BS EN ISO 3385 ,1995) describes the standard method for determining the dynamic cushioning performance of polyurethane foams. Samples of foam are impacted three times by a drop hammer and its peak deceleration obtained along with the residual set resulting from the impacts. The method states that it is primarily intended for quality assurance in packaging applications and again was deemed not to be sufficiently useful for this study to merit being adopted. None of the Standard Methods described in BS 4443 is aimed at determining the vibration isolation properties of polyurethane foam.

2.5 Summary of the literature review

Since the introduction of flexible polyurethane foams into the markets there have been many attempts to predict their behaviour under compression. Of these the most successful have been empirical expressions borne out of the results of much experimentation. The complex structure of these materials, distribution of cell size and anisotropy, make the development of realistic mathematical models based on measurements of the foam microstructure extremely difficult although recent advances in this field have been made²³.

The usual Standard Tests on polyurethane foam are designed to satisfy industry's need to produce effective cushioning for packaging and furnishings and most of the research work on these materials has been driven by this need. Even when the material is produced for use in carpet underlay the chief interest of manufacturers is the ability of the material to withstand constant use: i.e. its fatigue performance. Whilst this approach to testing is justified from the manufacturers' viewpoint it does little to assist in choosing open cell polyurethane foams for use as resilient layers, and therefore as vibration isolators, in floors.

No tests designed to assist in specifying flexible polyurethane open cell foams for use in lightweight shallow profile flooring systems have been identified. That this should be the case is unsurprising since, as was stated in Chapter 1, the only flooring systems available incorporating low density open cell polyurethane foam were designed by Mackenzie. However, as a result of the research described in this thesis there are now commercially available shallow profile systems incorporating open cell rebond foam.

Mackenzie has carried out field tests⁴⁷ to determine the acoustic response of flooring systems with flexible open cell polyurethane foam. Other research work into the usefulness of polymer foams as resilient layers in floors has been on small samples in the laboratory and directed at determining their dynamic response. There is little in the literature on this. Pritz³³, interested in determining the suitability of two such materials as resilient layers under floors, carried out his research into the dynamic responses of polystyrene and polyethylene because no reference could be found to these in the literature.

The only references to the use of open cell foam in flooring systems have come from Mackenzie's work. These materials appear to have been overlooked in favour of closed cell foams because of the, generally, better load bearing properties of the latter. In particular no information has been found in the literature or in discussions with manufacturers^{10,12,48,49} regarding the static stress-strain characteristics of rebound foam or its dynamic behaviour.

The work carried out by Sueyoshi et al^{40,41,42} again involves laboratory tests to identify correlation between the dynamic response of the different systems investigated and aspects of their performance in the field. This work has identified indicators of the shock absorbing properties of composite flooring systems but has not related these to impact sound pressure levels in rooms beneath such floors.

No method for relating the acoustic performance of lightweight shallow profile floating floors comprising resilient layers of flexible open cell polyurethane foam to the properties of their resilient layers has been identified.

The sound absorption of open cell foam has not been included in this review. Despite its importance for many acoustical applications the sound absorption of resilient layers beneath floors is not the most important property for impact sound insulation. There are many references to this subject in the literature but the absorption of sound within foams was considered to be, at best, peripheral to this research. The propagation of sound waves through the polyurethane foams of interest to this research has therefore been excluded from this study. Gudmundsson⁵⁰, whose work will be discussed later in this

thesis, attempted to measure the speed of sound propagation through mineral fibre. This was shown to be very difficult with results dependent on the nature of the sound source and the separation of the transducers (accelerometers) used in the research.

Gudmunsson concluded that it was better to use values obtained using traditional resonance methods to calculate the sound insulation of floating floors. It was felt that this was further justification for ignoring sound absorption and concentrating on the approach adopted in this research.

2.6 Conclusions

Searches of the literature showed that when flexible open cell polyurethane foams are subjected to increasing compressive stress they exhibit a clearly defined yield point after which they begin to collapse elastically. Should the yield stress for a resilient foam layer be exceeded when the floor is walked upon such a collapse is likely to be noticeable which in turn gives the impression of instability. If a floating floor does not offer sufficient stability it is unlikely to be specified no matter how good the acoustic properties. Before a foam is specified for use under a floor then its yield point should be determined.

Mathematical modelling of the static behaviour of flexible polyurethane foams is still being developed due to the complicated nature of these materials. Their behaviour under compression has been best described by empirical or semi-empirical models. An experimental approach to assessing their load bearing characteristics was therefore adopted. The method described in BS 4443 Part 1, to determine the stress-strain characteristics of the materials⁴⁶, was identified as one of the key methods for investigating the foams of interest in this research programme. It was not expected that this method would give useful information concerning the dynamic properties of the materials however.

There has been comparatively little research into the dynamic vibration isolation properties of polyurethane foams and the most successful work has been experimental in nature. Pritz is the only identified source of research into the dynamic properties of polymer foams under floating floors³³. He adopted an experimental approach to the determination of the dynamic Young's modulus and the loss factor of foams currently used under floating floors. Only Mackenzie has investigated the use of open cell

polyurethane foams in floating floors. His work has been experimental in nature but has concentrated on the acoustic performance of different systems. This research is a continuation of the work begun by Mackenzie. It seeks to relate the material properties of resilient layers to the acoustic performance of the systems in which they are incorporated. Both Pritz and Mackenzie had used an experimental approach and this was therefore the method of investigation adopted in this research.

BS EN 29052-1, Determination of dynamic stiffness - Materials used under floating floors⁵¹, was adopted for examining the dynamic properties of the foams to be studied. The literature had shown that the dynamic Young's modulus, and hence the effective dynamic stiffness, of polyurethane foam was unlikely to change significantly over the frequency range of interest to building acoustics. This method for obtaining the dynamic stiffness was therefore likely to be the best indicator of a material's suitability as an isolator under a floating floor. In addition the Method would also allow examination of the damping in the materials⁵² although, again, this was unlikely to change over the frequency range specified in BS 2750 Part 7.

This choice of testing method has recently been justified by the appearance of the Draft Standard prEN 12354-2⁵³ which specifies BS EN 29052-1 for determining the dynamic stiffness of materials used under floating floors so that impact sound insulation might be predicted.

Since no information could be found from any source on the static or dynamic properties of rebond polyurethane foam it was felt that this material in particular should be investigated in order to identify any characteristic behaviour. Any information found regarding its static or dynamic properties would be a useful contribution to understanding a material which is likely to become more widely used, as recycling techniques are improved.

The approach adopted in this research programme therefore was to use the Method described in BS 4443 to determine the stress-strain behaviour of the foams of interest in order to identify those which would give a floating floor sufficient stability. Then the dynamic stiffness of Standard specimens would be obtained according to the Method described in BS EN 29052-1. Field tests would then be carried to measure the impact

sound insulation of sections of lightweight shallow profile floating floor comprising resilient layers made from the foams studied in the laboratory.

Correlation between the impact sound insulation of the sections of floating floor and the results from the dynamic tests in the laboratory would be sought. If such correlation could be identified then a method for predicting the improvement in impact sound insulation obtained by using lightweight shallow profile floating floors of special interest to refurbishment projects could be proposed. In particular it was intended to seek a method for predicting the weighted standardised impact sound pressure level ($L'_{nT,w}$) for such floors since this is the indicator used to determine whether a separating floor meets the criterion for impact sound insulation specified in The Building Regulations Part E.

2.7 References

- 1 GIBSON L.J.; ASHBY M.F, *Cellular solids*, Pergamon, Oxford., 1988.
- 2 HOOKE R. *Micrographia*, The Royal Society, London., 1664.
- 3 CULLUM D.J., UK Patent No 14468, Improvements in the construction of floors, Filing Date 17 May 1935.
- 4 HOFBAUER G., German Patent No 714399, *Scall and warmedammende verbindung von im abstand voneinander angeordneten bauteilen*, Filing Date 17 December 1935.
- 5 FRY A. (ed), *Noise control in building services*, Sound Research Laboratories Ltd., Pergamon Press, Chapter 6, 1988.
- 6 BOATZ G., ILLGER H.W., RABE H, *Slabstock foams*, Polyurethane Handbook, 2 nd edition, Editor; Oertel G, Publ Hanser, 1993.
- 7 <http://www.pfa.org/intouch/ntouch41.txt>
- 8 Industry News, Flexible polyurethane foam is recoverable and recyclable, *J. Cellular Plastics*, 1994, Vol 30, No 2, 102-104.
- 9 SUH K.W. *Encyclopaedia of chemical technology, 4 th Edition*, Editor Kirk Othmer, 1994
- 10 COLLEY I, Virecon business manager, British Vita, Manchester, *Private communication*, 1996.
- 11 POOCH H. D. *Floor for gymnasium*, European Patent Application, No 90102959.5, Date of Registration 19 September 1990.
- 12 MURPHY R., Technical Manager, British Vita, Manchester, *Private communication*, 1995.
- 13 ISOPA-the European Isocyanate Producers' Association, *Fact sheet, isopa*; Avenue Evan Nieuwenhuysse 4; Box 9; Brussels Belgium, 1993.
- 14 HILYARD N.C, Stiffness and strength-flexible polymer foams, *Mechanics of Cellular Plastics*, Ed Hilyard N.C. Publ Applied Science Publishers Ltd. Barking, Essex, England., 1982.

-
- 15 HILYARD N.C., Hysteresis and energy loss in flexible polyurethane foams, *Low Density Cellular Plastics; Physical Basis of Behaviour*, Ed Hilyard N.C., Cunningham A., Chapman and Hall, London, 1994.
 - 16 COLLIER P., *The design and performance of non-linear vibration isolating materials*, PhD Thesis, Sheffield City Polytechnic, Sheffield, UK, 1985.
 - 17 GENT A.N., The deformation of foamed elastic materials, *Journal of Applied Polymer Science*, 1959, 1, 107-113.
 - 18 GENT A.N., Mechanics of foamed elastic materials, *Rubber Chem. Tech.*, 1963, 36, 597-610.
 - 19 RUSCH K.C., Load-compression behaviour of flexible foams, *Journal of Applied Polymer Science*, 1969, 13, 2297-2311.
 - 20 TIMOSHENKO S.P., GOODIER J.N., *Theory of elasticity, 3rd edition*, Mcgraw-Hill, New York, 1970.
 - 21 DEMENTEV A.G., TARAKANOV O.G., Effect of cellular structure on the mechanical properties of plastic foams, *Polymer Mech. USA*, 1970, 6(4), 594-602.
 - 22 DEMENTEV A.G., TARAKANOV O.G., Model analysis of the cellular structure of plastic foams of the polyurethane type, *Polymer Mech. USA*, 1970, 6(5), 744-749.
 - 23 KRAYNIK A.M., WARREN W.E., The elastic behaviour of low density cellular plastics, *Low Density Cellular Plastics; Physical Basis of Behaviour*, Ed Hilyard N.C., Cunningham A. Chapman and Hall, London, 1994.
 - 24 ABAQUS User's Manual, Version 5.2, 1992, Copyright Hibitt, Karlsson and Sorensen Inc. USA.
 - 25 SPERLING L.H., Basic viscoelastic definitions and concepts, *Sound and Vibration Damping with Polymers*, Ed Corsaro R.D., Sperling L.H., American Chemical Society, 1990
 - 26 SHESTOPAL V.O., CHILCOTT B., Vibration properties of packaging flexible urethane foams, *J Cellular Plastics*, 1988, Vol 24, 359-373.
 - 27 GEROK J., *Der versuchs und forschungsingenieur*, 1981, 4:30.
 - 28 CALCATERRA P.C., *Design guide for polyurethane foam isolation systems*, U.S. Naval Air Development Centre. 1965.

-
- 29 HILYARD N.C., LEE W.L., CUNNINGHAM A., Energy dissipation in polyurethane cushion foams and its role in dynamic ride comfort, *Proceedings Cellular Polymers International Conference*, Forum Hotel, London UK, 20-22 March, Rapra Technology, 1991.
- 30 STEVENS B.N.; SCOTT J.F.; BURCHELL D.J., A comparison of the dynamic fatigue performance of typical carpet underlayment foams, *J Cellular Plastics*, 1990, Vol 26, 19-37.
- 31 HAGER S.L.; CRAIG T.A., Fatigue testing of high performance flexible polyurethane foam, *J Cellular Plastics*, 1992, Vol 28, 284-303.
- 32 POLYURETHANE FOAM ASSOCIATION, 1993, *Intouch*, <http://www.pfa.org/intouch/ntouch41.txt>, Vol 3, No 2.
- 33 PRITZ T., Dynamic young's modulus and loss factor of plastic foams for impact sound isolation, *J Sound and Vibration*, 1994, Vol 178, 315-322.
- 34 PRITZ T., Dynamic strain of a longitudinally vibrating viscoelastic rod with an end mass, *Journal of Sound and Vibration*, 1982, 85 (2), 151-167.
- 35 PRITZ T., Frequency dependence of frame dynamic characteristics of mineral and glass wool materials, *Journal of Sound and Vibration*, 1986, 106 (1), 161-169.
- 36 PRITZ T., Non-linearity of frame dynamic characteristics of mineral and glass wool materials, *Journal of Sound and Vibration*, 1990, 136 (2), 263-274.
- 37 PRITZ T., Transfer function method for investigating the complex modulus of acoustic materials: rod like specimen, *Journal of Sound and Vibration*, 1982, 81 (3), 359-376.
- 38 VER I.L., Measurement of dynamic stiffness and loss factor of elastic mounts as a function of frequency and static load, *Noise Control Engineering*, 1974, 3 (3), 37-42.
- 39 SIM S., KIM K.J, A method to determine the complex modulus and Poisson's ratio of viscoelastic materials for fem applications, *Journal of Sound and Vibration.*, 1990, 141 (1), 71-82.
- 40 SUEYOSHI S; SCHNIEWIND A.P., Dynamic behaviour of wood strip over elastic underlayment composite flooring subjected to light impact loads, *Wood Sci. Technol.*, 1991, Vol 25, 309-318.

-
- 41 SUYEOSHI S; TONOSAKI M., Determination of localised dynamic behaviour of wood strip over foam rubber underlayment, composite flooring by random vibration, *Wood Sci. Technol.* , 1993, Vol 27, 11-21.
- 42 SUEYOSHI S.; TONOSAKI M.; ORIBE M., Localised vibration of composite wood flooring fastened to a concrete slab, *Japan Wood Research Society*, 1995, Vol 41, 31-36.
- 43 MACKENZIE, R.K. The development of a sound absorbing flooring system, 1986, *Proc IOA*, vol 8, 53-61.
- 44 BLAKE, R.E., Basic vibration theory, *Shock and vibration handbook, fourth edition*, ed. Harris C.M., 1996.
- 45 BS 4443, 1988, *British Standard Methods of Test for Flexible Cellular Materials, Parts 1-7*.
- 46 BS 4443, 1988, *British Standard Methods of Test for Flexible Cellular Materials, Part 1, Methods 5a and 5b, Determination of Compression Stress-strain Characteristics*.
- 47 MACKENZIE R.K., Upgrading of floors in refurbishment projects, *Proc. IOA*, 1993, Vol. 15, Part 15, 301-309.
- 48 VAN BUNDER T, ICI Europe Ltd, Everslaan 45, 3078 Everberg, Belgium, *private communication*, 1997.
- 49 SOFMAN M., Polyurethane Recycle and Recovery Council, Society of the Plastics Industry, 355 Lexington Avenue, 11 th Floor, New York, NY 10017, USA, *private communication*, 1996.
- 50 GUDMUNDSSON S., Sound insulation improvement of floating floors. A study of parameters, *Lund Institute of Technology, Department of Building Acoustics, Lund, Sweden*, 1984.
- 51 BS EN 29052-1: 1992, *Acoustics - determination of dynamic stiffness - materials used under floating floors in dwellings*.
- 52 CREMER L., HECKL M., UNGAR E.E., *Structure-borne sound, 2nd ed.*, Publ. Springer-Verlag , 1988.
- 53 prEN 12354-2, 1997, *Draft standard, building acoustics, estimation of acoustic performance of buildings from the performance of products, part 2: impact sound insulation between rooms*.

CHAPTER 3

STATIC BEHAVIOUR OF FLEXIBLE POLYURETHANE FOAMS

3.1 Introduction

This chapter briefly reviews the advantages of using flexible open cell polyurethane foams in lightweight shallow profile floating floors and emphasises the special usefulness of these systems for refurbishment projects. The laboratory tests carried out to determine the behaviour of virgin and rebond foams under compression are described and the results from these experiments are presented. The implications of the results for selecting polyurethane foams as resilient layers under floors are discussed and conclusions drawn regarding the relative usefulness of the different types of foam investigated.

3.2 Background

The advantages that flexible polyurethane foams have over the traditional mineral or glass fibre quilts as resilient layers were discussed in the introduction to this thesis. They often have better long term performance, they are more pleasant to handle and there are no problems associated with airborne fibres with these materials¹. For refurbishment projects they are particularly useful.

In converting large single dwellings into separate flats or improving the sound insulation of existing buildings during refurbishment it is often necessary to improve the impact sound insulation of floors. If the ceilings in rooms below cannot be lowered, because of ceiling height or the need to preserve architectural features, then the easiest way to improve a floor's acoustic performance without lifting floorboards is simply to lay a floating floor on the existing floor. Of course if it is a concrete floor which needs to be upgraded without altering the ceiling below then a floating floor is often the only option. It is desirable to keep increases in floor height to a minimum however in order to avoid unacceptably large steps up into rooms or having to increase door height. It is this need,

to minimise increases in floor height, that makes flexible polyurethane foams particularly useful.

The Building Regulations Part E state that resilient layers under floating floors made from mineral or glass wool quilts should be no less than 25 mm thick² and it is accepted that below this thickness the dynamic properties of the resilient layer are dominated by the air contained in the quilt³. A typical example of an easy to fit tongued and grooved flooring system comprising a fibre glass resilient layer was described in The Structural Engineer⁴. The resilient layer is 25 mm thick and glued to 18 mm flooring grade chipboard. Such a system raises the existing floor level by 43 mm which is often unacceptable. Indeed it has been argued⁵ that there is a need for modified specifications to the Building Regulations to accommodate the demand for systems which raise floor levels by less than 20 mm.

Floating floor systems are now commercially available comprising a 9 mm thick tongued and grooved medium density fibreboard (mdf) walking surface glued to a flexible open cell resilient layer with a thickness of 8 mm. It is such flooring systems that are of interest to this research, particularly so since the use of flexible open cell foam in floating floors is novel. Information on the performance under compression of flexible foams is obviously necessary before they can be specified for use as resilient layers. The first requirement of any floor is that it gives the required stability and the experiments described in the next section of this chapter were undertaken in order to assess the load bearing characteristics of different types of flexible polyurethane foam.

3.3 Testing method

The method adopted to assess the load bearing properties of the polyurethane foams is described in BS 4443 Method 5a⁶ which specifies the Standard Method for determining the stress-strain characteristics of flexible polyurethane foam. The stress-strain behaviour of open cell flexible polyurethane foam under compression is strongly dependent on its recent compression history, the shape of the specimen, the rate of compression and the shape of the indenter. The standard therefore specifies a number of conditioning cycles before any data are collected and also a standard specimen size, standard test speed and the shape of the platens.

Three samples of each material of interest were tested. The preferred test specimen size was used which is a right parallelepiped with square force bearing surfaces of side 100 mm and thickness 50 mm. The tests were carried out using a Hounsfield 10 KR testing machine controlled by a dedicated software package installed onto a computer. The platens were larger than the test specimens and their surfaces were smooth, but not polished, with the upper platen having a ball joint to ensure that both the surfaces were parallel. The test arrangement is illustrated in Figure 3.1.

First the two platens are moved towards each other until just touching and the ball joint is locked. This ensures that the two load bearing surfaces of the platens are parallel and there is no unwanted movement in the test system. The platens are then moved apart again. The sample is placed on the fixed lower platen and the upper platen moved towards the sample at a suitably low speed (5 mm/minute) until contact is made with the upper surface of the sample when the test begins.

The sample is strained up to 70% of its original thickness at a speed of 100 mm/minute at which point the direction of travel of the upper platen is reversed and the load is removed at the same speed of 100 mm/minute. When the upper platen returns to the position at which the test began, its direction is reversed again and another compression cycle is begun. The sample is subjected to three such conditioning cycles before the strain produced by a given compressive force is recorded on the fourth cycle.

As the work progressed the software controlling the compression testing machine was modified to give additional information. Firstly it was modified to give data for the initial curve from the first conditioning cycle as well as data from the final loading and unloading strokes. Later the software was further modified so that data from the unloading stroke of the first conditioning cycle could be recorded as well. When the data are imported into a spreadsheet it is a simple matter to convert the loads recorded to stresses which enables the production of stress-strain curves shown later in this chapter. Integration within the spreadsheet allows the calculation of the areas under the various curves which leads to the calculation of the energy dissipated per unit volume over both the first and final loading cycles as well as the energy absorbed per unit volume in the compressive deformations.

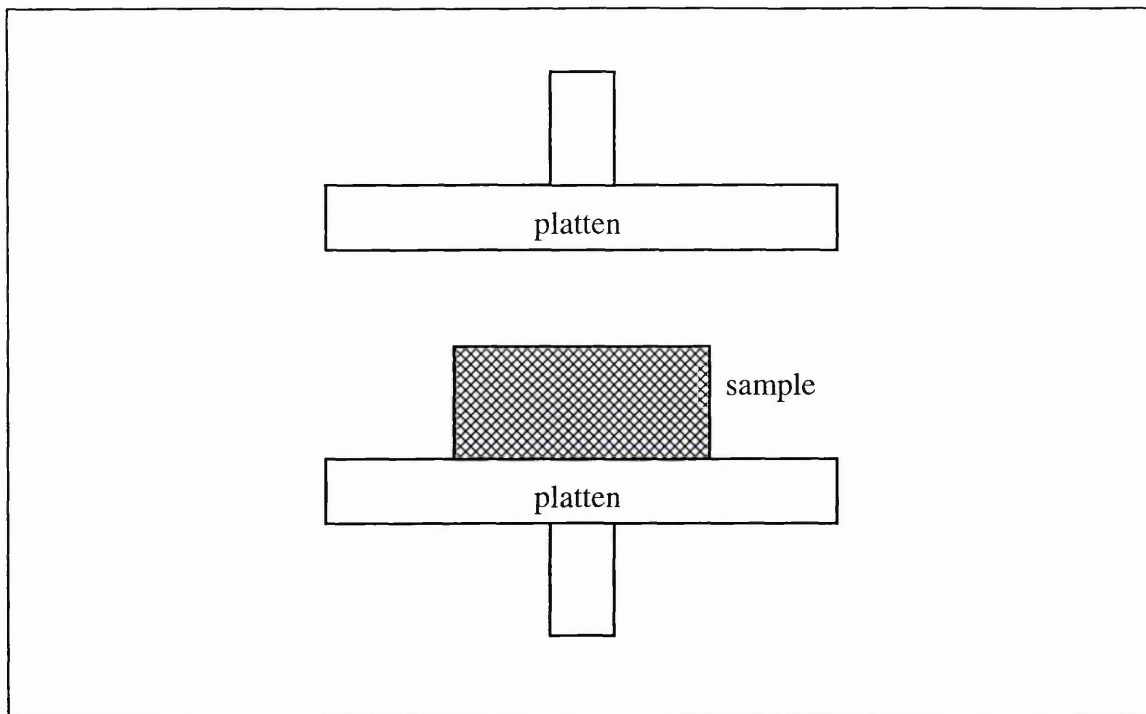


Figure 3.1: arrangement for compression tests.

Along with the other tests described in BS 4443 the method described above is primarily designed for testing the performance of cushions in furnishing. The relevance of the conditioning cycles can therefore be easily understood since sitting on a cushion usually involves relatively large strains with the compressive load applied for relatively long periods of time. Under a floating floor foam layers do not necessarily suffer this type of deformation. Furniture will impose a constant additional static load to the walking surface on the layer but, if the layer is to provide good isolation, this should not exceed the yield stress otherwise the layer will collapse and begin to behave more like a solid polymer and less like a foam.

Walking across a floor comprising a flexible foam resilient layer may cause loading in excess of the foam's yield stress but the load is usually immediately removed in a domestic situation leaving the foam to recover. It was felt, therefore, that data from the first conditioning cycle of the standard test ought to be considered when assessing the usefulness of foams as resilient layers under floors.

3.4 Results

Figure 3.2 shows stress strain curves from the final loading stroke from tests carried out as specified in BS 4443 Part 1 method 5a on four different densities of rebond foam.

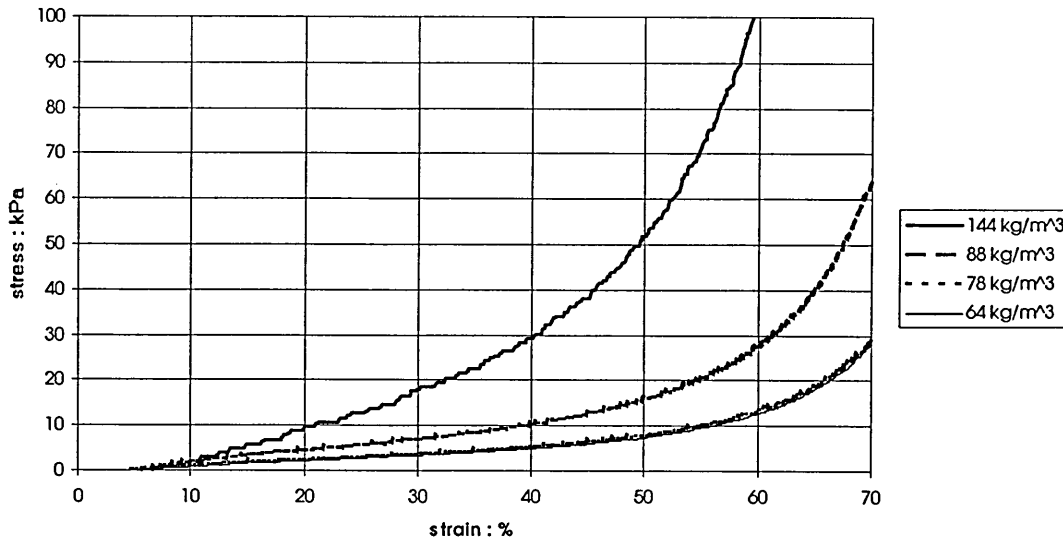


Figure 3.2: final loading curves for rebond open cell foams.

All the specimens exhibit almost linear behaviour up to strains of at least 40% after which the curves begin to rise more steeply. Higher levels of stress at given strains are seen as foam density increases. The results from tests carried out in the same manner on three different of virgin foams are shown in Figure 3.3.

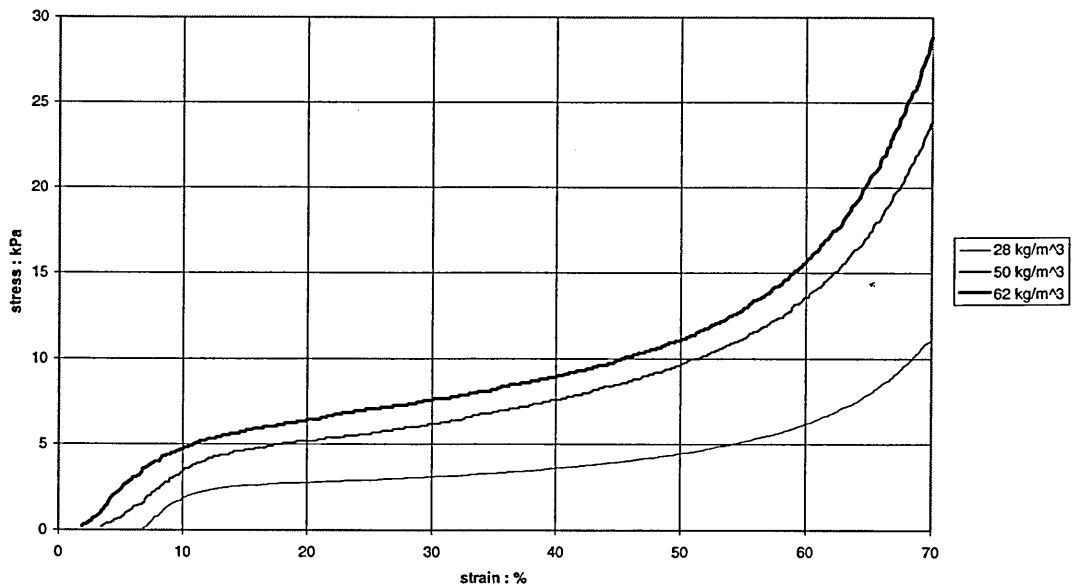


Figure 3.3: final loading curves for virgin open cell foams.

Examination of these curves clearly shows all the virgin foams have a yield point at a stress between 2 and 5 kPa followed by a more rapid increase in strain up to around 50% strain. Beyond this point, stress begins to increase rapidly as with the reconstituted foams. Results from the virgin foams again suggest that stress levels at given strains are higher in the denser foams.

The values for the Young's moduli of the foams given in Table 3.1 are taken from the gradients of the curves such as those shown in Figure 3.2 and Figure 3.3 which were produced from tests carried out according to BS 4443. For the rebond foams the modulus is defined by the gradient of the stress versus (decimal) strain curve up to 40 % strain. For the virgin foams the gradient up to the yield point (taken to be 10% strain) is used⁷.

foam density: kg/m ³	Young's modulus: kPa
64: rebond	13.0±0.2
78: rebond	13.2±0.9
88: rebond	24.4±1.7
144: rebond	93.7±4.8
28: virgin	50.4±4.7
50: virgin	56.7±4.3
62: virgin	55.7±5.7

Table 3.1: Young's modulus for the foams tested.

Figure 3.4, Figure 3.5 and Figure 3.6 show the initial loading and final unloading strokes as well as the final loading stroke for standard sized specimens of a rebond and two virgin foams having densities of 78 kg/m³, and 28 kg/m³ and 62 kg/m³ respectively. It can be seen that the low density open cell virgin foam is affected much more by the conditioning cycles in the test than the more dense foams. Its yield stress on the final loading stroke, at around 2 kPa, is less than half that on the first stroke (over 5 kPa) and the slope of the graph after the yield point is modified to a greater extent than that of the denser virgin foam.

When the yield stress is exceeded, on the first stroke, the 28 kg/m³ virgin foam continues to compress up to a strain of around 35% without any increase in stress but on the final stroke the loading curve has a slightly positive gradient after the yield point. With the two higher density foams the conditioning cycles had little effect on the shape of the loading curves although it can be seen that load bearing ability is reduced and neither foam recovers to its original thickness before the final loading stroke begins since these curves do not begin at the origin.

Examination of Figure 3.4 and Figure 3.6 shows that on both first and final loading strokes a given stress results in a greater strain in the rebond foam than in the 62 kg/m³ virgin foam for strains up to 60%. Between 60% and 70% strain the situation is reversed and at 70% strain the reconstituted foam has the higher level of stress. When the initial loading curves of Figure 3.4 and Figure 3.5 are examined it can be seen that initially the low density virgin foam is stiffer than the higher density reconstituted foam. Both the virgin foams begin to yield at roughly the same values of stress and strain on the first compression stroke.

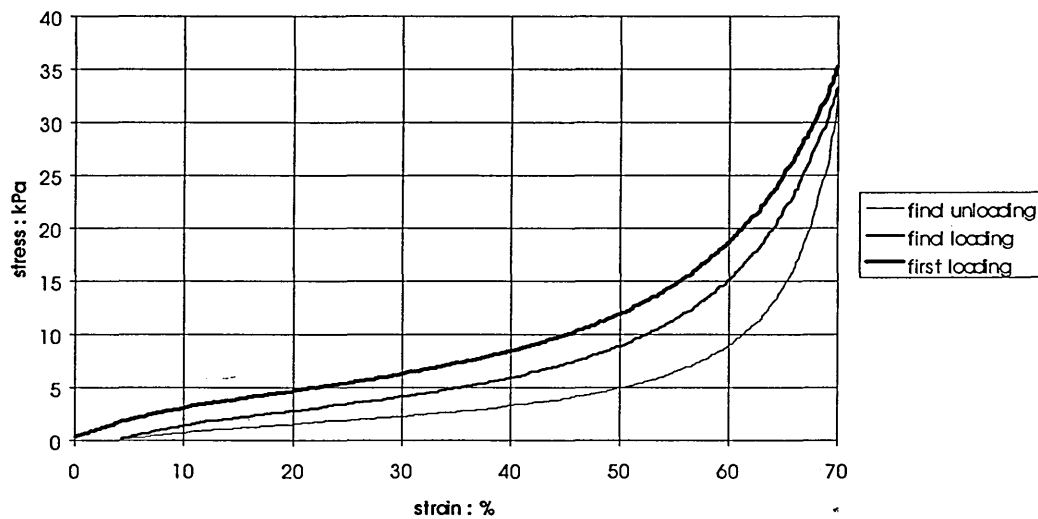


Figure 3.4: initial loading and final loading and unloading curves for rebond foam (78 kg/m³)

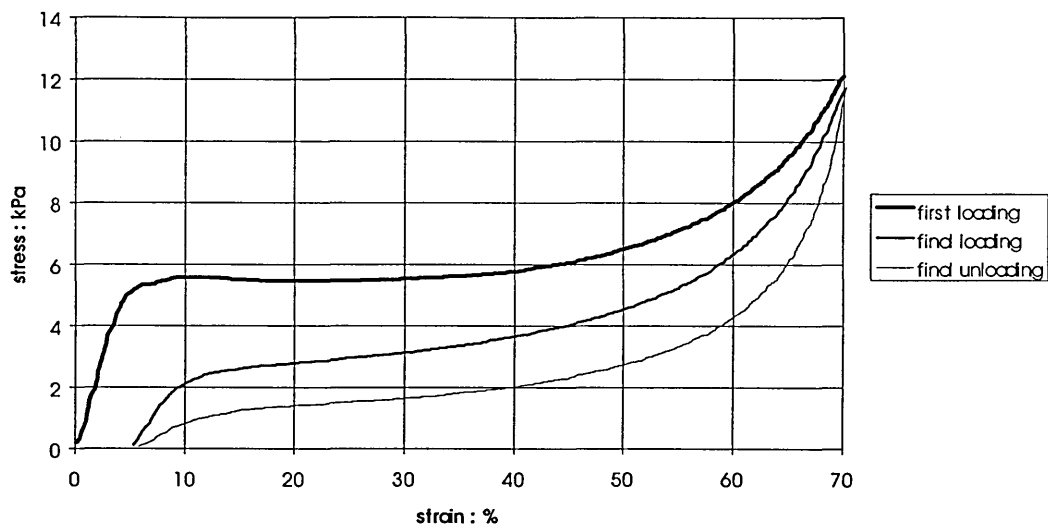


Figure 3.5: initial loading and final loading and unloading curves for virgin foam (28 kg/m³)

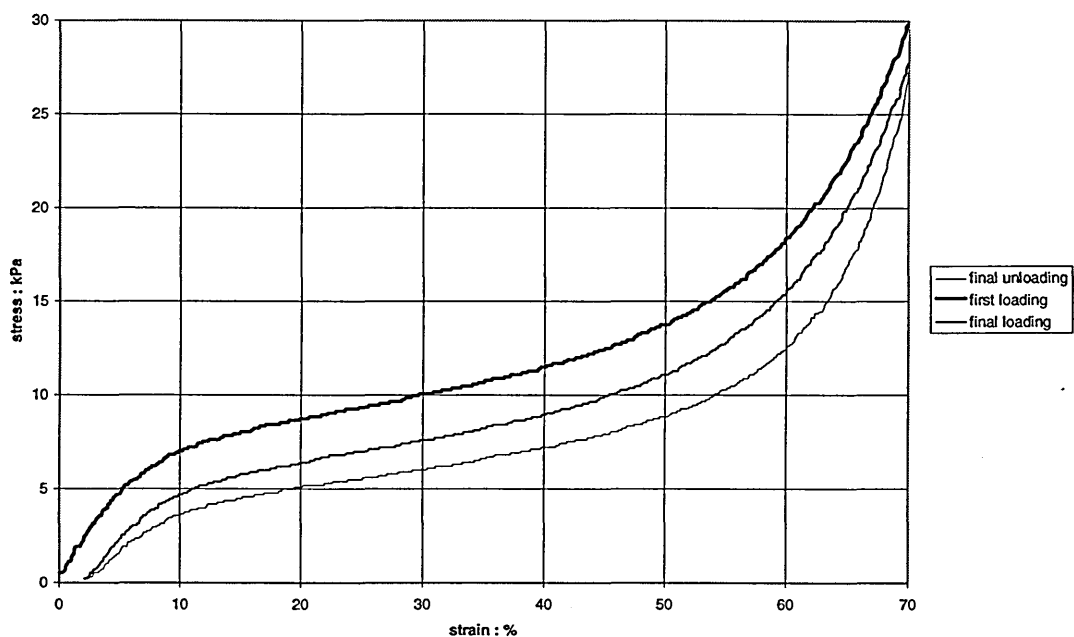


Figure 3.6: initial loading and final loading and unloading curves for virgin foam (62 kg/m³)

The difference between the Young's modulus of the foams before and after the conditioning cycles is illustrated more clearly in Table 3.2 which shows the comparison between the first and final loadings on just one specimen of each of the three foams. As in Table 3.1, the modulus for the rebond foam is taken as the gradient up to 40% strain

and for the virgin foams, the gradient up to the yield point. Clearly the 28 kg/m³ virgin foam is the most affected by the conditioning cycles.

type of foam and density: kg/m ³	Young's modulus: kPa first compression stroke	Young's modulus: kPa final compression stroke
rebond: 78	18.0	14.6
virgin: 28	113.3	45.3
virgin: 62	66.6	60.0

Table 3.2: the effect of conditioning on Young's modulus.

Table 3.3 shows the energy used in the deforming cycles shown in Figures 3.4, 3.5 and 3.6 . The areas under the first and final loading curves represent the energy absorbed per unit volume by the material on these cycles⁷. The area under the final unloading curve represents the energy stored in the foam and available to return it to its original shape after the final loading stroke, thus subtracting this value from the energy absorbed on the final stroke gives the energy dissipated on the final cycle. It can be seen that the 62 kg/m³ virgin foam absorbs most energy on both first and final compression strokes and also stores most energy on the final cycle. The reconstituted foam dissipates most energy over the final cycle and absorbs more energy than the 28 kg/m³ virgin foam on the first and final compression strokes as well as storing more energy than the lower density virgin foam after the final loading stroke.

	Energy absorbed per unit volume on first loading stroke kJ/m ³	Energy absorbed per unit volume on final loading stroke kJ/m ³	Energy stored per unit volume after final loading stroke kJ/m ³	Energy dissipated per unit volume on last cycle kJ/m ³
rebond foam 78 kg/m ³	6.9	5.2	3.3	1.9
virgin foam 28 kg/m ³	4.4	2.7	1.7	1.0
virgin foam 69 kg/m ³	8.3	6.6	5.4	1.2

Table 3.3: Energy involved in loading and unloading cycles

Figure 3.7 shows data from final loading curves of identically sized standard samples of two reconstituted and two virgin foams. The enlarged scale shows the differences in compression characteristics up to 40% strain more clearly. It is evident that the behaviour of the reconstituted foams is linear over this strain range with neither foam exhibiting the yield point which is clearly evident with both virgin foams. It is also noted that for the 62 kg/m³ virgin foam, once the yield point is passed, its curve has a similar gradient to those of the reconstituted foams.

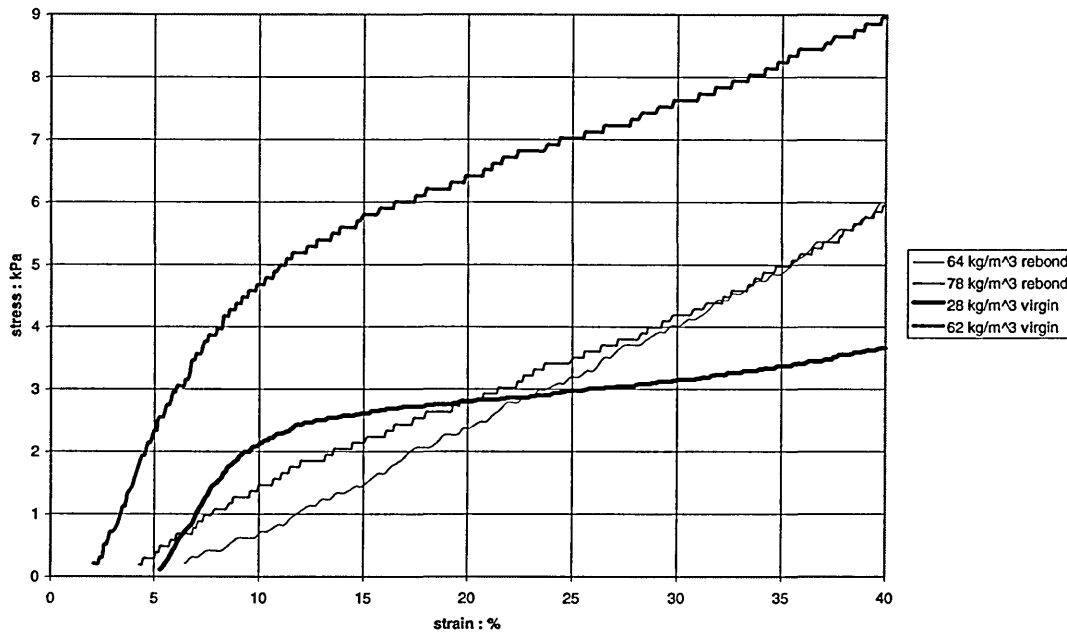


Figure 3.7: comparison of final loading strokes for reconditioned and virgin open cell foam.

Figure 3.8 shows an example of data from the first compression strokes on two standard samples of 78 kg/m³ rebond foam. One of the samples was deformed in the same direction in which the foam is compressed during its formation and the other perpendicular to this direction. Examination of the curves shows that when the foam is compressed in the perpendicular direction it is noticeably stiffer over the range of strain shown above about 4% strain. This different behaviour in the two directions is also illustrated in Figure 3.9 which shows data from a similar test carried out on a

polyurethane rebond foam of density 105 kg/m^3 which is made from scrap of the same density rather than a range of densities.

Here the difference between the curves at small strain is more marked although at 70% strain the two curves had converged. The scale was chosen for easy comparison with Figure 3.8 but the trend towards convergence at high strain can perhaps be seen from the chart. Consistent with all results from tests on reconstituted foams, no clearly defined yield point was observed with any of the samples.

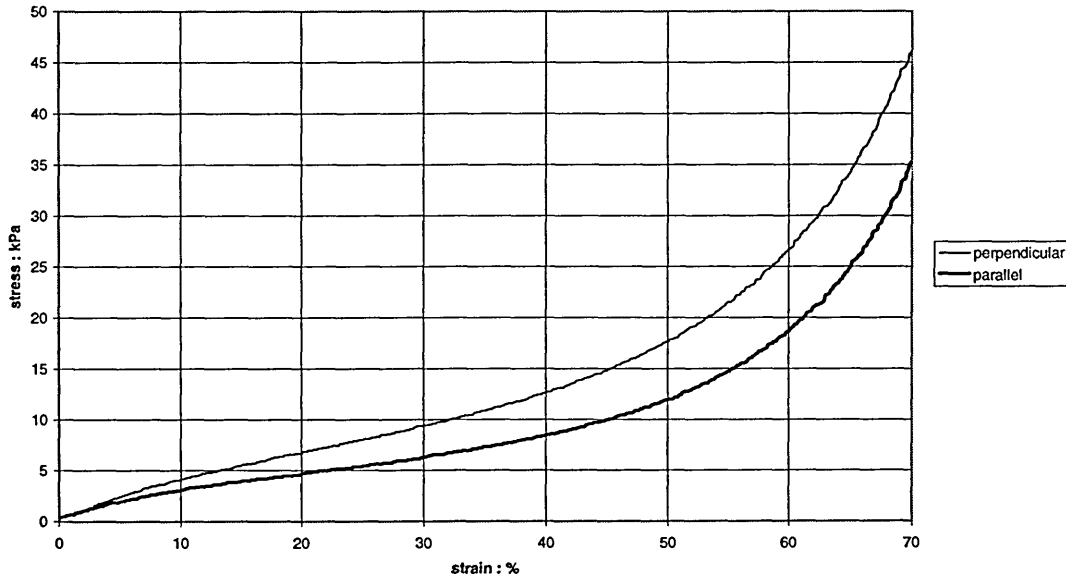


Figure 3.8: initial loading curves for 78 kg/m^3 reconstituted foam compressed parallel and perpendicular to the direction of compression in forming.

Figure 3.10 also shows the results of compressing reclaimed foam of a single density. The material compressed was loose crumb taken from a sample of the constituents from which the 78 kg/m^3 reconstituted foam is made. Crumbs of the same density were selected and placed in a square perspex mould which was placed on the lower platen of the testing machine. These were compressed in the same way as the other samples had been compressed. Data from the first and final compression cycles are illustrated. It can be seen that on neither of the compression strokes is there a yield point and that both of these curves are similar in shape to those produced from tests on the samples of reconstituted foam.

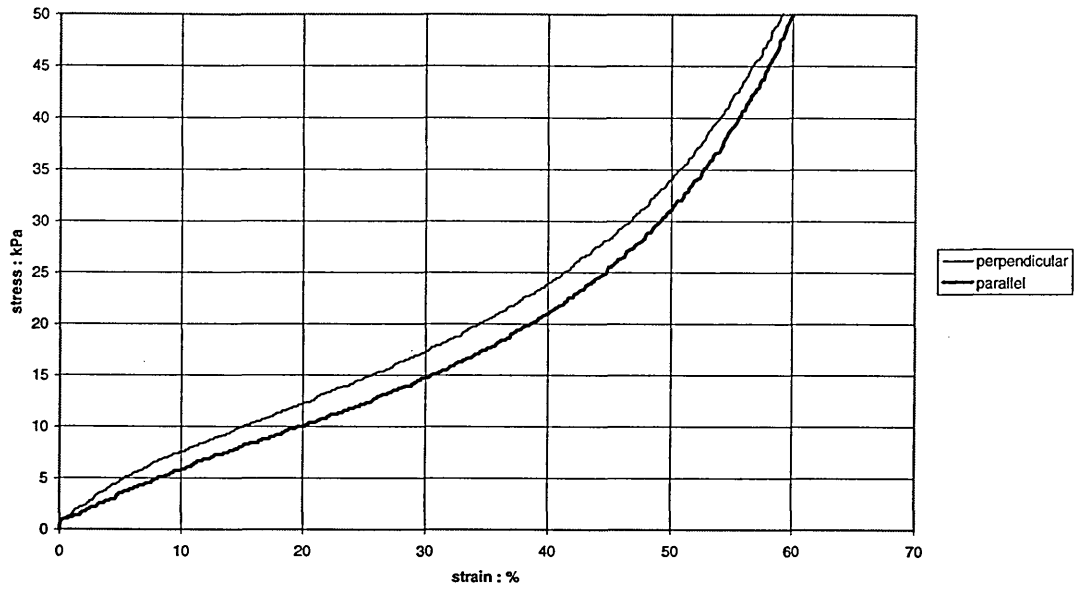


Figure 3.9: initial loading curves for single density reconstituted foam compressed parallel and perpendicular to the direction of compression in forming.

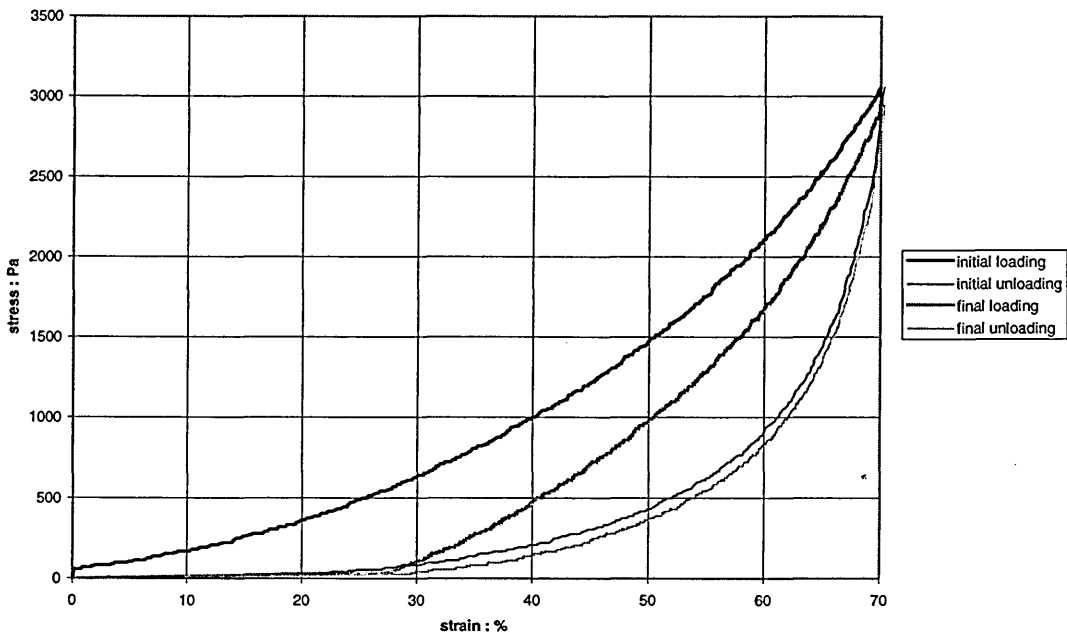


Figure 3.10: loading and unloading curves for single density polyurethane crumb.

3.5 Discussion

A lightweight shallow profile floating floor system using low density virgin open cell foam and having good impact sound insulation has been described previously⁵. The system comprises 9 mm thick tongued and grooved mdf boards to which the resilient layer is glued. Fitting such a system is relatively quick and easy since the boards are merely placed on the existing supporting floor then slotted together and glued along their joints. In order to reduce excessive movement, and therefore possible problems of fatigue, the joints are reinforced with a closed cell foam strip which deforms much less than the open cell foam under domestic loading. Despite this, noticeable deflections underfoot are still possible as the floating floor is walked on.

The relatively large and rapid deflections which may be suffered by systems comprising virgin foams are due to the characteristic behaviour of the material under compression, in particular the yield point associated with these materials. Figures 3.3, 3.5 and 3.6 show that the yield point is present on the first and final compression strokes of the Standard Test. The low density virgin foam whose behaviour is shown in Figure 3.5 is used in the flooring system described⁵ and, as Figure 3.5 shows, if the yield stress is reached by walking on the floor the resulting deflection is likely to be relatively large, rapid and therefore discernible.

Examination of Figures 3.5 and 3.6 shows that the Young's modulus of the 28 kg/m³ virgin foam is greater than that of the 62 kg/m³ foam on the first compression stroke although it is considerably more affected by the conditioning specified in the Standard Method. This is demonstrated more clearly in Table 3.2 which shows the Young's moduli for the foam specimens whose behaviour under compression is shown in Figures 3.4 to 3.6. Both the yield point and the Young's modulus of the 28 kg/m³ virgin foam are greatly reduced by the conditioning cycles.

Table 3.1 shows that the Young's moduli, and therefore the stiffnesses, of the virgin foams are very similar after the conditioning cycles although their yield stresses are very different. The values given are the mean values from tests on three different specimens and the potential error taken to be the standard deviation on the results. The potential errors in the results given in Table 3.2 were not estimated since only one specimen of

each foam was tested and the table included merely to illustrate more clearly the effect of the conditioning cycles on the specimens.

The 62 kg/m³ foam was the highest density virgin foam available and was therefore chosen for better comparison with the rebond foams. Both this and the 50 kg/m³ virgin foam are high resilience foams however and so their ability to withstand the conditioning cycles better is not surprising. Collier⁸ describes the difference in structure of conventional and high resilience foams. Conventional foams can be viewed as having cells made from beams or struts whereas the high resilience foams have cells which are more like shells having pores in these shell walls. This difference in their structure probably explains why the yield point, caused by the elastic buckling of the cell struts⁷, is more clearly defined with the conventional foam.

None of the rebond foams investigated exhibited the yield point characteristic of virgin open cell foams. In addition the Young's moduli for the 64 and 78 kg/m³ rebond foams were much less affected by the conditioning cycles of the Standard Test Method than the conventional low density virgin foam. The Young's modulus for the 64 kg/m³ rebond foam was reduced from 22.1 to 17.0 kPa by the conditioning cycles and as Table 2 shows the reduction in the modulus was only 3.4 kPa with the 78 kg/m³ rebond foam. This means that short term fatigue leading to softening in a rebond foam resilient layer is unlikely to be noticed by anyone walking on a floor comprising such material. The absence of a yield point also ensures that noticeable deflections of the walking surface are unlikely despite the fact that these two rebond foams are softer than all the virgin foams before their yield point.

A material's ability to recover to its original thickness after compression is an important consideration when it is being considered for use under floors. In terms of the energy available to accomplish this, Table 3.3 shows that the rebond foam is much better than the low density virgin foam. Amendment number 1 (1992) to BS 3379⁹ however, states that rebond foam has a poorer compression set than virgin foams although it has good fatigue performance. The Standard Method¹⁰ for determining compression set requires compressing the materials by 75% of their thickness for 72 hours at room temperature. Resilient layers under floors should not be subjected to such high strains for such times however and so this Standard will not necessarily provide useful information for

assessing foams for use under floors. Indeed Metzen¹¹ argues that subjecting expanded polystyrene to unrealistic loads prior to testing according to BS EN 29052-1 leads to underestimation of the material's dynamic stiffness when installed under a floor. Compression set was therefore not measured according to the Standard Method.

Table 3.3 also shows that the rebond foam dissipated more energy on the last loading and unloading cycle than the virgin foams. This greater hysteresis may mean that the rebond foam is the most highly damped and this aspect will be discussed further in Chapter 4 where the results from dynamic tests on these materials are described. The approach which yields the information given in Table 3.3 is probably more useful for assessing the suitability of foams for packaging than supporting floors however. For assessing suitability for use as a resilient layer, the most relevant information can be deduced from the gradients of the stress-strain curves without the need for integration. Integration does assist in the comparison of the different types of foam however which is a major aim of this chapter.

For clarity Figures 3.8 and 3.9 only show data from the first loading strokes from compression tests on two different reconstituted polyurethane foams. In both these figures, compressions in the direction of forming compression and at 90° to this direction are shown. It can be seen that the materials are stiffer perpendicular to the direction of forming compression. This is potentially significant for flooring systems using reconstituted polyurethane foam as a resilient layer since the acoustic properties may well be affected if the required thickness of foam is cut from the original block in different directions.

Searches of the Rubber and Plastics Research Association's (Rapra Technology Ltd) data base, the largest in the world on these materials, have failed to identify any references to the stress-strain characteristics of reconstituted polyurethane foams. Communications with the manufacturers of the reconstituted foams tested^{12,13}, ICI Polyurethanes (Europe)¹⁴ and the Polyurethane Recycle and Recovery Council (PURRC) USA¹⁵ have also failed to turn up any references to the behaviour under compression of reconstituted polyurethane foam. The only identified reference¹⁶ to this behaviour has resulted from this research. In particular no reference to the anisotropy exhibited by these materials has been found.

According to the manufacturers of the reconstituted foams tested, the foam whose loading curves are shown in Figure 3.9 is made from scrap foam having just one density. This is mostly by accident since the important characteristic as far as they and their customer are concerned is the colour of the finished products and it so happens that foam scrap of the required colour comes from a single density of slabstock foam. The 78 kg/m^3 foam by contrast contains a range of different densities¹² from 20 to 60 kg/m^3 . The single density foam was investigated in order to determine whether the stress-strain characteristics of the material were due to the fact that different densities of foam were present in the material or whether it was due to the recycling and reforming process.

Figure 3.9 suggests that the absence of a clearly defined yield stress is not caused by the range of different densities of scrap foam since there is no identifiable yield point in the curve. This is supported by the curves shown in Figure 3.10 which are plotted from data generated by compressing the loose crumb, of just one density, which goes to make the 78 kg/m^3 reconstituted foam. There is a large compression set shown in this Figure which is to be expected since the first stroke will remove many of the large voids left between the crumbs before it begins to crush the foam itself. The final loading stroke, however, has roughly the shape observed from 30% strain onwards in Figure 3.9 with no hint of any yield point.

The absence of a yield point with reconstituted polyurethane foam is possibly due to the fact the individual constituent chips, or crumbs, making up the material yield at different strains. Virgin foam is stiffer in its rise direction and after mixing and forming, the direction of greatest stiffness of the chips will be oriented at random. In addition to this, the forming process is likely to mean that some chips are pre-strained more than others in the finished material. This, especially when there are different densities of foam in the material, is likely to lead to chips yielding at different strains. The interactions between the chips are likely to be very complicated and a realistic model of the behaviour of reconstituted polyurethane foam is beyond the scope of this research but it is felt that the different yield points might well disguise a single yield point as laminating a panel can disguise a single resonance.

The behaviour described of reconstituted foams may well mean they offer advantages for other applications. In packaging or car headrests the foam used has to absorb a certain amount of energy whilst providing a rate of deceleration that will not damage the object it is there to protect. Virgin foams are typically initially stiffer than reconstituted foams and then they collapse much more rapidly up to the onset of densification. A material which deforms at a constant rate and has a constant stiffness up to the point of densification is likely to provide a more controlled and satisfactory deceleration. It is felt therefore that these materials are worthy of further research and that the description of their stress-strain characteristics is a useful initial contribution to this work.

3.6 Conclusions

Any resilient layer used under a floating floor must provide acceptable stability for those walking upon it in addition to providing isolation from the supporting floor and therefore impact sound insulation for rooms beneath the floor. Despite the Standard Method for obtaining the stress-strain behaviour of polyurethane foams being designed for assessing materials used for cushioning or packaging it provides useful information on their suitability for use under floors. By modifying the Standard Method to obtain data from the first compression cycle as well as the last, the Method becomes much more useful for assessing foams for use under floors. The modification also gives some information regarding the short term fatigue behaviour of the materials.

The yield point associated with all virgin polyurethane foams is not a useful characteristic for a layer used as an isolator under a floating surface. Exceeding the yield stress for a foam is undesirable since it leads to a rapid collapse of the material. The characteristic behaviour of rebond polyurethane foam suggests that, from the viewpoint of providing good support for a walking surface, it is better than virgin foam. At small strains it is softer than much less dense virgin foam as well as virgin foam of comparable density and its stiffness is constant up to 40% strain.

The static tests described in this chapter suggest that from a structural viewpoint therefore rebond foam is better suited as a resilient layer under a floating floor than virgin open cell foam. Subsequent chapters will discuss whether the material is likely to provide better isolation, and therefore better impact sound insulation, than virgin foam.

3.7 References

- 1 MACKENZIE R.K., Development of a sound absorbing flooring system, *Proc. IOA*, 1986, Vol. 8, 53-61.
- 2 DEPARTMENT OF THE ENVIRONMENT AND THE WELSH OFFICE, *Approved document E, resistance to the passage of sound*, 1991.
- 3 JOHANSSON C., ANGREN A., Development of a lightweight wooden joist floor, *Applied Acoustics*, 1994, 43, 67-79.
- 4 ACOUSTIC INSULATION, *The Structural Engineer*, 1996, Vol. 74 No 18, 17 September.
- 5 MACKENZIE R.K., Upgrading of floors in refurbishment projects, *Proc. IOA*, 1993, Vol. 15, Part 8, 301-308.
- 6 BS 4443, 1988, *British Standard Methods of test for flexible cellular materials, part 1, Methods 5a and 5b, Determination of compression stress-strain characteristics*.
- 7 GIBSON L.J.; ASHBY M.F, *Cellular solids*, Pergamon, Oxford, 1988.
- 8 COLLIER P., *The design and performance of non-linear vibration isolating materials*, PhD Thesis, Sheffield City Polytechnic, Sheffield, UK, 1985.
- 9 BS 3379, 1991, *Specification for flexible polyurethane cellular materials for load bearing applications*.
- 10 BS 4443, 1988 *British Standard Methods of test for flexible cellular materials, part 1, methods 6a and 6b, determination of compression set*.
- 11 METZEN H.A., Effect of pre-load on the dynamic stiffness of impact insulation materials and on the predicted impact sound insulation, *Proceedings of Internoise 96*, 1996, 1807-1810.
- 12 Private communication, Colley I., 1996, Virecon Business Manager, Soudan Street, Middleton, Manchester, M24 2DB.
- 13 Private communication with Rowland Murphy, 1996, Vitafoam, Technical Manager, Soudan Street, Middleton, Manchester, M24 2DB.
- 14 Private communication with Thomas Van Bunder, ICI Europe Ltd. Everslaan 45, 3078 Everberg, Belgium.

-
- 15 Private communication with M. Sofman, PolyUrethanes Recycle and Recovery Council, Society of the Plastics Industry, 355 Lexington Avenue, 11th Floor New York, NY 10017.
 - 16 HALL R, MACKENZIE R.K., Reconstituted versus virgin open cell foams in floating floors, *Building Acoustics*, 1995, Vol. 2, No. 2, 419-436.

CHAPTER 4

DYNAMIC BEHAVIOUR OF FLEXIBLE POLYURETHANE FOAM

4.1 Introduction

The results from the static tests described in the previous chapter showed that the characteristic behaviour of rebond foam makes it more suitable for providing support to a floating floor than virgin foam. The results also showed that at small strains rebond foam is softer than virgin foam. The literature had highlighted the importance of the dynamic stiffness of the resilient layers in floating floors on their acoustic performance. It had also shown that correlation between the static stiffness and the dynamic stiffness of these materials was unlikely to be found. The dynamic stiffness of the polyurethane foams of interest would have to be measured therefore.

This chapter describes the laboratory measurements of the dynamic stiffness of virgin and rebond foam specimens as well as the damping present in the various systems. The results from the measurements are discussed and the two types of material are compared. Finally the relationship between the dynamic stiffness of laboratory specimens and of resilient layers under floating floors is discussed. In order to relate the dynamic stiffness of resilient layers to that of test specimens of the layers the airflow resistivity of the materials must be measured. The airflow resistivity measurements are discussed in Chapter 5.

4.2 Background

When lossless, linear isolators, such as springs, are used to isolate a machine from a floor the degree of useful isolation provided can be estimated from static tests. In this situation if a mass (M) supported by a spring is acted on by a linear force then the force transmissibility (T_F) is given by¹

$$|T_F| = \frac{1}{1 - \left(\frac{f}{f_n}\right)^2}$$

Equation 4.1

where f = forcing frequency, Hz

f_n = natural frequency for the system given by¹

$$f_n = \frac{1}{2\pi} \sqrt{\frac{S}{M}} \text{ Hz}$$

Equation 4.2

where S = spring stiffness, N/m

M = mass, kg

When f is greater than $\sqrt{2}f_n$ then useful isolation is provided².

For a spring of stiffness, S , the deflection, Δ , caused by a mass, M , is given by

$$\Delta = \frac{Mg}{S} \text{ m}$$

Equation 4.3

where: g = acceleration due to gravity.

Substituting Equation 4.3 into Equation 4.2 leads to the following result:

$$f_n = \frac{1}{2\pi} \sqrt{\frac{g}{\Delta}} \text{ Hz}$$

Equation 4.4

The only variable on the right hand side of Equation 4.4 is the deflection (Δ) which means that f_n , and hence the onset of useful isolation, can be found simply by measuring the deflection caused by a static load. This is not the case with flexible open cell polyurethane foams however.

The literature showed that the impact sound insulation of floating floors depends primarily on the dynamic stiffness of their resilient layers. The literature also showed that nearly all researchers had found that the dynamic Young's modulus, and therefore the dynamic stiffness, of polyurethane foams cannot be determined from their static behaviour under compression^{3,4}. Recently Stewart⁵, who measured the dynamic

stiffnesses of closed cell polyurethane foam and other resilient materials, came to the same conclusion.

Stewart found the dynamic stiffnesses to be larger than the measured static stiffnesses by ratios varying from 1.3 to 7.7. The only proposed method identified for relating the static stress-strain behaviour of polyurethane foams to their dynamic stiffness^{6,7} is unsuitable for resilient layers under floors because measurements of the small deflections of the resilient layers desirable for good stability would render the method inaccurate. The dynamic stiffness of the polyurethane foams of interest had to be measured therefore.

Various methods for determining the dynamic stiffness of flexible polyurethane foams were discussed in Chapter 2 but it was concluded that the Method described in BS EN 29052-1⁸ should be adopted. This Method was chosen because it is the only current Standard Method identified for determining the dynamic stiffness of resilient layers under floors used throughout Europe. The Method is simple and monitoring the system response around the fundamental vertical resonance frequency allows measurement of the damping in the different test systems⁹.

BS EN 29052-1 only refers to damping because high levels may make the identification of the resonant frequency difficult from observation of the system's response amplitude: it is only the frequency of resonance that is important in the Method⁸. In highly damped systems the Standard⁸ recommends monitoring the input-output phase difference in order to identify the resonant frequency. The damping offered by the resilient layers is important however since this is the mechanism which controls the response of a floating floor at its resonant frequency. It has been established that adding resilience can reduce the impact sound insulation of floors around the resonant frequency^{10,11} due to increases in the amplitude of vibration. Increased damping may reduce the amplitude of the floating floor but it may also increase the force transmitted through the resilient layer to the supporting floor¹². Whether or not damping is useful in resilient layers under floors was not clear but might become more so as the research progressed. The damping in the systems was investigated therefore.

4.2.1 BS EN 29052-1

BS EN 29052-1 defines dynamic stiffness as the ratio of dynamic force to dynamic displacement. It identifies the fundamental vertical vibration of a standard mass-spring test system and uses this to calculate the apparent dynamic stiffness of the test specimen per unit area using the relationship:

$$f_r = \frac{1}{2\pi} \sqrt{\frac{S_{\text{dyn}}}{m_a}} \text{ Hz}$$

Equation 4.5

where f_r = the resonant frequency of the test system Hz

S_{dyn} = the apparent dynamic stiffness per unit area of the test specimen N/m^3

m_a = the total mass per unit area used during the test kg/m^2

In this method, it is assumed that the resilient specimen acts as a spring which supports the specified mass. The specimen stiffness is determined by rearranging Equation 4.5 and is then related to the stiffness of the resilient layer.

4.2.2 Resonant frequency

The peak values of the acceleration, velocity and displacement for a system subjected to forced vibration occur at slightly different frequencies^{12,13}. In systems with the usual, small, amount of damping the differences between the resonant frequencies is insignificant but with highly damped systems this may not be the case. The resonant frequencies are given by¹²

$$\text{displacement resonant frequency} = \frac{f_n}{\sqrt{1-2\zeta^2}} \text{ Hz}$$

Equation 4.6

$$\text{velocity resonant frequency} = f_n \text{ Hz}$$

Equation 4.7

$$\text{acceleration resonant frequency} = \frac{f_n}{\sqrt{1-2\zeta^2}} \text{ Hz}$$

Equation 4.8

$$\text{damped resonant frequency} = \frac{f_n}{\sqrt{1-\zeta^2}} \text{ Hz}$$

Equation 4.9

f_n = the undamped natural frequency of the system (Hz).

ζ = the damping ratio (or the fraction of critical damping¹²)

It has been demonstrated that systems comprising resilient layers of polyurethane foam exhibit viscous damping¹⁴. The phase angle between the response displacement and the excitation force of a single degree of freedom system with viscous damping excited by a force acting on the mass of the system is equal to 90° at the resonance frequency¹². The phase angle between the acceleration response and the excitation force of such a system is 180° different to this frequency which meant that the resonant frequency for the test system could be identified from the input-output phase difference.

In this thesis the frequency at which the input-output phase difference passed through -90° is taken to be the resonant frequency. Any difference between the frequencies of maximum response amplitude and -90° input-output phase shift is used to assist in estimating the potential error in the determination of the resonant frequency. This approach is justified because even with high levels of damping there can be confidence that the system's resonant frequency lies between the frequencies of 90° phase difference ± the frequency of maximum response amplitude. The approach would certainly give a better idea of the accuracy of the resonant frequency's determination than the resolution of the analyser which was ± 0.5 Hz over the test frequency range and could therefore only underestimate any uncertainty.

4.2.3 Damping

The damping in the test systems was obtained using the method adopted by Sueyoshi and Tonosaki¹⁵ who compared the damping in the systems they investigated by measuring their different damping ratios (ζ) which are defined as^{12,16}:

$$\zeta = \frac{\Delta f}{2f_r}$$

Equation 4.10

f_r = the resonant frequency of the system

Δf = the bandwidth between the frequencies corresponding to those values of mechanical impedance equal to:

$$\sqrt{2} \times (\text{minimum value of mechanical impedance}) \text{ Hz.}$$

Now the transfer acceleration and dynamic stiffness for the systems investigated are defined by Kurze¹⁷ as

$$\text{accelerance} = \frac{\text{output acceleration}}{\text{input force}} \text{ m / (Ns}^2\text{)}$$

Equation 4.11

$$\text{dynamic stiffness} = \frac{\omega^2}{|\text{accelerance}|} \text{ N / m}$$

Equation 4.12

ω = the radian frequency = $2\pi f$ where f is the frequency in Hz

Sueyoshi and Tonosaki¹⁵ cite Harris¹⁸ and define dynamic stiffness and dynamic mechanical impedance of the excitation point as

$$\text{dynamic stiffness} = \frac{\text{Force}}{\text{displacement}}$$

Equation 4.13

$$\text{mechanical impedance} = \frac{\text{Force}}{\text{velocity}}$$

Equation 4.14

$$\text{apparent mass} = \frac{\text{Force}}{\text{acceleration}}$$

Equation 4.15

The magnitude of the mechanical impedance and the dynamic stiffness can be obtained by integrating the reciprocal of the acceleration with respect to time once and twice respectively. This is the same as multiplying the reciprocal of the acceleration¹⁹ by ω and ω^2 , as shown by Equation 4.12, which can be carried out in a spreadsheet or by the analyser used in the tests. For ease, in this investigation the mechanical impedance was obtained using a spreadsheet having previously ascertained that this treatment gave the same results as using the analyser to do the integration. The damping in the different test systems was compared by monitoring their loss factors (η) given by^{9,12,16}:

$$\eta = 2\zeta$$

Equation 4.16

and ζ is defined as before.

The method for determining the damping in the different foam specimens described above has the advantage of simplicity and can be derived from the data used to produce the figures illustrated later in this chapter. Unfortunately when two resonances occur close together they cannot always be detected with this method²⁰. In such circumstances the method of Kennedy and Pancu is accepted as being the most accurate way of determining the damping in different systems^{20,21}. The method has greater accuracy because it makes use of the rapid change in phase between input and output around a resonance which is ignored in Sueyoshi's approach. This, more accurate method, was used to confirm that the more simple method described earlier gave acceptably accurate results.

Figure 4.1 illustrates Zaveri's construction²¹ for determining the loss factor using Kennedy and Pancu's approach. First, the real and the imaginary parts of the system's response to the excitation are plotted on mutually perpendicular axes. The best circle is then drawn through the data points that are the most widely spaced. In Figure 4.1 the

most widely spaced points are illustrated at frequencies ω_1 and ω_2 . Equidistant between these two points is ω_0 , the resonant frequency. α is the angle enclosed by the radii from the centre of the circle (or arc) to ω_1 and ω_2 . The loss factor is given by²¹:

$$\eta = \frac{2(\omega_2 - \omega_1)}{\omega_0 \tan(\alpha/2)}$$

Equation 4.17

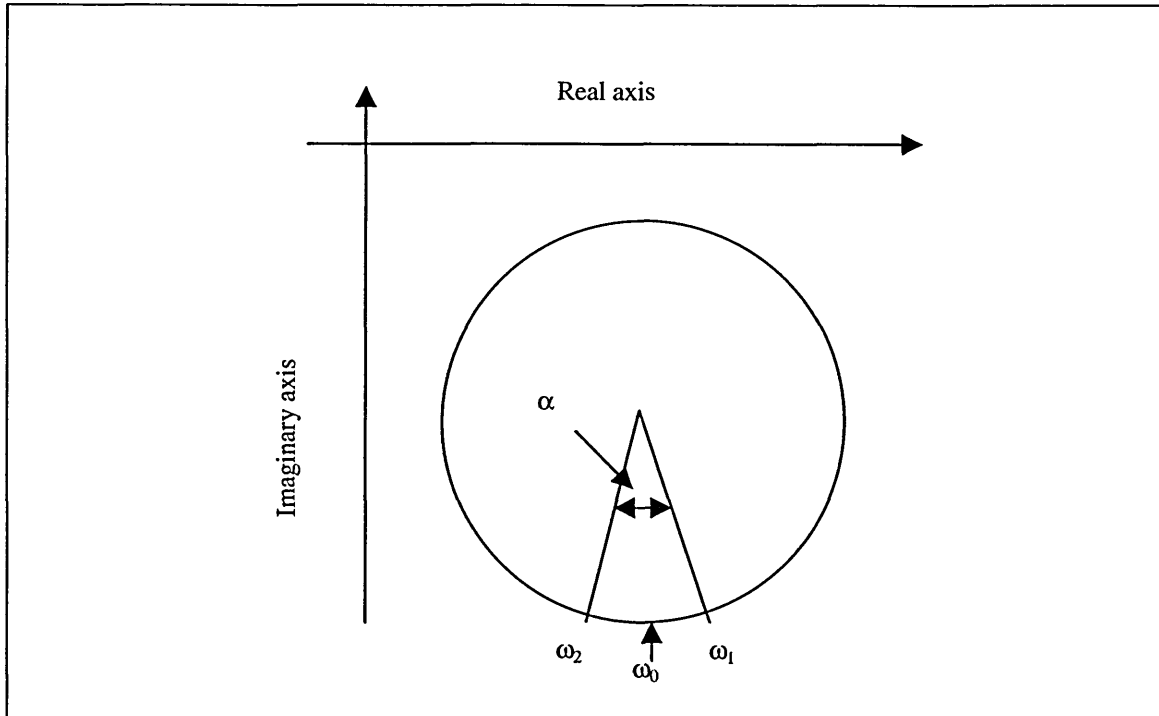


Figure 4.1: Kennedy and Pancu method for damping

4.3 Test method

4.3.1 Calibration

The force transducer and the accelerometer were calibrated before testing was begun. The accelerometer used in the tests was a B&K 4393 delta shear accelerometer which was calibrated using a B&K 1606 vibration pick up pre-amplifier with a built in shaker table. The accelerometer was screwed onto the shaker table and the table vibrated. In the drive system to the shaker table is a ball which begins to rattle when its peak acceleration equal to that due to gravity. By monitoring the output of the accelerometer with an oscilloscope, the point at which the vibration begins can be detected and at this point the acceleration of the plate will be equal to that due to gravity.

When the accelerometer had been calibrated, the force transducer was calibrated using a steel block of known mass suspended beneath a table. The system was excited with the Ling model 200 shaker used for the measurement of dynamic stiffness. The situation is illustrated in Figure 4.2.

The force transducer was placed between the block and the shaker. It was fastened to the block by a grub screw and excited using a stinger of length 127 mm made from 1.08 mm diameter piano wire. The, now calibrated, accelerometer was placed on the opposite face of the block and the input force and output acceleration were monitored as the frequency of the exciting signal was slowly swept between 5 and 100 Hz. Newton's second law (Force = mass \times acceleration) was then used to confirm the calibration of the force transducer by dividing the exciting force by the resulting acceleration. The relevant calibration curves are given in section 4.4 of this chapter.

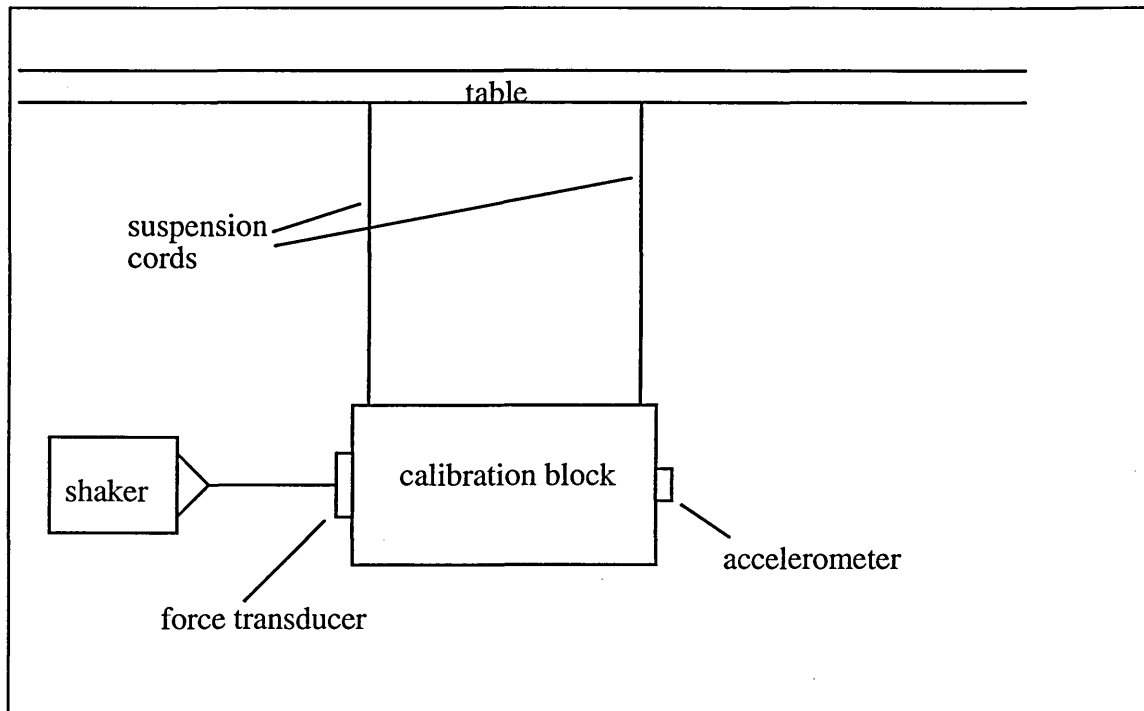


Figure 4.2: force transducer calibration

4.3.2 Laboratory experiments

The equipment and the experimental set-up used for the dynamic tests according to BS EN 29052-1 are illustrated in Figure 4.3. The load plate is a steel parallelepiped with top and bottom surfaces (200 ± 3) mm \times (200 ± 3) mm, as specified in the Standard, and

the load bearing surfaces of the samples used were also cut to this size. The total mass supported by the specimen in these tests, including transducers, was 7.53 kg. The resonant frequency of the systems was obtained by slowly sweeping a sine wave signal with constant amplitude over a frequency range sufficiently large to be able to observe the fundamental vertical resonance peak. The stinger used in the calibration of the force transducer was used to connect the shaker and the force transducer.

BS EN 29052-1 states that if the resonant frequency depends on the amplitude of the excitation force, the dependence should be determined and the resonant frequency found by extrapolation down to zero force amplitude. Investigation of the dependence amplitude on force was therefore carried out for the materials tested.

There is one deviation from the Method described in the Standard which is that the specified plaster of Paris layer between the sample and the load plate was not used. The purpose of this layer is to ensure that, with samples having an uneven load bearing surface such as those cut from rockwool slabs, the whole of the sample is excited during the test. It is important that the plaster of Paris has time to cure fully²², which takes 24 hours at normal temperatures, and had such a layer been used it would have slowed down testing considerably.

Since the virgin foam samples had smooth surfaces it was suspected that the layer was unnecessary for these samples. Experiments with different foams were undertaken to confirm this: such tests were also conducted on rebond foams. A set of results from tests conducted on a rebond foam is given in Section 4.4. A rebond foam was chosen as the example because such foams have surfaces with greater irregularities than the virgin foams. A rebond foam is therefore more likely to show the need for the plaster of Paris layer should this be the case.

The specimens were placed on the steel block, as shown, and the system excited by feeding a slowly swept sine wave of constant amplitude to the shaker from the dual channel analyser. The analyser was also used to monitor the output from the accelerometer and the force transducer. Three specimens of each material were tested as specified in the Standard. The steel block on which the samples were placed was machined flat and was used so that a dial gauge on a magnetic base could be fixed to it

in order to measure the thickness of the specimens according to the method described in BS 4443²³ before testing. It was then hoped to be able to measure accurately the thickness of the specimens under the load plate.

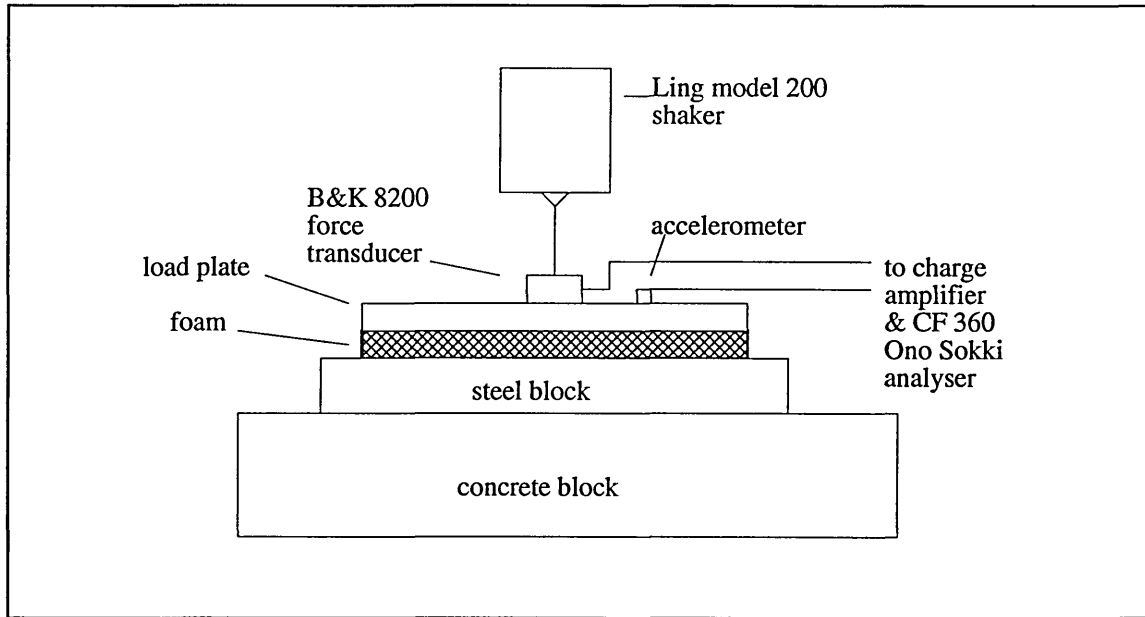


Figure 4.3: apparatus for measuring resonant frequency.

Tests were carried out on the materials whose static performance under compression was described in Chapter 3. After the initial results from relatively thin specimens had been analysed, experiments were conducted to observe the effect of increasing sample thickness on the stiffness of the specimens and the damping in the system.

4.4 Results

Figure 4.4 shows the calibration curve for the accelerometer obtained using the built in shaker of the vibration pick up pre-amplifier at the point where the ball in the drive to the shaker table just begins to shake. The curve represents the output signal from the accelerometer and the onset of vibration is confirmed by the distortion in the sine wave on the negative going slope. This corresponds to the acceleration of the table being equal to the acceleration due to gravity²⁴, 9.81 m/s^2 . It can be seen that the amplitude is 0.98 V where $1 \text{ V} \equiv 10 \text{ m/s}^2$.

Figure 4.5 shows the calibration curve for the force transducer up to 100 Hz. The curve shows the resultant from dividing the input force by the resultant acceleration. It can be seen that, apart from the distortion below 30 Hz, the curve remains at a constant level equivalent to the total mass of the block, including force transducer and accelerometer, 14.57 kg.

Examples of the results from a series of tests to determine whether the plaster of Paris layer specified in BS EN 29052-1 is necessary when polyurethane samples are tested are shown in 4.5 and Figure 4.7. Figure 4.6 shows three curves from data obtained from tests on the same sample of reconstituted foam tested with and without plaster of Paris and finally without the plaster but with an equivalent amount of weight added to the load plate. It can be seen that the three curves shown are not identical but the first peak occurs at the same frequency for each sample. Figure 4.7 demonstrates that with all the three curves the input-output phase difference passed through 90° at the same frequency. All the curves showing the input-output phase difference have been multiplied by -1 to give positive going curves instead of negative going curves. This format is used throughout this thesis and henceforth the negative sign of the phase difference at resonance will be ignored.

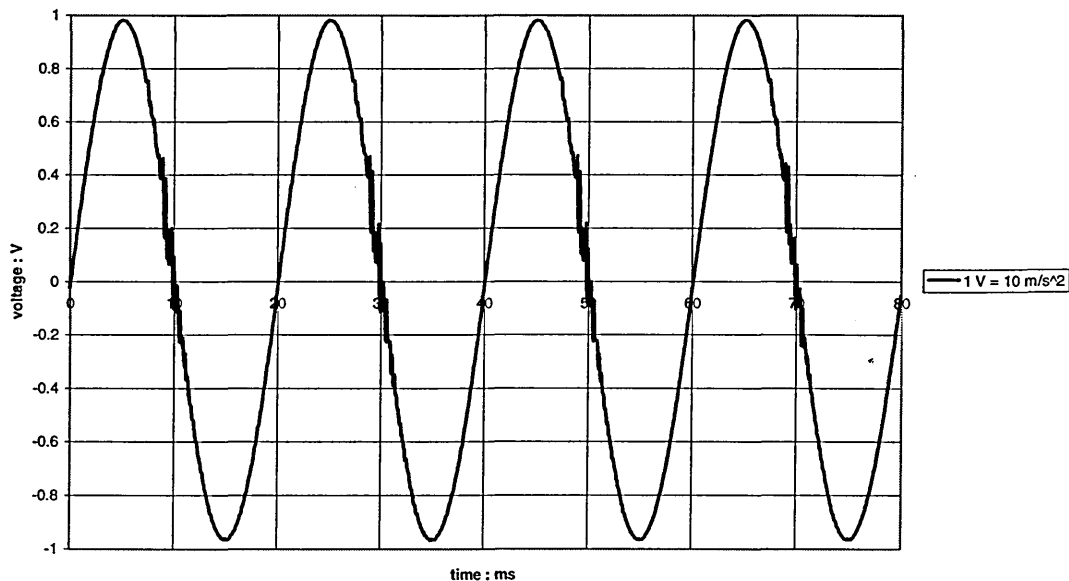


Figure 4.4: accelerometer calibration curve

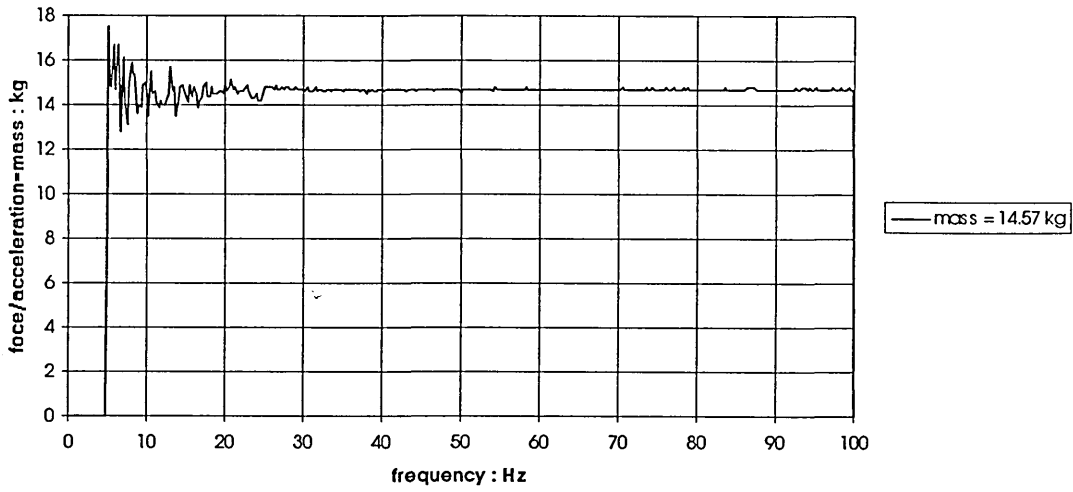


Figure 4.5: force transducer calibration curve.

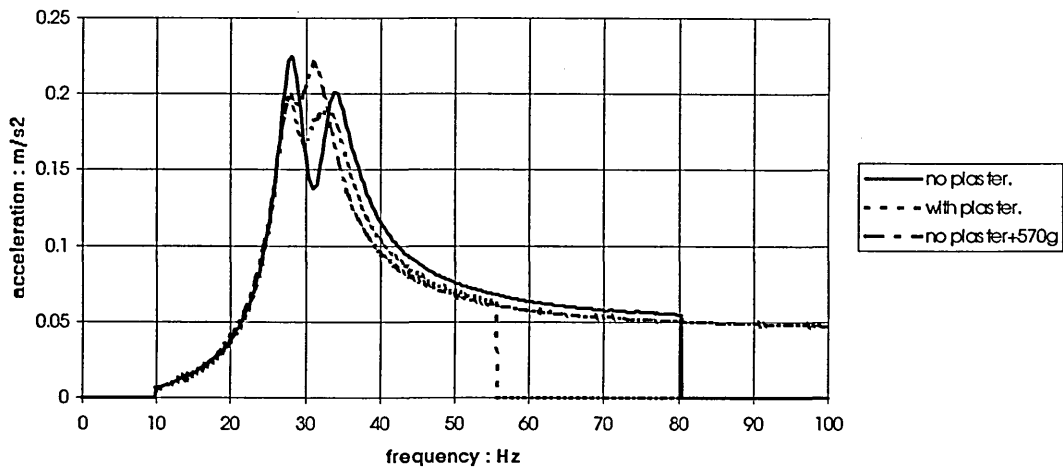


Figure 4.6: acceleration response from tests with and without plaster of Paris.

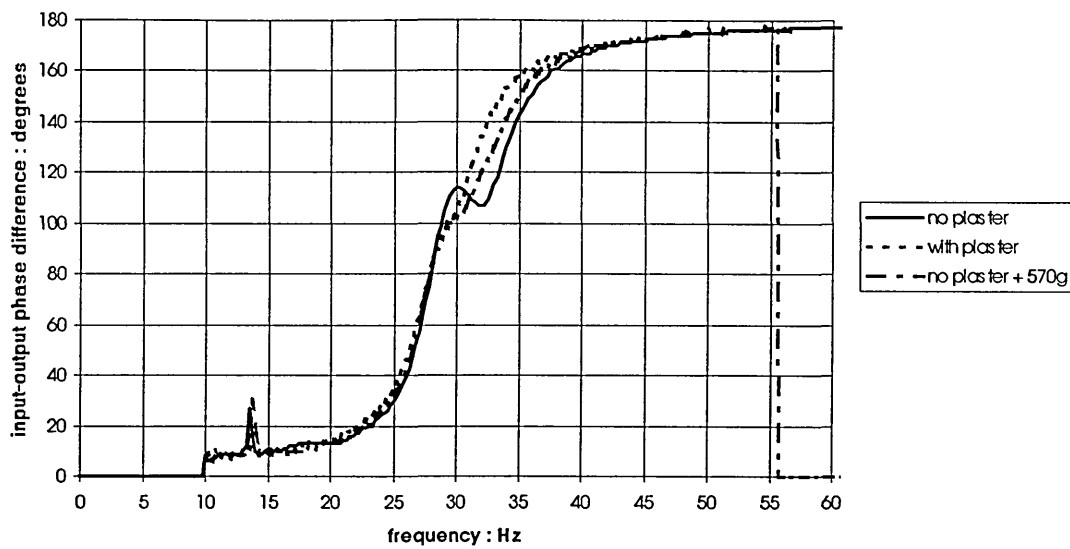


Figure 4.7: input-output phase difference with and without plaster of Paris.

Figures 4.8 to 4.10 show the response of the test system with the same rebound foam specimen subjected to three different input forces. It can be seen that the acceleration peaks remain unchanged in amplitude and frequency.

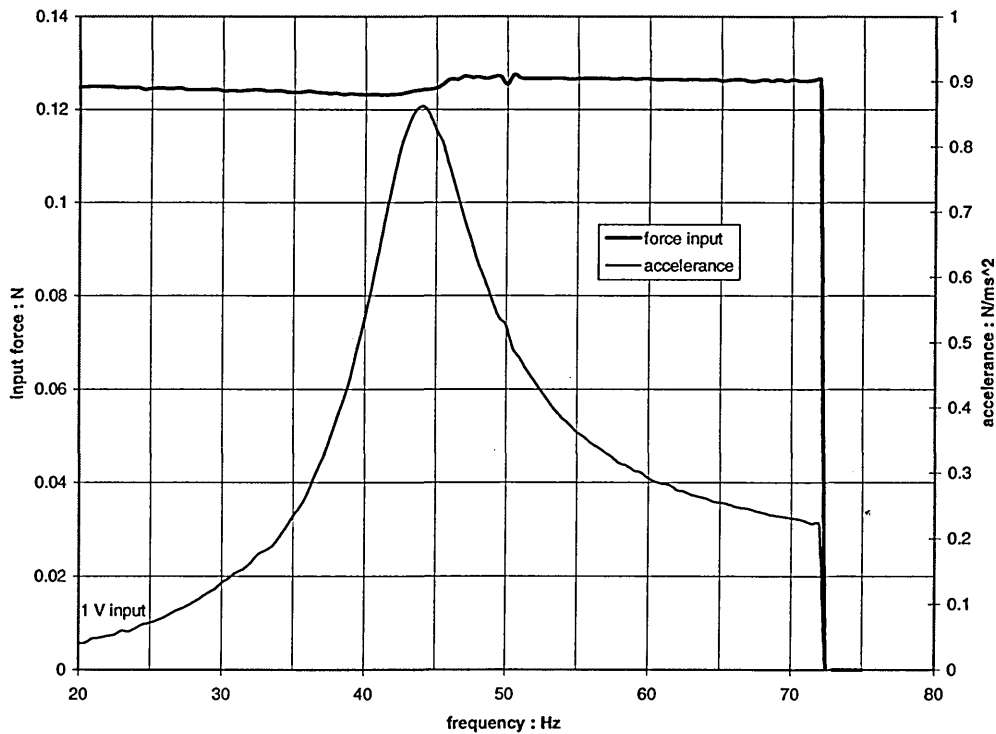


Figure 4.8: accelerance and input force for 144 kg/m² rebound foam; 1V input.

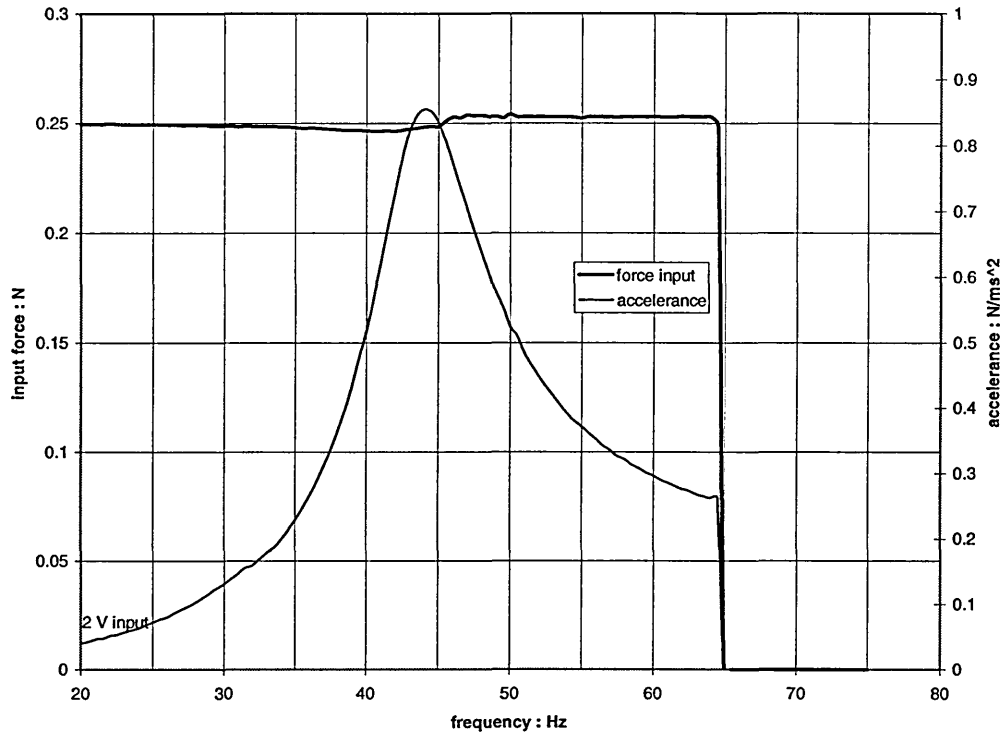


Figure 4.9: accelerance and input force for 144 kg/m² rebound foam; 2V input.

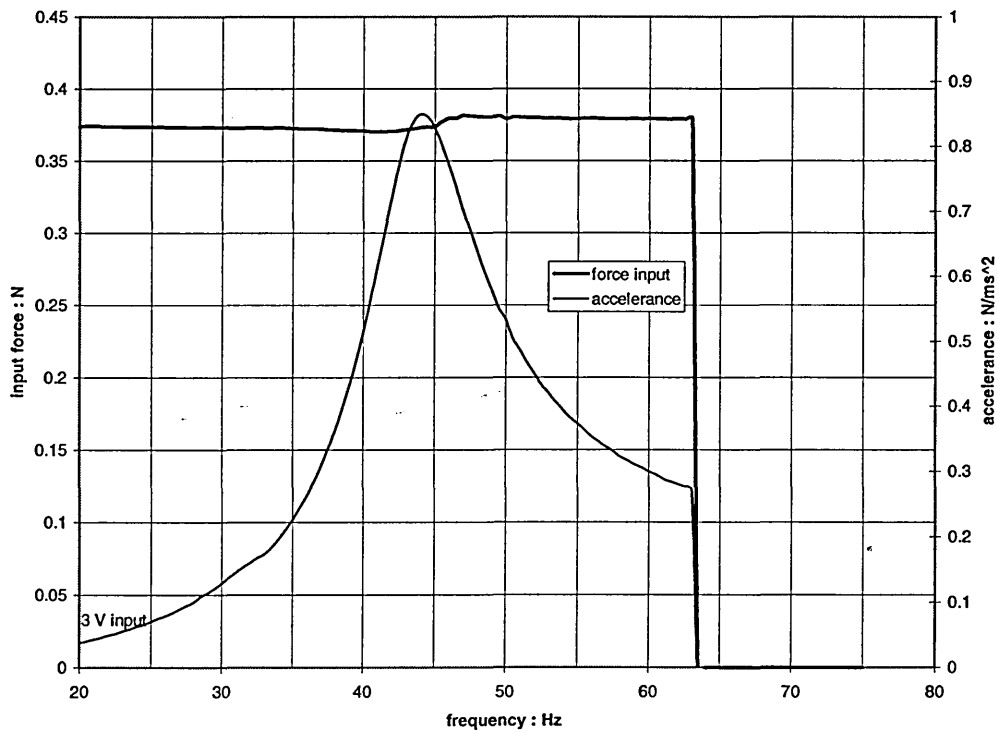


Figure 4.10: accelerance and input force for 144 kg/m² rebound foam; 3V input.

The results from extensive testing of virgin and rebond foams showed virgin foam specimens give the test system a higher natural frequency than the more dense rebond foams. This has been reported previously²⁵ and the complete set results need not be repeated here, especially as the results from identical tests will be presented in Chapter 7. Some of the results from this series of tests are included however because they help to illustrate points that are important to the development of this thesis.

The curves illustrated in Figures 4.11 to 4.12 show examples of the system response with specimens of different types of foam. It can be seen that although the 28 kg/m^3 virgin foam is the thickest specimen and has by far the lowest density, the test system had the highest resonant frequency with this material. The lowest resonant frequency was exhibited by the system with the 64 kg/m^3 rebond foam as can be seen by comparing Figure 4.13 with the others in this series.

Examining the curves also shows that the highest values for the accelerance at the resonant frequency occurred in the systems with virgin foams. The accelerance at resonance for the system with the 62 kg/m^3 virgin foam was particularly high, at least twice the value observed with the lower density virgin foam. Figures 4.7 to 4.11 also show that the frequency of maximum response amplitude never differs from the frequency at which the input-output phase difference is equal to 90° by more than 3 Hz.

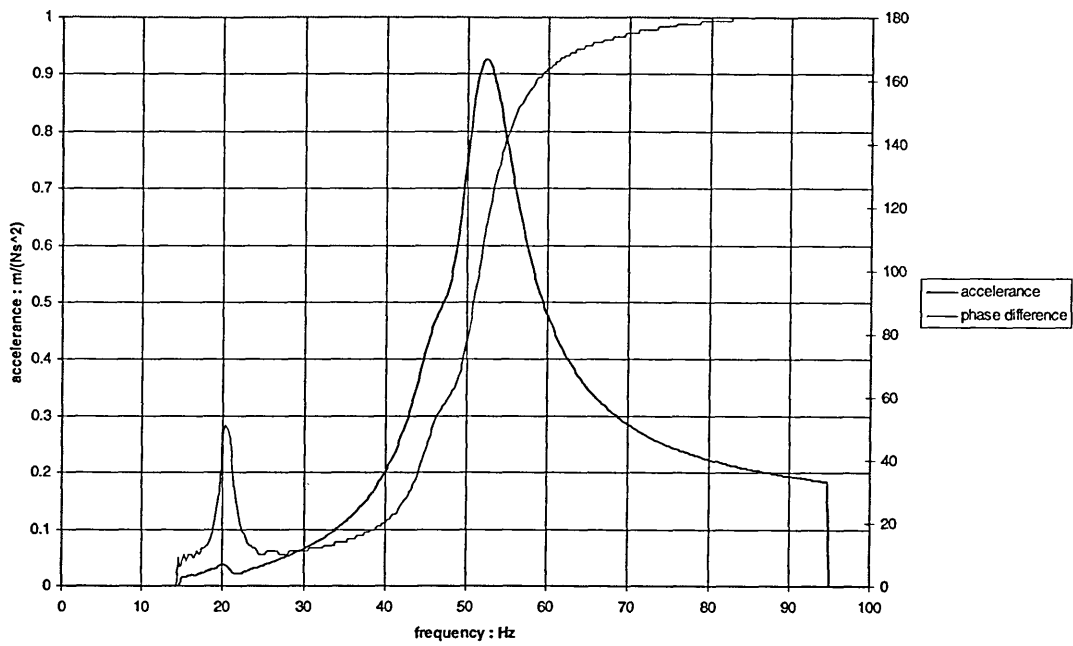


Figure 4.11: system response with a 28 kg/m^3 virgin foam specimen, 16.2 mm thick:

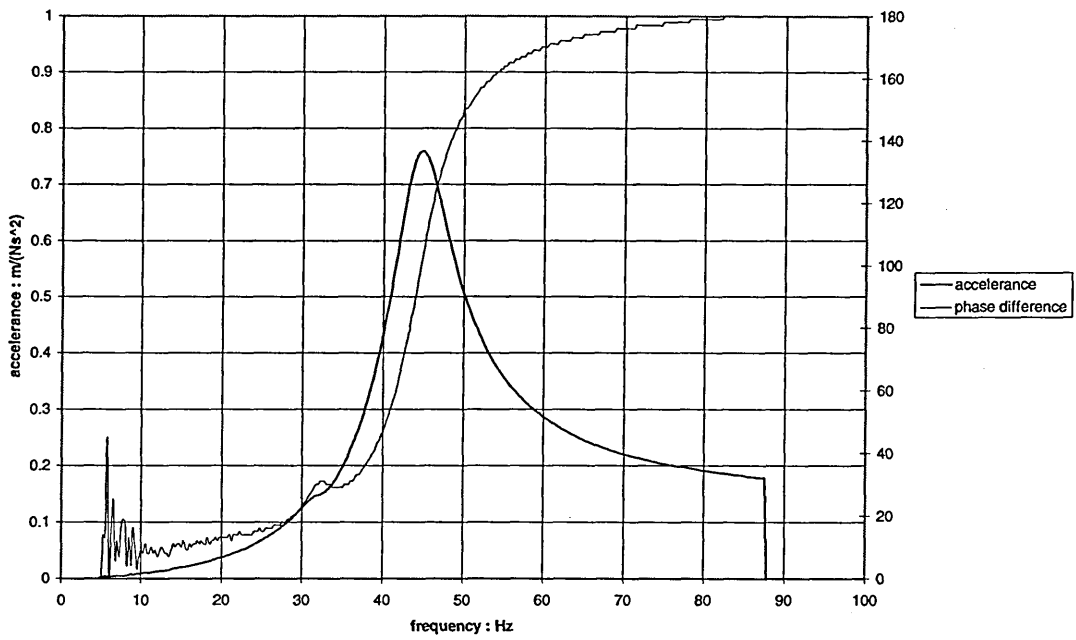


Figure 4.12: system response with a 144 kg/m^3 rebond foam specimen, 13.2 mm thick.

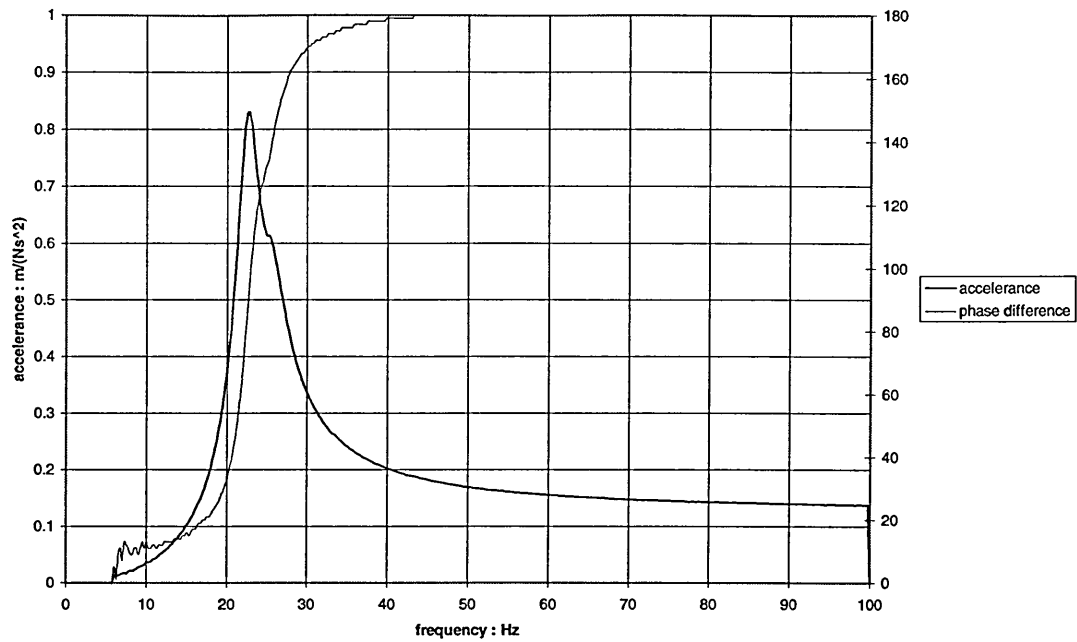


Figure 4.13: system response with a 64 kg/m³ rebond foam specimen, 12.6 mm thick.

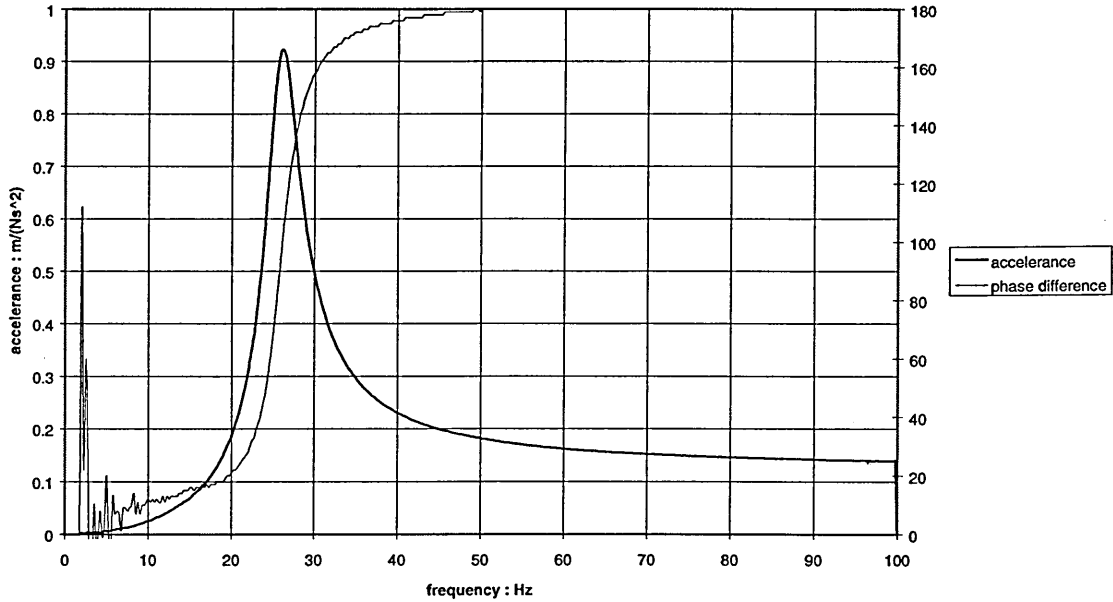


Figure 4.14: system response with a 78 kg/m³ (measured 69 kg/m³) rebond foam specimen, 13.2 mm thick.

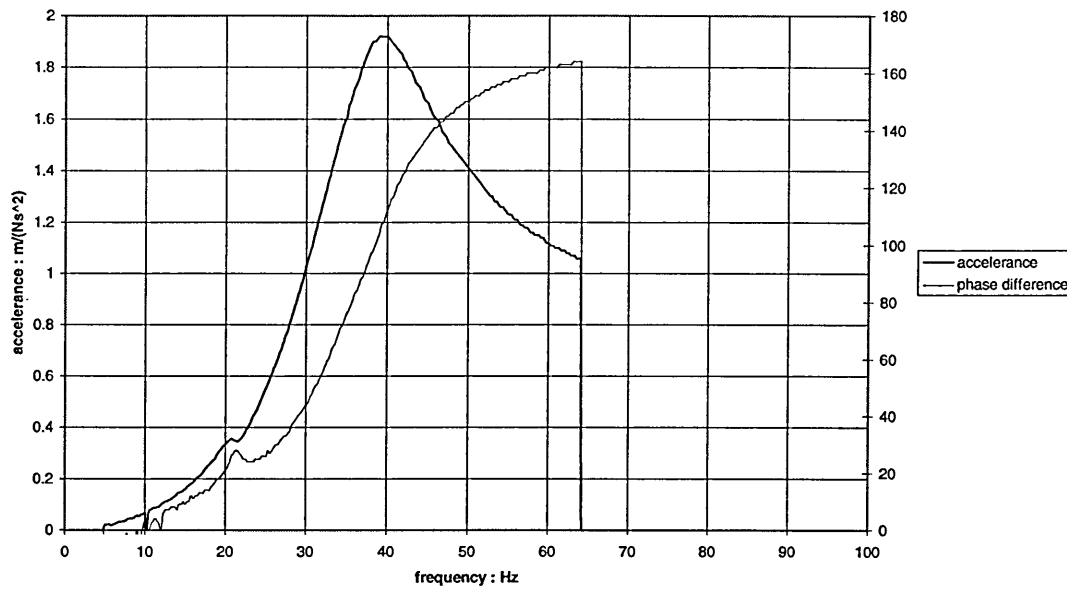


Figure 4.15: system response with a 62 kg/m³ (measured 69 kg/m³) virgin foam specimen, 9.6 mm thick.

Figure 4.16 shows the variation of test system resonant frequency with specimen thickness for a series of different foams. It can be seen that resonant frequency for a given thickness of rebond foam increases as the density increases, although this is not obvious from observation of the curves corresponding to the two least dense rebond foams. The resonant frequency is seen to decrease as the specimen thickness is increased. The figure also shows that the 62 kg/m³ virgin foam gave the system a higher resonant frequency than all but the most dense reconstituted foam.

The values for the dynamic stiffness (S_{dyn}) and the loss factor (η) for the different thicknesses and types of foam whose resonant frequencies are shown in Figure 4.16 are given in Table 4.1. The densities given in bold are those provided by the manufacturer of the foam and those in brackets the densities obtained from measurements in the laboratory. With all but the 78 kg/m³ foam the damping in the system is reduced as the specimen thickness increases. Static stiffnesses (S) are also included for comparison. These were calculated using the values for the Young's moduli of the foams determined according to the method of BS 4443²⁶ described in Chapter 3. The potential error in the

static stiffnesses has been ignored since there is little point in giving values of stiffness to more than one decimal place for this comparison

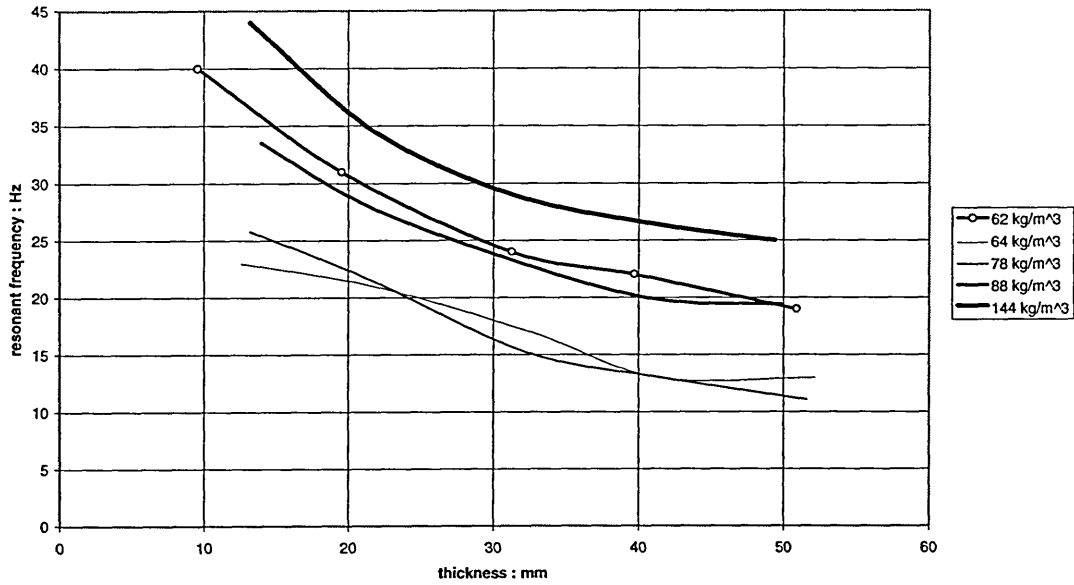


Figure 4.16: test system resonant frequency with specimens of different types and thicknesses of foam.

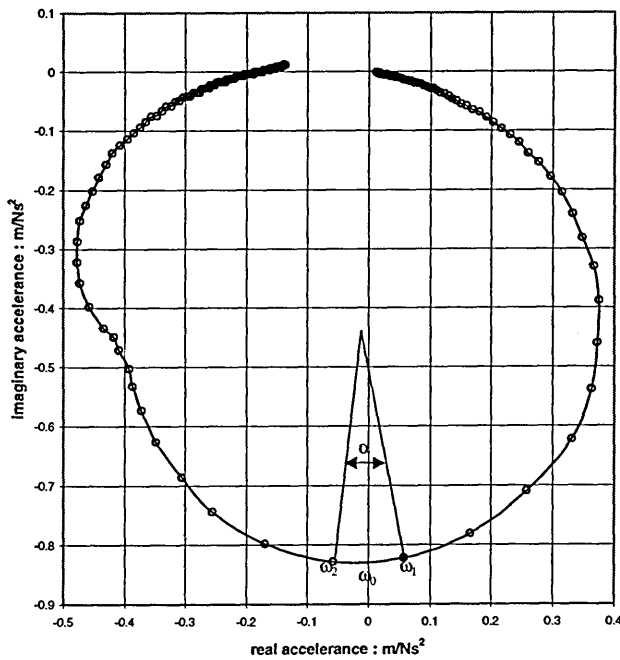


Figure 4.17: system response with a 64 kg/m³ rebond foam specimen, 12.6 mm thick, Kennedy and Pancu method.

The data shown in Figure 4.13 are represented in Figure 4.17 in the form required for Kennedy and Pancu's method for determining the loss factor of the test system. The loss factor (η) derived from this graph was found to be 0.14. The value for η was 0.15 using Sueyoshi and Tonosaki's method with the data in Figure 4.13, i.e. using the width of the mechanical impedance peak at (maximum/ $\sqrt{2}$) points.

density kg/m ³	thickness mm	S MN/m ³	S _{dyn} MN/m ³	loss factor
rebond 64 (60)	12.6	1.0	3.8±0.2	0.16±0.02
	21.7	0.6	3.3±0.1	0.17±0.03
	32.6	0.4	2.2±0.1	0.13±0.03
	41.3	0.3	1.3±0.1	0.13±0.04
	52.2	0.2	1.3±0.1	0.11±0.04
rebond 78 (69)	13.2	1.0	5.0±0.2	0.15±0.02
	21.5	0.6	3.6±0.2	0.16±0.02
	32.2	0.4	1.7±0.7	0.25±0.03
	41.4	0.3	1.3±0.1	0.19±0.05
	51.6	0.3	0.9±0.1	0.16±0.03
rebond 88 (86)	14.0	1.7	8.2±1.8	0.25±0.02
	21.4	1.1	5.8±0.2	0.15±0.02
	31.2	0.8	3.9±0.1	0.16±0.02
	40.9	0.6	3.0±0.1	0.16±0.03
	49.8	0.5	2.8±0.1	0.13±0.03
rebond 144 (140)	13.2	7.1	14.4±0.3	0.18±0.02
	21.8	4.2	9.1±0.3	0.17±0.02
	31.4	3.0	6.3±0.2	0.15±0.02
	40.7	2.3	4.9±0.2	0.14±0.02
	49.4	1.9	4.6±0.2	0.13±0.02
virgin 62 (69)	9.6	5.8	10.3±1.5	0.47±0.02
	19.5	2.9	7.1±2.8	0.43±0.02
	31.3	1.8	3.8±0.5	0.39±0.02
	39.7	1.4	3.6±0.2	0.19±0.03
	51.0	1.1	2.7±0.1	0.21±0.03

Table 4.1: comparison of static and dynamic stiffness and loss factor for different types and thicknesses of foam specimen.

4.5 Discussion

The curves showing the outputs for the accelerometer and force transducer shown in Figures 4.3 and 4.4 illustrate that they are both in good calibration. Figure 4.4 shows that at the onset of the vibration discussed earlier, the output voltage from the accelerometer was equivalent to 9.8 m/s, the acceleration due to gravity. The resultant curve from the force transducer calibration shown in Figure 4.5 is a constant value equivalent to the mass of the calibration block and the transducers at all frequencies above 25 Hz. The irregular trace below this frequency was due to lateral movements being introduced into the system which were unavoidable given the method of excitation. The calibration curves confirm that there can be confidence in the subsequent measurements in this programme.

The results shown in Figure 4.6 and Figure 4.7 demonstrate that the plaster of Paris layer specified in BS EN 29052-1 is not necessary when testing polyurethane flexible foam samples of the specified shape. The curves do not have identical shapes but it can be seen that the initial peak for all three test configurations occurs at the same frequency with only the magnitude of the first peak changed by the inclusion or non inclusion the of plaster of Paris. That the initial peaks occur at the resonance frequency of the system is confirmed by the input-output phase difference curves shown in Figure 4.7. Since only the frequency of resonance is required by the Standard, the slight differences in the curves are not important and not using the plaster of Paris layer is justified. Figures 4.8 to 4.10 are examples showing the result of varying the input force to the test system. No difference was observed in the system response from varying the input force with any of the specimens tested.

The results shown in Figure 4.11 to Figure 4.15 show that the frequencies at which the system response amplitude was at a maximum varied little from that frequency at which the input-output phase difference passed through 90°. The curves show that the difference was never greater than 3 Hz but it tended to increase as the system damping increased. This explains the greater uncertainty in the values for dynamic stiffness (S_{dyn}) for systems with high damping given in Table 4.1. The uncertainty in each individual measurement of the resonant frequency was taken to be the difference between the frequency of maximum response amplitude and the frequency at which the

input-output phase difference passed through 90° as was discussed earlier in this chapter. It can also be seen that the magnitude of the acceleration at the resonant frequency is greatest with the virgin foams, particularly so with the high density virgin foam.

The 62 kg/m^3 virgin foam was tested so that virgin and reconstituted foams of similar density could be compared (in fact its density was exactly the same as the 78 kg/m^3 (manufacturer's data) rebond foam when these were measured in the laboratory). This virgin foam was the most highly damped material, as is suggested by the width of the acceleration curve in Figure 4.15 and as can be seen from Table 4.1. It would appear therefore that greater hysteresis observed with the rebond foam in the static tests is not necessarily an indicator of more damping in a material in dynamic tests. The high acceleration peak at the resonance is probably due to the fact that this is designed to be a high resilience foam.

Collier⁶ describes high resilience and conventional polyurethane foams and the behavioural differences between the two types appear to be due to their structure. The cells in high resilience foams are essentially spherical shells of polymer with individual cells connected to their neighbours by pores in the shell wall. The cells in conventional foam are made from struts and are thus more like the Gibson and Ashby model²⁷ described in Chapter 2. The high resilience virgin foam is the most expensive of the materials tested. This together with its high acceleration peak and damping suggests that the material would not be chosen for use as a resilient layer under a floating floor.

The dynamic stiffness of the foam samples is inversely proportional to their thickness^{3,6,9} and so it is to be expected that the resonant frequency for the tests systems should fall as the thickness of the foam specimens was increased. This was observed in all the tests carried out. In addition as the density of the rebond foams increased, so did the specimen stiffness for a given thickness although the two lowest density rebond foams (measured in the laboratory as 60 and 69 kg/m^3) had very similar stiffnesses. This is perhaps not surprising when one considers the closeness of their densities.

The load plate used in the dynamic tests imposed a static load of 1.9 kPa on the test specimens which is below the yield stress for the final loading strokes of the 50 mm

thick virgin foams tested as can be seen most clearly in Figure 3.8 of the previous chapter. It is considerably below the first compression stroke yield stress of these specimens as can be seen below in Figure 4.18. The strain induced in the samples by this stress is around 2% and at such low strains the virgin foams are at their stiffest, before the onset of densification.

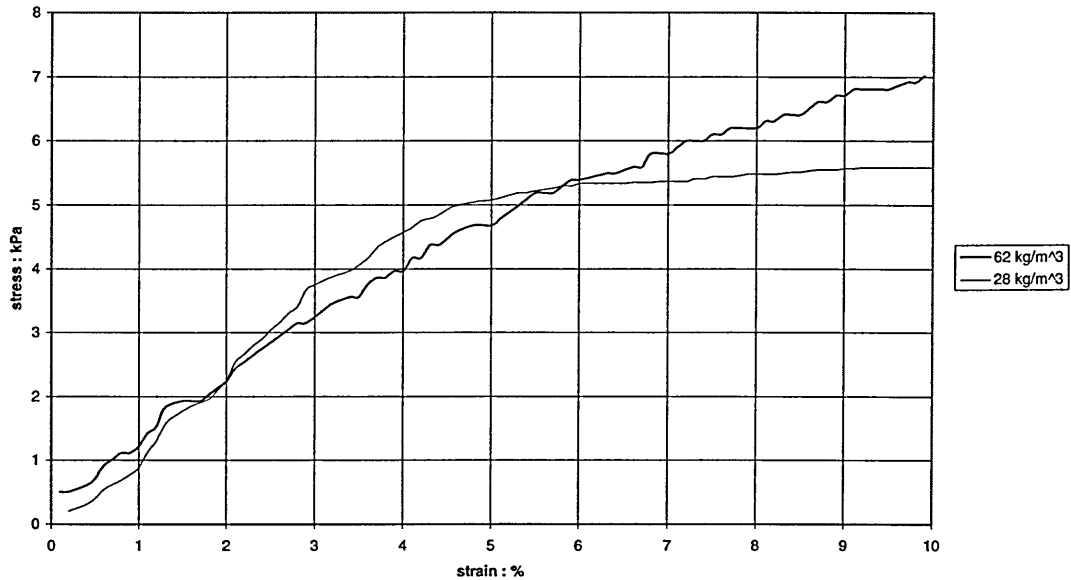


Figure 4.18: first loading strokes for 62 and 28 kg/m³ virgin foam.

Comparison of the static and dynamic stiffness using data from the first compression stroke in the static tests is more suitable since BS EN 29052-1 does not specify any conditioning of the test specimens. It is not surprising that there is no correlation between the specimen dynamic stiffness and the static stiffness determined according to BS 4443. Table 4.2 is therefore included below so that a comparison can be made when the static stiffness is determined without any conditioning. Figure 4.19 and Figure 4.20 show graphical representations of the data in Table 4.2. The static stiffnesses were obtained from the data used to produce Figures 3.5 and 3.6.

Figure 4.19 indicates that when the data point corresponding to a static stiffness of 0.8 MN/m³ is ignored there is good correlation between the static and dynamic stiffnesses ($S_{dyn} = 3.2552.S$) as is indicated by the value $R^2 = 0.9921$, where R^2 is the coefficient of determination. The correlation is not as good when this point is included ($S_{dyn} =$

3.4829.S and $R^2 = 0.9261$). For both regression lines, the intercept was set to zero since the correlation between static and dynamic stiffness was not significantly changed by not doing so (and setting the intercept to zero obviously produces a simpler equation). With the virgin foam (see Figure 4.20), the correlation between static and dynamic stiffness was significantly worse with the intercept set to zero ($R^2 = 0.8886$ compared with 0.9551).

The data in Table 4.2 suggest that there may be a simple linear relationship between the static and dynamic stiffnesses of the two types of foam although this is likely to be different for each different type of foam. For the rebond foam, the dynamic stiffness would appear to be between approximately 3.3 and 3.6 times greater than the static stiffness. For the virgin foam the relationship is slightly more complicated being, approximately, given by: $S_{dyn} = 1.4.S + 1.3 \text{ MN/m}^3$. The evidence derived from Figure 4.19 and Figure 4.20 is by no means conclusive however. It should be noted that the estimated error in the dynamic stiffness of the 32.2 mm thick specimen ($S = 0.6 \text{ MN/m}^3$) was $\pm 41\%$ of the mean value and the point on Figure 4.19 corresponding to $S = 0.8 \text{ MN/m}^3$ does not fit well with the other data on the chart..

density kg/m ³	thickness mm	S MN/m ³	S _{dyn} MN/m ³
rebond 78 (69)	13.2	1.5	5.0±0.2
	21.5	0.8	3.6±0.2
	32.2	0.6	1.7±0.7
	41.4	0.4	1.3±0.1
	51.6	0.3	0.9±0.1
virgin 62 (69)	9.6	6.9	10.3±1.5
	19.5	3.4	7.1±2.8
	31.3	2.1	3.8±0.5
	39.7	1.7	3.6±0.2
	51.0	1.3	2.7±0.1

Table 4.2: comparison of static and dynamic stiffness using data from the first compression in the static tests.

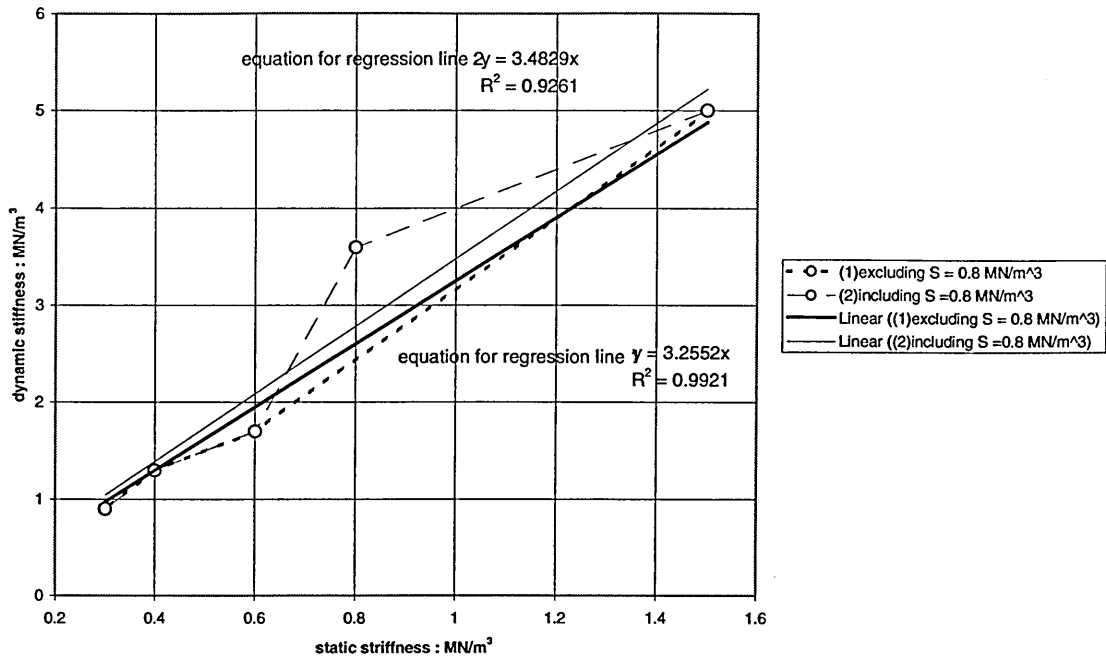


Figure 4.19: dynamic versus static stiffness for rebond foam
 (measured density = 69 kg/m^3)

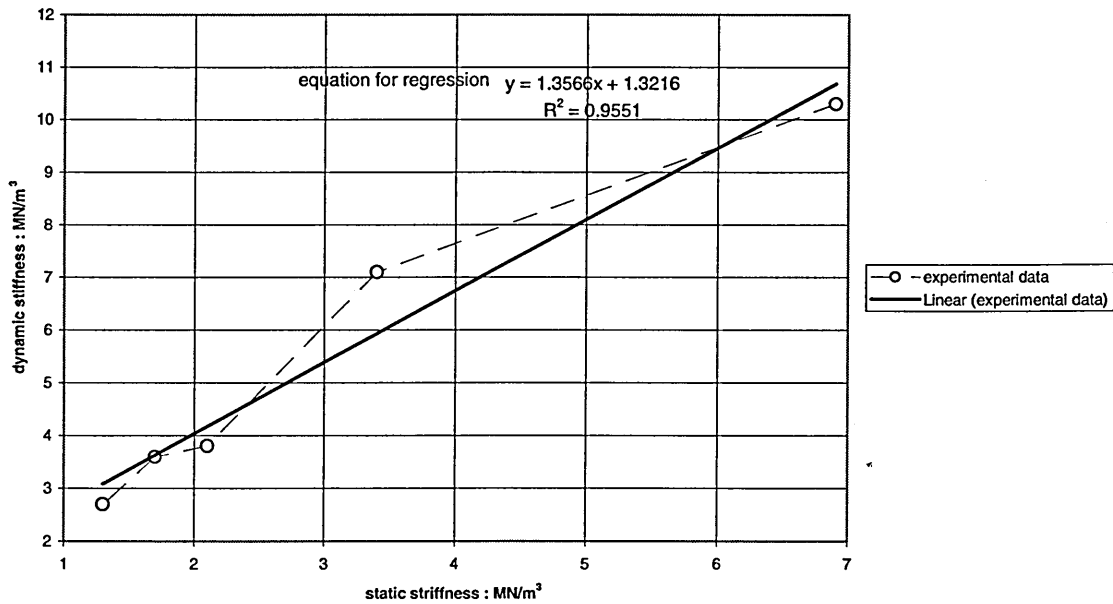


Figure 4.20: dynamic versus static stiffness for virgin foam
 (measured density = 69 kg/m^3)

The low stress imposed by the load plate on the specimens meant that changes in specimen thickness due to the stress were too small to measure accurately. For the virgin foams especially, where the imposed load of the plate caused a strain of approximately 2%, it was especially difficult to measure the change in thickness. The specimen thickness under the load plate is required only for calculating the dynamic stiffness of the air contained in porous materials however. With rebond foam especially, variations in thickness across the small test specimens in the order of 10% were not uncommon. Measuring the thickness of the specimens prior to testing and assuming an appropriate uncertainty in their thickness is therefore sufficiently accurate for this test programme.

The modification to the Standard Test Method described in Chapter 7 makes the measurement of specimen thickness unnecessary. The steel block was therefore not used in these (later) tests and the samples were placed directly on the concrete block which had a smooth surface. Placing samples on the steel block or the concrete block had no effect on the results obtained.

The data presented in Table 4.1 do not suggest that there is any simple relationship between specimen thickness and loss factor although it can be seen that all the foams exhibit relatively high damping. The comparison between the two methods for calculating the loss factor of the 64 kg/m³ rebond foam is significant however. This result was chosen to illustrate the comparison because Figure 4.13 shows evidence of a resonance fairly close to the main resonance peak. If Sueyoshi and Tonosaki's simple method for calculating η were to be insufficiently accurate for the purposes of this research then one would expect significant differences between their method and that of Kennedy and Panu . There is no significant difference between the two methods.

The methods were also compared with the data obtained from tests on the 62 kg/m³ virgin foam since the peaks are less symmetrical than the others presented. For the thinnest specimen tested the Kennedy and Panu method returned a value for η of 0.39 rather than that given in Table 4.1. None of the values of η for the other thicknesses of this high density virgin foam varied by more than 0.01 however, although the damping in the systems with two thinnest high resilience specimens is very high. Use of the

simpler method is therefore justified in this research. Further justification of this statement is given later in this thesis.

Before the dynamic stiffnesses of the specimens used in the standard tests⁸ can be related to those of resilient layers under floating floors the airflow resistivity must be determined. This is described in Chapter 5. Once the airflow resistivity has been determined correlation between the results from the laboratory tests described in this chapter and the performance of the lightweight floating floors of interest to this research can be sought.

The method of BS EN 29052-1 cannot be used to determine the dynamic stiffness of resilient layers under floors whose airflow resistivity is less than $10 \text{ kPa}\cdot\text{s}/\text{m}^2$ however and so the airflow resistivities of the materials had to be established. It also remained to demonstrate correlation between the test results obtained in the laboratory and the acoustic performance of flooring systems using flexible polyurethane foams as the resilient layer.

4.6 Conclusions

It has been demonstrated that the plaster of Paris layer specified in BS EN 29052-1 is not necessary when testing flexible polyurethane foam specimens. It is therefore possible to carry out testing on these materials much more quickly than when testing fibre quilts where the plaster of Paris layer has been shown to make a difference to the test results²².

The results from the dynamic tests show that the relatively high density rebond foams had lower dynamic stiffnesses than a high resilience virgin foam of similar density and conventional foams with much lower density. The dynamic stiffnesses of all but the most dense rebond foam were lower than those of the virgin foams tested. The results from tests on the most dense, high resilience, virgin foam suggested that this would not be favoured for use under a floor. The specimens made from the $28 \text{ kg}/\text{m}^3$ virgin foam, already used in shallow profile floating floors, had the highest dynamic stiffness of any tested. The stress-strain characteristics of this material, discussed in Chapter 3, also suggested that it was not the best choice of material for a resilient layer. Rebond foams appeared to be the best materials to use under floating floors.

The results presented in this chapter suggest that it may be possible to identify a simple quantitative relationship between the static and dynamic stiffnesses of polyurethane foams. This relationship is likely to be different for each different type of foam and possibly different for different foams of the same type. The identification of such a relationship is, therefore, not necessarily a goal worth pursuing since the dynamic stiffness of the foam specimens is relatively easily identified using the method described in this chapter (and in BS EN 29052-1).

The static stiffnesses does provide a guide to the likely relative dynamic stiffnesses of different materials since it has been shown that as static stiffness of the foams increases so does the dynamic stiffness. The only method identified for relating static stiffness to dynamic stiffness is not applicable to resilient layers under floors because the magnitudes of the strains likely to be suffered by a resilient layer are so small that accurate measurement is not possible with the equipment available.

The simple method for estimating the damping in the foams investigated used by Sueyoshi and Tonasaki is sufficiently accurate for use in this research. This is especially the case since BS EN 29052-1 only mentions damping because it may make the determination of the test system's resonant frequency difficult.

4.7 References

- 1 FRY A. (Ed), *Noise control in building services*, Sound Research Laboratories Ltd., Pergamon Press, 1988.
- 2 MUSTER D, PLUNKETT R., Isolation of vibrations, *Noise Reduction*, Ed Beranek L.L., Mcgraw-Hill Book Company, New York, 1960.
- 3 HILYARD N.C., , stiffness and strength-flexible polymer foams, *Mechanics of Cellular Plastics*, Ed Hilyard N.C. Publ Applied Science Publishers Ltd. Barking, Essex, England, 1982.
- 4 VER I.L., Measurement of dynamic stiffness and loss factor of elastic mounts as a function of frequency and static load, *Noise Control Engineering*, 1974, 3 (3), 37-42.
- 5 STEWART M. A., *Sound transmission through a chipboard floating floor supported on a concrete slab*, PhD thesis, Heriot-Watt University, 1996.
- 6 COLLIER P., *The design and performance of non-linear vibration isolating materials*, PhD Thesis, Sheffield City Polytechnic, Sheffield, UK, 1985.
- 7 HILYARD N.C., LEE W.L., CUNNINGHAM A., Energy dissipation in polyurethane cushion foams and its role in dynamic ride comfort, *Proceedings Cellular Polymers International Conference*, 20-22 March, Forum Hotel, London UK, Rapra Technology , 1991.
- 8 BS EN 29052-1: 1992, *Acoustics - Determination of dynamic stiffness - Materials used under floating floors in dwellings*.
- 9 CREMER L., HECKL M., Ungar E.E., *Structure-borne sound*, 2nd ed., Publ. Springer-Verlag, 1988.
- 10 Ver I.L., Interaction of sound waves with solid structures, *Noise and Vibration Control Engineering*, (Ed) Beranek L.L., Ver I.L., 245-367, Publ. John Wiley and Sons Inc. 1992.
- 11 W.E. BLAZIER, DUPREE R.B., Investigation of low frequency footfall noise in wood-frame multifamily building construction, *J. Acoust. Soc. Am.*, 1994, 96 (3), 1521-1532.
- 12 BLAKE R.E., Basic vibration theory, *Shock and Vibration Handbook*, Ed Harris C.M., 4th Edition, Chapter 2, Publ Mcgraw-Hill, New York, 1996.

-
- 13 KINSLER E.K., FREY A.R., *Fundamentals of acoustics*, 2nd ed, John Wiley and Sons Inc., New York, USA, 1962.
 - 14 SUEYOSHI S.; TONOSAKI M.; ORIBE M., Localised vibration of composite wood flooring fastened to a concrete slab, *Japan Wood Research Society*, 1995 Vol. 41, 31-36.
 - 15 SUYEOSHI S; TONOSAKI M., Determination of localised dynamic behaviour of wood strip over foam rubber underlayment, composite flooring by random vibration, *Wood Sci. Technol.* , 1993, Vol. 27, 11-21.
 - 16 JONES D.I.G., Applied damping treatments, *Shock and Vibration Handbook*, Ed Harris C.M., 4th Edition, Chapter 37, Publ McGraw-Hill, New York, 1996.
 - 17 KURZE U.J., Laboratory measurements of vibro-acoustic properties of resilient elements, *Acta Acoustica*, 1994, 2, pp 483-490.
 - 18 CHU A.S., ELLER E.E., WHITTIER R.M., Vibration transducers, *Shock and Vibration Handbook*, Ed Harris C.M., 4th Edition, Chapter 2, Publ McGraw-Hill, New York, 1996.
 - 19 CF-350/360 Dual Channel FFT Analyser Instruction Manual, Ono Sokki Co. Ltd.
 - 20 WHITE R.G., Vibration testing, *Noise and vibration*, 713-753, Publ. Ellis Horwood Ltd., 1982.
 - 21 ZAVERI K., *Modal analysis of large structures-Multiple exciter systems*, ISBN 8787355035, Bruel and Kjaer, 1985.
 - 22 HOPKINS C., 1995, Private communication, BRE Acoustics Section.
 - 23 BS 4443, 1988, Part 1, *Flexible cellular materials, measurement of dimensions of test specimens, methods 1a and 1b.*
 - 24 KAYE G.W.C., LABY T.H., *Tables of physical and chemical constants*, 13 th edition, Longmans Green and Co. Ltd, London, 1966.
 - 25 HALL R., MACKENZIE R.K., Reconstituted versus open cell foams in floating floors, *Building Acoustics*, 1995, Vol. 2 No 2, 419-436.
 - 26 BS 4443, 1988, Part 1, *Flexible Cellular Materials, Determination of compression stress-strain characteristics.*
 - 27 GIBSON L.J.; ASHBY M.F., *Cellular solids*, Pergamon, Oxford, 1988.

CHAPTER 5

AIRFLOW RESISTIVITY

5.1 Introduction

The laboratory tests conducted on the different types of foam had suggested that flexible rebond open cell foam would be better to use as the resilient layer under floating floors than virgin open cell foam. Although the dynamic tests described in the previous chapter showed that the rebond foam specimens generally had lower dynamic stiffness than the virgin foams, specimen dynamic stiffness cannot be related to that of a resilient layer without knowledge of the airflow resistivity of the material. It was therefore necessary to measure the airflow resistivity of the foams of interest.

This chapter describes the relationship between the stiffness of the specimens measured under laboratory conditions and that of resilient layers under floors. It describes the measurement of airflow resistivity and presents the results obtained. The results are discussed and conclusions are drawn which, in subsequent chapters, lead to a modification to the Standard Method for determining the dynamic stiffness of resilient layers under floors. The modification leads ultimately to a method for predicting the weighted standardised impact sound pressure level ($L'_{nT,w}$) when lightweight floating floors are used on concrete supporting floors.

5.2 Background

According to BS EN 29052-1¹ (the Standard Method for determining the dynamic stiffness of resilient layers under floating floors) knowledge of the airflow resistivity of the materials being tested is required in order to relate the dynamic stiffness of the specimen to that of the material when used as a resilient layer under a floating floor. Since the test specimens and the excitation amplitudes used in the procedure¹ are small, the stiffness of the air contained in the sample has no effect on the test results. The air is free to move laterally in and out of the sample². Under a floating floor this is not the case and the stiffness of the air contained in the resilient layer must be considered. The

significance of the air stiffness is determined by the stiffness of the foam material itself and the lateral airflow resistivity (r) of the foam¹.

BS EN 29052-1 states that for materials with high airflow resistivity ($r > 100 \text{ kPa.s/m}^2$), the apparent dynamic stiffness per unit area of the sample (S_{dyn}) is equal to the dynamic stiffness of the material when used under a floating floor (S_{layer}).

$$S_{\text{layer}} = S_{\text{dyn}} \quad \text{N / m}^3$$

Equation 5.1

For intermediate airflow resistivity where:

$$10 \text{ kPa.s/m}^2 < r < 100 \text{ kPa.s/m}^2$$

the dynamic stiffness per unit area of the resilient material under the floating surface is given by:

$$S_{\text{layer}} = S_{\text{dyn}} + S_{\text{air}} \quad \text{N / m}^3$$

Equation 5.2

where S_{air} = stiffness per unit area of the air enclosed in the material.

The stiffness of the enclosed air is calculated by

$$S_{\text{air}} = \frac{P_o}{d\epsilon_m} \quad \text{N / m}^3$$

Equation 5.3

where p_o = atmospheric pressure (Pa)

d = thickness of the resilient layer (m)

ϵ_m = the porosity of the material

When $p_o = 0.1 \text{ MPa}$ and $\epsilon_m = 0.9$ then¹:

$$S_{\text{air}} = \frac{111}{d} \quad \text{MN / m}^3$$

Equation 5.4

where d is in mm

For low airflow resistivity, $r < 10 \text{ kPa.s/m}^2$, then sample stiffness and resilient layer stiffness are equal and $S_{\text{layer}} = S_{\text{dyn}}$ if the dynamic stiffness of the enclosed air is small compared with that of the test specimen. If the dynamic stiffness of the enclosed air is not small when compared with the dynamic stiffness of the sample and $r < 10 \text{ kPa.s/m}^2$ then the Standard cannot be used¹ to determine the dynamic stiffness of the material when it is used under a floating floor. It was therefore necessary to measure the airflow resistivity of the materials to be used as resilient layers in sections of floating floor so that the relationship, according to BS EN 29052-1, between the dynamic stiffness of the laboratory samples and the dynamic stiffness of the resilient layers could be established.

BS EN 29052-1 states that the airflow resistivity of the materials investigated should be determined by one of the methods described in BS EN 29053³. Method A described in this Standard was adopted.

5.2.1 Measurement of airflow resistivity

The Standard Method³ for obtaining the airflow resistivity of a material is to measure the pressure drop across a sample of known dimensions and to use these measurements to calculate the airflow resistivity. The airflow resistance (R) of a test specimen is given by³:

$$R = \frac{\Delta p}{q_v} \quad \text{Pa.s / m}^3$$

Equation 5.5

where

Δp = pressure difference (Pa).

q_v = volumetric airflow rate passing through the specimen (m^3/s).

The specific airflow resistance (R_s) is given by:

$$R_s = RA \quad \text{Pa.s / m}$$

Equation 5.6

A = the cross sectional area of the specimen (m^2)

The airflow resistivity (r) is given by

$$r = \frac{R_s}{d} \quad \text{Pa.s/m}^2$$

Equation 5.7

where d = sample thickness (m).

5.3 Test method

The apparatus used to obtain the airflow resistivities of the samples is illustrated in Figure 5.1. The measurement cell is square in cross section with sides of 100 mm (area = 10^4 mm^2) and is 300 mm in depth. The sample is supported on an open mesh 100 mm above the bottom of the chamber where the air inlet and outlet are located. A rotary vacuum pump was used to generate the airflow required for the test and the plenum used to give an airflow rate as constant as possible.

The pressure difference between atmospheric pressure and the pressure in the chamber beneath the specimen was measured. The Standard requires that the differential pressure drop across the specimen be measured at a linear air speed of 0.5 mm/s through the specimen which corresponded to a volumetric flow rate of 300 cc/min for this apparatus. The air flow rate was therefore measured using a Platon flow meter with a range between 60 and 600 cc/min.

The samples of material were prepared such that their sides were slightly larger than 100 mm, as specified in the Standard, in order to prevent air leakage between the samples and the sides of the measurement chamber. The thickness of the samples in the chamber was measured using micrometer callipers between the measuring points shown in Figure 5.1.

Three specimens of each foam were tested using the apparatus. The airflow resistivities of the rebond foams were obtained in the direction of the materials' forming compression and in the direction perpendicular to this. Similarly the airflow resistivity for the virgin foam was obtained in the rise direction for the foam and perpendicular to this direction. The differential pressure was measured at increasing and then decreasing volumetric flow rates between 100 and 600 cc/min: the flow rate was increased, or

decreased, by 100 cc/min between each measurement so that anomalies due to taking only one measurement, at 300 cc/min, could be avoided.

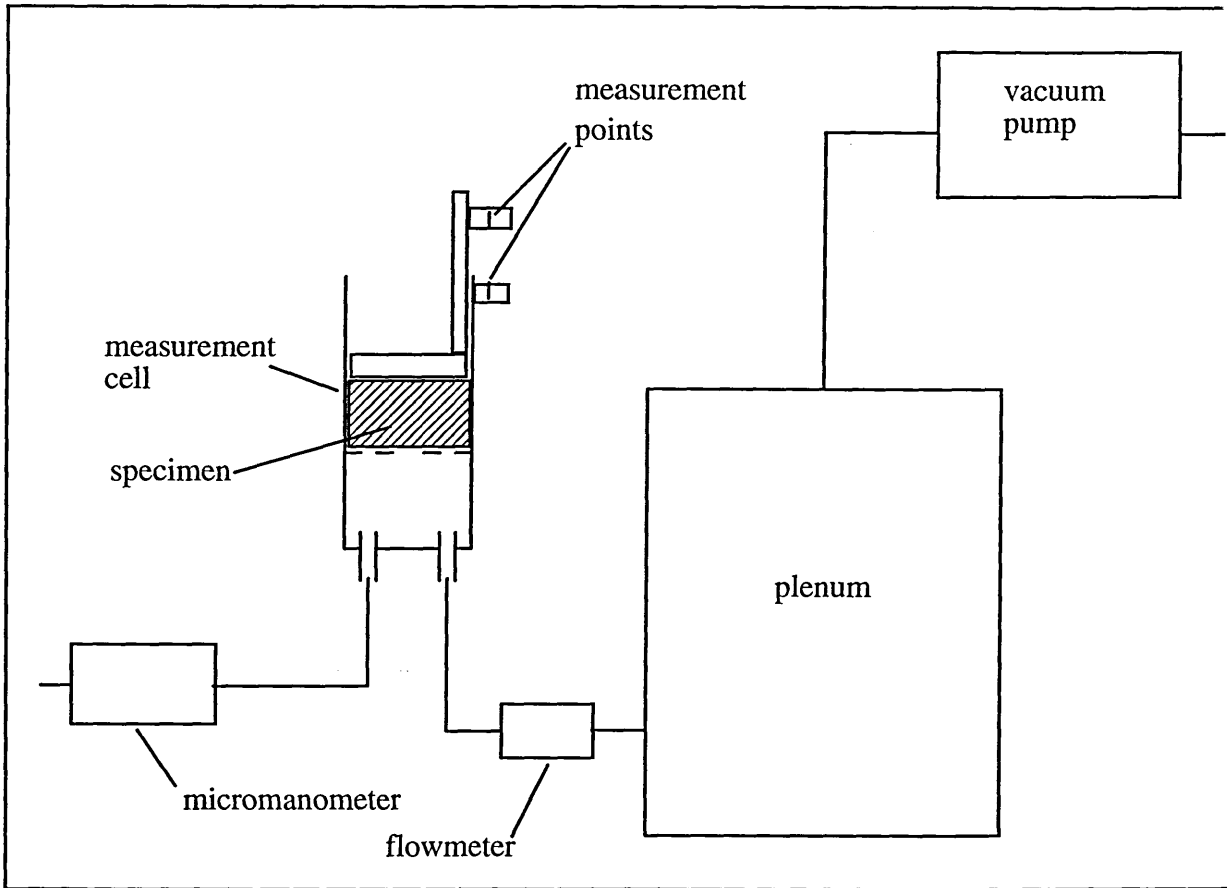


Figure 5.1: apparatus for measuring airflow resistivity

The micromanometer used initially to measure the pressure difference was a Furness Instruments FCO 11 model 1 with a sensitivity of ± 0.1 Pa which meant that for some low airflow resistivity materials the instrument was being used at the limits of its usefulness at low airflow rates. For these foams the measurements were repeated using a Furness FCO 11 model 2 micromanometer with sensitivity ± 0.01 Pa. In order to verify that the apparatus was sufficiently accurate to determine whether the stiffness of the air (S_{air}) in a resilient layer had to be added to that of the test specimen (S_{dyn}) the airflow resistivities of several foams were measured using a different apparatus at the Building Research Establishment (BRE). This apparatus had a test chamber with the

same cross-sectional area and shape as the one manufactured for this research and had been used to measure the airflow resistivities of fibre quilts.

5.4 Results

Results from tests according to BS EN 29053 are shown in Table 5.1 and Table 5.2. Table 5.1 shows the results from a series of tests on different types of reconstituted foam. The values for airflow resistivity in the direction perpendicular to the forming compression are shown in bold. Those in the direction of forming compression are given in italic. It can be seen that the airflow resistivity for these materials increases as the density of the foam increases. The difference in the airflow resistivity in the two directions is insignificant.

density kg/m³	airflow resistivity kPa.s/m²	standard deviation kPa.s/m²	airflow resistivity kPa.s/m²	standard deviation kPa.s/m²
64 (60)	6.0	0.2	<i>6.3</i>	<i>0.5</i>
78 (69)	7.6	0.3	<i>7.0</i>	<i>0.3</i>
88 (86)	13.4	0.5	<i>13.1</i>	<i>0.90</i>
144 (140)	33.0	1.0	<i>32.5</i>	<i>3.0</i>

Table 5.1: airflow resistivity for rebond foam (measured density in brackets)

Table 5.2 shows airflow resistivity values for the virgin foam used in flooring samples which were to be tested in the field. The results show that the foam has a slightly higher airflow resistivity at right angles to its rise direction. Comparison with Table 5.1 shows that the airflow resistivity in both directions is higher than the airflow resistivities of the much more dense 64 and 78 kg/m³ reconstituted foams.

virgin foam 28 kg/m³	airflow resistivity kPa.s/m²	standard deviation kPa.s/m²
rise direction	12.0	0.1
perpendicular to rise direction	13.7	1.8

Table 5.2: airflow resistivity for virgin foam

5.5 Discussion

Measurements of the airflow resistivity of the foams were made only because it was necessary to know whether to use Equation 5.2 or Equation 5.1 to calculate the dynamic stiffness of a resilient foam layer under a floating floor. The precise value of the airflow resistivity of the foams was not of special interest to this research therefore. The requirement was merely to be confident that the airflow resistivity lay in the range $10 \text{ kPa}\cdot\text{s}/\text{m}^2 < r < 100 \text{ kPa}\cdot\text{s}/\text{m}^2$ or above or below this range.

The efforts to verify that the apparatus was sufficiently accurate to allow the determination of dynamic stiffness of the materials to be used as resilient layers according to BS EN 29052-1 were nevertheless felt necessary. Taking measurements on the same samples with two sets of apparatus was an easy way of confirming the accuracy of the system constructed for this research programme. The results showed insignificant differences. It was therefore demonstrated that the apparatus used in this research programme was sufficiently accurate to allow the determination of the dynamic stiffnesses of polyurethane foam resilient layers.

Thin layers of foam for resilient layers are most likely to be cut from the blocks produced in the manufacture of the materials in the direction illustrated in Figure 5.2 because of the widths of foam required. This is increasingly the case as foam density increases due to the smaller thicknesses of the blocks. With the low density rebond foams, however, it is possible to cut the resilient layers from the top or from the sides of the rebond block and airflow resistivity had to be determined in each direction.

It can be seen from Table 5.1 that there is no significant difference in the airflow resistivity in either direction with the rebond foams. The two more dense rebond foams have higher airflow resistivities and the dynamic stiffness for these materials, when used as resilient layers, is calculated using Equation 5.2 according to BS EN 29052-1. The dynamic stiffness of resilient layers made from the virgin foam can also be calculated using Equation 5.2. The airflow resistivities of the 64 and 78 kg/m^3 rebond foams are less than $10 \text{ kPa}\cdot\text{s}/\text{m}^2$ and therefore the dynamic stiffnesses of the air contained in the foams and the dynamic stiffnesses of the foam materials themselves need to be compared to determine whether BS EN 29052-1 can be used with these materials.

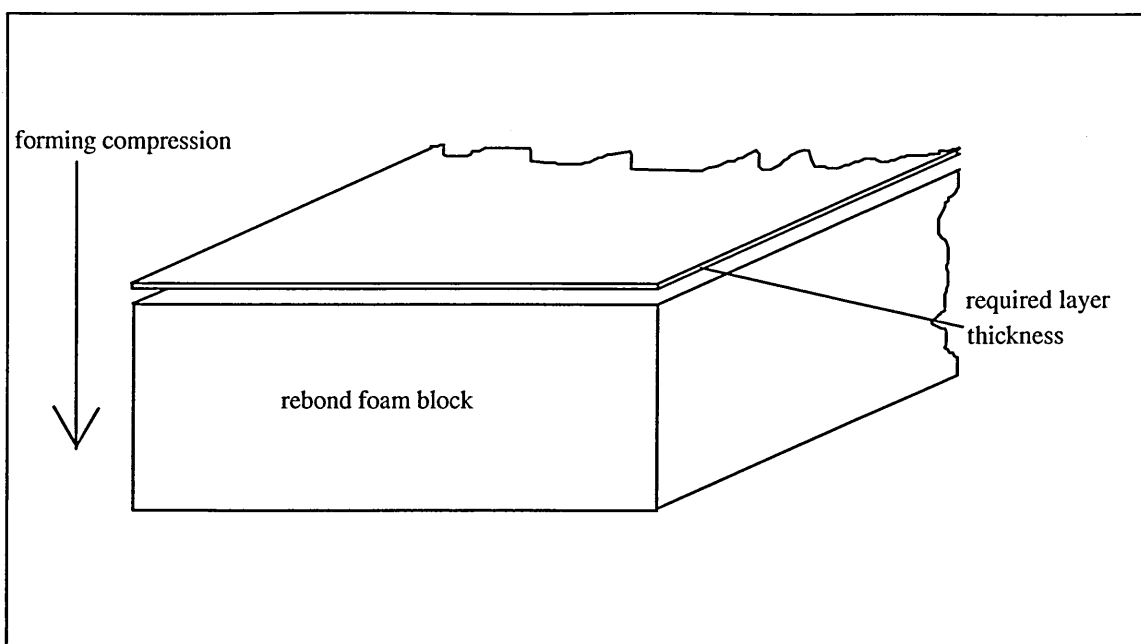


Figure 5.2: cutting required thickness from block

Table 5.3 (on Page 97) shows the comparisons between the dynamic stiffness of the different thicknesses of rebond foam specimens and the air stiffness for each thickness calculated using Equation 5.4. It can be seen that for none of the thicknesses of either foam is the air stiffness insignificant. The Method described in BS EN 29052-1 therefore cannot be used to determine the dynamic stiffness of resilient layers under floors made from these materials.

The airflow resistivity of the virgin foam appears to vary between the rise direction and the directions perpendicular to this direction, although more measurements would have to be taken to confirm this given the potential error in the values presented in Table 5.2. Although this is an open cell foam some remnants of cell walls remain. The apparent slightly higher airflow resistivity perpendicular to the rise direction is probably due to greater numbers of significant cell membranes remaining from the forming process. Figures 5.3 and 5.4 illustrate this. These and the subsequent micrographs were obtained using a scanning electron microscope (SEM). Many of these membranes are likely to be ruptured when the foam is subjected to large strains however⁴ so it may be that there is little or no difference once the foam has been in use for a while.

density kg/m ³	thickness mm	S _{dyn} MN/m ³	S _{air} MN/m ³
64	12.6	3.9	8.8
	21.7	3.3	5.1
	32.6	2.2	3.4
	41.3	1.3	2.7
	52.2	1.3	2.1
78	13.2	5.0	8.4
	21.5	3.6	5.2
	32.2	1.7	3.4
	41.4	1.3	2.7
	51.6	0.9	2.2

Table 5.3: Comparison of sample stiffness and air stiffness for different thicknesses of rebond foam.

The remaining membranes in the low density virgin foam may well explain why its airflow resistivity is greater than that of the much denser 64 and 78 kg/m³ rebond foams. Figure 5.5 shows that there are no significant membranes to be seen in the 78 kg/m³ foam.

Investigations with the SEM showed no discernible difference in the structure of this, 78 kg/m³ rebond, foam when micrographs were taken in different directions. Figures 5.6 and 5.7 show micrographs of the 144 kg/m³ rebond foam taken in different directions. With this foam the view perpendicular to the forming compression shows that the cell walls are more closely pressed together than with the lighter rebond foam (Figure 5.5). The view in the direction parallel to forming shows that the cell walls are not so distorted as in the perpendicular direction but nevertheless the airflow resistivity was virtually identical in the two directions.

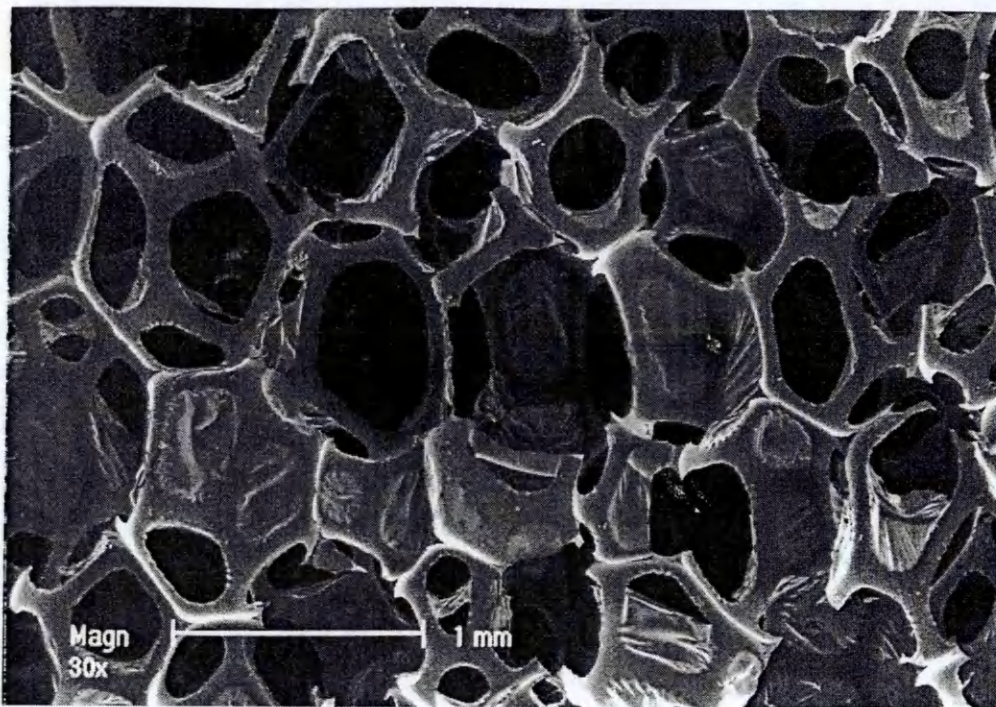


Figure 5.3: micrograph of 28 kg/m³ virgin foam, taken perpendicular to the rise direction

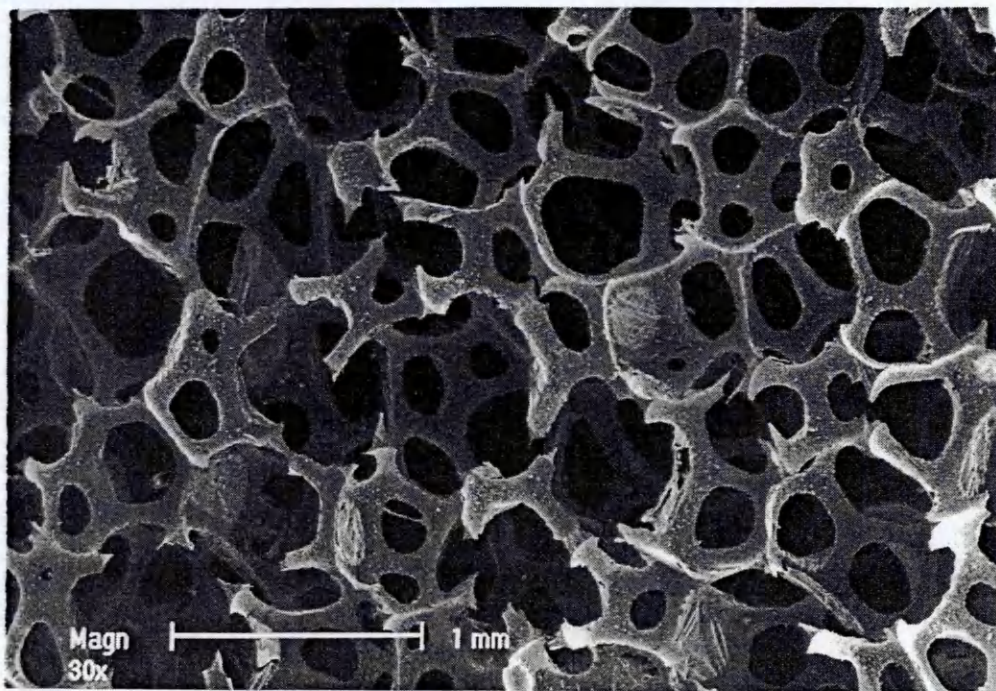


Figure 5.4 micrograph of 28 kg/m³ virgin foam, taken in the rise direction

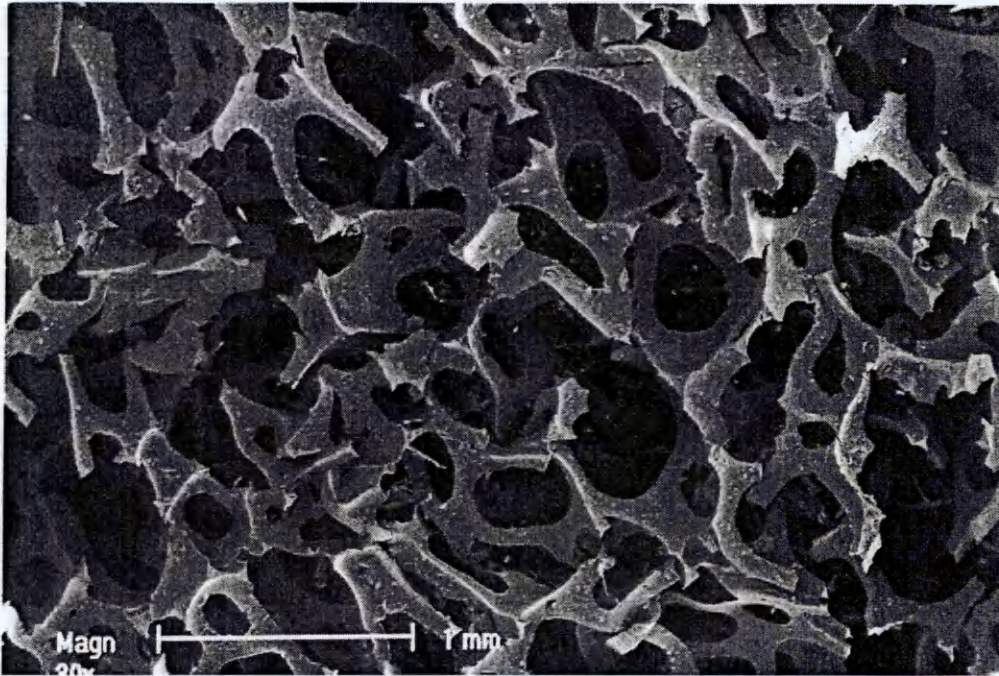


Figure 5.5: micrograph showing 78 kg/m³ rebond foam, taken perpendicular to the forming compression

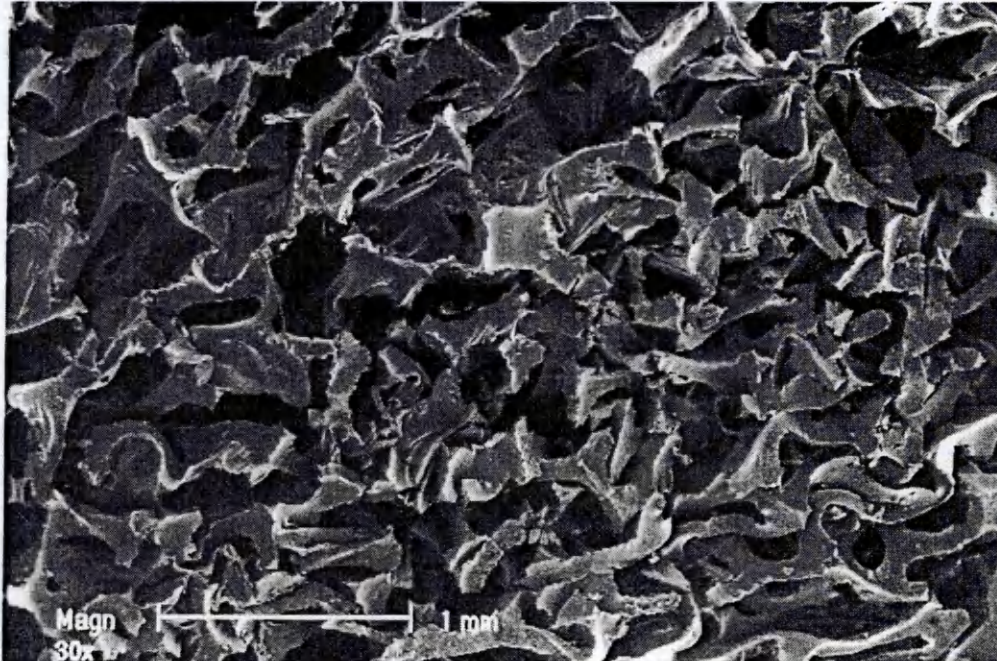


Figure 5.6: micrograph showing 144 kg/m³ rebond foam, taken perpendicular to the forming compression

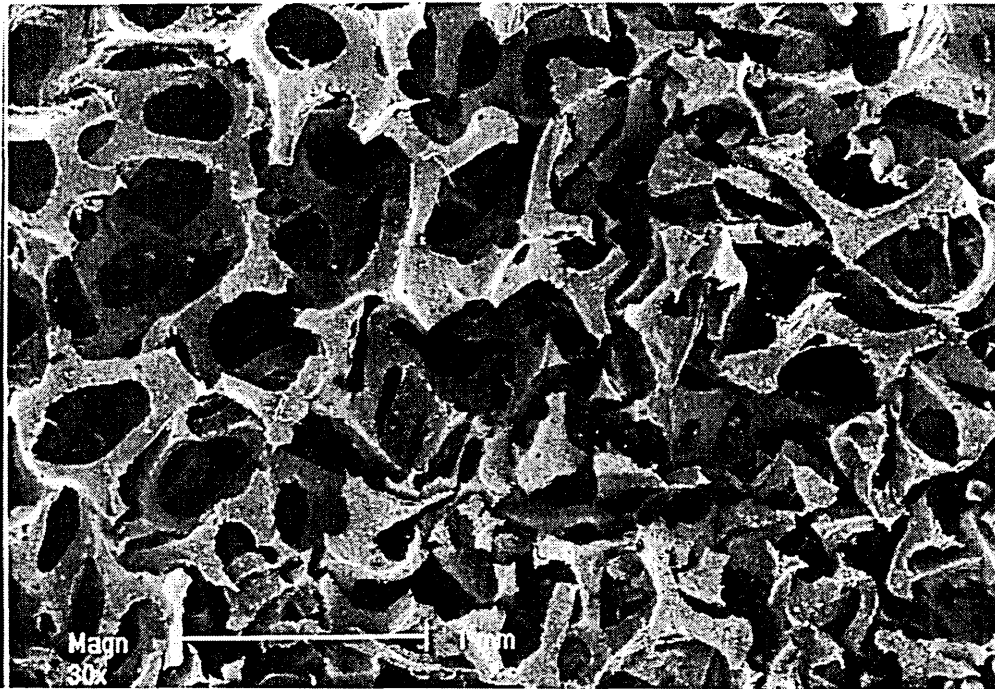


Figure 5.7: micrograph showing 144 kg/m³ rebond foam, taken parallel to the forming compression

The micrographs support the proposal that the remaining membranes are significant for the airflow resistivity of open cell polyurethane foams.

5.6 Conclusions

The rebond foams had unexpectedly low airflow resistivity when compared with the much lower density virgin open cell foam and it is thought that this is due to the rebond foam manufacturing process removing the remnants of the cell membranes. The two lowest density rebond foams had airflow resistivities less than 10 kPa.s/m². It has been shown that the stiffness of the air contained in these specimens is significant when the dynamic stiffnesses of resilient layers made from these materials is to be calculated. BS EN 29052-1 cannot be used to determine the dynamic stiffness of resilient layers under floating floors comprising these materials therefore.

The results from the tests described in Chapter 3 suggested that their static stress-strain characteristics would make these foams better than low density virgin foam for use as resilient layers however. The results from the dynamic tests presented in Chapter 4 showed that the laboratory specimens made from these materials also had the lowest dynamic stiffnesses. These foams were therefore of considerable interest to this research programme. A method for including the stiffness of the air contained in the laboratory specimens in the measurement of their apparent dynamic stiffness had therefore to be devised to enable the determination of the dynamic stiffness of resilient layers comprising these foams. It was concluded that the best way to achieve this was to modify the test method described in BS EN 29052-1. This will be discussed further in Chapter 7.

5.7 References

- 1 BS EN 29052-1, 1992, *Acoustics-determination of dynamic stiffness-Materials used under floating floors in dwellings.*
- 2 CREMER L., HECKL M., UNGAR E.E., *Structure-borne sound, 2nd ed.*, Publ. Springer-Verlag , 1988.
- 3 BS EN 29053, 1993, *Acoustics, materials for acoustical applications - Determination of airflow resistance.*
- 4 COLLIER P., *The design and performance of non-linear vibration isolating materials*, PhD Thesis, Sheffield City Polytechnic, Sheffield, UK, 1985.

CHAPTER 6

FIELD MEASUREMENTS OF IMPACT SOUND

6.1 Introduction

The work described in the previous chapter showed that the two lowest density rebond foams tested have such low airflow resistivities that the Method described in BS EN 29052-1 cannot be used to determine their dynamic stiffness when used as resilient layers under floors. Their stress-strain behaviour and the results from measurements of the dynamic stiffness of specimens of these materials suggested that they would be the best foams to use as resilient layers under lightweight floating floors however.

Identifying their likely usefulness as resilient layers under floors led to discussions with the foam manufacturers. These, in turn, led to a programme of development with a company wishing to produce and market shallow profile lightweight floating floors. The development programme is briefly described because the results from this justify the interest in the 78 kg/m^3 rebond foam in particular as a resilient layer. Section 6.3 describes the field tests to measure the impact sound insulation of specimens of floating floor with different resilient layers. These were undertaken as a first step towards developing a method for predicting the improvement in impact sound insulation from using these lightweight floating floors. The results from the tests are presented and discussed. Concluding remarks regarding the development of a prediction method are to be found in the final section of this chapter.

6.2 Background: development programme

Lightweight floating flooring systems were to be produced which were intended to be easy to install and to give good impact sound insulation. The chosen form was of tongued and grooved sections which could be placed on an existing floor then quickly pushed together and glued into place. The most important part of the systems, the resilient layer, had still to be decided upon. It had already been demonstrated that rebond foam had better compression stress-strain characteristics than virgin foam for

use under floating floors and it had been decided to use a rebond foam. Dynamic tests had shown that rebond foam gave the laboratory test system described in Chapter 4 a lower natural frequency than virgin foam. It remained to identify the most suitable type of rebond foam to use and the optimum thickness for this application.

A series of tests was undertaken in the laboratory which has been described by Bougdah and Hall¹. The choice of the density of rebond foam and its thickness was based on the need to keep the flooring systems as shallow as possible, economics (the denser the rebond the more expensive it is) and the need for good isolation. It was assumed that the foam layer which gave the test system the lowest natural frequency was the most likely to give useful isolation over the widest range of frequencies. This approach took no account of the stiffness of the air enclosed in such a resilient layer but did at least allow comparisons between different materials and thicknesses. As a result of these tests, a resilient layer comprising an 8 mm thickness of 78 kg/m³ rebond foam was chosen for the systems.

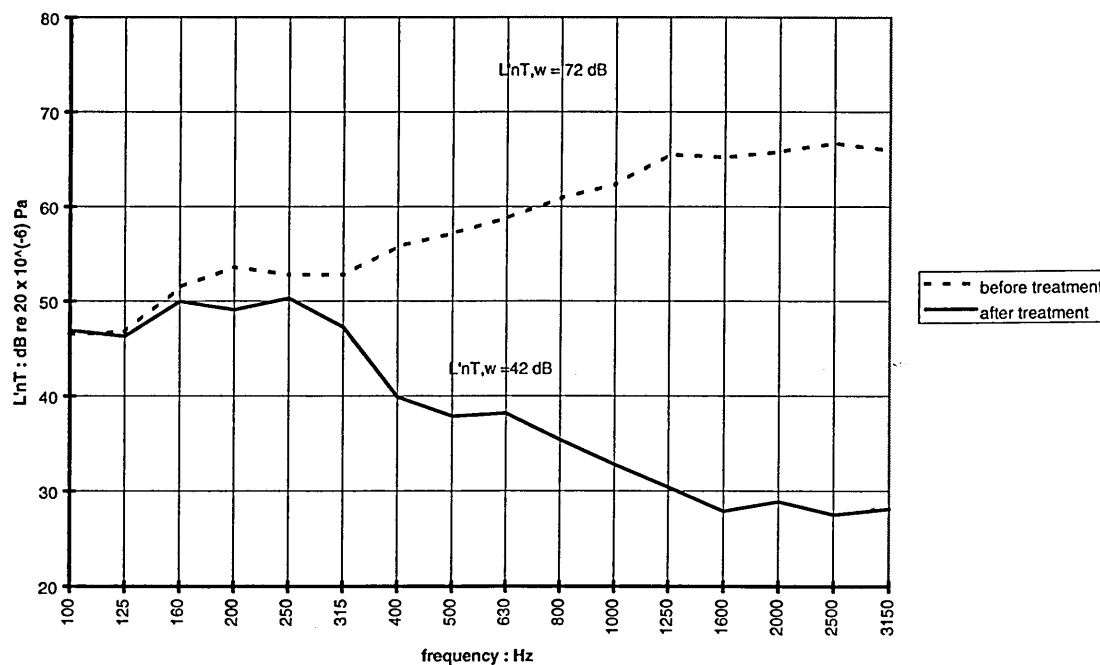


Figure 6.1: concrete floor before and after treatment with mdf system

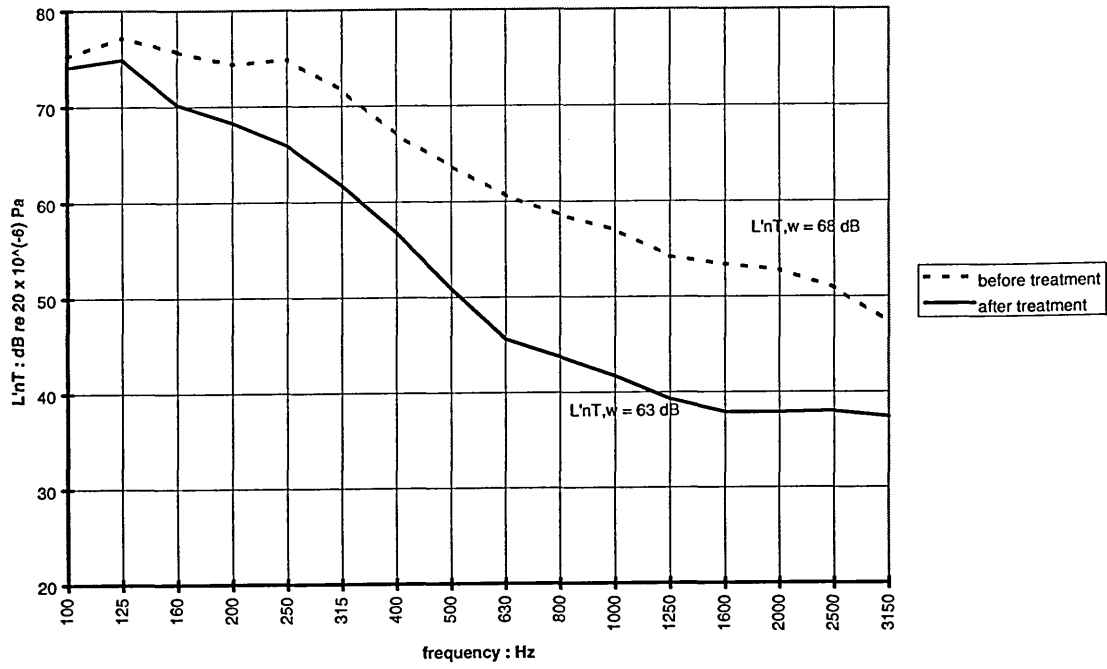


Figure 6.2: wooden floor before and after treatment with mdf system

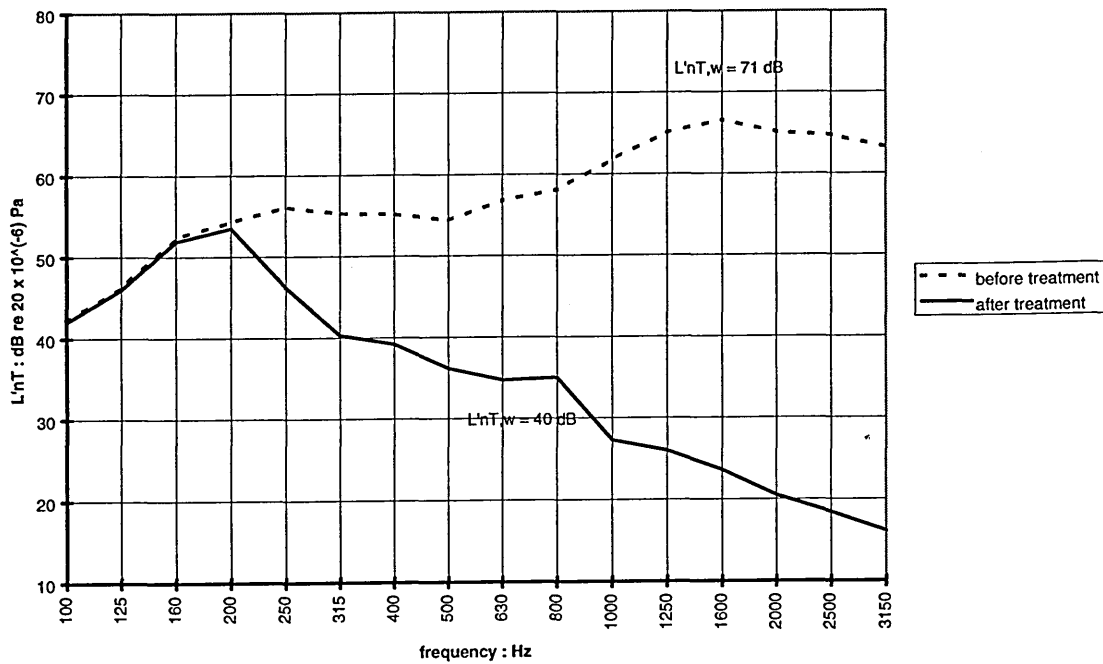


Figure 6.3: concrete floor before and after treatment with chipboard system

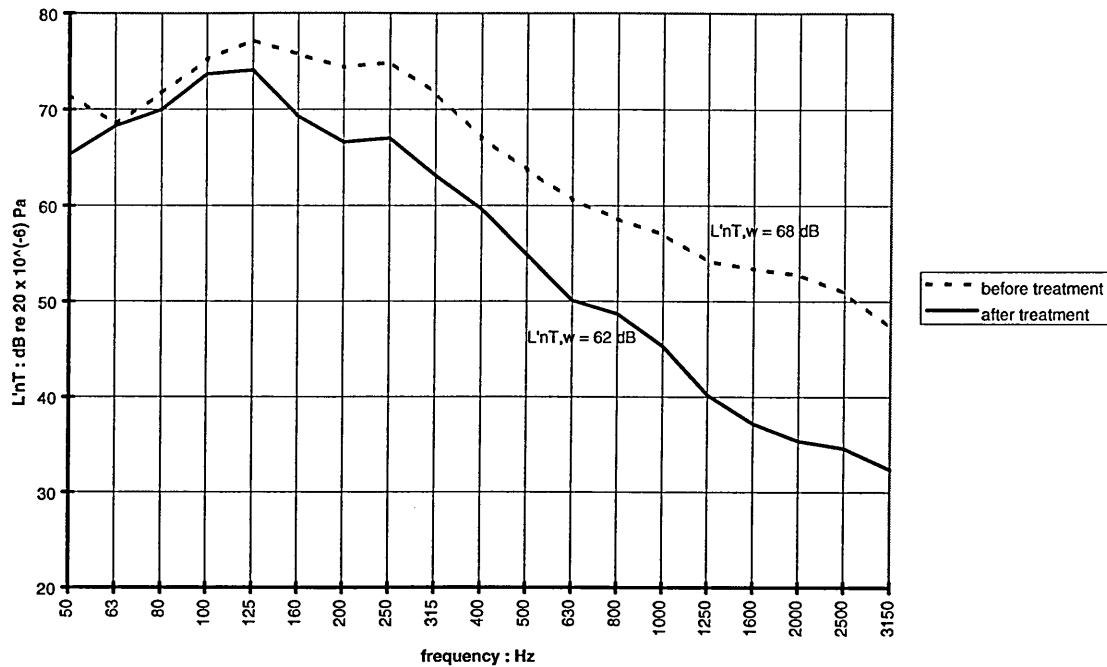


Figure 6.4: wooden floor before and after treatment with chipboard system

Having decided upon the design of the proposed products a small quantity of these were produced and their acoustic performance was tested in the field. The tests were carried out according to BS 2750 Part 7² on both wooden and concrete floors and showed that the products performed well in both situations as is shown by Figures 6.1 to 6.4. Both mdf and flooring grade chipboard systems were produced. The mdf used was 9 mm thick and the chipboard 18 mm.

On the concrete floor a (3.6 x 4.2) m² section of mdf flooring and a (2.4 x 6.0) m² section of chipboard flooring were tested on a much larger supporting floor. The performance of the two systems was then measured on timber a supporting floor in a large Victorian house which was to be refurbished. The floor was (4.1 x 4.75) m² in area and was completely covered by the floating floor. These floating floor systems are now being produced and are commercially available.

It remained to correlate the results of the laboratory tests on the foams with the acoustic performance of systems in the field which incorporated them as resilient layers however. In particular a method for predicting the likely improvement in impact sound insulation to be derived from using such a floating floor was needed, especially given growing

availability of such systems. The first step in the development of such a method was to carry out field tests to measure the acoustic performance of these floors with as many different types of resilient layers as possible.

6.3 Testing method

Field tests were carried out according to the method described in BS 2750 Part 7² to obtain the standardised impact sound pressure level beneath a concrete floor with an area of 29.5 m² in a (receiving) room having a volume of 85.4 m³, with and without floating floor samples. Since small (1.13 m x 0.52 m) samples of mdf flooring were used, only one (central) position was used for the standard tapping machine. This position was marked so that the samples of flooring could be placed in the same position for each test. Sound level measurements were carried out using a building acoustics analyser which controlled a rotating boom holding the condenser microphone used to sample the sound pressure. Measurements were taken in the Standard third octave bands between 100 and 3150 Hz.

The reverberation time in the receiving room was measured in three different positions as the rotating boom was stepped around one complete rotation. Two sets of measurements were taken so the reverberation time was calculated using six different measurements and at least three positions. The impact sound level was averaged, as the boom rotated continuously, over 48 s (three rotations each taking 16 s to complete) for the bare floor and 32 s for each of the samples of flooring. Background levels in the receiving room were measured over six rotations of the boom each taking 16 s, in order to ensure that any unrepresentative measurements caused by doors banging etc. could be discarded without compromising the validity of the results obtained.

Measurements were taken on two occasions and the impact sound level in the receiving room due to the standard tapping machine on the bare floor was measured at the start of each test series. On the first occasion mdf floating floor samples with resilient layers of different thicknesses of the same rebond foam (78 kg/m³) were tested. On the second occasion the same mdf flooring with different densities of rebond foam and one virgin foam were tested. Most of the floating floor samples originally had strips of denser foam around the two tongued edges. These were cut off with a circular saw as were the grooves on the other two sides to leave samples with the dimensions given earlier (1.13

m x 0.52 m). A full sized sample (1.2 m x 0.6 m) which had an 8 mm layer of 78 kg/m³ rebond attached was tested to see whether cutting the samples down had any significant effect on the results.

6.4 Results

The results from the field tests on the samples of mdf floating floor are shown in Table 6.1 and Table 6.2. Graphical representation of the data is given in Figure 6.5 and Figure 6.6. The data presented in these are from identically sized samples of 9 mm thick mdf : only the resilient layers are different. It can be seen from Figure 6.5 that the resilient layer comprising 6 mm thick rebond foam performs significantly worse than the thicker layers in the frequency range 200 to 1000 Hz and that, although there is little overall difference in performance between the three other layers, as the thickness of the layer increases so the acoustic performance of the floating floor specimen improves between 100 and 1000 Hz.

The different acoustic performance of the sections of flooring is reflected in the figures for the weighted standardised impact sound pressure level ($L'_{nT,w}$) given in Table 6.1 which show an improvement of 1 dB for an increase in the thickness of the resilient layer of 2 mm between 12 and 16 mm. The flooring sample with the 6 mm thick resilient layer gave a value for $L'_{nT,w}$ of 45 dB, 2 dB worse than the next thinnest layer and the maximum value for L'_{nT} occurred at 250 Hz. The maximum L'_{nT} values for the systems with thicker foam layers occurred at 200 Hz, with the 12 mm layer, and at 160 Hz with systems having 14 and 16 mm layers.

The performance of the floating floor samples with different types of foam as the resilient layer can be compared by examining Table 6.1 and Figure 6.6. The foam layers were of roughly equal thickness and all were considerably more dense than the only virgin foam tested. Figure 6.6 shows that the 128 kg/m³ foam had the worst performance of the rebond foams. All the other rebond foams had very similar performance across the whole frequency range shown although the 64 and 96 kg/m³ rebond foams had the best performance up to 250 Hz. The highest values of L'_{nT} for all the rebond foam systems were recorded in the 200 Hz third octave band with the lowest value in this band being recorded with the system comprising the lowest density rebond.

The floating floor sample with the virgin foam layer had the best performance between 100 and 200 Hz after which its behaviour was similar to the 128 kg/m³ rebond foam system. For the sample with the virgin foam layer, the highest value for L'_{nT} was recorded in the 250 Hz third octave band although at 200 Hz L'_{nT} was only 0.5 dB lower. The L'_{nT,w} values for these systems hardly varied, all were 44 dB apart from the 128 kg/m³ resilient layer system which was 45 dB. The two most dense rebond resilient layers reduced the acoustic performance of the supporting floor at frequencies below 250 Hz.

The comparison between the two sizes of flooring samples with the 8 mm rebond resilient layer can be seen in Figure 6.7 which shows virtually no difference in the performance of the two samples below 400 Hz and very little difference above this frequency. Both samples gave L'_{nT,w} values of 45 dB and both virtually identical maximum values for L'_{nT} of 56.3 dB, for the smaller sample, and 56.1 dB at 250 Hz.

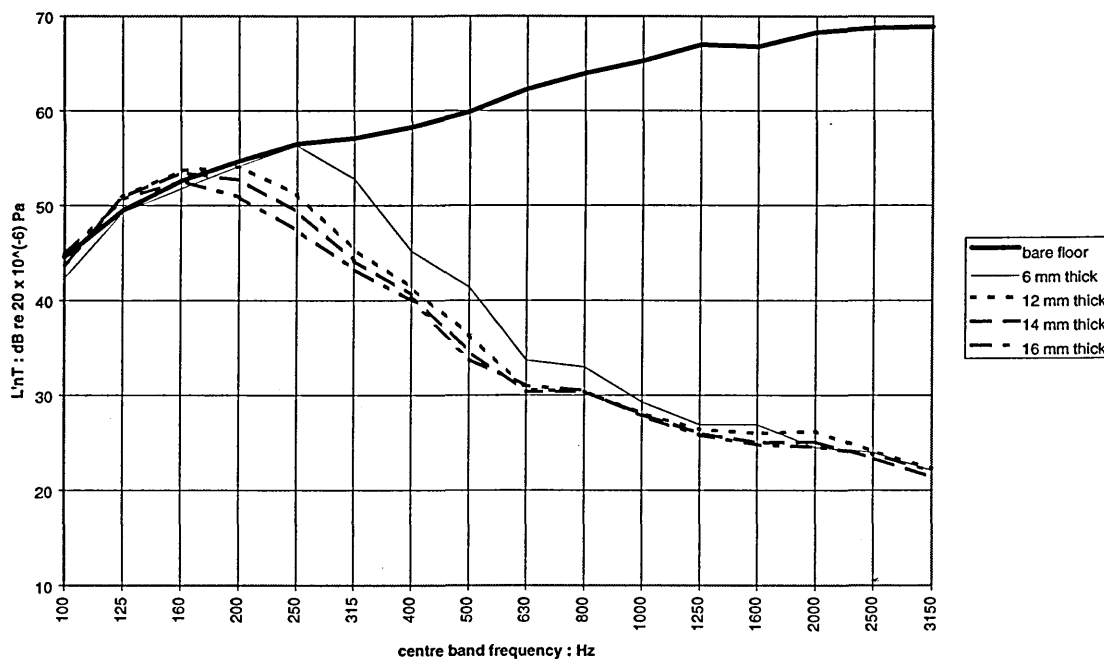


Figure 6.5: L'_{nT} for different thicknesses of 78 kg/m³ rebond.

L'_{nT}					
centre band frequency: Hz	bare floor dB	6 mm dB	12 mm dB	14 mm dB	16 mm dB
100	44.6	42.4	43.8	43.9	44.9
125	49.5	49.3	51.0	50.9	50.7
160	52.6	51.8	53.7	53.5	52.6
200	54.7	54.2	54.1	52.7	50.9
250	56.5	56.3	51.2	49.4	47.4
315	57.1	52.8	45.4	44.2	43.3
400	58.3	45.2	41.4	40.6	40.0
500	59.9	41.4	36.4	34.6	33.8
630	62.3	<i>33.7</i>	<i>30.6</i>	<i>30.4</i>	<i>31.0</i>
780	64.0	33.0	<i>30.4</i>	<i>30.4</i>	<i>30.5</i>
1000	65.3	<i>29.3</i>	<i>28.1</i>	<i>28.0</i>	<i>27.8</i>
1250	67.0	<i>26.9</i>	<i>26.4</i>	<i>26.0</i>	<i>25.8</i>
1600	66.8	26.9	26.0	25.0	24.8
2000	68.3	<i>24.5</i>	26.2	25.1	<i>24.6</i>
2500	68.8	<i>24.0</i>	<i>24.1</i>	<i>23.4</i>	<i>23.8</i>
3150	68.9	<i>22.1</i>	<i>22.3</i>	<i>21.4</i>	<i>22.0</i>
$L'_{nT,w}$	74	45	43	42	41

Table 6.1: impact sound pressure level for systems with different thicknesses of 78 kg/m³ rebond foam layers

Figures in italic are adjusted for background levels.

		L'_{nT}: re 20 x 10⁻⁶ Pa				
		resilient layer density: kg/m³				
		rebond				virgin
centre band frequency Hz	bare floor	64	96	128	144	28
100	44.7	43.6	43.3	43.6	44.4	42.2
125	47.7	47.6	48.2	47.7	48.6	46.8
160	52.6	52.9	54.7	54.2	55.1	52.6
200	54.8	54.8	56.1	57	56.2	54
250	56.2	53.6	53.7	56.3	53.7	54.5
315	58	49.1	47.8	51.3	48.4	52.2
400	58	44	43	44.9	43	45.4
500	60.2	39.3	38.5	42.5	38.1	41.1
630	61.4	30.8	31.3	35.1	31	33.3
780	62.8	30.5	30	32.2	30.1	33.7
1000	64.8	27.2	27.2	28.8	28	29.6
1250	65.9	25.4	26.1	26.6	26.5	28.1
1600	66.7	26.4	25.6	26.8	26.6	28.9
2000	67.7	26	26.3	26.1	26.4	26.8
2500	67.7	24.9	24.2	25.3	24.5	25.1
3150	67.9	23.2	23.2	24.3	23.4	21.9
L'_{nT,w}	73	44	44	45	44	44

Table 6.2: impact sound pressure levels for systems with different resilient layers

Figures in italic are adjusted for background levels.

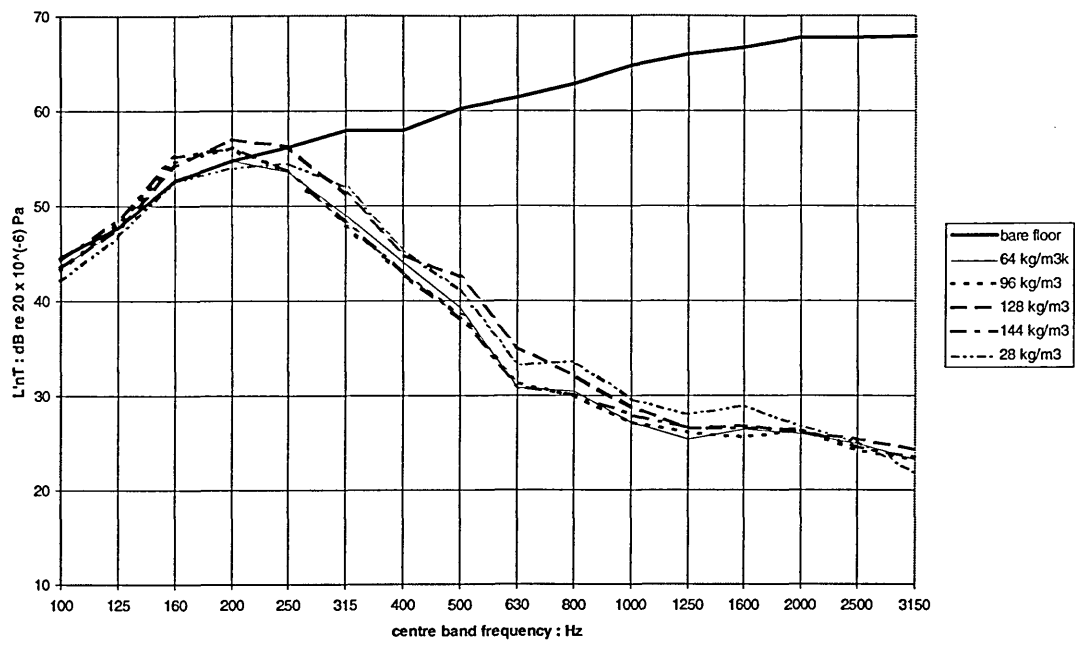


Figure 6.6: L'_{nT} for different resilient layers

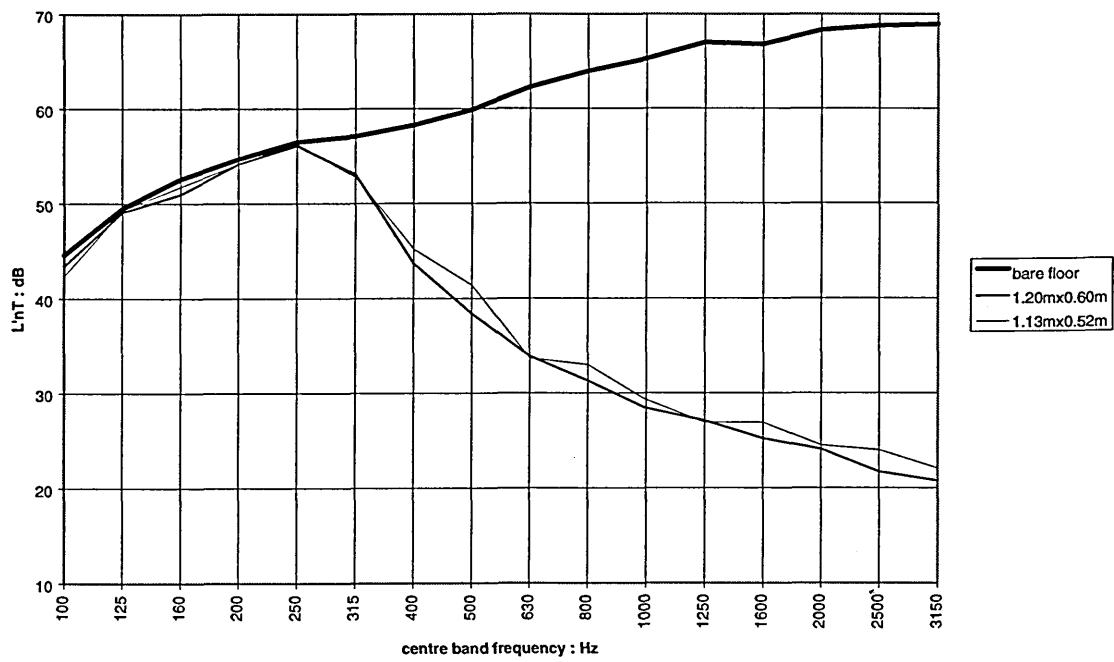


Figure 6.7: comparison of different sized samples with 78 kg/m³ rebond resilient layer

6.5 Discussion

The dynamic stiffness of a resilient layer under a floating floor is inversely proportional to its thickness³. It was therefore expected that the systems with different thicknesses of the same, 78 kg/m³, rebond foam would perform better as the layer thickness increased. The results presented in the previous section show this to be the case. However, the results suggest that the stiffness of the air in the thin polyurethane resilient layers might not dominate their performance in the same way that it does in fibre quilts. There is no point in making a fibre quilt layer less than the 25 mm thickness specified in the Building Regulations⁴ because below this thickness, the stiffness of the air enclosed dominates⁵. With the rebond polyurethane foam there is a measurable difference between the four thicknesses investigated.

The $L'_{nT,w}$ values in Table 6.1 suggest that there is a linear relationship between $L'_{nT,w}$ and resilient layer thickness over the small range of thickness tested. This is illustrated in Figure 6.8 which shows error bars to illustrate the uncertainty in each measurement point on the chart. A potential error of ± 1 mm was assumed in the measurement of the thickness of the resilient layers which was equivalent to the average standard deviation of a set of 15 measurements taken with each layer. The error in $L'_{nT,w}$ was taken to be ± 1 dB which is the limit of accuracy of the Standard rating procedure⁶, this is discussed further in Chapter 8.

The apparent linear relationship between thickness and $L'_{nT,w}$ could not be confirmed for other thicknesses or types of foam because none were available. Such a simple relationship would be surprising however. There is no linear relationship between the dynamic stiffness of the foam samples and their thickness and, as will be explained in Chapter 8, the improvement in impact sound insulation is proportional to the logarithm of the reciprocal of the natural frequency of the floating floor multiplied by 40.

Figure 6.6 is a graphical representation of the data given in Table 6.2. These show the results from measurements with flooring specimens having different densities of foam as resilient layers. It can be seen that although the systems perform differently all but one had the same value for $L'_{nT,w}$. This perhaps serves to demonstrate the insensitivity of the rating procedure and to emphasise the significance of the performance around a

system's resonant frequency. It is noted however that only the systems with the least dense rebond and the virgin foam did not reduce the impact sound insulation of the supporting floor around what appears to be a resonance for these systems. Nevertheless, if correlation were to be identified between laboratory tests and impact sound insulation it would be expected that the dynamic stiffness of specimens from these materials would be very similar.

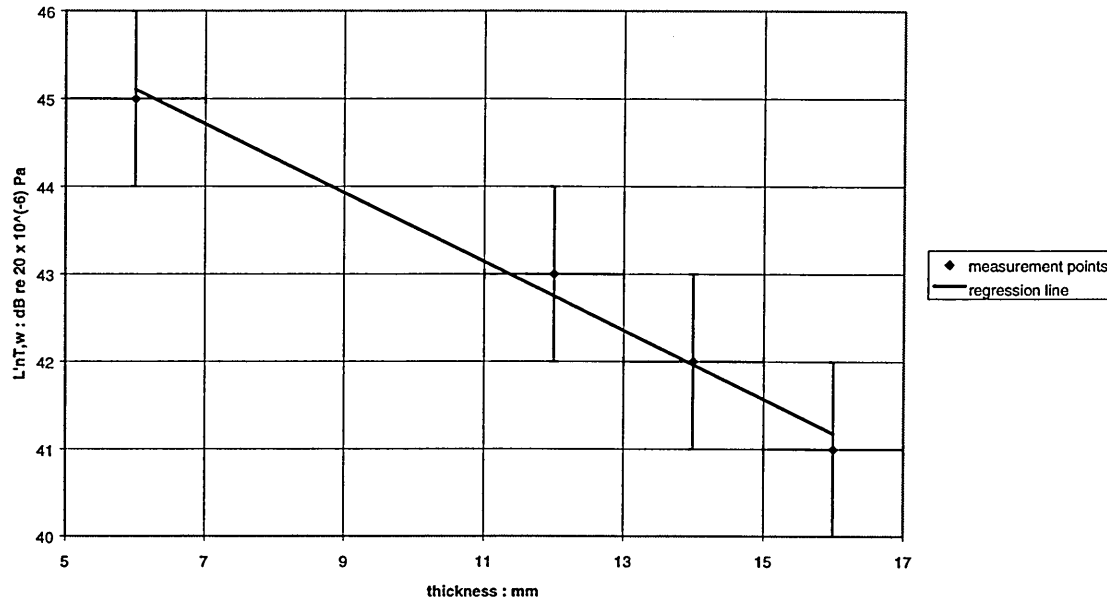


Figure 6.8: $L'_{nT,w}$ versus thickness for 78 kg/m^3 rebond foam layers.

6.6 Conclusions

The field tests on the samples of floating floor systems comprising different thicknesses of the same resilient layer showed that as the thickness of the resilient layer increased the acoustic performance of the system improved. The dynamic tests discussed in Chapter 4 had shown that as the thickness of the test specimens increased their dynamic stiffness was reduced. It ought to be possible, therefore, to relate the results from laboratory tests such as these to the acoustic performance of the systems with the different layers. However, for the reasons discussed in Chapter 5, it would be necessary to include the effect of the air in the laboratory test specimens if a method for predicting the acoustic performance of lightweight floating floors were to be developed. This will be discussed in the next chapter.

It was decided that specimens should be cut from the resilient layers of the systems tested in the field so that these could be tested in the laboratory. Attempts should also be made to include the effect of the air enclosed in the specimens in these laboratory tests since the 78 kg/m^3 rebond foam had an airflow resistivity less than $10 \text{ kPa}\cdot\text{s/m}^2$. The approach adopted is described in the next chapter which provides the link to the final part of the prediction method for $L'_{nT,w}$. Lastly it was shown that removing the tongued and grooved joints and thereby reducing the size of the sections of flooring did not affect their impact sound insulation significantly. It remains to be seen whether individual sections of floating floor can realistically represent the performance of complete floors.

The systems comprising the denser foam layers generally performed less well and tended to reduce the impact sound insulation for the system between 125 and 250 Hz. $L'_{nT,w}$ remained virtually constant for all the different systems with resilient layers of similar thickness. This result could be significant. It suggests that denser foam could be specified for use under a floor without significantly worsening the rating of the system if extra load bearing capability were required.

6.7 References

- 1 Bougdah H., Hall R., Impact sound insulation of floors using recycled polyurethane foam, *Proc CLIMA 2000*, 1997.
- 2 BS 2750, 1978 , *Measurement of sound insulation in buildings and of building elements, Part 7, Field measurements of impact sound insulation of floors.*
- 3 HILYARD N.C., Hysteresis and energy loss in flexible polyurethane foams, *Low Density Cellular Plastics; Physical Basis of Behaviour*, Ed Hilyard N.C., Cunningham A. Chapman and Hall, London , 1994.
- 4 DEPARTMENT OF THE ENVIRONMENT AND THE WELSH OFFICE, *The Building Regulations, Resistance to the passage of sound, Approved Document E* 1991.
- 5 JOHANSSON C., ANGREN A., Development of a lightweight wooden joist floor, *Applied Acoustics*, 1994, 43, 67-79.
- 6 BS 5821, 1982, *Rating the sound insulation of buildings and of building elements, part 2, Method for rating the impact sound insulation.*

A NEW METHOD FOR MEASURING THE DYNAMIC STIFFNESS OF RESILIENT LAYERS

7.1 Introduction

The importance of the dynamic stiffness of resilient layers in the sound insulation of floating floors is stated in the Building Regulations¹. In order to predict the performance of the lightweight floating floor sections tested in the field, the dynamic stiffness of their resilient layers must therefore be determined. The review of the literature has established that this dynamic stiffness includes the contribution of the air contained in the material comprising the resilient layer^{2,3}. Due to the small specimen size and small amplitudes used in the Method described in BS EN 29052-1 the air contained in the specimens has no effect on the test results²: the air is free to move laterally in and out of the sample.

BS EN 29052-1 states that in order to relate the dynamic stiffness of a resilient layer under a floor to that of laboratory specimens, the airflow resistivity of the material must first be measured. For materials having intermediate airflow resistivity ($100 \text{ kPa}\cdot\text{s}/\text{m}^2 > r > 10 \text{ kPa}\cdot\text{s}/\text{m}^2$) the stiffness of the air contained must be added to that of the specimen⁴. If the airflow resistivity of such a layer is less than $10 \text{ kPa}\cdot\text{s}/\text{m}^2$ and the calculated air stiffness is significant compared with the specimen dynamic stiffness then the Method described therein cannot be used. The results presented in Chapter 5 showed this to be the case with two of the rebond foams, in particular the $78 \text{ kg}/\text{m}^3$ rebond foam which is used in commercially available flooring systems. It was therefore felt that a method of including the dynamic stiffness of the air contained in the laboratory test specimens had to be developed.

This chapter describes a series of laboratory tests to find the dynamic stiffness of specimens cut from the resilient layers of the sections of flooring used in the field tests

described in Chapter 6. The Standard Method to determine the apparent dynamic stiffness of laboratory specimens from resilient layers was described in Chapter 4. A novel modification to the method is proposed which includes the effect of the air contained in the specimens in the determination of apparent dynamic stiffness. This means that the specimens' dynamic stiffness can be directly related to that of resilient layers, comprising the same foam, under floating floors. This, in turn, ought to allow the prediction of the impact sound insulation offered by floating floors comprising these layers. There remains the problem of the low load imposed by the lightweight floating floors of interest to this research on the resilient layer however. BS EN 29052-1⁴ states that it does not apply to systems with such lightweight floating surfaces. The method for predicting the impact sound insulation of these lightweight floating floors is discussed in Chapter 8.

Although the measurement of damping is not required by the BS EN 29052-1 the method specified does allow its measurement. Since the damping in a resilient layer may significantly affect the performance of floating floors at their resonant frequency it was felt that the data collected should be used to estimate the loss factors of the different types of foam. The damping in the test systems was therefore measured and the results obtained are compared with those of other researchers investigating the performance of virgin foams. No reference to the damping inherent in rebond foam has been found.

7.2 Testing method

When closed cell foams are tested according to the method described in BS EN 29052-1 a fillet of petroleum jelly is used to seal the joint between the specimen and the base on which it is placed. The fillet is needed to ensure that air does not move laterally beneath the test specimen since this could affect the results obtained from the test. It was decided that a fillet of petroleum jelly could also be used with the open cell foam specimens to prevent the air moving laterally out of the sample. By so doing it was intended that the stiffness of the air contained in the test specimen, as well as the stiffness of the foam itself, would play a part in the tests.

Three foam specimens were cut from each of the samples of floating floor whose

acoustic performance had been measured on the concrete supporting floor. The specimens were cut from the resilient layer as shown in Figure 7.1 and tested using the method and apparatus described in Chapter 4 to determine the system's resonant frequency. The dynamic stiffness of the specimens was then calculated as described in Chapter 4.

When the resonant frequency with each specimen had been obtained, the edges of the specimen and the joints between the base and the load plate were completely sealed with petroleum jelly and the test was repeated. This is illustrated in Figure 7.2. Sealing the specimen should contain the air within the test system and in this way the stiffness of the air in the specimen could be included in the laboratory tests. The sealed specimen resonant frequency was then obtained and the dynamic stiffness calculated as before.

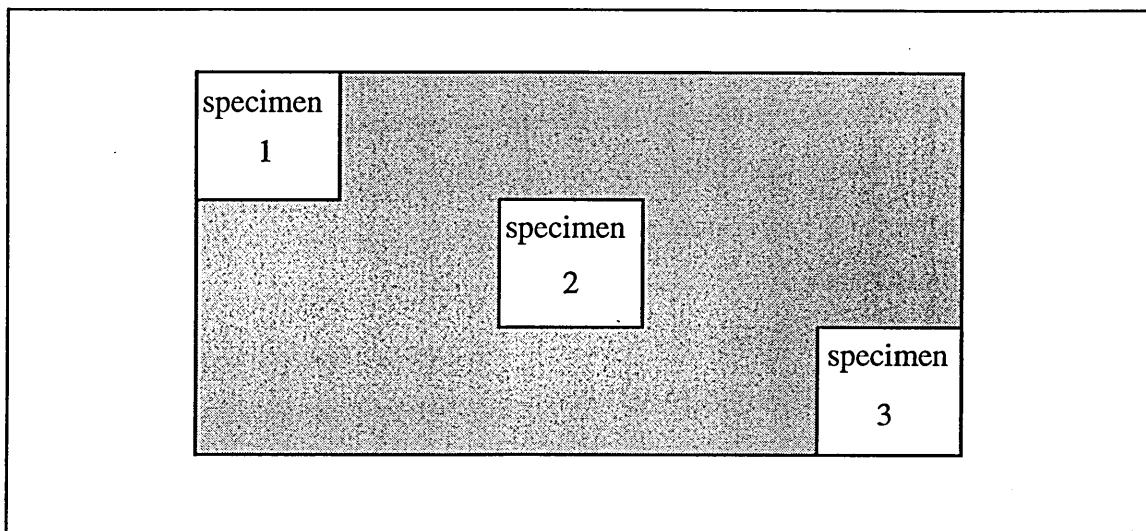


Figure 7.1: specimens cut from floating floor resilient layer.

This approach meant that the dynamic stiffness of the unsealed specimens could be obtained and the air stiffness calculated, using Equation 5.4, and added to the specimen stiffness. The value for dynamic stiffness obtained in this manner could then be compared with the dynamic stiffness of the same test specimen with its edges sealed. It could then be seen whether sealing the edges of the sample gave the expected increase in specimen dynamic stiffness.

In addition to determining the dynamic stiffness of the specimens the damping in the

test systems was also measured using the method adopted by Sueyoshi and Tonosaki⁵ which was described in Chapter 4. This would allow the damping of the reconstituted foams to be compared with the damping in virgin foams measured by other researchers. It could also be seen whether sealing the test specimens had any effect on the damping in the test system.

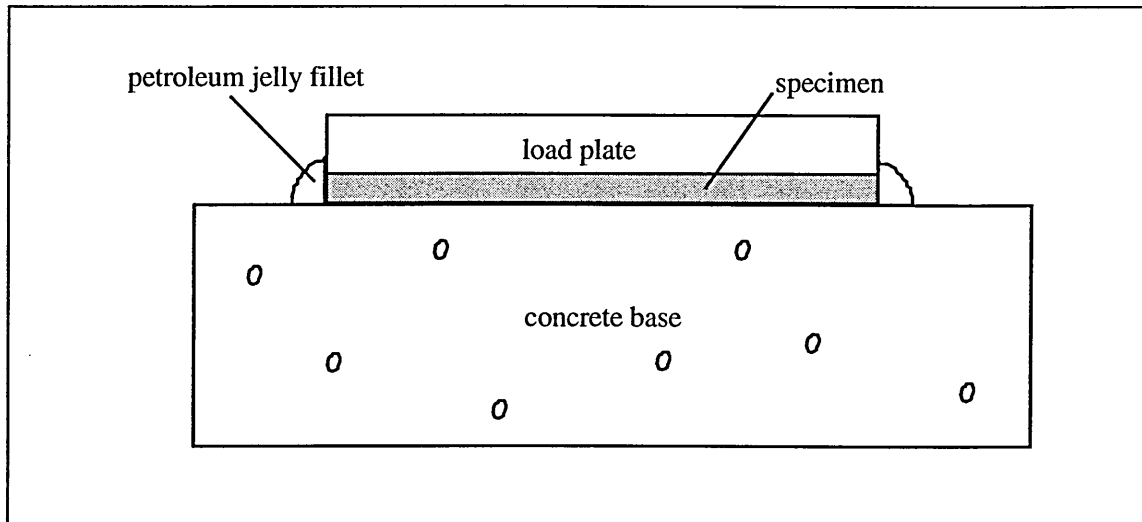


Figure 7.2: petroleum jelly sealing the edges of the test specimen.

7.3 Results

Table 7.1 shows the resonant frequencies and the calculated values for the dynamic stiffnesses of the different test systems. In each case the mean value obtained from the specified⁴ three test specimens is given with the standard deviation of the values shown in brackets. The standard deviations were used to estimate the potential error in the values of dynamic stiffness.

The limits of error in the values for dynamic stiffness in the last column include the estimated errors in the determination of resonant frequency and assume a variation of ± 1 mm in the thickness of the foam layers. Comparison of the values for dynamic stiffness in the last two columns shows that, although some values lie within the estimated limits of accuracy, the test systems with the sealed specimens generally give higher values for dynamic stiffness than using the calculated the air stiffness.

Table 7.2 shows the results from the measurements of the damping in the unsealed and sealed test systems. Again the values shown are the mean values from three tests, in each case, with the standard deviations used to estimate the accuracy of the measurements. The mean values of the loss factors for all but the 128 kg/m³ foam are higher when the specimens are sealed but, when the potential errors in the values are considered, only with the 28 kg/m³ virgin foam did there appear to be any significant increase in damping measured.

Examples of the accelerance and input-output phase difference curves for the test system with the 6 mm thick 78 kg/m³ rebond foam are shown in Figures 7.3 and 7.4. It can be seen that the output response peak is significantly reduced by sealing the system as well as being shifted to a higher frequency. All the examples of the accelerance curves presented show the response of the test system before and after the edges of the same test specimen were sealed.

density of foam: kg/m ³	thickness of foam: mm	f _r unsealed: Hz	f _r sealed: Hz	sample dynamic stiffness unsealed: MN/m ³	sample dynamic stiffness sealed: MN/m ³	material dynamic stiffness plus calculated air stiffness: MN/m ³
64	10	45.5(1.0)	64.0(1.5)	15.4±0.7	30.4±1.5	26.5±2.1
96	11.5	43.0(2.5)	62.5(2.5)	13.7±1.7	29.0±2.4	23.4±1.6
128	9	62.5(1.0)	74.0(1.0)	29.0±1.0	40.7±1.1	41.3±2.6
144	11	44.0(1.0)	62.0(1.5)	14.4±0.6	28.6±1.4	24.5±1.6
28	8	62.0(1.0)	76.0(2.0)	28.6±0.8	42.9±2.3	42.5±2.8
78	6	42.5(1.0)	80.0(3.5)	13.4±0.6	47.6±4.2	31.9±4.3
78	12	31.0(1.0)	53.5(1.5)	7.1±0.5	21.3±1.2	16.4±1.3
78	14	27.5(2.0)	47.5(1.5)	5.6±1.0	16.8±1.0	13.5±1.6
78	16	24.0(1.5)	44.0(1.0)	4.3±0.5	14.4±0.6	11.2±1.0

Table 7.1: resonant frequency and dynamic stiffness for the test system with different foam specimens.

The damping in the 128 kg/m³ rebond foam appeared to be significantly reduced by sealing the specimen and examples of the system response for a sealed and an unsealed specimen are shown in Figure 7.5 and Figure 7.6. It can be seen that there is evidence of another resonance in Figure 7.6 and so the value for the loss factor was checked using Kennedy and Pancu's method⁶. The value for the loss factor (η) obtained was 0.14, identical to that obtained using Sueyoshi and Tonosaki's method. There is little difference in the amplitudes of the output response but the sealing the specimen has shifted the resonance curve peak to a higher frequency. With the other rebond foams sealing the specimens does not appear to have had a significant effect on the damping in the systems.

density of foam: kg/m ³	thickness of foam: mm	loss factor (unsealed)	loss factor (sealed)
64 kg/m ³	10	0.15(0.03)	0.17(0.02)
96 kg/m ³	11.5	0.26(0.03)	0.22(0.02)
128 kg/m ³	9	0.19(0.02)	0.14(0.01)
144 kg/m ³	11	0.19(0.03)	0.19(0.02)
28 kg/m³	8	0.12(0.02)	0.19(0.02)
78 kg/m ³	6	0.24(0.05)	0.30(0.03)
78 kg/m ³	12	0.20(0.03)	0.27(0.06)
78 kg/m ³	14	0.23(0.07)	0.25(0.03)
78 kg/m ³	16	0.20(0.05)	0.26(0.02)

Table 7.2: loss factors for the tests systems.

With the virgin foam, sealing the sample increased the damping significantly as can be seen by examination of Table 7.2. Figures 7.7 and 7.8 show examples of the system response with the virgin foam. It can be seen that the accelerance peak is significantly reduced by sealing the system.

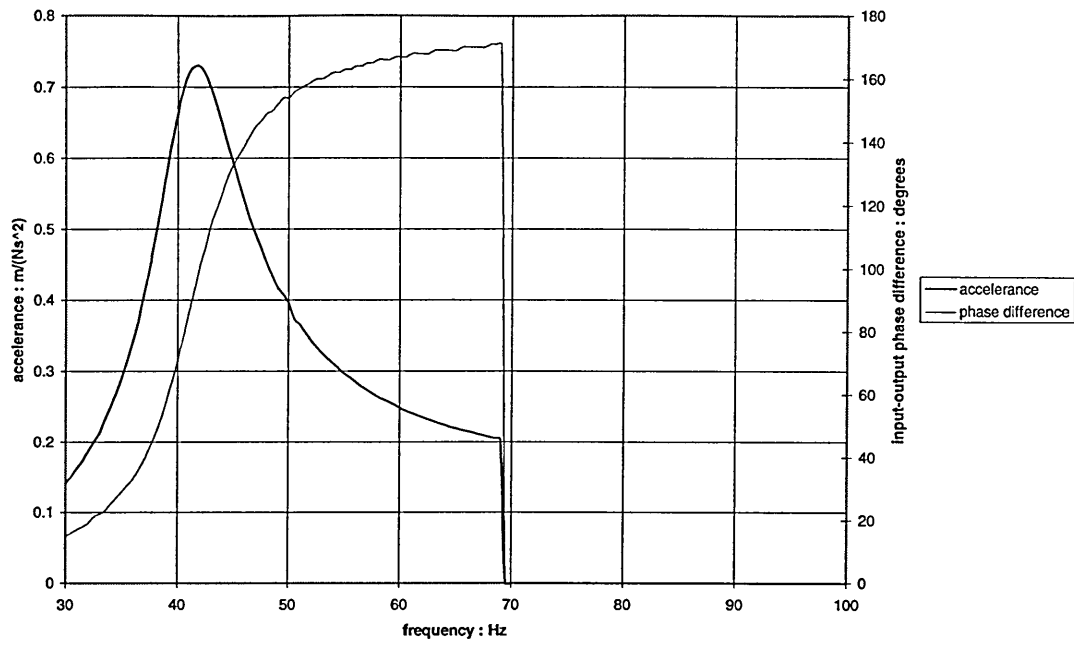


Figure 7.3: test system with 78 kg/m³ rebond; unsealed specimen

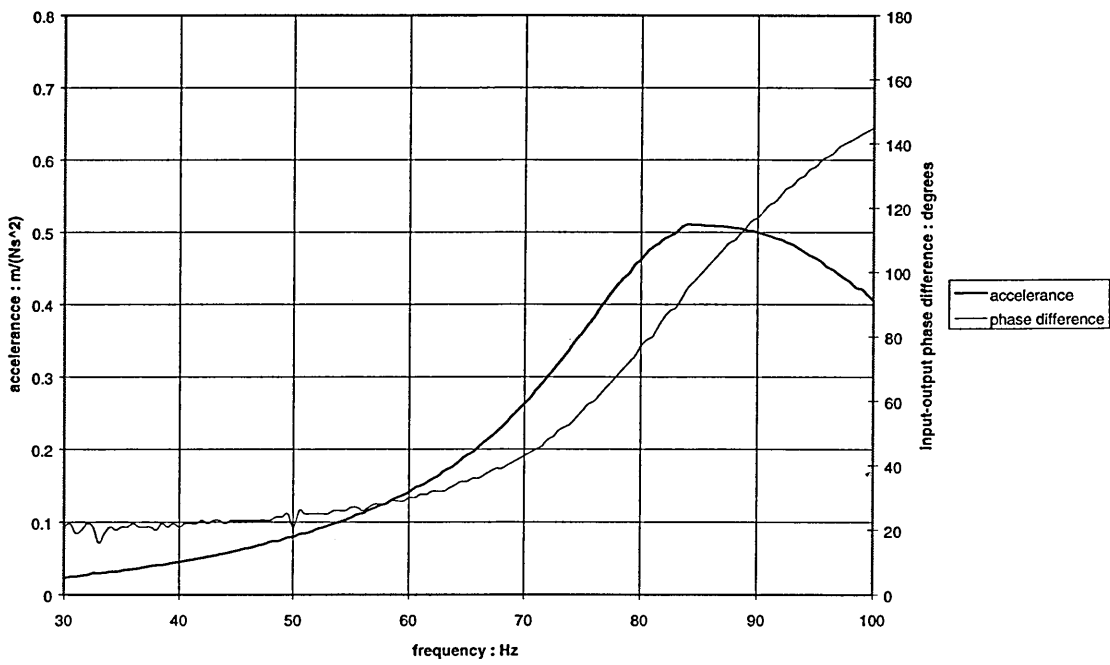


Figure 7.4: test system with 78 kg/m³ rebond; sealed specimen

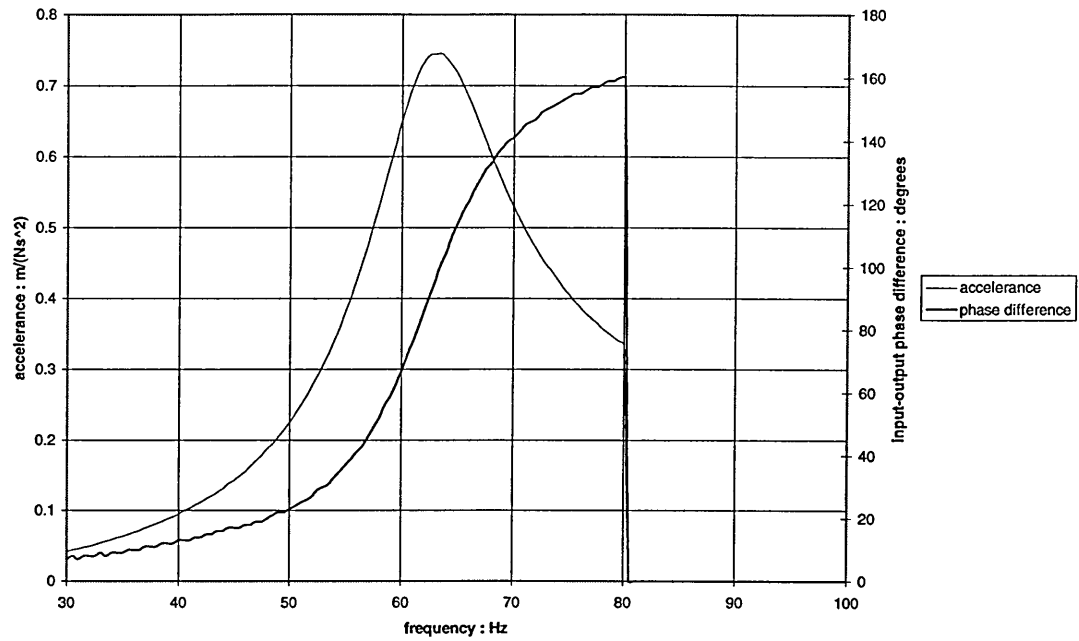


Figure 7.5: test system with 128 kg/m^3 rebond; unsealed specimen

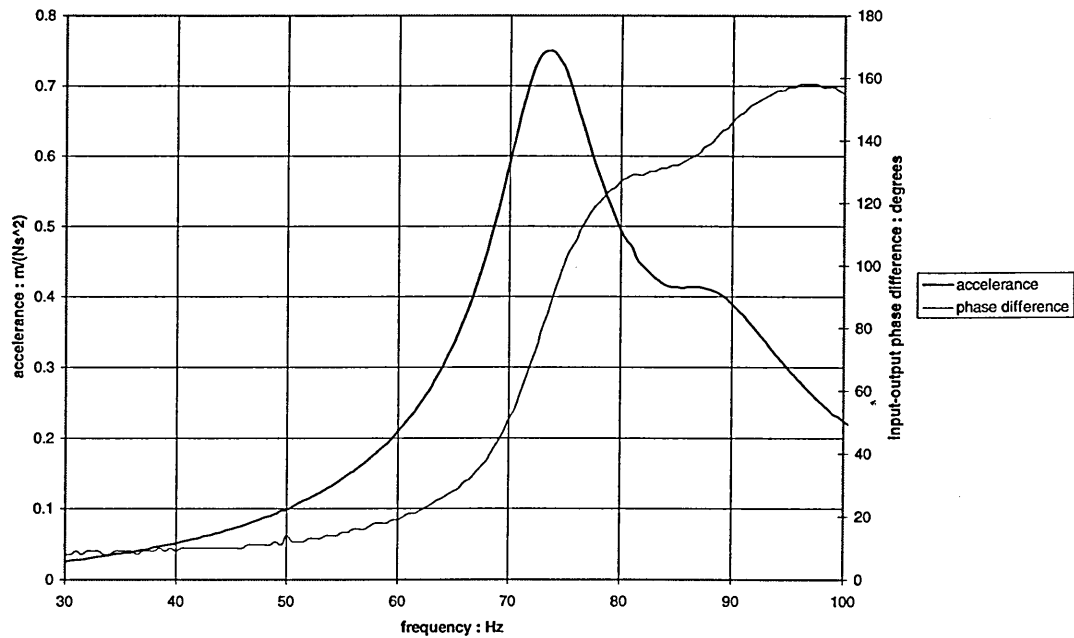


Figure 7.6: test system with 128 kg/m^3 rebond; sealed specimen

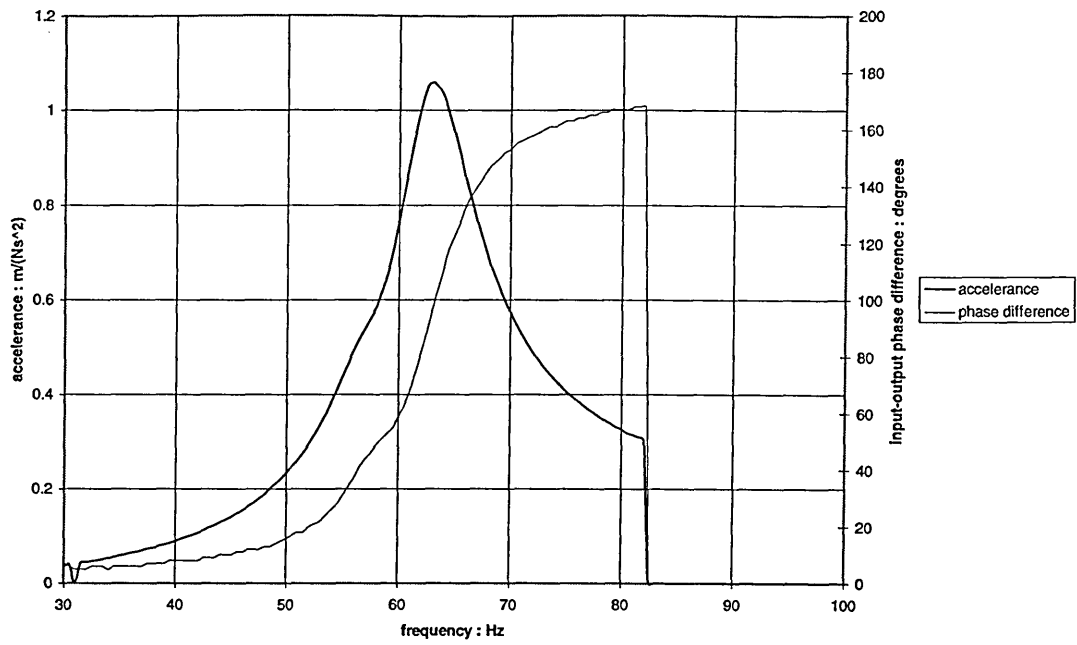


Figure 7.7: test system with 28 kg/m^3 virgin foam; unsealed specimen

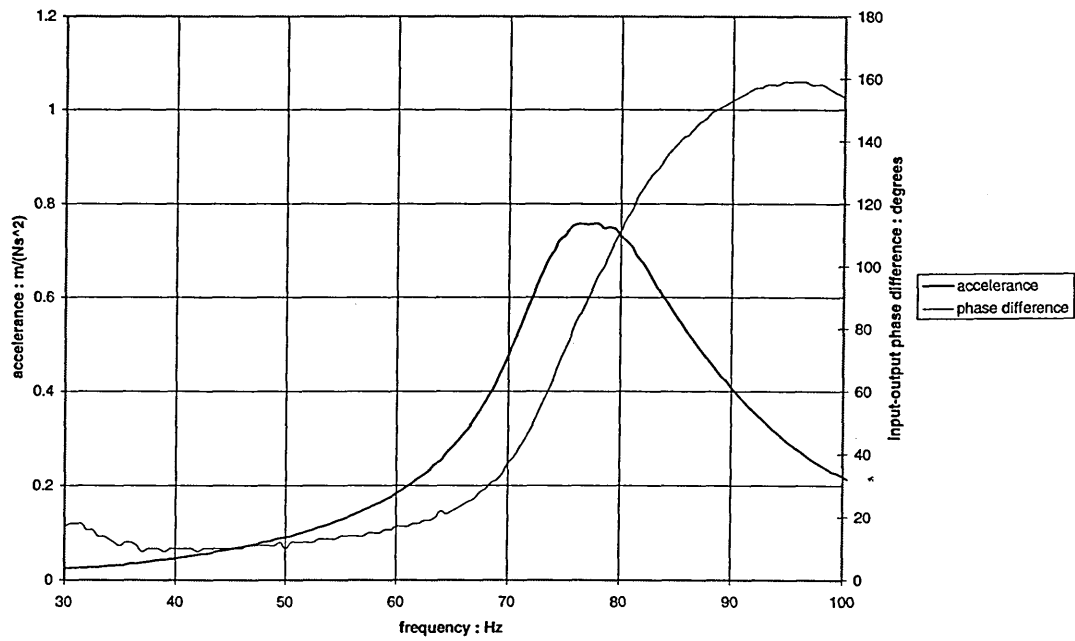


Figure 7.8: test system with 28 kg/m^3 virgin foam; sealed specimen

7.4 Discussion

The objective of the series of tests described in this chapter was to include the effect of the stiffness of the air contained in the test specimens in order to estimate the dynamic stiffnesses of the resilient layers of the sections of flooring tested in the field. This was particularly important for the 64 and 78 kg/m³ rebond foams due to their airflow resistivities being less than 10 kPa.s/m² (demonstrated in Chapter 5). This, according to BS EN 29052-1, means that the Method⁴ cannot be used to determine the dynamic stiffness of resilient layers under floating floors comprising these foams.

Not all the foams used as resilient layers in the field tests had had their airflow resistivities measured due to the unavailability of suitable samples but Table 5.1 shows that airflow resistivity increases with foam density for rebond foams. It also shows that rebond foams with densities between 96 and 144 kg/m³ have airflow resistivities between 10 and 100 kPa.s/m² so, according to the Standard⁴, Equation 5.4 can be used to calculate the stiffness of the air enclosed in the resilient layers.

Examination of Table 7.1 shows that, in most cases, the dynamic stiffness of the sealed test specimen was slightly higher than the value obtained by adding the calculated air stiffness to the dynamic stiffness of the unsealed specimen. When the estimated limits of accuracy in these values are taken into account however it can be seen that there is reasonably good agreement between the two methods of estimating the dynamic stiffness of the resilient layers. This is illustrated in Table 7.3 which shows the difference between the two methods in the third column. Only with the very thin (6 mm) 78 kg/m³ rebond foam is the difference in stiffness (ΔS_{dyn}) greater than 11% compared with the dynamic stiffness of the sealed systems. The uncertainty in the measurement of resilient layer thickness was taken to be ± 1 mm, as in the previous chapter, since it was found that the layer thickness varied by at least this amount over the area of the flooring sections.

density of foam: kg/m ³	thickness of foam: mm	ΔS_{dyn} MN/m ³	ΔS_{dyn} %
64 kg/m ³	10	0.8	3
96 kg/m ³	11.5	1.6	5.5
128 kg/m ³	9	0	0
144 kg/m ³	11	1.1	4
28 kg/m³	8	0	0
78 kg/m ³	6	7.2	15
78 kg/m ³	12	2.4	11
78 kg/m ³	14	0.7	4
78 kg/m ³	16	1.6	11

Table 7.3: difference in the values of resilient layer dynamic stiffness produced by the two methods of including the air stiffness.

It should be noted, when comparing the two sets of values for the dynamic stiffness including air stiffness, that Equation 5.4 is derived from Equation 5.3 and assumes an atmospheric pressure of 0.1 MPa and foam porosity of 0.9. Realistic variations from these two values of atmospheric pressure and porosity give insignificant differences in the values of air stiffness produced by using Equations 5.3 and 5.4. Equation 5.3 also assumes that the compression of the resilient layers take place isothermally however.

Cremer et al² state: for fibre quilts, at low frequencies, considering the thermal capacity and thermal conductivity of the fibres, isothermal compression is most likely. Previous research, reviewed by Hilyard^{7,8}, suggests that in the frequency range used in these laboratory tests, isothermal compression is also most likely with polyurethane foams. Equation 5.4 should hold for the calculation of air stiffness in these polyurethane foams therefore, despite the thermal capacity and thermal conductivity of the polymer frame material being substantially different from those of the fibres in quilts.

The uncertainty in the values of dynamic stiffness with the sealed and unsealed systems

given in Table 7.1 was estimated using the standard deviation from the set of three tests with each foam. The error in each individual measurement, estimated as described in Chapter 4, was also included. It can be seen, in Table 7.1, that the resonant frequencies of the sealed and unsealed test systems varied little over the three tests conducted with each type of foam. The value of the resonant frequency is the most likely source of error in the determination of dynamic stiffness since the square of this value is used in its calculation. A better idea of the accuracy of the Method would be gained from carrying out more tests on more samples and perhaps over a range of temperatures. Such an investigation was considered to be beyond the scope of this research programme because of the time and resources involved. Also, as was mentioned in the previous chapter, the procedure for rating the impact sound insulation of floors is only accurate to ± 1 dB.

It is felt however that the differences in the values of dynamic stiffness including air stiffness are sufficiently small that it can be claimed that there is insignificant difference in the two methods of including the air stiffness. Sealing the edges of the test specimens therefore results in the dynamic stiffness of the air enclosed in the specimen being realistically included in the laboratory tests.

The loss factors of the systems, given in Table 7.2, show that the rebond foams all exhibit a higher degree of damping than the virgin foam. The value for the virgin foam ($\eta = 0.12$) is in good agreement with the values obtained by Pritz^{9,10} for a 32 kg/m^3 polyurethane foam ($\eta \approx 0.1$). Pritz does not state that the foam has open cells but in a later work¹¹ he gives the loss factor of a polyethylene foam of density $\approx 30 \text{ kg/m}^3$ containing closed cells as about 0.1. Collier¹² found that $\eta \approx 0.1$ for virgin open cell polyurethane foam at small strains and 10 Hz and Sueyoshi and Tonosaki¹³ found the loss factor of their foam rubber to be around 0.08 although this contained closed cells. It appears therefore that the values for the loss factors measured in this programme of research are in agreement with those of other researchers.

It is difficult to generalise about the effect of sealing the test specimens on damping. The damping in the system with the virgin foam was significantly increased by sealing

the specimens but this was not necessarily so with the rebond foams. The mean values for the loss factors with the 78 kg/m^3 rebond foam increased when the specimens were sealed but when the estimated limits of accuracy are considered the increase is not significant. With the other rebond foams only the damping with the 128 kg/m^3 foam appeared to be significantly affected by sealing the specimens and in this case there was a reduction in damping. It is noted that this foam is also much stiffer than the other rebond foams which was suggested by the results of the field tests presented in the previous chapter. As air moves within the foam during sinusoidal excitation energy is lost to friction. Since sealing the test specimens prevents the air enclosed in them from moving laterally in and out of the test system it would be expected that the damping would be reduced in this circumstance. This only appeared to be the case with the 128 kg/m^3 foam.

It is likely that the fillet of petroleum jelly contributed significantly to the damping with the majority of the foam specimens but did not do so with the 128 kg/m^3 foam. This does not explain why the damping appeared to be significantly reduced with the virgin foam however. The measured dynamic stiffness of the virgin foam was virtually the same as that of the much more dense rebond foam. It may be that the internal structure of the virgin foam is important. Perhaps the remnants of cell walls play an important part in energy absorption as they are deformed during testing.

The measured value of η for the sealed system with the 128 kg/m^3 foam given in Table 7.2 was confirmed using Kennedy and Pancu's method. For completeness the shape of the curve constructed is shown in Figure 7.9. It can be seen that the smaller resonance around 87 Hz is clearly identified by the smaller circle on the curve. Despite this resonance, the comparison of the two methods for determining η showed again that the simpler method, of Sueyoshi and Tonosaki, is sufficiently accurate.

As was stated in Chapter 4, the damping in test specimens is only mentioned in BS EN 29052-1 because high levels may make the resonant frequency of the test system difficult to identify. Whether or not sealing the samples increases the damping in the test system is unimportant to the method for predicting the performance of floating floor

being developed. Damping may be important in the performance of floating floors however since it is this mechanism which is most significant in controlling the amplitude of vibrations around a system's resonant frequency¹³.

In a system comprising a mass subjected to forced vibration which is vertically separated from a heavier base by a parallel spring damper system with viscous damping, the magnitude of the force transmitted to the base is directly proportional to the damping in the system (η) as well as the stiffness¹⁴. The higher the damping therefore the greater will be the transmitted force at frequencies greater than $1.4f_0$, where f_0 is the floating floor mass-spring resonance frequency. It is perhaps of note, therefore, that Figure 6.6 indicates that the specimen of flooring comprising the 28 kg/m^3 virgin foam had the best performance around 200 Hz despite being stiffer than all the other foams.

It has been reported that a sample of floating floor with a rebond foam layer gave better performance at the resonance frequency than a system with the same thickness of virgin foam when placed on a timber supporting floor¹⁵. This was not observed in the tests on the concrete supporting floor described in Chapter 6 however: around its resonant frequency the virgin foam performed better than the other foam layers of similar thickness. The virgin foam was the least damped specimen prior to sealing its edges and after this was still one of the least damped. More results are needed before conclusions can be drawn but the relative importance of stiffness and damping on the acoustic performance of floating floors comprising polyurethane foam layers may be worthy of more research.

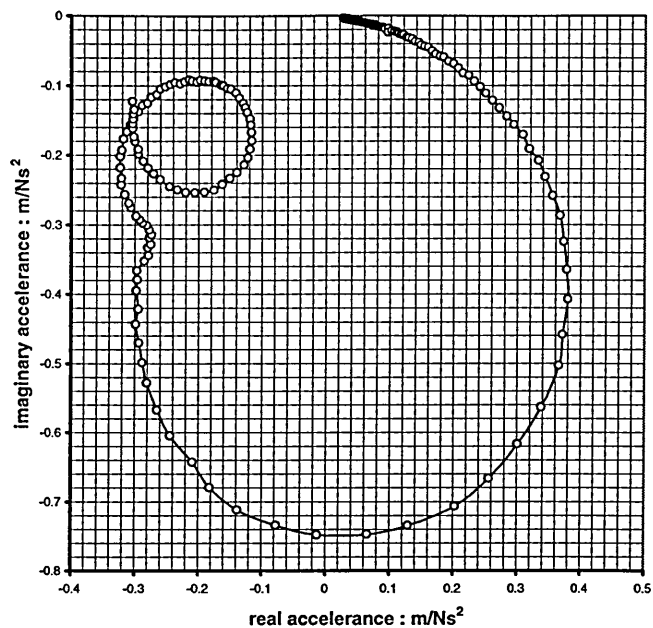


Figure 7.9: Kennedy and Pancu construction for η

7.5 Conclusions

From comparisons with other research and the results from the virgin foam tested in this research it appears that the rebond polyurethane foams are more highly damped than the virgin foams from which they are made. However, when measurements of damping are made using the test system described in BS EN 29052-1 the system should not be sealed.

The effect of the air enclosed in porous resilient layers under floating floors has to be included when estimating their dynamic stiffness. The results presented in this chapter demonstrate that sealing the edges of the specimens means that the effect of the air contained in them is included in laboratory tests. This should therefore allow the dynamic stiffness of the tests specimens to be taken as being representative of the dynamic stiffness of resilient layers under floating floors. This is particularly important for the 64 and 78 kg/m³ rebond foams since it allows the determination of their dynamic stiffness, when used under floors, despite their low airflow resistivity.

prEN 12354¹⁶ shows that the improvement in impact sound insulation obtained when a floating floor is placed on a supporting floor can be calculated if the mass-spring resonance frequency of the floating floor is known. The mass-spring resonance frequency is determined using the dynamic stiffness of the resilient layer so the modification to the method described in BS EN 29052-1 should allow ΔL to be calculated. Only the extreme lightness of the floating mdf surface remains to be accounted for. The choice of the prediction method is the subject of Chapter 8.

7.6 References

- 1 DEPARTMENT OF THE ENVIRONMENT AND THE WELSH OFFICE, *The Building Regulations, Resistance to the passage of sound, Approved Document E*, 1991.
- 2 CREMER L., HECKL M., UNGAR E.E., *Structure-borne sound*, 2nd ed., Publ. Springer-Verlag, 1988.
- 3 JOHANSSON C., ANGREN A., Development of a lightweight wooden joist floor, *Applied Acoustics*, 1994, 43, 67-79.
- 4 BS EN 29052-1, 1992, *Acoustics-Determination of Dynamic Stiffness-Materials used under Floating Floors in Dwellings*.
- 5 SUYEOSHI S; TONOSAKI M., Determination of localised dynamic behaviour of wood strip over foam rubber underlayment, composite flooring by random vibration, *Wood Sci. Technol*, 1993., Vol. 27, 11-21.
- 6 ZAVERI K., *Modal analysis of large structures-Multiple exciter systems*, ISBN 8787355035, Bruel and Kjaer, 1985.
- 7 HILYARD N.C., Dynamic mechanical behaviour, *Mechanics of Cellular Plastics*, Ed Hilyard N.C. Publ Applied Science Publishers Ltd. Barking, Essex, England, 1982.
- 8 HILYARD N.C., Hysteresis and energy loss in flexible polyurethane foams, *Low Density Cellular Plastics; Physical Basis of Behaviour*, Ed Hilyard N.C., Cunningham A. Chapman and Hall, London, 1994.
- 9 PRITZ T., Transfer function method for investigating the complex modulus of acoustic materials: spring-like specimen, *Journal of Sound and Vibration*, 1980, 72 (3), 317-341.
- 10 PRITZ T., Transfer function method for investigating the complex modulus of acoustic materials: rod like specimen, *Journal of Sound and Vibration*, 1982, 81 (3), 359-376.
- 11 PRITZ T., Dynamic young's modulus and loss factor of plastic foams for impact sound insulation, *Journal of Sound and Vibration*, 1994, 178 (3), 315-322.
- 12 COLLIER P., *The design and performance of non-linear vibration isolating materials*, PhD Thesis, Sheffield City Polytechnic, Sheffield, UK, 1985.

-
- 13 SUYEOSHI S; TONOSAKI M., Determination of localised dynamic behaviour of wood strip over foam rubber underlayment, composite flooring by random vibration, *Wood Sci. Technol.* , 1993, Vol. 27, 11-21
 - 14 BLAKE R.E., Basic vibration theory, *Shock and Vibration Handbook*, Ed Harris C.M., 4th Edition, Chapter 2, Publ Mcgraw-Hill, New York, 1996.
 - 15 MACKENZIE R.K., HALL R., Developments in the application of flexible open-cell polymer foams for impact sound reduction in floors, *Proc IOA*, 1996, Vol. 18 Part 3, 29-38.

IMPACT SOUND INSULATION OF FLOATING FLOORS

8.1 Introduction

Chapters 6 and 7 contain the results from acoustic tests conducted on the lightweight floating flooring and the results from laboratory measurements of dynamic stiffness respectively. The aim of this chapter is to identify a method of correlating the acoustic performance of the sections of floor with the results from the laboratory tests so that the impact sound insulation of lightweight floating floors can be predicted. Therefore, a review of earlier work into the prediction of impact sound is presented here. The relative merits of the different approaches to predicting the impact sound insulation of floating floors are discussed in relation to this research and the choice of prediction model adopted is justified.

A review of previous research into the measurement of the impact sound insulation of floors is presented later, in Chapter 10, which considers the usefulness of the ISO tapping with the lightweight floating floors of interest to this thesis. This chapter, therefore, concentrates on different approaches to the prediction of impact sound insulation. The impact sound insulation of floors has been the subject of much research but this thesis is concerned only with floating floors. Specifically, lightweight shallow profile floating floors comprising polyurethane foam resilient layers on concrete supporting floors. Therefore, although there is a huge body of research covering the performance of floors, e.g. timber joist floors, only the work relevant to this research is discussed in detail.

8.2 Background

According to Gudmundsson, in his review of the work on impact sound insulation of floating floors¹, the improvement in impact sound insulation (ΔL) due to the addition of a floating floor was defined by Gösele in 1948² as the difference between the sound

level in the receiving room with and without the floating floor. The first theoretical model identified for predicting ΔL is that described by Cremer³ and first published in 1952⁴. Cremer's model provided theoretical basis for the frequency dependence of ΔL , already identified empirically by Gösele⁵.

$$\Delta L = 40 \log \left(\frac{f}{f_0} \right) \text{ dB}$$

where f and f_0 represent the frequency of excitation and the floating floor's mass-spring frequency respectively. Cremer's model was possible because the addition of a floating floor does not change the characteristics of the ceiling in the receiving room. The absorption power and the radiating power of the ceiling associated with the floor remain the same⁶.

Cremer considered floating floors to be "locally reacting" which means that the force on the floating surface is transmitted to the supporting floor in the immediate vicinity of the excitation point. His model assumes that there is no reverberant field, due to reflections from the edge of the floating floor, contributing to the sound transmitted through the supporting floor to the receiving room below. This means that the floating floor is considered either to be of infinite extent or to consist of a material with internal damping sufficiently high to render the effect of edge reflections insignificant. However, it became apparent that there could be large deviations from the simple expression for ΔL derived by Cremer¹.

Deviations from Cremer's model can often be attributed to bridging of the resilient layer. There can be other explanations for the deviations: one of which is that, for some types of floating floor, the reflections from the edge of the floating slab are significant. This was, and is, the case with lightly damped floating slabs and in particular with the commonly used sand/cement screeds. Research aimed at modelling ΔL for lightly damped floors with significant edge reflections was therefore conducted.

In 1971, VÉR's important work on impact sound isolation, which included a model for predicting ΔL for lightly damped floating floors was published⁷. He derived an expression describing ΔL for floating floors supported on resilient mounts which

suggested that ΔL increased by 30 dB per decade (rather than Cremer's predicted 40 dB per decade).

According to Gudmundsson¹, it was VÉR who first described floors as locally and resonantly reacting. In deriving his expression, VÉR assumed that the impact sound transmission to the receiving room occurred over the whole area of the floating slab rather than at the point of excitation, as with Cremer's model. Therefore it was the resonant behaviour of the slab which determined the impact sound transmission.

Both Cremer's and VÉR's models assume that the resilient layer between the supporting floor and the floating floor can be treated as a lumped element, or as many lumped elements. The resilient layer is, therefore, regarded as a spring, or springs, with stiffness but no mass. At high frequencies, the mass of the resilient layer cannot be ignored and the layer has to be treated as a wave medium with distributed mass and stiffness.

According to Gudmundsson¹, this occurs at relatively low frequencies with the materials likely to be used in buildings. Gudmundsson therefore approached the prediction of ΔL from the premise that the resilient layer can be treated as a wave medium¹. This, along with the approaches to modelling the performance of floating floors mentioned above is discussed in detail in the next section.

8.3 The prediction of impact sound insulation with floating floors

8.3.1 Locally reacting floating floors

Cremer's model for the prediction of ΔL is important historically and will be described in detail because there are mistakes in the notation in the most widely available derivation of the model³. The author hopes that a detailed explanation will assist those who might find difficulty in following the derivation through for the first time. For this reason, the variables are, mostly, assigned the same symbols used in the aforementioned text³. Cremer based his derivation on the fact that floating floors can be modelled as two parallel plates coupled by a locally reacting interlayer of dynamic stiffness S_{dyn} . The plates each have bending stiffnesses B_1 and B_2 and uncoupled bending wave numbers k_1 and k_2 . The subscripts 1 and 2 refer to the floating floor and the supporting floor respectively.

The small pressure exerted on the two plates by the resilient layer is given by

$$S_{\text{dyn}}|\zeta_{d1} - \zeta_{d2}| \quad \text{N/m}^2$$

Equation 8.1

Where the variables (ζ_d) represent the vertical displacement amplitude of the coupled plates. Assuming only sinusoidal excitation of the plates and taking ζ to represent the phasors (rotating vectors) of the displacement, one obtains the following two coupled bending wave equations³:

$$-B_1 \nabla \nabla \zeta_1 - S_{\text{dyn}} (\zeta_1 - \zeta_2) = -\omega^2 m_1 \zeta_1$$

Equation 8.2

$$-B_2 \nabla \nabla \zeta_2 - S_{\text{dyn}} (\zeta_2 - \zeta_1) = -\omega^2 m_2 \zeta_2$$

Equation 8.3

where $\nabla = \frac{\partial^2}{\partial x^2} + \frac{\partial^2}{\partial y^2} + \frac{\partial^2}{\partial z^2}$ and m_1 and m_2 represent the surface densities of the two plates.

Using $\omega_1 = \sqrt{\frac{S_{\text{dyn}}}{m_1}}$ and $\omega_2 = \sqrt{\frac{S_{\text{dyn}}}{m_2}}$ (the natural frequencies of the two mass-spring systems comprising a plate and the resilient layer) one can substitute for S_{dyn} in Equations 8.2 and 8.3.

The bending stiffness of plates is given by³ $B = \frac{\omega^2 m}{k^4}$ and so also substituting for B_1

and B_2 in the two equations leads to

$$\left[\nabla \nabla - k_1^4 \left(1 - \left(\frac{\omega_1}{\omega} \right)^2 \right) \right] \zeta_1 - k_1^4 \left(\frac{\omega_1}{\omega} \right)^2 \zeta_2 = 0$$

Equation 8.4

$$-k_2^4 \left(\frac{\omega_2}{\omega} \right)^2 \zeta_1 + \left[\nabla \nabla - k_2^4 \left(1 - \left(\frac{\omega_2}{\omega} \right)^2 \right) \right] \zeta_2 = 0$$

Equation 8.5

Combining the two equations above leads to an 8th order differential equation which may be written³

$$\{(\nabla\nabla - k_I^4)(\nabla\nabla - k_{II}^4)\}(\zeta_{1,2}) = 0$$

Equation 8.6

Equation 8.6 implies that, for positive values of k_I^4 and k_{II}^4 , on each plate there is a bending wave field and a near field. The wave numbers k_{I1} and k_{21} refer to the bending wave fields of the floating floor and the supporting floor respectively. Similarly, k_{I11} and k_{211} represent the near fields on the two floors. These two pairs of coupled bending wave numbers are obtained from the solution of:

$$k_{I,II}^4 = 0.5 \left[k_1^4 \left\{ 1 - \left(\frac{\omega_1}{\omega} \right)^2 \right\} + k_2^4 \left\{ 1 - \left(\frac{\omega_2}{\omega} \right)^2 \right\} \right] \\ \pm \sqrt{\left(0.25 \left[k_1^4 \left\{ 1 - \left(\frac{\omega_1}{\omega} \right)^2 \right\} - k_2^4 \left\{ 1 - \left(\frac{\omega_2}{\omega} \right)^2 \right\} \right]^2 + k_1^4 k_2^4 \frac{\omega_1^2 \omega_2^2}{\omega^4} \right)}$$

Equation 8.7

The resonance frequency for the system comprising the two plates and the resilient layer is given by:

$$\omega_{12} = \sqrt{(\omega_1^2 + \omega_2^2)}$$

Equation 8.8

Above ω_{12} , k_I and k_{II} tend towards k_1 and k_2 respectively. Below this frequency k_{II} does not exist and k_I tends to:

$$k_I^4 = \omega^2 \left(\frac{m_1 + m_2}{B_1 + B_2} \right)$$

Equation 8.9

Cremer relates the displacement phasors (ζ) and the wave numbers (k) as

$$\frac{\zeta_{2I}}{\zeta_{1I}} = \frac{\left(\frac{\omega_2}{\omega}\right)^2}{\frac{k_1^4}{k_2^4} - 1 + \left(\frac{\omega_2}{\omega}\right)^2} = \varepsilon_I$$

Equation 8.10

$$\frac{\zeta_{1II}}{\zeta_{2II}} = \frac{\left(\frac{\omega_1}{\omega}\right)^2}{\frac{k_{II}^4}{k_I^4} - 1 + \left(\frac{\omega_1}{\omega}\right)^2} = -\varepsilon_{II}$$

Equation 8.11

ε_I and ε_{II} were chosen so that they have small positive values at high frequencies, when the coupling is weak.

In his discussion of the impedance of plates³, Cremer shows that the wavefield that would be produced on the supporting floor, in the absence of the floating floor, needs a force (F_0) at the point of excitation given by

$$F_0 = 8jB_2k_2^2\zeta_{20}$$

Equation 8.12

where $j = \sqrt{-1}$

For the floating floor system, Cremer assumes point excitation of the floating slab, which produces cylindrically spreading waves with corresponding near fields. The rotationally symmetric field produced at a given point on the plate depends on its distance from the point of excitation (at $r = 0$) and is described by Hankel functions of the second kind (H_0^2). Cremer states that the asymptotic expressions for the Hankel functions may be used;

$$H_0^2(r) \approx \frac{j2}{\pi} \ln r \text{ for } |r| \ll 1$$

$$H_0^2(r) \approx \sqrt{\frac{2}{\pi r}} e^{-j(r-\pi/4)} \text{ for } |r| \gg 1$$

The boundary conditions at the origin are such that the total force acting on the floating slab is equal to the exciting force and the force on the supporting slab is equal to zero.

Hence;

$$F_0 = 8jB_1(k_1^2\zeta_{11} - \epsilon_{11}k_{11}^2\zeta_{211})$$

Equation 8.13

$$0 = 8jB_2(\epsilon_1k_1^2\zeta_{11} + k_{11}^2\zeta_{211})$$

Equation 8.14

At frequencies above ω_{12} , $k_1^2 = k_{11}^2$ and it is shown that for the floating floor

$$\zeta_{11} = \frac{F_0}{8jB_1k_1^2}$$

Equation 8.15

The above is identical to Equation 8.12 except that, here, the subscripts refer to the floating floor. However, the amplitude is greater than when the supporting floor is excited directly, the ratio of the amplitudes being inversely proportional to the ratio of

the driving point impedances of the two slabs³. i.e. $\frac{\zeta_{11}}{\zeta_{20}} = \frac{Z_2}{Z_1}$.

Cremer shows that the type I wavefield in the supporting floor can be ignored because it is so small and that the type II wavefield in the floating slab can also be neglected.

Since ΔL is defined as the difference in impact sound pressure level measured without and with a floating floor, without any knowledge of the supporting floor's properties,

ΔL can be found from;

$$\Delta L = 20 \log \left(\frac{\zeta_{20}}{\zeta_{211}} \right) \text{ dB}$$

Equation 8.16

where ζ_{211} is obtained using;

$$\zeta_{211} = - \left(\frac{k_1^2}{k_{11}^2} \right) \zeta_{21}$$

Equation 8.17

and

$$\left| \frac{\zeta_{2II}}{\zeta_{2I}} \right| = \frac{k_I^2}{k_{II}^2} \approx \frac{k_1^2}{k_2^2}$$

Equation 8.18

Cremer describes the subsequent substitutions necessary to obtain the result

$$\Delta L = 40 \log \left(\frac{f}{f_o} \right) \text{ dB}$$

Equation 8.19

Since the errors identified in the original notation³ in the derivation have been corrected, the steps between Equation 8.17 and Equation 8.19 need not be presented here. The problem encountered by the author was that some of the equations, identified as being necessary for the required substitutions, contained errors as did some of the equations leading to their derivation. Once the errors are identified, the derivation of Equation 8.19 from Equation 8.17 is simple.

For lightweight floating floors, Cremer introduces a modification to Equation 8.19.

With all floating floors, at a certain frequency, the cut off frequency (f_{co}), the mass impedance of the tapping machine hammers becomes significant. For heavy concrete floating floors f_{co} is above the upper frequency range of interest to building acoustics. Lightweight floating floors have much lower driving point impedances than concrete floating slabs and the mass impedance of the tapping machine hammers can become significant at much lower frequencies. If f_{co} lies within the building acoustics frequency range then the effect of the hammers must be compensated for. The cut off frequency is given by³

$$f_{co} = \frac{Z}{2\pi m_o} \text{ Hz}$$

Equation 8.20

where m_o = the mass of the hammer (0.5 kg).

Z = the driving point impedance of the floating floor given by^{3,8}

$$Z = 2.3c_L\rho h^2 \text{ Ns/m}$$

Equation 8.21

where: c_L = the longitudinal wave speed in the floating floor (m/s).

h = the thickness of the floating floor (m).

ρ = the density of the floating floor (kg/m^3).

The modified equation is³

$$\Delta L = 40 \log\left(\frac{f}{f_o}\right) + 10 \log\left[1 + \left(\frac{f}{f_{co}}\right)^2\right] \text{ dB}$$

Equation 8.22

Cremer et al demonstrate good agreement between predicted and measured values of ΔL up to around 1000 Hz^3 for both relatively heavy and lightweight floating floors. At higher frequencies, predicted and measured values diverge but the predicted improvement in impact sound insulation shows good correlation with the measured data given for a range of ΔL up to 40 dB.

8.3.2 Resonantly reacting floating floors

It is well known that measurements of the impact sound insulation often yield results which do not agree with the improvement in ΔL predicted by Equation 8.19. With lightweight floors, this has been shown to be caused by the reduced power input to the floating slab above the critical frequency. With floating slabs such as sand/cement screeds Equation 8.19 often overestimates ΔL however. As stated earlier in this chapter, deviations from Equation 8.19 were explained in terms of the effects of sound bridges across the resilient layer coupling the two plates together³. Gudmundsson, in 1984, considered this to be the most often cited reason for the deviations from the theoretical values but emphasised the importance of Gösele's work¹.

Gösele suggested that the best agreement between measured and predicted results occurred when the resilient layer was relatively stiff and suggested two possible sound transmission paths apart from the forced wave in Cremer's theory. One was due to

lateral airborne sound propagation between the plates, which was mentioned by Cremer, although resilient layers with high airflow resistivity should prevent this being significant. The other was resonant transmission.

Gudmundsson describes Gösele's method of identifying this source of transmission¹. A concrete floating floor was constructed that was larger than the supporting floor and measurements were carried out using a standard tapping machine. The results from the measurements obtained in the receiving room for impact excitation of the floating slab directly above the supporting floor were compared with those obtained when the floating floor was excited outside the area of the supporting floor. At low frequencies, excitation directly above the supporting slab produced much higher transmission than excitation outside the area of the supporting slab. This was not the case at high frequencies however. Here, there was little difference in the sound transmission resulting from the different excitation positions. This was compelling evidence that resonant transmission is significant above particular frequencies for certain types of floating slab.

Vér's research into the impact sound insulation of floating floors⁷ was mentioned in the introduction to this chapter. For locally reacting floating floors, Vér simply cites Cremer and presents Equation 8.19. There is a much more detailed explanation of his approach to describe the problem of resonant sound transmission, which was to use Statistical Energy Analysis (SEA).

Vér assumed the floating slab to be rigid, lightly damped and finite in size with the power input (W_{in}) to this slab by the tapping machine given by

$$W_{in} = F_{rms}^2 Y_1 \quad \text{Watts per octave.}$$

Equation 8.23

F_{rms} = the root mean square force (N)

Y_1 = the driving point mobility of the floating slab (m/Ns)

The other assumptions were;

1. The slab is supported by individual resilient mounts.
2. There is no correlation between the motion of the slab at the different mounts.

3. There is no lateral sound propagation between the floating slab and the supporting floor.
4. Each mount can be considered to have the impedance of a pure spring.
5. The power transmitted between the two slabs is transmitted only through the resilient mounts.
6. The average point input impedance of both slabs is the same as that of infinite slabs having the same thickness, surface density and comprising the same materials as the finite slabs.
7. The motion of the floating slab is not affected by the presence of the supporting slab.
8. The power transmitted by moments is negligible compared with that transmitted by forces.
9. Radiation power losses can be neglected.

Vér describes the power balance in the floating slab as

$$W_{in} = W_{d1} + W_{12} - W_{21} \quad \text{Watts}$$

Equation 8.24

and in the supporting slab as

$$W_{12} = W_{d2} + W_{21} \quad \text{Watts}$$

Equation 8.25

where the subscripts (1) and (2) refer to the floating and supporting slabs respectively and the subscript d refers to power dissipated in the designated slab. The subscripts (12) and (21) describe whether the power flows from slab 1 to slab 2 or vice versa.

Vér shows that the power transmitted from the floating slab to the supporting slab through a single resilient spring is given by;

$$W = v_1^2 K_{12}(\omega) \quad \text{Watts}$$

Equation 8.26

v_1^2 is the space averaged mean square velocity of the floating slab. K_{12} is given by;

$$K_{12} = \frac{|Z_m|^2 Y_2}{1 + 2 \operatorname{Re}\{Z_m\}(Y_1 + Y_2) + |Z_m|^2 (Y_1 + Y_2)^2}$$

Equation 8.27

Z_m is the impedance of a single resilient spring and $\operatorname{Re}\{\}$ represents the real part of the variable. Y_1 and Y_2 represent the mobilities of the floating and supporting slabs respectively. The power transmitted by n mounts is therefore obtained by multiplying Equation 8.26 by n .

In order to obtain ΔL one needs to determine the velocity of the supporting floor resulting from the force acting on the floating slab. This is given by⁷

$$\frac{v_2^2}{v_1^2} = \frac{K_{12}(\omega)n'}{\rho_{s2}\omega\eta_2 + K_{21}(\omega)n'}$$

Equation 8.28

n' = the number of resilient springs per unit area

ρ_{s2} = the surface density of slab 2

η_2 = the loss factor of slab 2

$$K_{21}(\omega) = K_{12}(\omega) \left(\frac{Y_1}{Y_2} \right)$$

Vér writes Equation 8.24 in terms of the characteristics of the floating floor system and then inserts Equation 8.28 into it to determine v_1^2 . These operations enable the determination of the mean square velocity of the composite floor (v_c^2). The sound power radiated into the receiving room by the composite floor ($W_{c,r}$) is given by

$$W_{c,r} = v_c^2 \rho c \sigma_r A \quad \text{Watts}$$

Equation 8.29

where ρ = the density of air (kg/m^3)

c = the speed of sound in air (m/s)

σ = the radiation efficiency of the ceiling

A = area (m^2)

The mean square velocity of the supporting slab when excited directly by the tapping machine (v_{s2}^2) is given by

$$v_{s2}^2 = \frac{F_{rms}^2 Y_2}{\rho_{s2} \omega \eta_2 A} \quad \text{m/s}$$

Equation 8.30

This leads to ΔL , given by

$$\Delta L = 10 \log \left(\frac{v_{s2}^2}{v_c^2} \right) \quad \text{dB}$$

Equation 8.31

Vér states that, above a certain frequency, ΔL is given by

$$\Delta L \approx 10 \log \left(\frac{Y_2 \rho_s \omega \eta_1}{Y_1 K_{12}(\omega) n'} \right) \quad \text{dB}$$

Equation 8.32

and for a typical floating floor, this leads to the high frequency approximation:

$$\Delta L \approx 10 \log \left[2.3 c_L h_1 \eta_1 n' \left(\frac{\omega^3}{\omega_1^4} \right) \right] \quad \text{dB}$$

Equation 8.33

c_L is the longitudinal wavespeed (m/s) in the floating slab and h_1 is its thickness (m).

ω_1 is the fundamental resonance of the floating slab given by

$$\omega_1 = \sqrt{\left(\frac{s n'}{\rho_{s1}} \right)} \quad \text{rad/s}$$

where s = the dynamic stiffness of an individual resilient spring (N/m)

ρ_{s1} = the surface density of the floating slab (m/s^2)

Substituting for ω_1 in Equation 8.33, therefore yields

$$\Delta L \approx 10 \log \left[\frac{2.3 c_L h_1 \eta_1 \rho_{s1}^2 \omega^3}{n' s^2} \right] \text{ dB}$$

Equation 8.34

Equation 8.34 is also quoted elsewhere^{8,9} and indicates that, assuming the damping in the floating slab and the dynamic stiffness of the resilient mounts are frequency independent, ΔL increases by 30 dB per decade for resonantly reacting floating floors.

8.3.3 The resilient layer as a wave medium

In his review of the wave medium approach to the prediction of ΔL , Gudmundsson cites the earlier work of Lindblad who treated the resilient layer as a wave medium with impedance $Z_s = \sqrt{E_s \rho_s}$.

where E_s is the dynamic modulus and ρ_s is the density of the resilient layer.

The speed of sound in the layer is given by $c_s = \sqrt{\frac{E_s}{\rho_s}}$ and the wavenumber given by

$$k_s = \frac{\omega}{c_s}.$$

Lindblad states, for the primary wave,

$$\frac{\tau_{\text{total construction}}}{\tau_{\text{supporting slab}}} = \left| \frac{2Z_s}{j\omega m_1} \right|^2$$

where τ represents the transmission coefficient. This can be written;

$$\Delta L_1 = 20 \log \left(\frac{\omega m_1}{2 \rho_s c_s} \right)$$

Equation 8.35

Considering the losses in the resilient layer,

$$\Delta L_{\eta} = -10 \log(e^{-k_s \eta_s h_s})$$

Equation 8.36

The effect of multiple reflections between the two slabs was estimated by considering the interlayer as a one-dimensional space leading to;

$$\Delta L_r = 10 \log \left(1 + \frac{1}{2k_s \eta_s h_s} \right)$$

Equation 8.37

k_s , η_s , and h_s are the wave number, the loss factor and the thickness of the resilient layer separating the two slabs respectively.

Equation 8.37 was considered to be a high frequency complement to Cremer's solution, which is valid at low frequencies. At higher frequencies ΔL is given by

$\Delta L_1 + \Delta L_{\eta} - \Delta L_r$. i.e.;

$$\Delta L = 20 \log \left(\frac{\omega m_1}{2\rho_s c_s} \right) - 10 \log(e^{-k_s \eta_s h_s}) - 10 \log \left(1 + \frac{1}{2k_s \eta_s h_s} \right) \text{ dB}$$

Equation 8.38

Lindblad further developed his theory¹ with the inclusion of a complex reflection factor for sound pressure at the floating and supporting slabs¹⁰. Following Lindblad's work, Gudmundsson included the wave behaviour of the resilient layer in Cremer's Fourier transform approach to deriving the improvement in impact sound insulation from adding a floating floor.

Gudmundsson starts his model's derivation by describing a linear mechanical system:

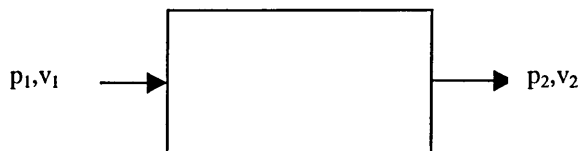


Figure 8.1; linear four pole mechanical system

The system is excited by the pressure (p_1) which results in the input velocity (v_1). The velocity (v_2) on the output side results in the pressure (p_2). For a plate, the system becomes¹

$$\begin{bmatrix} p_1 \\ v_1 \end{bmatrix} = \begin{bmatrix} 1 & (Z_p + Z_f) \\ 0 & 1 \end{bmatrix} \begin{bmatrix} p_2 \\ v_2 \end{bmatrix}$$

Equation 8.39

where Z_p is the impedance of the plate and Z_f is the radiation loading.

When the mechanical system is a spring it is described by¹

$$\begin{bmatrix} p_1 \\ v_1 \end{bmatrix} = \begin{bmatrix} 1 & 0 \\ (j\omega/s) & 1 \end{bmatrix} \begin{bmatrix} p_2 \\ v_2 \end{bmatrix}$$

Equation 8.40

where s is the dynamic stiffness of the spring and ω the radian frequency. Coupling two plates by a spring leads to¹;

$$\begin{bmatrix} p_1 \\ v_1 \end{bmatrix} = \begin{bmatrix} 1 & (Z_{p1} + Z_f) \\ 0 & 1 \end{bmatrix} \begin{bmatrix} 1 & 0 \\ (j\omega/s) & 1 \end{bmatrix} \begin{bmatrix} 1 & Z_{p3} \\ 0 & 1 \end{bmatrix} \begin{bmatrix} p_3 \\ v_3 \end{bmatrix}$$

Equation 8.41

where, here, the subscripts 1 and 3 refer to the floating and the supporting plates separated by the resilient layer.

For a spring with distributed mass (ρ_s), wavenumber (k_s) and phase velocity (c_s)

Equation 8.40 becomes;

$$\begin{bmatrix} p_1 \\ v_1 \end{bmatrix} = \begin{bmatrix} \cos(k_s h_2) & j\rho_s c_s \sin(k_s h_2) \\ \left\{ \frac{j \sin(k_s h_2)}{\rho_s c_s} \right\} & \cos(k_s h_2) \end{bmatrix} \begin{bmatrix} p_2 \\ v_2 \end{bmatrix}$$

Equation 8.42

The losses in the resilient layer are included using a complex wavenumber (k_s^*) where;

$$k_s^* = k_s \left(1 - j \frac{\eta_2}{2} \right)$$

Equation 8.43

Gudmundsson evaluates Equation 8.41, with the modifications to the spring element described in order that it is treated as a wave medium, and then assumes point loading to obtain the improvement in impact sound insulation. He then compared the results of an exciting force acting on the floating floor (or plate) and on the supporting floor (or plate) to derive an expression for ΔL .

The resilient layer was first treated as a homogenous isotropic wave medium and later the effects of anisotropy in the layer were included in the model. This was done because the speed of the sound wave parallel to the direction of the mineral fibres, that Gudmundsson studied, is known to be about three times greater than in the direction perpendicular to the fibres¹. The results from the two different treatments were compared with the results from laboratory measurements.

The comparison revealed what was acknowledged by Gudmundsson to be a serious drawback¹ with his wave medium model of the resilient layer. This was that the same resilient layer had to be modelled differently in order to give reasonable correlation with measurement data depending on the type of floating floor. With floating concrete slabs, modelling the resilient layer as an anisotropic wave medium gave better correlation. For floating chipboard floors modelling the layer as a homogenous wave medium gave better results.

Gudmundsson also considered SEA analysis to solve the problem of predicting the impact sound insulation of floating floors over the whole building frequency range. His approach was to use Cremer's solution, modified to include the wave behaviour of the resilient layer, up to the frequency at which resonant transmission began to dominate the sound transmission. At frequencies above this point SEA was used. Unfortunately the correlation between the results from this model and measurements was poor and it proved to be difficult to combine the two approaches to modelling ΔL . It proved difficult to "sew the two solutions together" as Gudmundsson put it¹.

It is interesting to note that, for the SEA analysis, the solution was easier to derive when the supporting floor was considered to be excited rather than the floating slab.

Reciprocity means that there is no difference between the two approaches. It is also of note that although Gudmundsson states that the improvement in airborne sound insulation and impact sound insulation due to the addition of a floating floor should be identical, this was not observed. The difference appears to have been attributed to unwanted flanking transmission.

8.4 Discussion of the prediction models

Vér's method for predicting ΔL arose, in part, from the need to give a theoretical explanation of the deviation between the results from Cremer's analytical model and measurement data gathered on lightly damped floating floors. pr EN 12354-2¹¹, which is aimed at unifying prediction methods in building acoustics, presents an equation which, like that derived by Vér, predicts an increase in ΔL of 30 dB per decade for lightly damped sand/cement screeds. Vér's equation is derived for floating floors supported by individual resilient mounts rather than a continuous layer however.

Unfortunately one cannot simply increase the number of mounts until one has, in effect, a continuous layer because this violates one of his basic assumptions. i.e. There is no correlation between the motion of the slab at the different mounts.

Impact sound transmission was also modelled by Nilsson¹² who considered the floating floor to be supported by a continuous resilient layer and a simply supported supporting floor excited by a bending moment at one of the supports. His solution for forced transmission was the same as Cremer's. He produced three different solutions for resonant transmission which depended upon the nature of the floating and supporting slabs. However, Gudmundsson considered that Nilsson might have "driven his simplifications too far" in deriving his final expression for resonant transmission¹ resulting in its being applicable only to a narrow frequency region.

Using resonant sound transmission models to predict the performance of the floating floor systems of interest to this research would not appear to be the best approach therefore. Vér's approach is inapplicable because it requires individual mounts rather than a continuous resilient layer and Nilsson's is not considered to be applicable over a wide frequency range. Even Gudmundsson's SEA extension to the forced solution

proved to be unsuccessful. Also, resonant transmission takes place at relatively high frequencies for particular flooring systems (although the frequency at which resonant transmission begins to dominate varies with different floating floor systems). At low frequencies, it is accepted that forced transmission dominates and this is “covered” by Cremer’s theory which leads to a 40 dB per decade improvement in ΔL . The results from the field tests on the small sections of floating floor described in Chapter 6 suggest that $L'_{nT,w}$ is dominated by the performance of the flooring sections up to 500 Hz. Assuming resonant transmission to be the dominant mechanism might not, therefore, be the first choice even if a suitable model had been identified.

Modelling the resilient layer as a wave medium allows the damping in the layer to be included in the calculation of ΔL . Since the measurement of damping with the polyurethane foam test specimens was described in Chapter 4 it might appear to be advantageous to adopt a prediction method for ΔL in this research which included damping as well as dynamic stiffness. The problem with so doing is that although the damping of the test specimens can be measured, this is not necessarily representative of the damping in a resilient layer beneath floating floor. The research reviewed in Chapter 2 which determined that the changes in damping, for the resilient materials studied, over the building acoustics frequency range were insignificant was conducted on small specimens.

Vér attributes deviations from the predicted 40 dB and 30 dB per decade slopes for ΔL observed with some field measurements to the possible frequency dependence of the damping in the slabs comprising the floating floor system. It may be the case that the loss factors in resilient layers vary with frequency when in place beneath floating floors, where the effect of the air enclosed may be significant. Also, as Gudmundsson’s research showed, it is difficult to determine the wavespeed in the resilient layer. The wave medium model did not appear to be the best choice for use in predicting ΔL . The most compelling argument for not adopting a wave medium model for the resilient layer is the need to adopt different models with different types of floating floor comprising identical resilient layers in order to achieve reasonable correlation with experimental data¹.

A successful model for predicting ΔL for lightweight floating floors has been presented³. Cremer et al demonstrated excellent correlation between predicted and measured values over a range of ΔL of 40 dB although in this case the lightweight floating surface comprised 12 mm thick wood plate rather than mdf. The good correlation was achieved by accounting for the reduced force input of the tapping machine hammers above the cut off frequency (f_{co}). Cremer determined that f_{co} for the lightweight wooden floor was 223 Hz. Gudmundsson found that the correction for reduced force input was necessary at frequencies greater than 550 Hz¹ for 22 mm thick chipboard. The method most likely to be the most suitable for predicting the performance of the mdf floating flooring appeared to be that described by Cremer therefore.

8.5 Conclusions

Adopting a model for predicting ΔL for the mdf floating flooring that assumes resonant transmission to be the dominant mechanism can be rejected. None has been identified that is applicable for a continuous resilient layer and for which the performance over a range of frequencies must be considered. The problems identified in determining the parameters necessary to describe the resilient layer as a wave medium (propagation speed and damping) rule out this approach also. Cremer et al demonstrated excellent correlation between measured and predicted ΔL for a lightweight timber floating floor by modifying Equation 8.19 to account for the mass impedance of the tapping machine hammers above f_{co} . This approach also has the advantage of simplicity and is therefore the method adopted for predicting ΔL in this research.

The mass spring resonance frequency can be determined from the mass and dimensions of the floating floor sections and the results from the measurement of the dynamic stiffness of the resilient layers. All that remains is to determine the driving point impedance of the mdf floating surface, and hence the cut off frequency, then to use Equation 8.22. This will be described in Chapter 9.

8.6 References

- 1 GUDMUNDSSON S., Sound improvement of floating floors. A study of parameters, *und Institute of Technology, Department of Building Acoustics, Lund, Sweden*, 1984.
- 2 GÖSELE K., Zur messmethodik der trittschalldämmung, *Gesundheitsing*, Vol 70, 1948.
- 3 CREMER L., HECKL M., UNGAR E.E., *Structure-borne sound, 2nd edition*, Publ. Springer-Verlag, 1973.
- 4 CREMER L., Theorie des klopf-schalles bei decken mit schimmendem estrich, *Acustica*, Vol 2, 1952.
- 5 GÖSELE K., Zur berechnung der trittschalldämmung von massivdecken, *Gesundheitsing*, Vol 72, 1951.
- 6 BOLT R.H., LUKASIK S.J., NOLLE A.W., FROST A.D.(Ed), *Handbook of acoustic noise control*, Publ McGregor and Werner Inc, Dayton Ohio, USA, 1952.
- 7 VÉR I.L., Impact noise isolation of composite floors, *JASA*, 1970.
- 8 VÉR I.L., Interaction of sound waves with solid structures, *Noise and Vibration Control*,(Ed) Beranek L.L., Vér I.L., 270-361, Publ. McGraw-Hill Book Company, 1971.
- 9 VÉR I.L., Interaction of sound waves with solid structures, *Noise and Vibration Control Engineering*,(Ed) Beranek L.L., Vér I.L., 245-367, Publ. John Wiley and Sons Inc, 1992.
- 10 LINDBLAD S.G., "Akustik V"(text book for undergraduate students), Lund Institute of Technology, Department of Building Acoustics, 1983.
- 11 prEN 12354-2, 1997, *Draft Standard, Building acoustics, Estimation of acoustic performance of buildings from the performance of products, Part 2: Impact sound insulation between rooms*.
- 12 NILSSON A.C., Some acoustical properties of floating floor constructions, *JASA*, 1977, Vol 61 No 6.

PREDICTING IMPACT SOUND INSULATION

9.1 Introduction

Chapter 8 explained how knowledge of the dynamic stiffness of a resilient layer allows the prediction of ΔL when a floating floor comprising the material is placed on a supporting floor. This chapter uses the results from the measurements of dynamic stiffness, presented in Chapter 7, to predict ΔL for the lightweight mdf sections of flooring tested in the field and to compare the predictions with the measured results. However, Cremer showed that, with lightweight floating floors, the force input to the floating surface is reduced due to the significant effect of the mass impedance of the tapping machine hammers. Therefore, compensation for the reduction in input force must be made above a cut off frequency (f_{co}) which is determined by the driving point impedance of the lightweight surface.

This chapter describes the method used to determine the driving point impedance of the mdf and determine f_{co} . Following this, Equation 8.22 is used to predict ΔL for the mdf flooring sections. Close correlation is found between the measured and predicted results. Comparison is also made with measurements on two different concrete supporting floors with much larger sections of floating floor. Lastly a simple method for predicting the weighted standardised impact sound pressure level ($L'_{nT,w}$) is proposed for a lightweight shallow profile floating floor on a concrete supporting floor whose sound insulation properties are known.

9.2 Predicting the impact sound insulation of floating floors

The improvement in impact sound insulation (ΔL) in a given frequency band produced by fitting a floating floor on a supporting floor is obtained by measuring L'_{nT} (in field measurements) before and after fitting the floating floor. ΔL is given by the difference in the two values of L'_{nT} . The prediction of the acoustic performance of structures from knowledge of the properties of the materials from which they are made is obviously an

extremely useful aid to designing buildings with good sound insulation. It has therefore been the subject of considerable research. Recently Gerretsen extended his earlier model for predicting airborne insulation¹ to cover impact sound insulation². The Draft Standards prEN 12354-1³ and prEN 12354-2⁴, have come about due to the need to standardise the prediction of acoustic performance and deal with the calculation of acoustic insulation between rooms for airborne sound and impact sound. Both Draft Standards cite Gerretsen's work and also lean on the much earlier work of Cremer Heckl and Ungar⁵.

prEN 12354-2 deals with the estimation of impact sound through floors and in particular with the estimation of the acoustic performance of floating floors. The Draft Standard contains nomograms for the prediction of the weighted impact sound reduction index⁶ (ΔL_w) of floating floors comprising sand and cement screed and asphalt floating floors supported by resilient layers having a given dynamic stiffness. None of the nomograms is useful for a floating floor with a surface density less than 15 kg/m² however which means that the shallow profile floating floors of interest in this research programme are not covered by the Draft Standard. The Draft Standard states that BS EN 29052-1⁷ should be used to determine the dynamic stiffnesses of the resilient layers under the floating floors. BS EN 29052-1 however states that because of the low static load imposed on the resilient layers by the mdf in the lightweight floating floors under discussion. It would appear, therefore, that the method described in BS EN 29052-1 cannot be used to determine their dynamic stiffness.

9.3 Driving point impedance of mdf

The driving point impedance (Z) of the mdf was evaluated using Equation 8.21. The thickness and the density of the material were easily obtained but the longitudinal wave speed in the material had to be measured. This was achieved by carrying out measurements as described by VÉR⁸ using a similar technique to that adopted by Craik⁹ to measure the longitudinal wave speed in building elements. The measurements were carried out using a sample of the mdf flooring tested in the field. Two Bruel and Kjaer type 4333 accelerometers and the dual channel Ono Sokki analyser were used for the measurements.

The mdf flooring was placed on a concrete floor and the two accelerometers (A and B) were attached to it with beeswax and separated from each other by 1m. The accelerometers were fixed to the mdf with their axes of highest sensitivity parallel to the direction of propagation of the longitudinal wave. The output from each accelerometer was fed to a channel of the analyser and longitudinal waves in the mdf were induced by tapping the edge of the flooring sample with a light metal hammer. The output from the accelerometer nearest to the point of excitation was used to trigger the analyser and the time for the impulse to travel the distance between the two accelerometers was recorded. Measurements were taken with the impulses travelling in both directions (from A to B with A providing the trigger pulse and from B to A with B providing the trigger pulse).

9.4 Prediction of $L'_{nT,w}$

Equation 8.19 is valid for frequencies greater than the resonance frequency (f_0). Around f_0 it is often observed that the impact sound insulation of a supporting floor is reduced by the addition of a floating floor¹⁰. Below f_0 it is unlikely that the addition of a floating floor will lead to any significant increase in impact sound insulation⁵. In this research, after the addition of the floating floor, values of L'_{nT} are calculated by subtracting values of ΔL , generated by Equation 8.22, from the measured values obtained when the bare supporting floors were tested. The curve generated by Equation 8.22 is projected onto the axis corresponding to a 0 dB improvement in ΔL and at this point, and at all third octave frequencies below this point, ΔL is equated to zero.

9.5 Results

9.5.1 Longitudinal wave speed in mdf

The results from measurements to find the longitudinal wave speed of sound in the mdf used for the flooring samples can be seen in Table 9.1 which shows that c_L can be taken to be (2400 ± 135) m/s. The first eight values are the results from measurements with the pulses travelling in the opposite direction to that which provided the results in the rest of the Table. There was no significant difference in the measured values in the two directions, (2389 ± 127) m/s and (2417 ± 135) m/s, so the value quoted (2400) m/s is the mean of the whole series of measurements. The standard deviation in the measurements

of the longitudinal wave speed (± 135 m/s) was taken to be the potential error in the value of wave speed quoted.

9.5.2 Prediction of ΔL

The density of the mdf used was 790 kg/m^3 for all the samples except for that with the virgin foam which was 720 kg/m^3 . The cut off frequencies (f_{co}) were obtained using Equations 8.20 and 8.21 and found to be 112 Hz for the 790 kg/m^3 mdf and 102 Hz for the 720 kg/m^3 mdf.

The predicted values of ΔL , obtained using Equation 8.22, for the different small sections of floating floor on the concrete supporting floor are shown in Figures 9.1 to 9.9. It can be seen that the correlation between the predicted values for ΔL and those obtained from field measurements is good over a range of ΔL up to 40 dB and of frequency up to 1000 Hz. This is consistent with previous research work⁵ which, for heavier floating floors, found good agreement for frequencies between the natural frequency of the floating floor (f_n) and $4f_n$.

The worst fit with the measured values of ΔL is seen in Figure 9.3 and Figure 9.4 which compare predicted and measured data for the flooring systems comprising the 14 and 16 mm thick layers of the 78 kg/m^3 rebond foam. Equation 8.22 overestimates ΔL for both these systems. Figure 9.10 compares measured and predicted data for the large ($3.6 \text{ m} \times 4.2 \text{ m} = 15.1 \text{ m}^2$) section of floating floor on a different, hollow block, concrete supporting floor: here again the correlation between measured and predicted data is reasonable up to 1000 Hz.

In Table 9.2 the results for the 28 kg/m^3 virgin foam are given in bold and those for the large section of floating floor (15.1 m^2) with the 6 mm layer of 78 kg/m^3 rebond foam in italic. Also included are predicted and measured $L'_{nT,w}$ from a council flat after refurbishment. In this case an mdf system with the 8 mm thick virgin foam resilient layer was fitted. The results are shown in bold italic. The separating floor was concrete with a sand and cement screed.

time for pulse to travel 1 m	longitudinal wave speed
ms	m/s
0.39	2564
0.43	2325
0.43	2325
0.44	2272
0.42	2370
0.41	2461
0.45	2207
0.39	2586
0.30	2500
0.30	2500
0.32	2343
0.28	2679
0.29	2586
0.31	2419
0.41	2461
0.46	2156
0.43	2349
0.48	2081
0.41	2415
0.41	2438
0.40	2485
0.41	2415
0.44	2286
0.40	2485
0.43	2349
0.41	2462
0.40	2509
mean wave speed	2402
standard deviation	132

Table 9.1: longitudinal wave speed

density of foam: kg/m ³	thickness of foam: mm	predicted L' _{nT,w} : dB	measured L' _{nT,w} : dB
64	10	44	44
96	11.5	43	44
128	9	45	45
144	11	43	44
28 (virgin)	8	45	44
78	6	45	45
78	12	43	43
78	14	42	42
78	16	41	41
78 (15.1m ²)	6	43	42
28 (virgin)	8	57	56

Table 9.2: comparison of predicted and measured L'_{nT,w}.

Comparisons of the predicted L'_{nT} and L'_{nT,w} values for the flooring samples tested in the field can be seen in Figures 9.11 to 9.19. At frequencies above 1000 Hz the predicted and measured values of L'_{nT} diverge but in all cases the predicted weighted standardised impact sound pressure level, L'_{nT,w}, shows excellent agreement with the measured value. Figures 9.20 and 9.21 compare the predicted and measured results for the 15.1 m² section of rebond floating floor and the refurbished council flat respectively. This close correlation between measured and predicted L'_{nT,w} also holds for these much large sections of flooring.

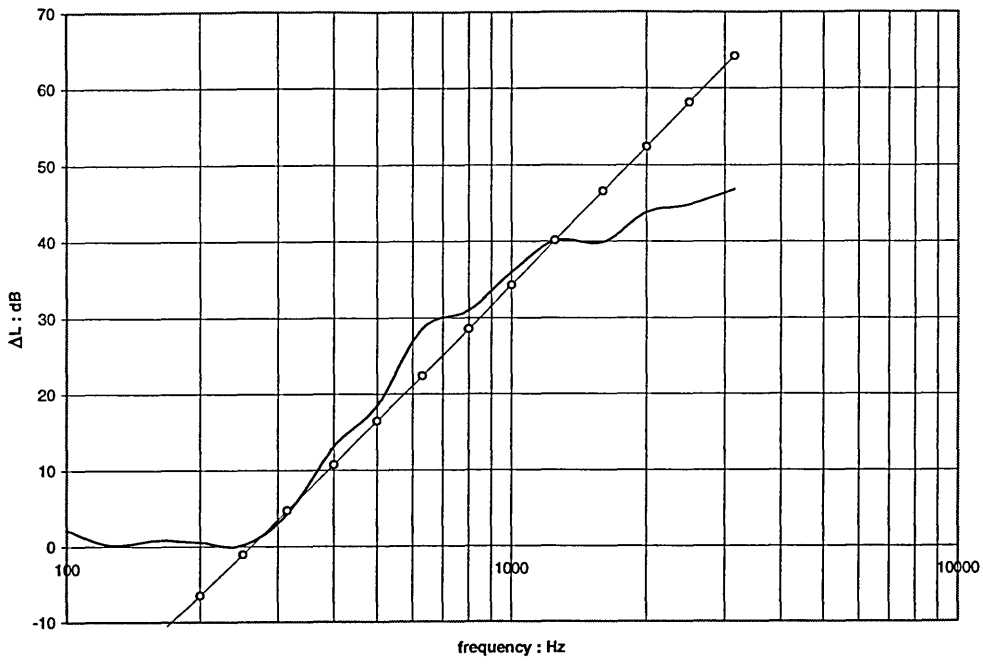


Figure 9.1: ΔL for 6 mm thick 78 kg/m³ rebond.

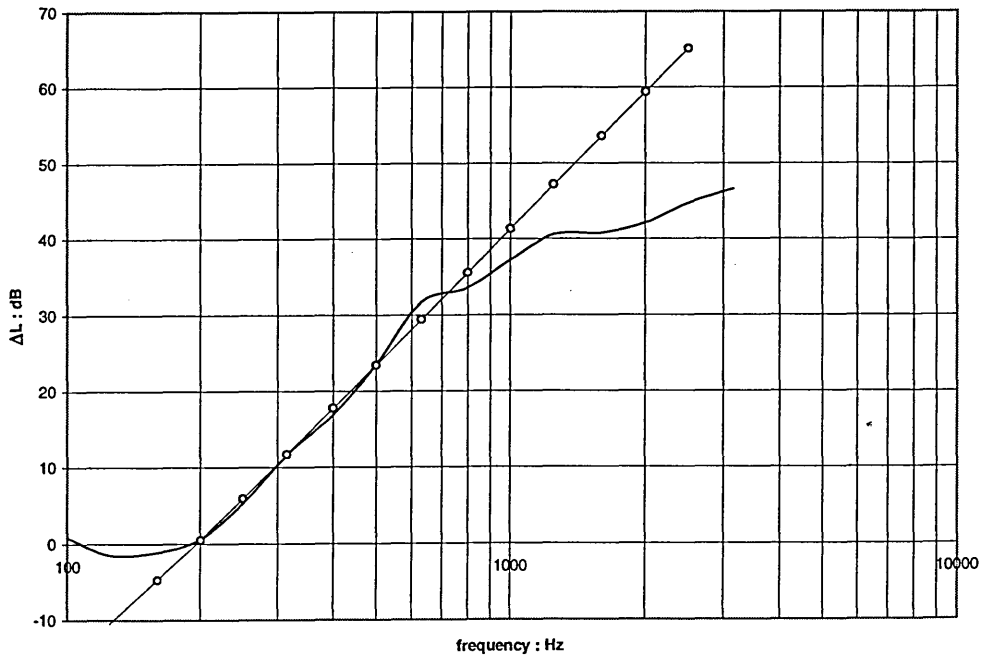


Figure 9.2: ΔL for 12 mm thick 78 kg/m³ rebond.

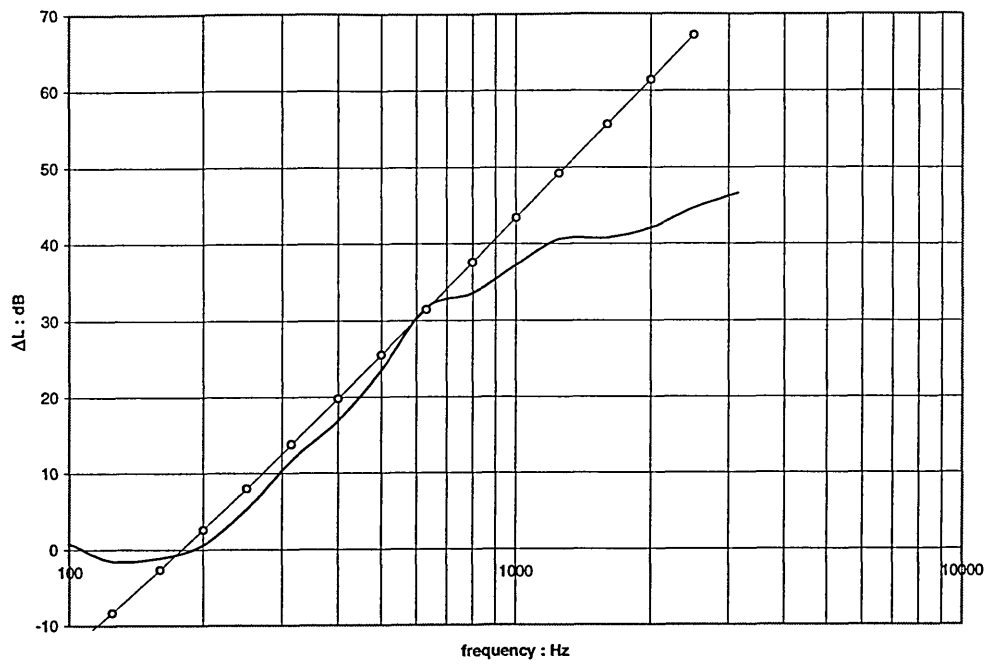


Figure 9.3: ΔL for 14 mm thick 78 kg/m³ rebond.

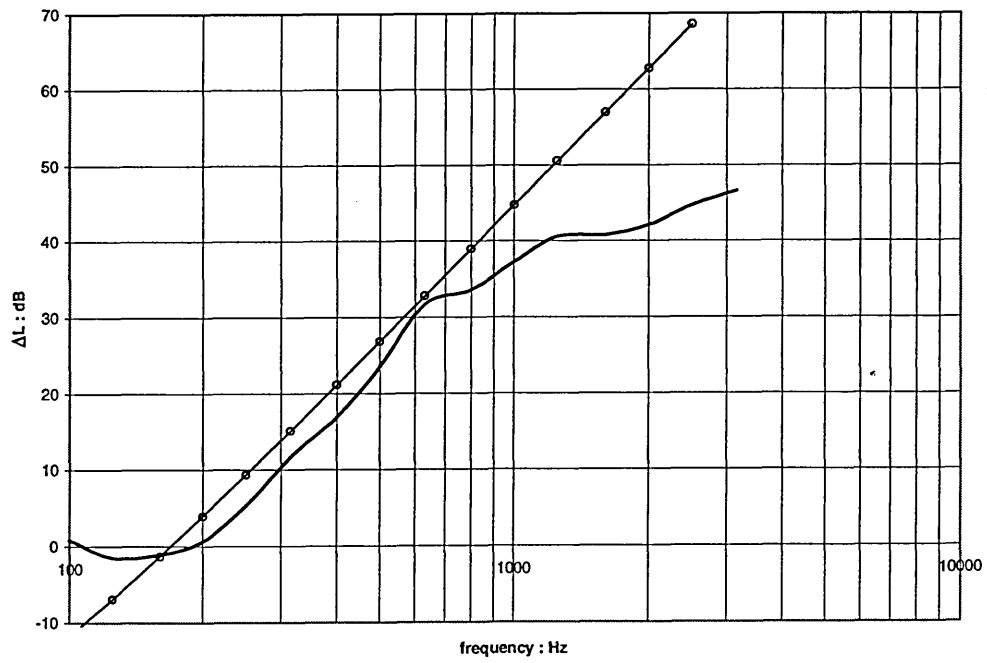


Figure 9.4: ΔL for 16 mm thick 78 kg/m³ rebond.

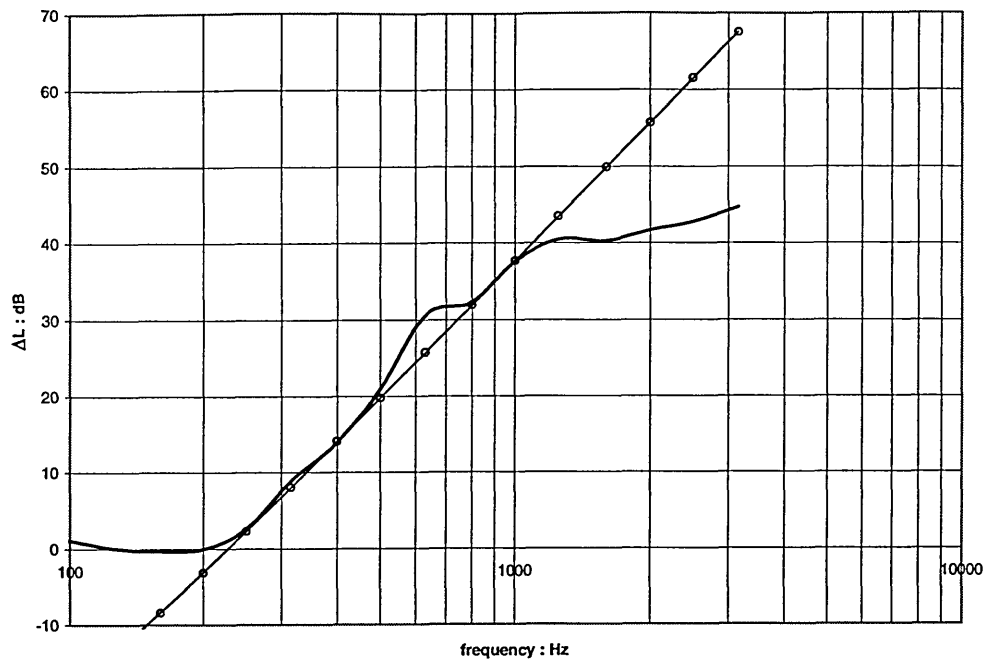


Figure 9.5: ΔL for 10 mm thick 64 kg/m³ rebond.

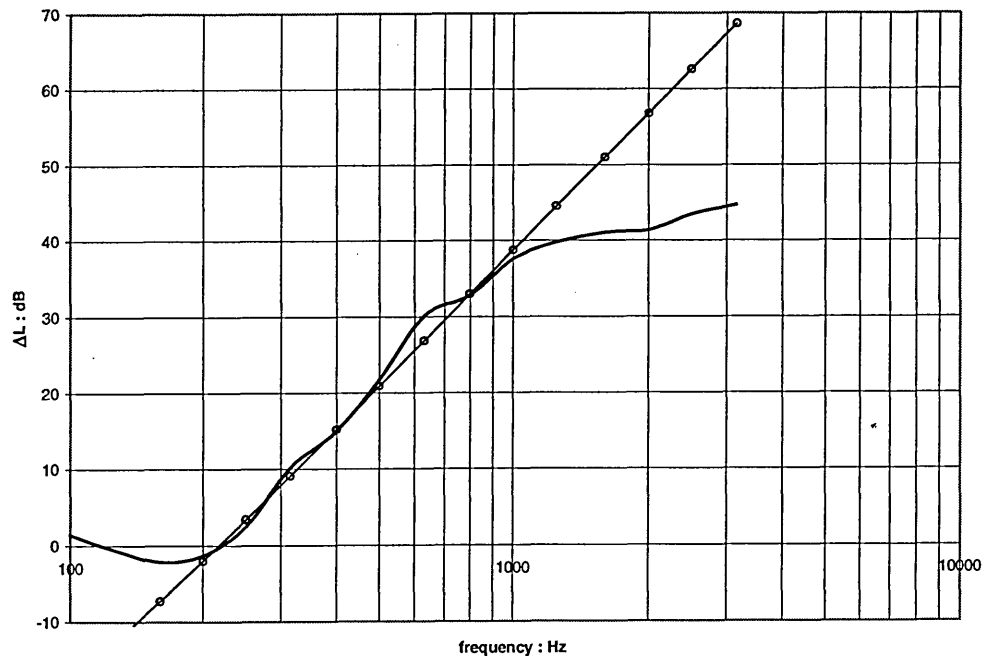


Figure 9.6: ΔL for 11.5 mm thick 96 kg/m³ rebond.

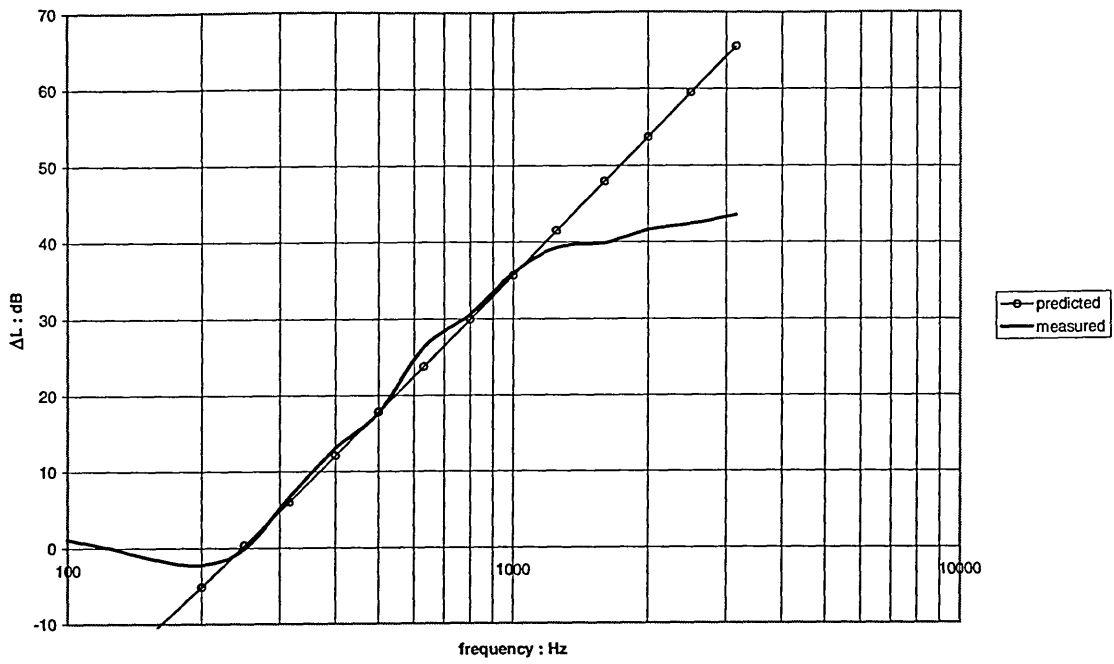


Figure 9.7: ΔL for 9 mm thick 128 kg/m³ rebond.

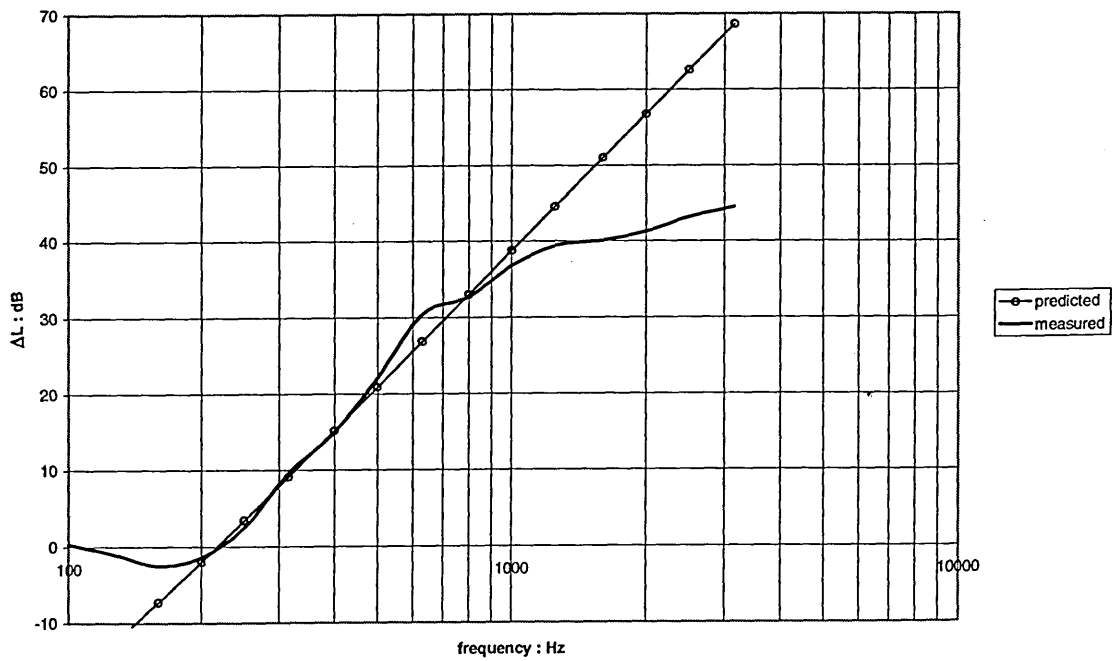


Figure 9.8: ΔL for 11 mm thick 144 kg/m³ rebond.

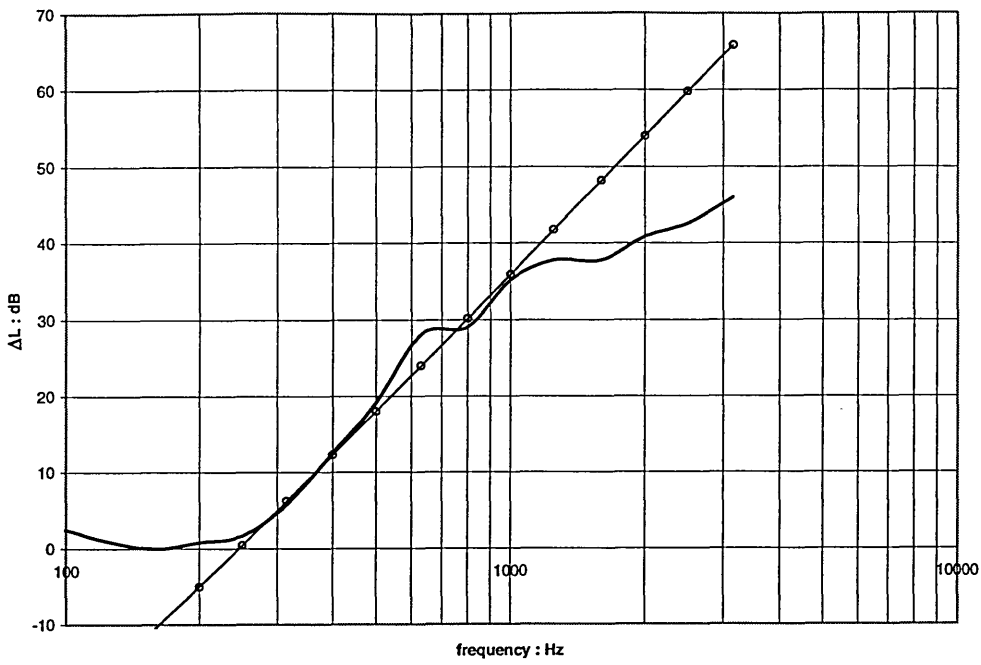


Figure 9.9: ΔL for 28 kg/m^3 virgin foam.

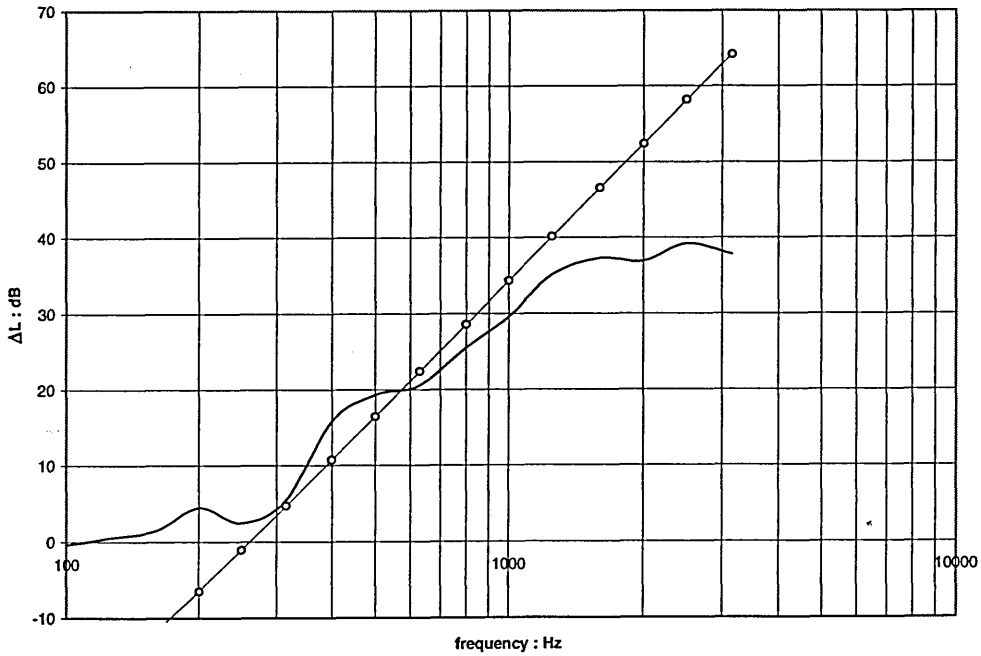


Figure 9.10: ΔL for 15.1 m^2 floating floor with 8 mm thick 78 kg/m^3 rebond.

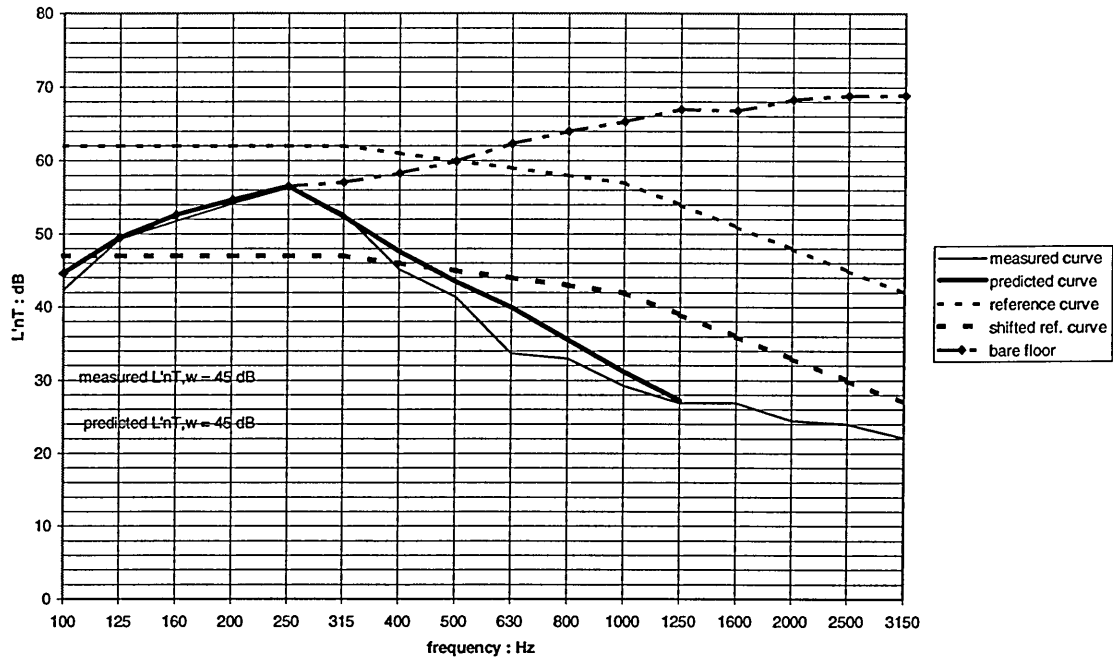


Figure 9.11: L'_{nT} for 6 mm thick 78 kg/m³ rebond.

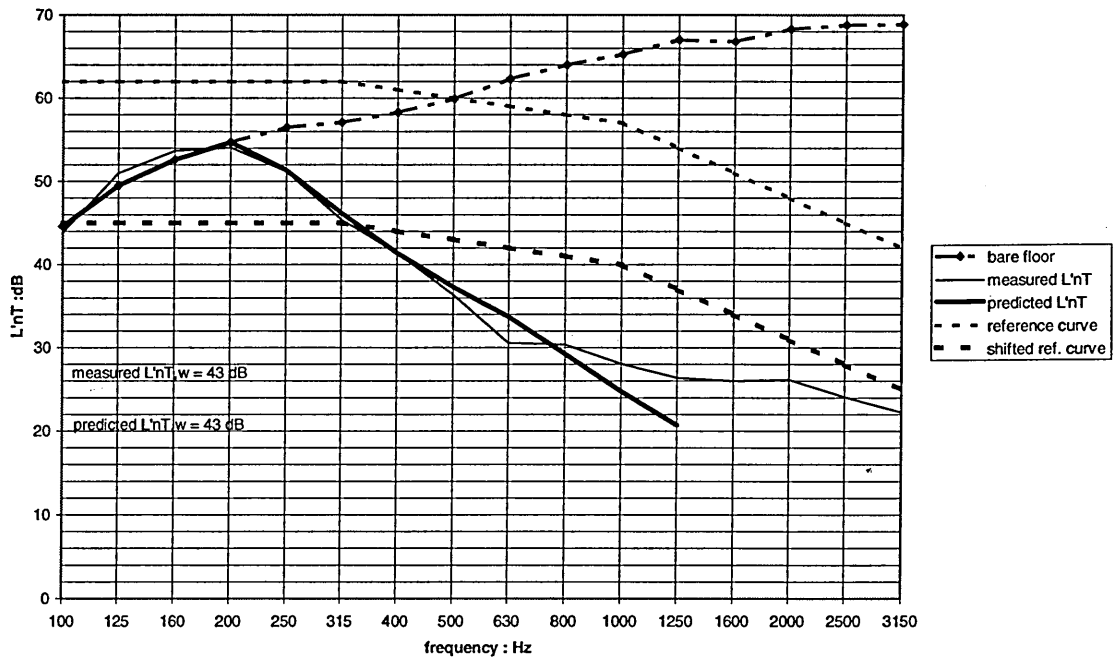


Figure 9.12: L'_{nT} for 12 mm thick 78 kg/m³ rebond.

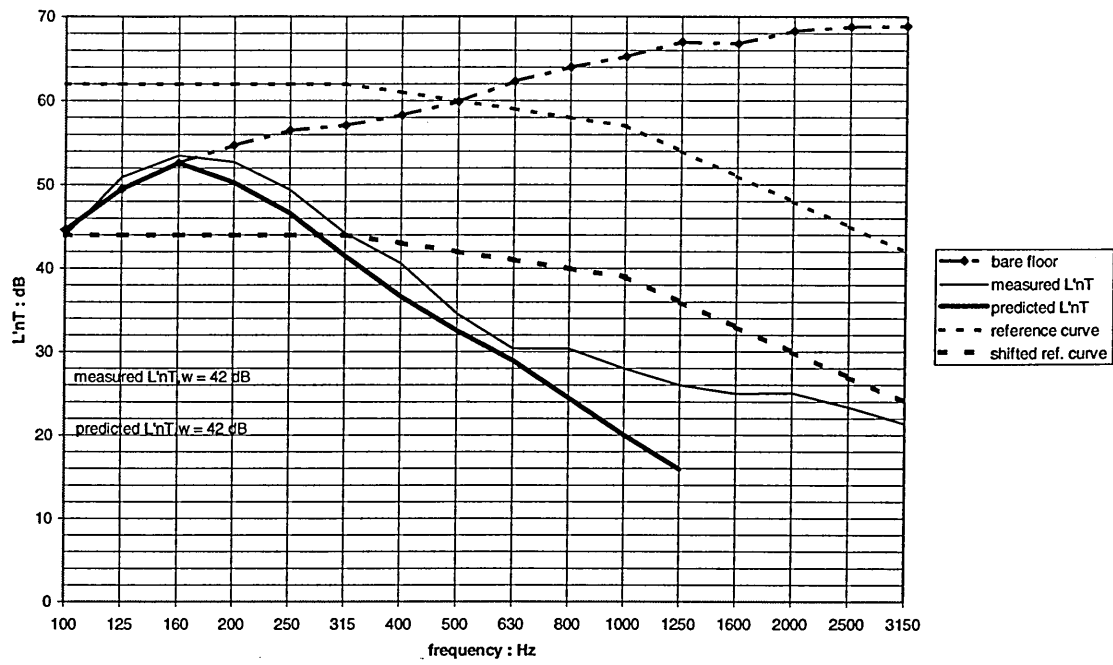


Figure 9.13: L'_{nT} for 14 mm thick 78 kg/m^3 rebond.

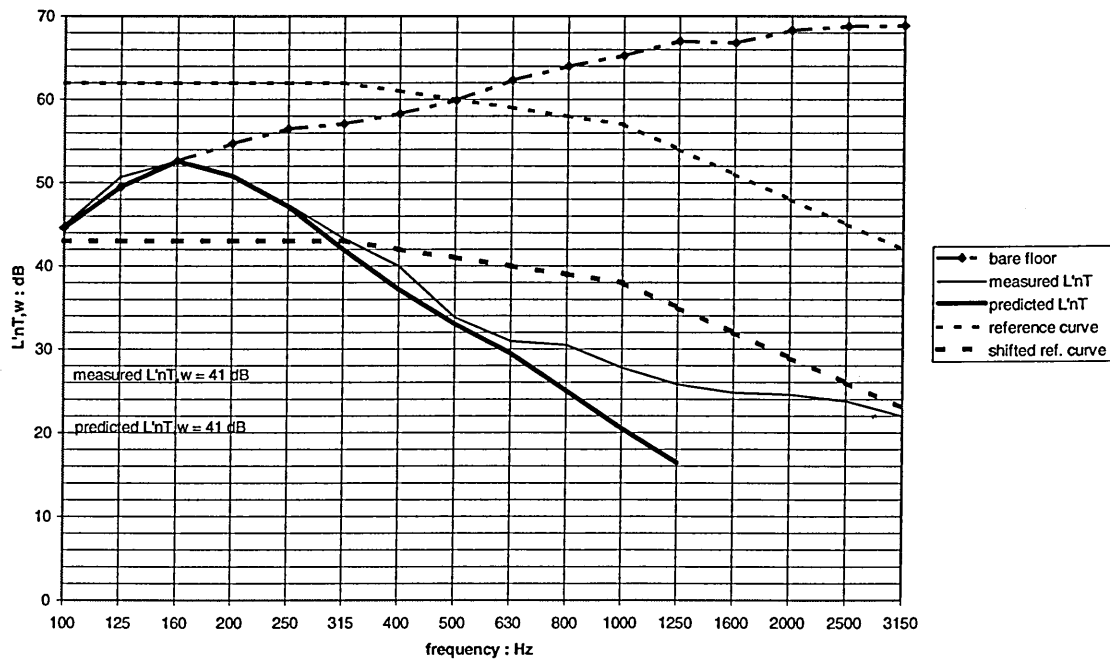


Figure 9.14: L'_{nT} for 16 mm thick 78 kg/m^3 rebond.

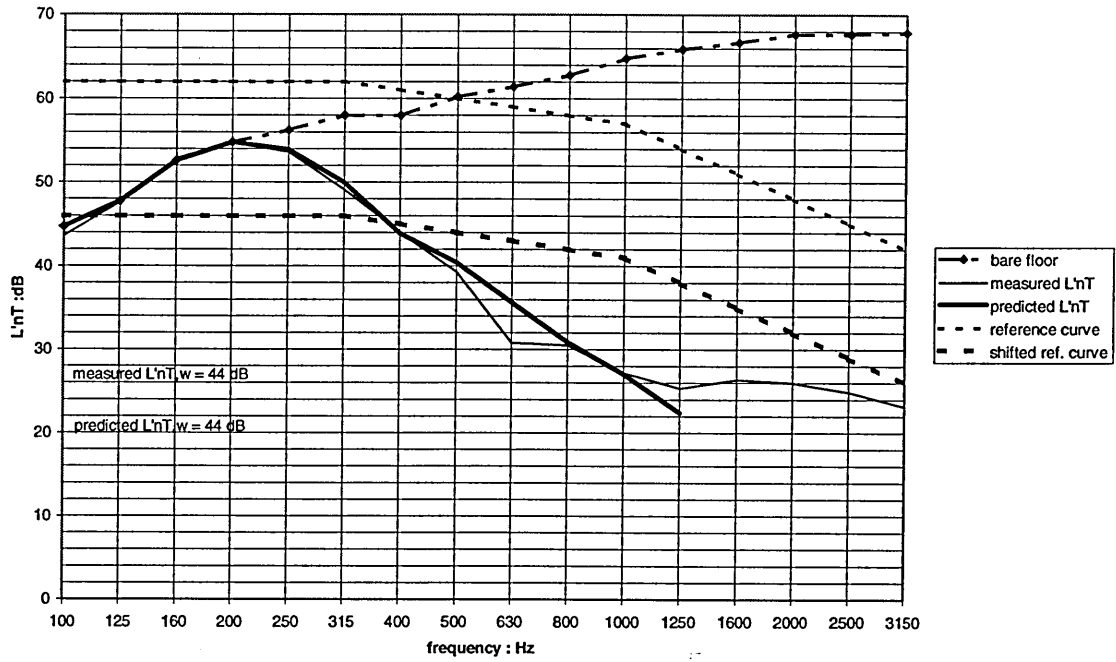


Figure 9.15: L'_{nT} for 10 mm thick 64 kg/m^3 rebond.

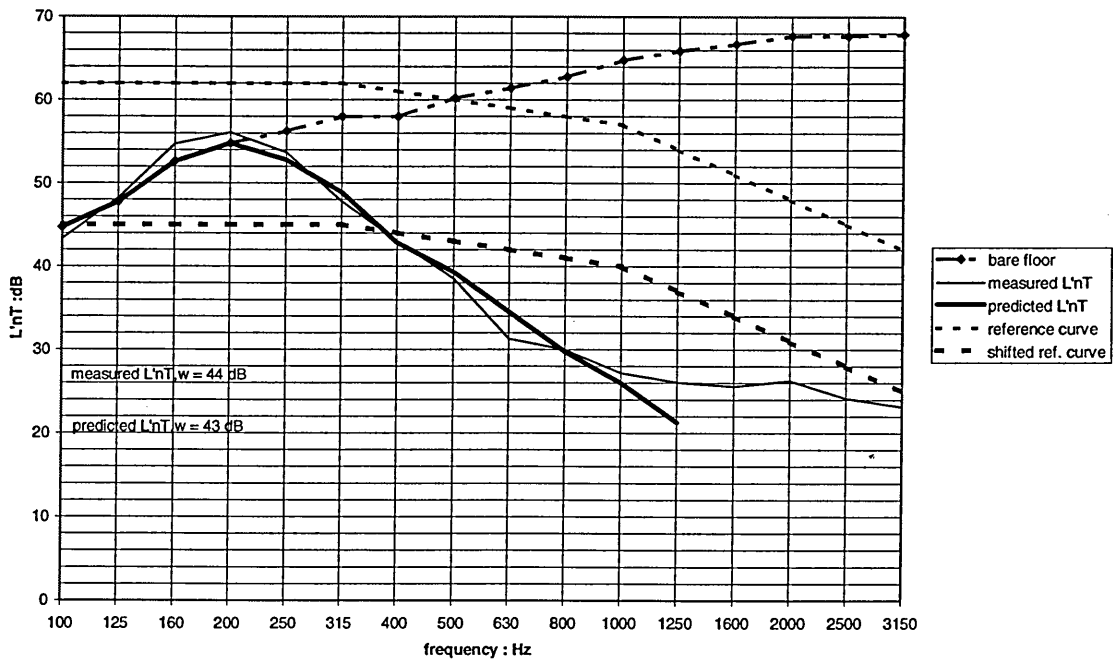


Figure 9.16: L'_{nT} for 11.5 mm thick 96 kg/m^3 rebond.

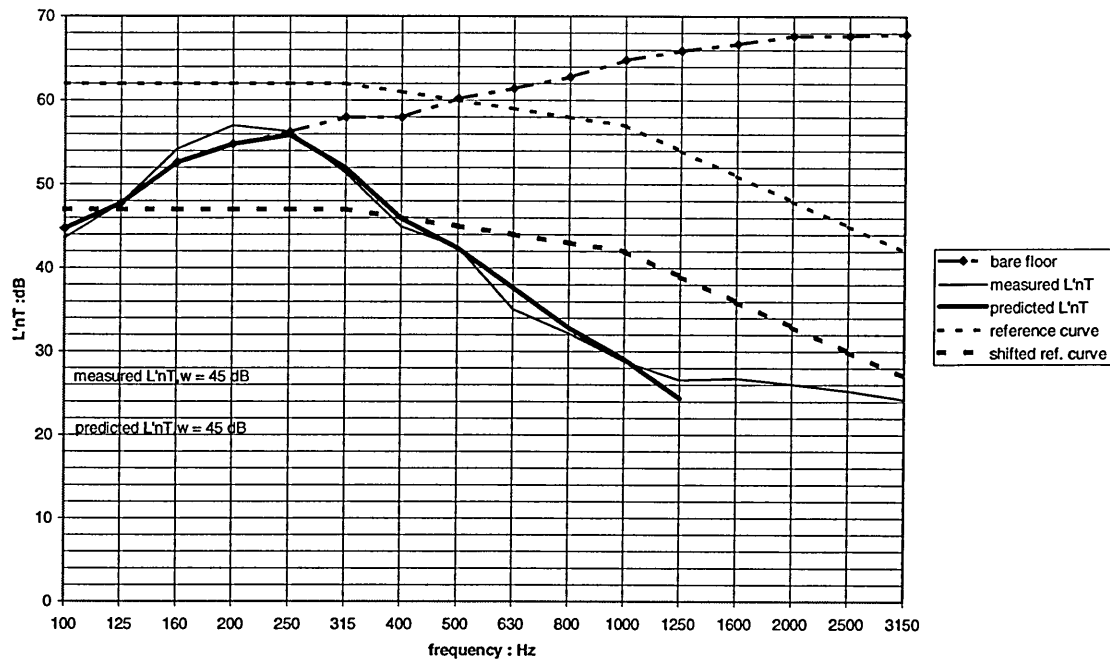


Figure 9.17: L'_{nT} for 9 mm thick 128 kg/m³ rebond.

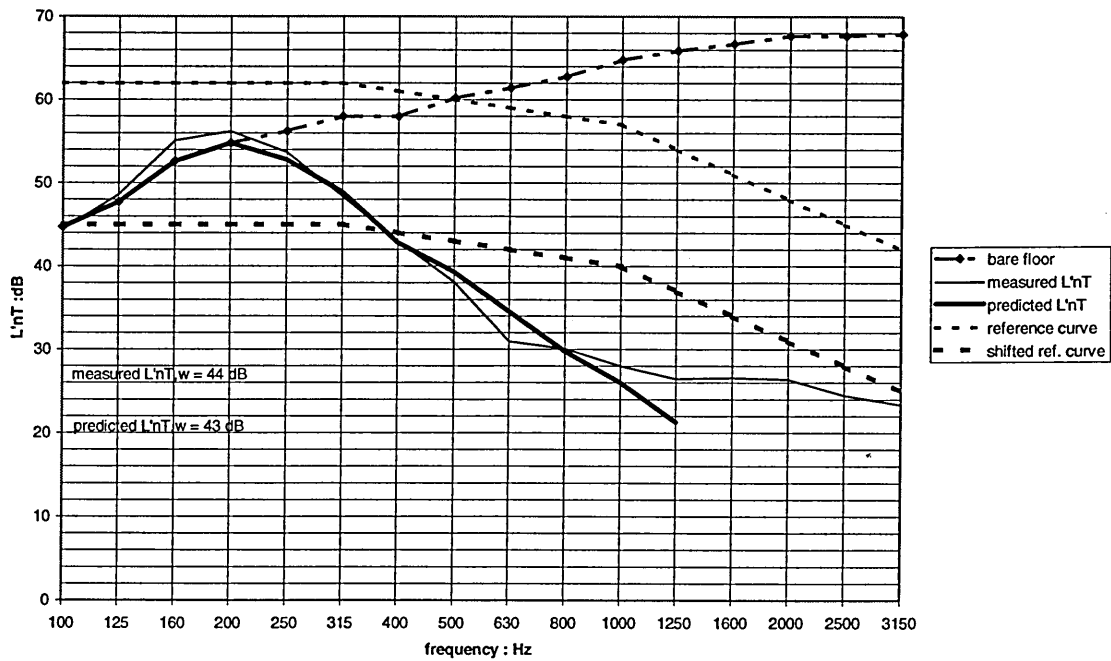


Figure 9.18: L'_{nT} for 11 mm thick 144 kg/m³ rebond.

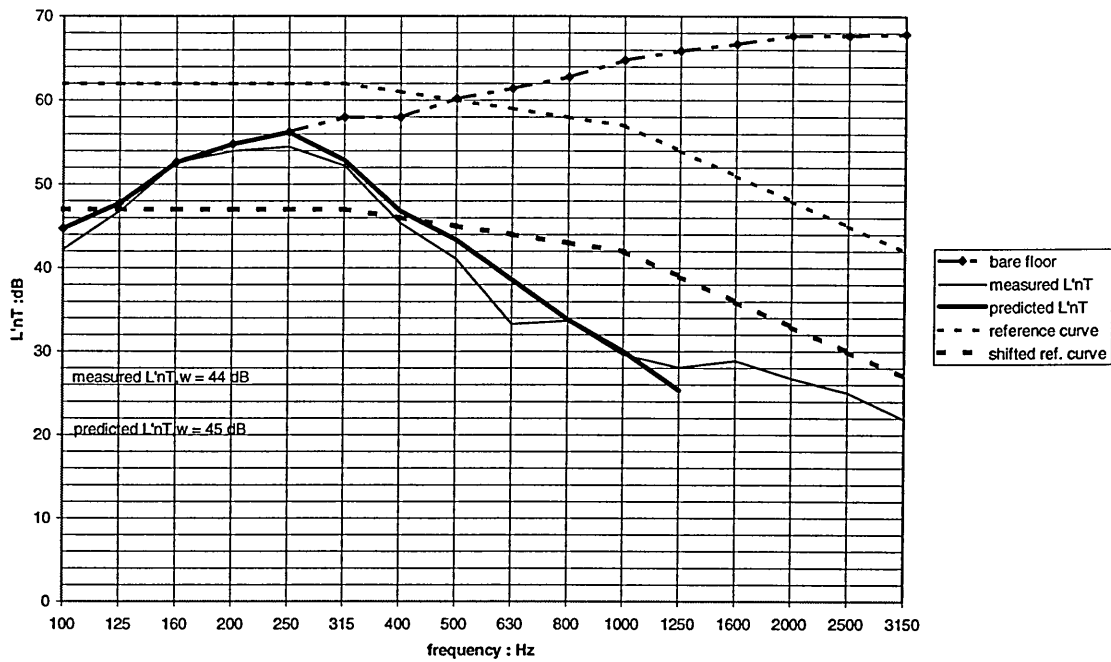


Figure 9.19: L'_{nT} for 8 mm thick 28 kg/m^3 virgin foam.

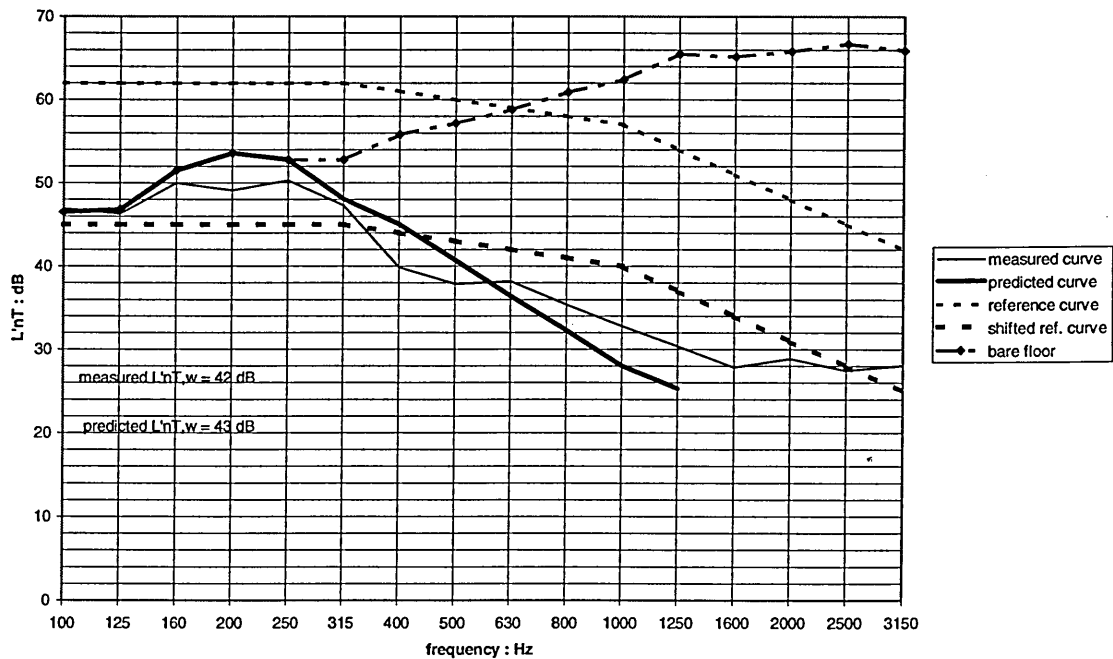


Figure 9.20: L'_{nT} for 15.1 m^2 section of mdf flooring with 6 mm 78 kg/m^3 resilient layer.

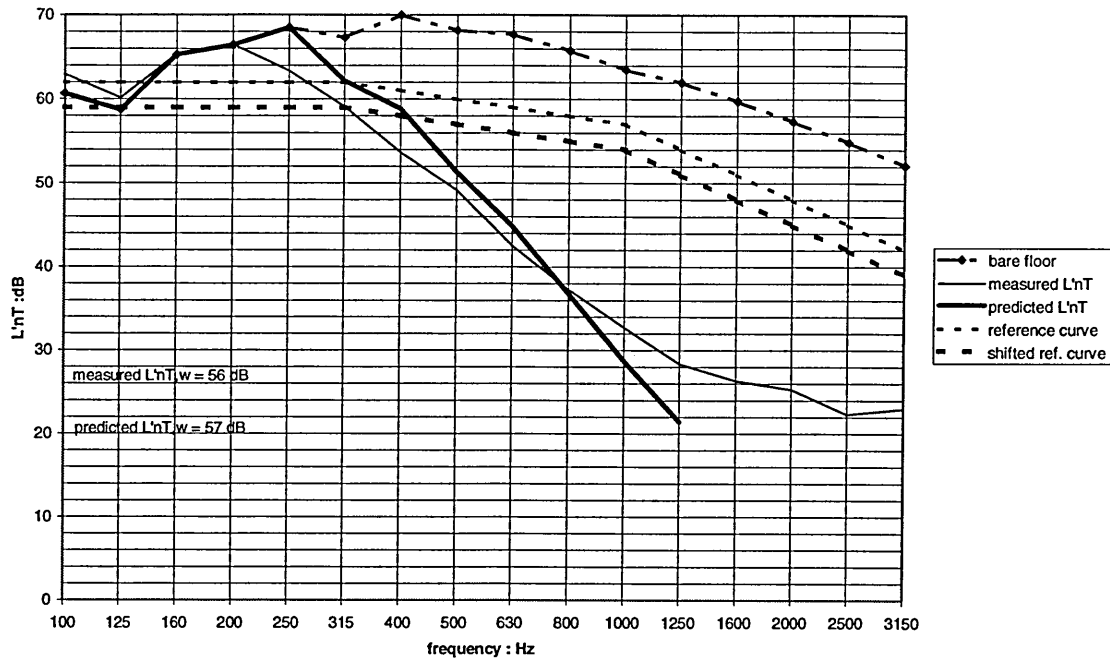


Figure 9.21: L'_{nT} for refurbished floor in council flat

9.6 Discussion

The value for the longitudinal wave speed in the mdf used as the walking surface of the floating floor systems tested is in agreement with the results from measurements carried out in other recent research¹¹ where it was found to be 2500 m/s. This value is within the estimated range of accuracy of the measurements carried out in the laboratory as part of this research programme. The value, 2400 m/s, quoted as the measured longitudinal wave speed is the mean of the measurements given in Table 1 and the potential error in the value is taken to be the standard deviation of the series of measurements.

It should be noted that the separation of the two accelerometers, only 1 m, was limited by the size of the flooring sections. It can be seen, from Table 1, that only four results are given for measurements with the pulse travelling in one direction compared with 13 results in the other. The reason for this is that, with the set of four results, the second accelerometer was close to the edge of the flooring section and it was sometimes difficult to decide where the start of the pulse began and therefore what to take as the

transit time for the pulse. Similar problems were described by Craik⁹ although the separation of his accelerometers was much greater and made such uncertainty insignificant. Here the distortions in the second pulse were probably due to reflection from the edge of the mdf. Measurements taken in the other direction did not suffer from such distortion probably because of the increased distance from the edge. However, despite the small separation of the accelerometers, given the resolution of the analyser (± 0.004 ms) and the number of measurements made, using the measured value in Equation 8.21, (2400 ± 130) m/s, can be justified.

The Figures showing the comparisons of the predicted and measured values of ΔL are shown on a logarithmic frequency axis to allow easy comparison with previously published research work⁵. The predicted values illustrated in Figures 9.1 to 9.10 show excellent agreement with the measured data over a 40 dB range in ΔL and over a range of frequency up to 1000 Hz. The greatest deviations between measured and predicted ΔL are seen with the systems comprising 14 and 16 mm layers of 78 kg/m^3 rebond foam and the large area of floating floor. Even here the correlation between predicted and measured data is reasonable up to 1000 Hz.

Above 1000 Hz it was expected that the predicted values would deviate from those measured. Cremer et al⁵ state that predictions based on Equation 8.19 essentially amounts to comparing a practically achievable case with an ideal one. It cannot be assumed that comparisons based on Equation 8.22 can be regarded differently. No matter how good the improvement in ΔL the levels in the receiving room will not be reduced below the background levels recorded in the absence of impact excitation by fitting a floating floor. Unless, that is, there was significant airborne sound transmission from the source room contributing to receiving room levels and this, transmission, was reduced by the floating floor. An unlikely occurrence under the conditions of this measurement series which is why the predicted values of L'_{nT} have not been shown for frequencies above 1250 Hz in the figures above.

Good correlation between measured and predicted ΔL , and consequently measured and predicted L'_{nT} , at frequencies above 1000 Hz is not important for predicting the likely $L'_{nT,w}$ value when concrete floors are covered with the lightweight mdf systems. Figures

9.11 to 9.21 all show that frequencies above 500 Hz have no effect on $L'_{nT,w}$. Indeed, the single figure rating of the systems comprising the lightweight floating floor is determined by the performance of the bare concrete floor up to the observed resonance frequency. The performance of the floating floor is significant only at the resonance frequency and in the two or three third octave frequency bands above this.

The most important factor in the success of the method's prediction of $L'_{nT,w}$ is its ability to identify the point at which improvement in ΔL is likely to begin. Even the reduction of impact sound insulation around the observed resonance frequency does not adversely affect the prediction significantly. The method for rating the impact sound insulation of floors⁶ states that the reference curve should be moved towards the measured response curve for the floor being rated in steps of 1 dB in order to find $L'_{nT,w}$. This method therefore has an accuracy of ± 1 dB at best and variations of this magnitude are not uncommon in field measurements on the same floor.

The potential error in the values for the longitudinal wave speed in mdf and the resonant frequency of the laboratory test system have been estimated. When the maximum potential errors are added to the wave speed and the resonant frequency and are used in the prediction of ΔL , the maximum difference in the value of $L'_{nT,w}$ obtained was 1 dB and in nearly all cases no difference in $L'_{nT,w}$ resulted from such treatment. Given the above results and the accuracy of the Standard Rating Method lengthy error analysis is irrelevant here.

Experimentally, the best justification for the prediction method are the results from the large supporting floor on which the 15.1 m² section of floating floor was placed, and those from the complete floating floor in the refurbished council flat. Both sets of results give close correlation between $L'_{nT,w}$ from measurements and from those generated by Equation 8.22. There is a difference of 1 dB between the results for the, complete, lightweight floating floor comprising virgin foam. For the rebond system there is a difference of 2 dB. In both cases the predicted results led to an underestimate of $L'_{nT,w}$ which, for prediction, is better than an overestimate of the benefits of a floating floor.

The good agreement observed between the $L'_{nT,w}$ values from measured and predicted data on the large areas and on the single sections of lightweight floating floor suggests that testing small sections in the field may give a good indication of the impact sound insulation of complete floating floors. It would have been desirable to carry out additional tests with large areas of floating floor or complete floating floors. Unfortunately the cost of producing and fitting the floating floors put this beyond the scope of this research programme. However, the question of whether tests on the single sections can be useful for predicting the performance of complete floating floors is examined further in Chapter 10.

9.7 Conclusions

The results in this chapter for the predicted values of ΔL show excellent agreement with the measured data first presented in Chapter 6. All the $L'_{nT,w}$ values for the single sections of floating floor derived from predicted and measured data lie within 1 dB of each other. Comparison of the measured and predicted ratings of the large section of floating floor comprising rebond and for the complete floating floor comprising virgin foam also show close agreement. These results suggest that impact sound insulation measurements on single sections of lightweight floating floor may give a good indication of the acoustic performance of complete floors. This will be investigated further in Chapter 10.

The predicted values of ΔL were obtained using the resonant frequencies of the different test specimens using the sealed laboratory test system described in Chapter 7. They are therefore further confirmation that sealing the test system realistically includes the effect of the air contained in the specimens. This, in turn, means that the dynamic stiffness of the specimens (MN/m^3) is the same as the resilient layers. Sealing the test system, described in BS EN 29052-1, therefore means that the dynamic stiffness of resilient layers with airflow resistivities less than $10 \text{ kPa}\cdot\text{s}/\text{m}^2$ can be determined with acceptable accuracy in the laboratory.

Using Cremer's method for compensating for the effect of the tapping machine hammers when predicting ΔL with lightweight floating floors gave as good correlation with measured data as can be seen from the results of this much earlier work. The

correlation between predicted and measured ΔL held over the same range of 40 dB.

Compensating for the effect of the tapping machine hammers therefore means that BS EN 29052-1 can be used to determine the dynamic stiffness of resilient layers subjected to loadings as low as 0.07 kPa under floating floors. This is considerably less than the 0.4 kPa lower limit of applicability stated in the Standard.

9.8 References

- 1 GERRETSEN E., Calculation of the sound transmission between dwellings by partitions and flanking structures, *Applied Acoustics*, 1979, 12, 413-433.
- 2 GERRETSEN E., Calculation of airborne and impact sound insulation between dwellings, *Applied Acoustics*, 1986, 19, 245-264.
- 3 prEN 12354-1, 1997, *Draft Standard, Building Acoustics, Estimation of Acoustic Performance of Buildings from the Performance of Products, Part 1: Airborne sound insulation between rooms.*
- 4 prEN 12354-2, 1997, *Draft Standard, Building Acoustics, Estimation of Acoustic Performance of Buildings from the Performance of Products, Part 2: Impact sound insulation between rooms.*
- 5 CREMER L., HECKL M., UNGAR E.E., *Structure-borne sound, 1st edition*, Publ. Springer-Verlag, 1973.
- 6 BS 5821, 1984, *Rating the sound insulation of buildings and of building elements, part 2, Method for rating the impact sound insulation.*
- 7 BS EN 29052-1: 1992, *Acoustics - Determination of dynamic stiffness - Materials used under floating floors in dwellings.*
- 8 VÉR I.L., Interaction of sound waves with solid structures, *Noise and Vibration Control Engineering*, (Ed) Beranek L.L., Vér I.L., 245-367, Publ. John Wiley and Sons Inc, 1992.
- 9 CRAIK R.J.M., The measurement of the material properties of building structures, *Applied Acoustics*, 1982, Vol. 15, 275-282.
- 10 W.E. BLAZIER, R.B. DUPREE, Investigation of low frequency footfall noise in wood-frame multifamily building construction, *J. Acoust. Soc. Am*, 1994. 96 (3), 1521-1532.
- 11 HOPKINS C, 1996, Private Correspondence, BRE Acoustics Section.

TESTING SMALL SECTIONS OF FLOATING FLOOR

10.1 Introduction

Chapter 9 compared impact sound insulation measurements on single sections of lightweight floating floor with predicted results calculated using the measured dynamic stiffness of their resilient layers. Good correlation between predicted and measured results was demonstrated both with small sections and also with larger sections of floating floor. The question of whether testing small sections of floating floor gives a realistic indication of the performance of large floating floors remains to be answered however.

For the small sections of floating floor to give similar impact sound insulation under a tapping machine as a large area of floating floor then most of the force on a complete floating layer must be transmitted to the supporting floor in the vicinity of the excitation point. This is VÉR's definition^{1,2} of a locally reacting floating floor for which Equation 8.19 holds. The results from Chapter 9 suggest that impact sound insulation tests on small sections of the lightweight floating floor of interest to this research can usefully be used to predict the impact sound insulation of complete flooring systems.

However, further investigation of this is required. A large area of floating floor may support bending waves that a single section does not. In addition, the contribution of the enclosed air in a resilient layer is likely to be reduced with a single small section since the air will be free to move laterally in and out of the layer.

This chapter describes the approach adopted to determine the usefulness of tests on small sections of floor. Measurements of the driving point mobility of single sections of floating floor are compared with those made on larger sections. Impact tests carried out using small and large sections of floating floor on a concrete supporting floor are described and the results presented. The results allow conclusions to be drawn concerning the validity of tests on small sections of floating floor.

10.2 Background

Equation 8.22 is based on the assumption that a floating slab can be regarded as an infinite plate i.e. that there are no reflections from the edges of the plate causing a reverberant field. This assumption has been shown to be reasonable for highly damped floating surfaces such as asphalt^{3,1} where the reverberant field on the plate is insignificant due to the reflected bending waves being highly damped. This is not the case when the floating floor is thick, rigid and lightly damped such as with concrete screeds. Although the predicted results in Chapter 9 showed good correlation with measured values of ΔL it was not demonstrated that lightweight shallow profile mdf floating floors can justifiably be treated as infinite plates. Nor has it been shown that the results from the single sections of flooring tested are representative of complete floors.

If it could be demonstrated that the results of impact sound insulation tests on single sections of lightweight floating floor are representative of the performance of complete floors then an important point would be made. It is obviously considerably quicker and cheaper to test a section of floating floor lain on a supporting concrete slab than to fit and test a complete floor. Any means of facilitating more economical testing of novel floating floors is likely to have a positive impact on product development. Such a result may therefore be important. Consequently it was felt necessary to explore the validity of the use of single sections of lightweight floating floor in order to assess the performance of full floors.

In a locally reacting floating floor the impact force is transmitted to the supporting floor in the vicinity of the excitation position and, as has been stated, there is no significant reverberant field. A first step towards validating the use of small sections of floor would be to determine whether the single sections of floor exhibit piston-like behaviour or whether they support bending modes. It could then be determined whether the behaviour of the single plates was modified when attached to other sections of floating floor. Measuring the driving point mobility of the sections of floating floor in these two situations appeared to be the way forward. Such an approach would enable the collection of data describing any modal frequencies and the magnitude of the driving point mobility could be compared with the theoretical mobility of an infinite plate

derived from Equation 8.21. The driving point mobility of an infinite plate is given by^{1,4};

$$Y = \frac{1}{Z} \text{ m/(Ns)}$$

Equation 10.1

10.3 Experimental method

Lack of resources meant that single sections of mdf flooring could only be compared with larger sections rather than with a complete floating floor. Six 1.2 m x 0.6 m sections of floor were arranged on a concrete supporting floor as indicated in Figure 10.1. Mobility was measured using a force hammer comprising a Bruel and Kjaer type 8200 force transducer. A Bruel and Kjaer type 4333 accelerometer, two Bruel and Kjaer type 2615 charge amplifiers and an Ono Sokki type 360 dual channel analyser were also used. Measurements were made in the corner of board 2 (2 cm from boards 2 and 4) and at 100 mm intervals from the centre of board 4 up to 500 mm. In all 9 measurements were made with the group of six boards including three taken in the centre of board 4. Measurements were taken on two different single sections of board at their centres and 100 mm from their centres.

Later, field tests were also carried out using the mdf floating floor and two rooms vertically separated by a concrete floor at BRE's premises in Garston (UK). A Norsonics type 830 building acoustics analyser was used with a Norsonics tapping machine. The microphone used was a Bruel and Kjaer type 4165 half-inch microphone. Eight sections of floating floor were fitted together on the supporting floor and the impact sound pressure level in the room below measured according to BS 2750 Part 7⁵. The arrangement of the flooring sections is illustrated in Figure 10.2. The total area of floating floor was 5.8 m² and four measurements were made with the tapping machine across joints, another five were made with the machine in the centre of the boards. Measurement of the impact sound insulation of the separating floor was carried out at four positions prior to laying the floating floor. The ceiling of the receiving room was 12.6 m² in area. The floor of the source room had an area of 19 m². Both rooms had identical width (3.6 m) but the source room was longer (5.3 m c.f. 3.5 m). The

measurements were carried out on the portion of separating floor directly above the receiving room.

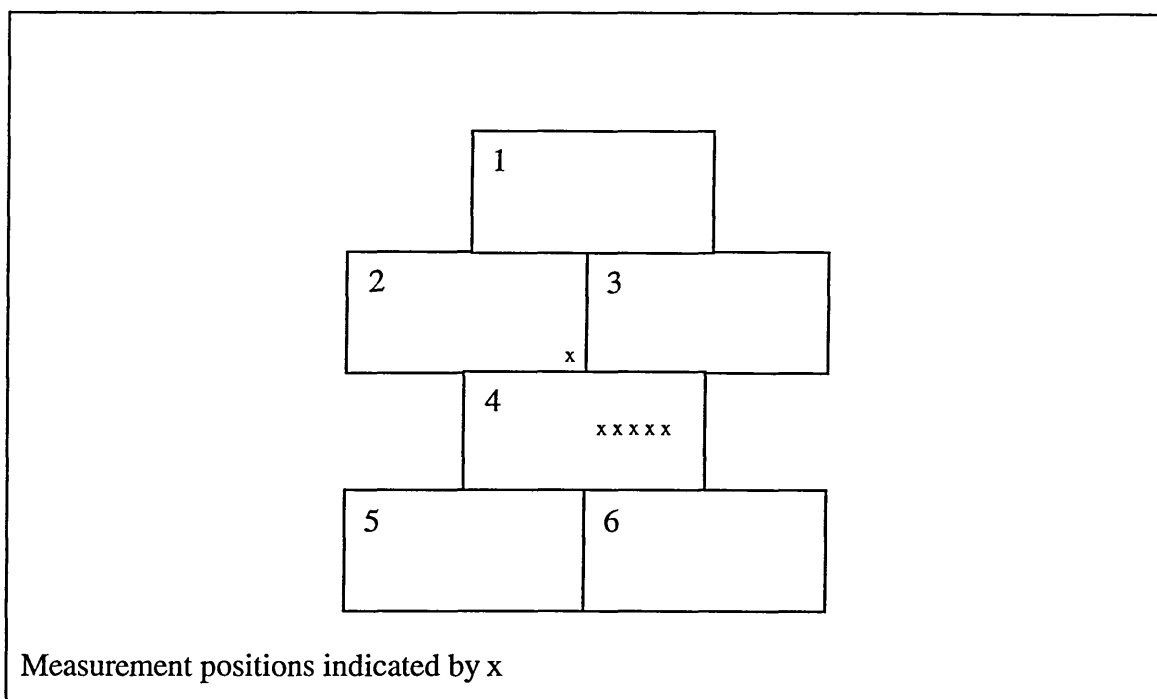


Figure 10.1; arrangement of floating floor sections for mobility tests.

The positions of the flooring sections on the separating floor had been marked and following the sequence of measurements described, measurement of impact sound insulation was conducted with the tapping machine in three different positions. Each position being marked, the tapping machine was placed in the centre of the flooring sections or in the centre of the rectangle which would be covered by the flooring section. Three different sections of floor were used and in each position measurements were taken on the bare floor, on the section of floating floor and on the section of floating floor with its edges completely sealed with petroleum jelly. A thick fillet of petroleum jelly was applied to all four edges of the boards. It was particularly thick on the two tongued edges where the void between the edge of the resilient layer and the edge of the mdf was completely filled.

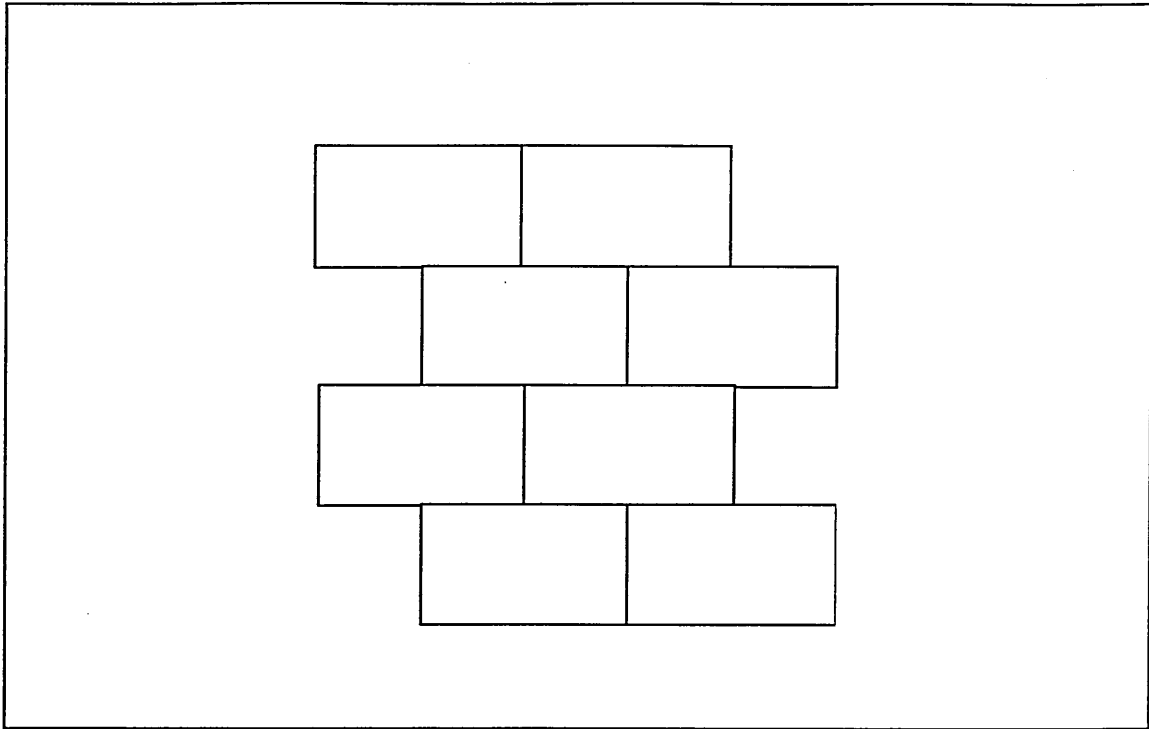


Figure 10.2; arrangement of flooring sections for impact sound insulation test.

10.4 Results

The results of the measurements of the driving point mobility (Y) are illustrated in Figures 10.3 to 10.5. For easier comparison, the results from the mobility measurements on the single boards and the boards attached to others are presented on the same axes. The logarithmic scale used has meant that the results from measurements in the frequency ranges 100 Hz to 1000 Hz and 1000 Hz to 2000 Hz had to be presented separately.

It can be seen that the curves obtained from the single sections of floating floor and the sections fastened to others are very similar but the results in the two frequency ranges illustrated in Figure 10.4 and Figure 10.5 are different to those observed below 100 Hz. Below 100 Hz it can be seen that the mobility peaks occur at the same frequencies (55 Hz and 95 Hz) although the magnitude of the mobility peaks is reduced when the boards are attached to others.

Between 100 Hz and 1000 Hz the peaks from both sets of measurements again, for the most part, occur at the same frequency or are within 2.5 Hz (the resolution of the analyser) of each other. In this frequency range the mobility peaks from the

measurements with six boards do not always lie beneath the curve obtained from measurements on the single board. However, in this frequency region the average mobility lies much closer to the calculated value for an infinite plate of mdf with the same density and thickness as the ones tested. Between 200 Hz and 500 Hz the values are 2.73×10^{-3} m/Ns and 2.72×10^{-3} m/Ns respectively for the group of six boards and the single board compared with the infinite plate mobility of 2.83×10^{-3} m/Ns. Above 2000 Hz the small peaks superimposed on the general trends of the two curves begin to occur at different frequencies but the general trend is that the mobilities are roughly the same apart from the minimum in the single board mobility between 1400 Hz and 1500 Hz.

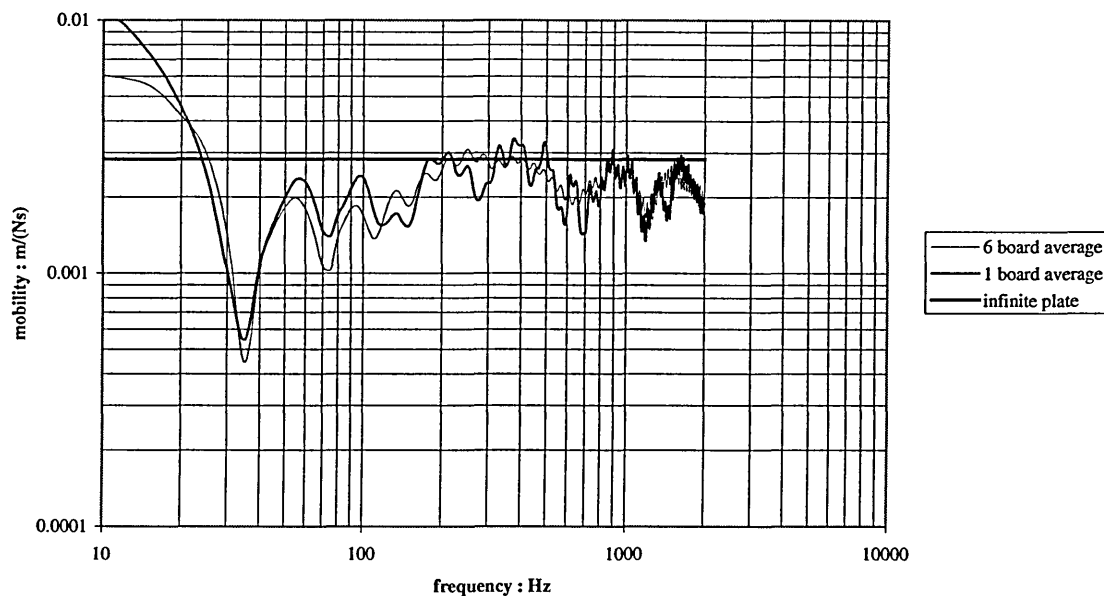


Figure 10.3: average driving point mobility for single boards and for boards attached to others.

Figure 10.6 shows the comparison of the improvement in ΔL from the different impact sound insulation measurements described in the previous section. For all three situations $L'_{nT,w}$ was 47 dB although it can be seen that the gradients of the ΔL curves for the large section of flooring and the single section with its edges sealed are very similar at frequencies between the 200 Hz and 500 Hz third octave bands.

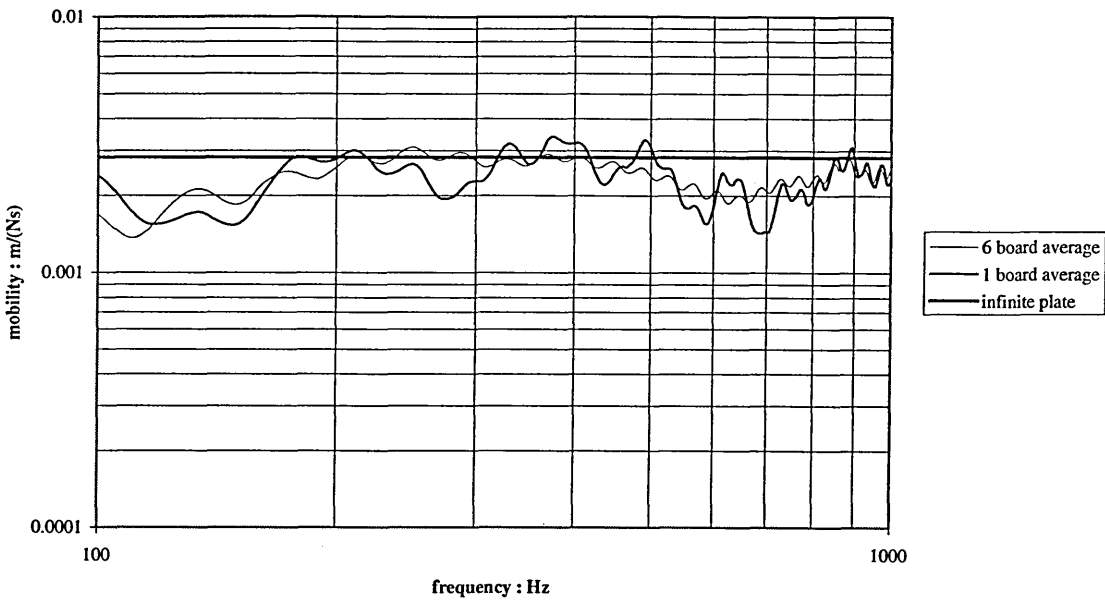


Figure 10.4: average driving point mobility for single boards and for boards attached to others, 100 Hz to 1000 Hz.

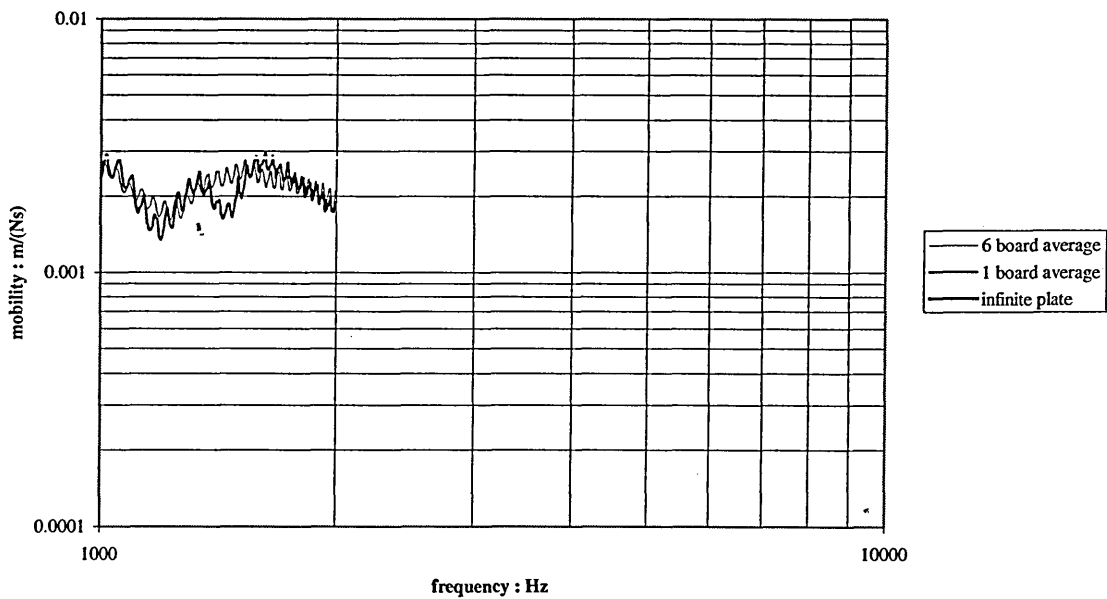


Figure 10.5: average driving point mobility for single boards and for boards attached to others, 1000 Hz to 10000 Hz.

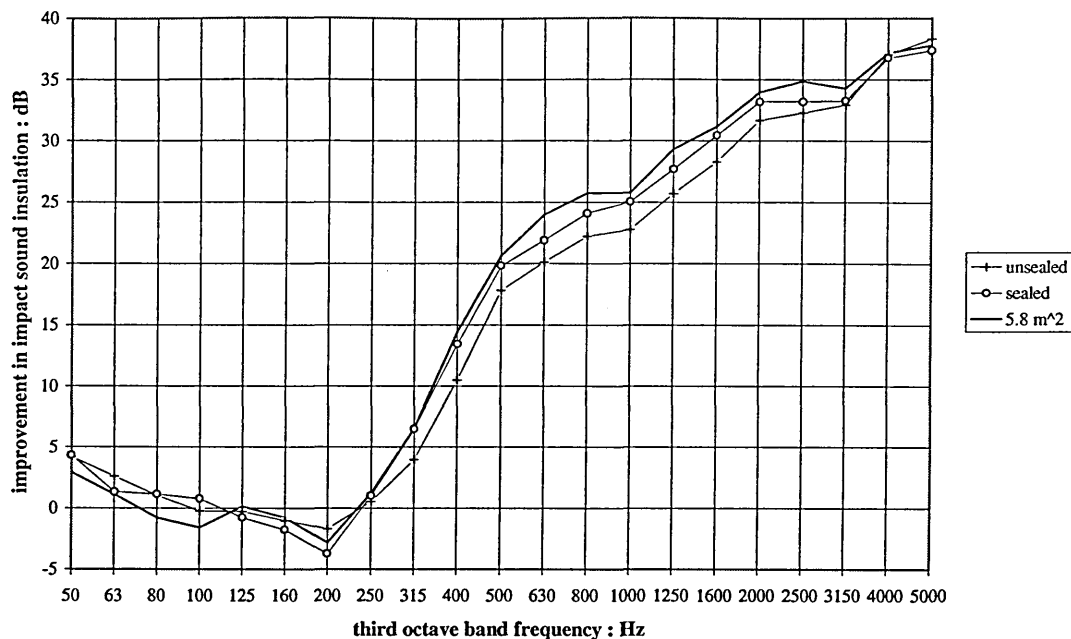


Figure 10.6; ΔL with single sections and larger section of floating floor.

10.5 Discussion

The measurements of mobility for the two situations discussed in this chapter show that the mdf does not behave like a piston when subjected to impact excitation. The presence of mobility maxima and minima at different frequencies is clearly seen. However, the important outcome from the measurements is the close similarity between the mobility curves from the single sections of flooring and flooring areas comprising sections fastened together. This close similarity helps in evaluating the legitimacy of testing single sections of flooring when an indication of the performance of complete floors is of interest.

The reduced height of the mobility peaks below 100 Hz when the sections of flooring are fixed together, compared with the results for the single sections, suggests that there is more damping in this circumstance. It is likely that some of the energy is transmitted across the joints rather than being reflected back from the edges of the flooring boards. The frequencies at which the peaks occur are unaltered however.

In the frequency range between 100 Hz and 1000 Hz the relationship between the two curves shown in Figure 10.4 becomes more complicated than in the frequency range below 100 Hz. All but a few peaks occur at the same frequency but here the curves

cross and the flooring section attached to others exhibits higher mobility than the single boards at some frequencies. However, the close similarity between the average mobility and the infinite plate mobility in the frequency range is significant. Between 200 Hz and 500 Hz the measured average mobilities and that of an infinite plate of the same material and thickness are virtually identical. This adds weight to the argument that using the impedance of an infinite plate to calculate the cut off frequency in Equation 8.22 is justified. Especially so since this frequency range is the most significant in determining the $L'_{nT,w}$ value for the systems comprising the lightweight floating flooring on the concrete supporting floors. Above 1000 Hz the trend appears to be for the mobilities to converge although between 1400 Hz and 1500 Hz the single section of flooring has the lower mobility.

The results from the mobility measurements suggest that the performance of lightweight floating floors comprising the tongued and grooved mdf sections investigated is dominated by the performance of the individual sections. The floors can therefore be considered to be locally reacting and the use of Equation 8.22 to predict the improvement in impact sound insulation when they are fitted on concrete supporting floors is justified. There is further justification for this statement. Other research has shown⁶ that bridging the resilient layer on lightweight floating floors has little effect on their measured sound insulation if the bridge (e.g. a nail or a screw) is ≥ 1 m from the tapping machine.

The results of the impact sound insulation tests presented in Figure 10.6 also add weight to the proposal that the tests conducted on the small individual sections of the floating floor can be taken to be a good indication of the impact sound insulation of a complete lightweight floor. The single figure rating, $L'_{nT,w}$, was the same for each of the three situations but the close similarity of the curves for the large section of floating floor and the single section with its edges sealed suggest that sealing the edges of single sections results in performance very close to that of larger areas of floating floor.

Sealing the edges resulted in the greatest reduction in impact sound insulation around the resonance frequency for the flooring system tested. The reduction in performance at this frequency is likely to be caused by reduced damping in the resilient layer. When the resilient layer is sealed the air contained can no longer move laterally in and out from

beneath the mdf. This may result in reduced damping, as the air no longer moves through the foam with the resulting energy loss due to friction. Certainly one would expect damping to be a significant controlling factor at this frequency.

It is not clear why sealing the edges should improve the impact sound insulation of the single section above 250 Hz. One might expect that the sound insulation would be reduced when the air was prevented from moving out of the layer due to increased stiffness. In fact it is clear from Figure 10.6 that the unsealed single section performed worst. It is also demonstrated that any changes in the stiffness of the resilient layer were not sufficiently significant to move the resonant frequency to a higher third octave band. The most likely explanation for the performance of the sealed sections being better than the unsealed sections is that there was sufficient petroleum jelly applied their edges to increase the damping of the mdf. Comparison with the results from the measurements on the larger section of floating floor suggest that the restraint on the edges of the flooring sections due to the petroleum jelly must have been similar to that provided by the connections to other flooring sections.

10.6 Conclusions

The results presented in this chapter support the argument that the performance of the lightweight shallow profile tongued and grooved floors is governed by the performance of the individual sections. This suggests that such floors can be described as locally reacting and that their contribution to the improvement of the impact sound insulation of concrete supporting floors can justifiably be calculated using Cremer's equation (Equation 8.22 in this thesis). It also adds weight to the argument that single sections of floating floor can legitimately be used to assess the impact sound insulation of complete systems.

The results of the impact sound insulation measurements presented in this chapter demonstrate that sealing the edges of the single section of floating floor resulted in closer performance to the larger section of flooring. This is likely to be due to the sealant restraining the edges of the flooring sections. This may not occur with heavier and stiffer floating surfaces. It may not occur if the sealed edges resulted in an increase in the contribution of the air stiffness sufficient to move the resonance frequency to a higher third octave band. Further tests need to be carried out before firm conclusions

can be drawn but the results of the impact sound insulation measurements presented, along with the mobility measurements, suggest that further comparisons of small sections and complete floors would be useful. If it could be demonstrated that sealed single sections generally gave similar results to complete systems then product development might become easier and less expensive.

10.7 References

- 1 VÉR I.L., Interaction of sound waves with solid structures, *Noise and Vibration Control Engineering*, 245-367, (Ed) Beranek L.L., Vér I.L., Publ. John Wiley and Sons Inc, 1992.
- 2 VÉR I.L., HOLMER C.I., Interaction of sound waves with solid structures, *Noise and vibration control*, (Ed) Beranek L.L., 270-357, Publ McGraw-Hill Inc, 1971.
- 3 prEN 12354-2, 1997, *Draft Standard, Building Acoustics, Estimation of Acoustic Performance of Buildings from the Performance of Products, Part 2: Impact sound insulation between rooms.*
- 4 CREMER L., HECKL M., UNGAR E.E., *Structure-borne sound, 1st edition*, Publ. Springer-Verlag, 1973.
- 5 BS 2750, 1978, *Measurement of sound insulation in buildings and of building elements, Part 7, Field measurements of impact sound insulation of floors.*
- 6 MACKENZIE R.K., 1996, Private correspondence, Napier University.

THE RATING OF FLOORS

11.1 Introduction

The use of the tapping machine in the measurement of impact sound insulation of floors has long been questioned. This chapter reviews previous research into its applicability for measuring the impact sound insulation of floors. The correlation between the rating of floors determined from measurements with the tapping machine and subjective impressions of impact sound insulation is also reviewed. The usefulness of using the tapping machine with the very thin lightweight floors of interest to this research is then discussed with particular reference to non linearity. As an introduction to this discussion the development of the Standard tapping machine and ISO 140 is briefly outlined

11.2 Review of measurement of impact sound insulation

A comprehensive review of the development of ISO 140 was produced by Schultz in 1980¹. More recently McKell² gave an overview of this history as an introduction to her thesis on the impact sound insulation of floors. Both works describe various types of impact sound source and the tapping machine specified in ISO 140-8³ bears a close resemblance to that of a machine used in 1929 by Chrisler and Snyder⁴. The machine comprised five rods raised by a motor driven cam which allowed one rod to fall every fifth of a second. The weight of the hammers is thought to be about two pounds¹ (approximately 0.9 kg). This early tapping machine was used simply to provide sufficient noise to be measured by the early sound level monitors^{1,2} rather than to produce the type of impulse generated by footsteps for example.

According to the Building Regulations Part E, separating floors are required to provide adequate impact sound insulation but walking is not the only activity which produces impact sound in floors. Children and adults jumping and running are sources of impacts

with different force-time histories and therefore produce different sound frequency spectra.

It has been shown that the force-time history of an impact due to an activity such as jumping can be significantly affected by the use of the knees and that running on tiptoe produces a different force-time spectrum to running using heel and toe⁵. It is therefore impractical to construct a single sound source capable of accurately reproducing all the different types of impact on floors produced by human activity in dwellings. However walking is considered to be the most significant source of annoyance due to sound transmission through separating floors^{6,7}.

Since the force-time spectrum produced by the tapping machine is substantially different to that of people walking, as is the sound spectrum produced in a receiving room, many researchers have questioned its usefulness for measuring impact sound insulation. Mckell² points out that most of the power in footsteps is contained in the 250 Hz third octave band or below. From investigations of timber joist floors, using an experimental set up similar to that used in earlier research⁵, Shi et al⁸ demonstrate that the power radiation generated by the tapping machine gives less low frequency radiation and more high frequency radiation in comparison with power radiation from an actual footfall.

The problems associated with measuring the impact sound insulation of floors were perhaps most eloquently described by Lindblad who suggested that acousticians have the choice of making worthless or meaningless measurements¹. A sound source used in the field which accurately reproduces footfalls on floors will produce measurements which are worthless because the resulting sound pressure levels are too low to measure accurately. By hitting the floor harder in order to be able to measure impact sound more easily, meaningless measurements result which give no indication of how the floor would behave when walked upon.

It would appear from the foregoing discussion that the tapping machine is an unsatisfactory impact sound source for assessing the impact sound insulation of floors. There is a significant body of opinion that rejects this however. For all its inadequacies, the tapping machine does produce measurable sound levels in the field which allows the comparison of floors. In addition to this, if “realistic” laboratory tests on different floor

constructions were used to predict field performance, Gerretsen⁶ argues that their performance in the field is likely to vary due to inconsistent installation. In these circumstances the standard tapping machine is considered by a considerable school of thought to be as good a sound source as any. Research has therefore been directed towards improving the system of rating floors described in ISO 717 Part 2⁹ in attempts to improve the correlation between subjective and objective assessments of floors.

11.3 Rating of floors

Research has shown that the current Standard method for the rating of floors does not always give good correlation between the rating value and the subjective satisfaction with the performance of separating floors^{2,6,7,10}. It is no simple task to design a rating system that does provide good correlation however. The objective of preventing annoyance due to the unwanted transmission of impact noise is complicated, not least because there is no simple definition of what constitutes annoyance. For some it might be high levels of unwanted impact sound for others merely being able to detect the sound transmitted through a floor is sufficient to cause annoyance. People also respond differently to sound depending on its frequency. Again, in such circumstances it could be argued that the tapping machine is as good a source of impact sound as any other.

There is another good reason for continuing to use the tapping machine for measuring impact sound levels: it is desirable for any modified rating method to produce a single figure rating having a simple relationship with existing values produced by the method in ISO 717-2. Several researchers therefore argue that continuing to use the tapping machine and modifying the rating curve in the Standard is the most sensible method of providing better correlation between the objective and the subjective performance of floors^{6,7,10}.

The most significant source of dissatisfaction with the ISO rating curve is that it gives insufficient weight to low frequency sound. As an example of this Bodlung¹⁰ compares a concrete and a wood joist floor having the same ISO indices despite the fact that the wood joist floor performs significantly worse in the frequency range below 250 Hz and should therefore provide worse insulation against footsteps noise. Bodlung goes on to investigate the correlation between the subjective performance of floors and rating values provided by using the Standard method of shifting a reference curve towards

measured third octave band impact sound levels but using different reference curves. He concludes that correlation is improved by the use of a curve with the emphasis on low and mid frequency bands. A straight line between 50 and 1000 Hz with a gradient of 1 dB per third octave is proposed. Earlier Gerretsen⁶ had proposed using modified noise rating (NR) curves to give better correlation. Both Gerretsen and Bodlung favour continuing to use the tapping machine as the source of impact sound in the measurement of impact sound insulation.

In their comparison of different methods of rating the insulation of floors against impact sound Fothergill and Carman⁷ also considered that the ISO tapping machine should continue to be used despite its limitations. Even so, alternative sources of impact sound were investigated in their research. A standard (ISO) tapping machine was modified to simulate a woman walking and sand bags dropped onto the floor were used. These had been found to represent children jumping reasonably well. One of the conclusions from this research was that the reference curve specified in ISO 717-2 is not the optimum shape to produce good correlation between the ratings and subjective impressions of the impact sound insulation of floors. It was considered that correlation could be improved by measuring down to the 50 Hz third octave band and by using a straight line curve having a slope of 3 dB per octave. The authors did not feel that the results from their research alone made a conclusive case for changing the reference curve in the Standard however.

The most recent contribution identified to the debate on the usefulness of the ISO tapping machine is that made by Warnock¹¹ in December 1998 in a paper presented to an international conference in on the performance of timber buildings. The paper presented results and conclusions derived from measurements on about 190 different floors. Different devices were used to generate impact sound and the spectra from these were compared to those generated by male walkers (about 90 kg) wearing hard rubber soled shoes. Warnock states that whilst the spectra produced by walkers and mechanical impactors may vary, it is sufficient that there be good correlation between the sound pressure levels produced by the impactors and the walkers. If the correlation is good then the levels produced by the impactor can be adjusted to produce a spectrum more like that produced by a walker.

Warnock showed that the ISO tapping machine is almost as good as the best of the different impactors tested. Good correlation between walkers and the tapping machine was demonstrated for all the floor surfaces tested, except carpet, up to at least 500 Hz. It was concluded that there is no need to stop using the tapping machine for the testing of floors but that it would be useful to measure levels down to 50 Hz.

The debate over the most appropriate method for measuring impact sound insulation and rating floors will continue. Impact sound insulation is measured in Japan with a car tyre dropped from a fixed height¹² although this machine is not practical for work in the field¹¹. Recent research in Sweden¹³ on wood joist floors has shown that sandbags dropped from different heights can represent adults and children running and jumping on such floors reasonably well. However it appears that the ISO tapping machine will continue to be used for the foreseeable future.

11.4 Lightweight floating floors

The question of whether the tapping machine is appropriate for testing the lightweight floating floors of interest to this research remains to be answered. Good correlation between measured and predicted improvements in impact sound insulation was demonstrated in Chapter 9. However, Lindblad¹⁴ shows that if the tapping machine hammers do not rebound after striking a resilient floor covering then there is a 6 dB improvement compared with the situation where the hammers strike a hard surface and rebound without losses. Lindblad states that the condition for rebound is;

$$\sqrt{KM} < 2Z_m$$

Equation 11.1

Here, M is the mass of the hammer (0.5 kg) and Z_m is the driving point impedance of the floating slab.

Gudmundsson¹⁵ investigated a range of floating floors on mineral fibre resilient layers. He compared¹⁵ the spectrum of the force input to the surface of a concrete supporting floor by a tapping machine hammer with the force spectrum obtained when the same hammer strikes the surface of a chipboard floating floor. This comparison shows that, with the chipboard floating floor, the force begins to decrease at the “cut off” frequency

(f_{co}) which for the chipboard is 550 Hz. Gudmundsson shows that when the force, above f_{co} , is corrected by ΔF where;

$$\Delta F = 10 \log \left[1 + \left(\frac{f}{f_{co}} \right)^2 \right] \text{ N}$$

Equation 11.2

(the same as the correction applied in Equation 8.22) the force put into the chipboard is the same as that input to the concrete supporting slab.

In addition, Gudmundsson shows that at frequencies below f_{co} the force put into the floating chipboard surface is 5 to 6 dB lower than that input to the concrete supporting floor. Gudmundsson uses Equation 11.1 to determine that the tapping machine hammers do not rebound on chipboard floating floors and suggests that this lack of rebound may explain the difference in force levels in the frequency range up to f_{co} .

Gudmundsson considers K (in Equation 11.1) to be dominated by the stiffness of the resilient layer. He cites Lindblad¹⁴ but describes K as compliance. Lindblad¹⁴ refers to K as the “compliance factor”. Dimensional analysis of Equation 11.1, in addition to Lindblad’s derivation, reveals that K represents stiffness in the equation.

If the tapping machine puts less force into a lightweight floating floor, due to the hammers not rebounding, than into a concrete supporting floor then it can be argued that the impact sound insulation of such lightweight systems cannot be measured according to the method described in ISO 140-7. The question of whether the tapping machine hammers do rebound on the mdf and whether this affects the rating of systems comprising mdf floating floors was therefore examined in this research.

There is a further point to consider: the mass of the tapping machine (approximately 10.5 kg for the Norsonics machine used in this research) imposes little strain on the polyurethane resilient layer of the systems examined in this research. If walking on the systems causes the polyurethane resilient layer to be strained beyond the linear region of the stress-strain curves shown in Chapter 3 then using the tapping machine to measure impact sound insulation will not give realistic results. This was also investigated therefore.

11.5 Experimental method

11.5.1 Tapping machine hammers on mdf and concrete

Tests were conducted to determine the amount of time that the tapping machine hammers remain in contact with the surfaces of lightweight mdf floating floors and concrete floors. A simple electrical circuit was used as shown in Figure 11.1. A thin strip of aluminium foil was attached to the surface under test with adhesive tape. A 1 k Ω resistor was placed in the circuit and the voltage drop across the resistor was measured when the hammer struck the aluminium foil and completed the circuit. By so doing it was possible to measure the time that the hammer was in contact with the test surface. An Ono Sokki dual channel analyser (type 360F) was used to record the output from the circuit and was triggered on the positive going edge of the pulse.

11.5.2 The deflection of lightweight floating floors under walking

The likely deflection suffered by the thin 78 kg/m³ layer of rebond foam used in the commercially available lightweight floating floor system was investigated using an Ono Sokki dual channel analyser (type 360F), a Bruel and Kjaer type 4333 accelerometer and a Bruel and Kjaer type 2635 charge amplifier. A single section of floating floor (1.2 m x 0.6 m) was placed on a large concrete floor and the accelerometer attached to its surface, close to the centre, with beeswax. A 90 kg male wearing soft rubber soled shoes stepped on the section of floating floor as close to the accelerometer as possible when walking and then when hopping and landing heavily with his heel close to the accelerometer. The floating floor section was approached from both directions perpendicular to its longer sides.

The recorded displacement was averaged over 16 measurements after which there was no discernible difference in the recorded pulse. The analyser used to record the pulses was triggered on the rising edge of the pulse and an audible warning sounded to indicate any instrument overloads. Measurements where overloads were indicated were not included in the averaging.

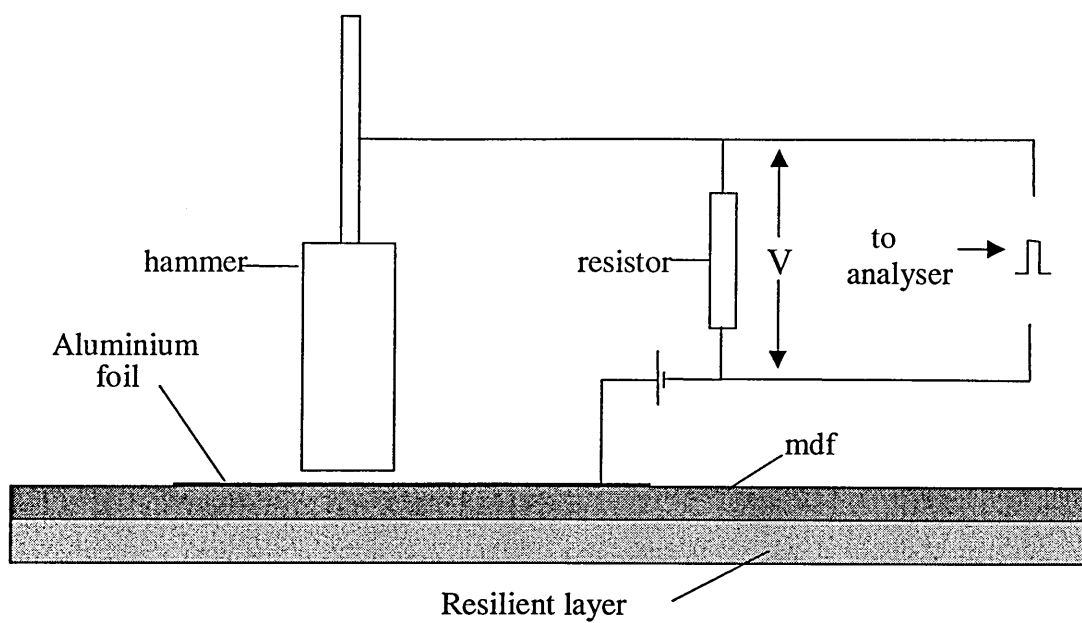


Figure 11.1; circuit for measuring hammer contact time.

11.6 Results

The results of the tests to determine how long the tapping machine hammers remained in contact with the mdf and concrete surfaces are shown in Figure 11.2 and Figure 11.3. It can be seen that the time spent in contact with the mdf surface by the hammer is over three times that spent in contact with the concrete surface. 4.7 ms compared with 1.3 ms.

Figure 11.4 shows the results of the investigation into the deflection suffered by the mdf floating surface when walked upon. The maximum deflection occurs when the section of floor is stamped upon heavily and is approximately 1.3 mm.

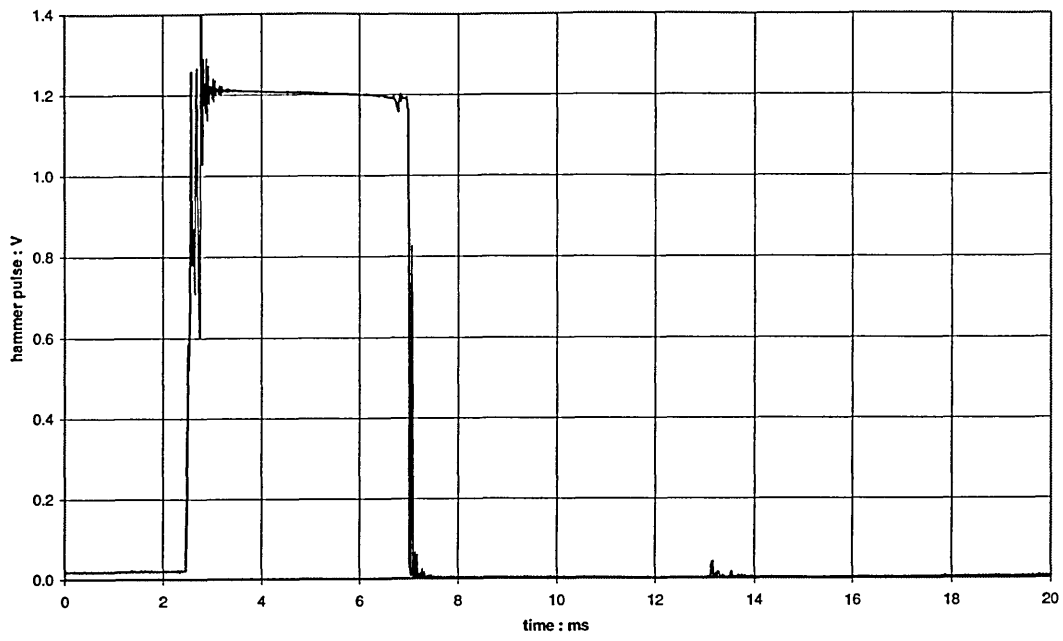


Figure 11.2; tapping machine hammer on mdf.

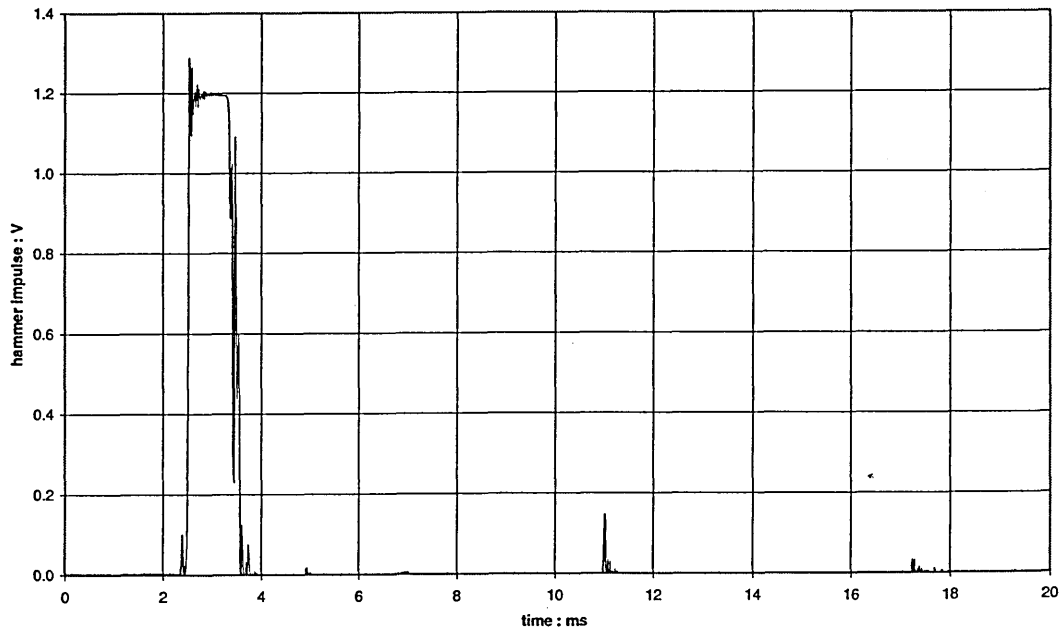


Figure 11.3; tapping machine hammer on concrete.

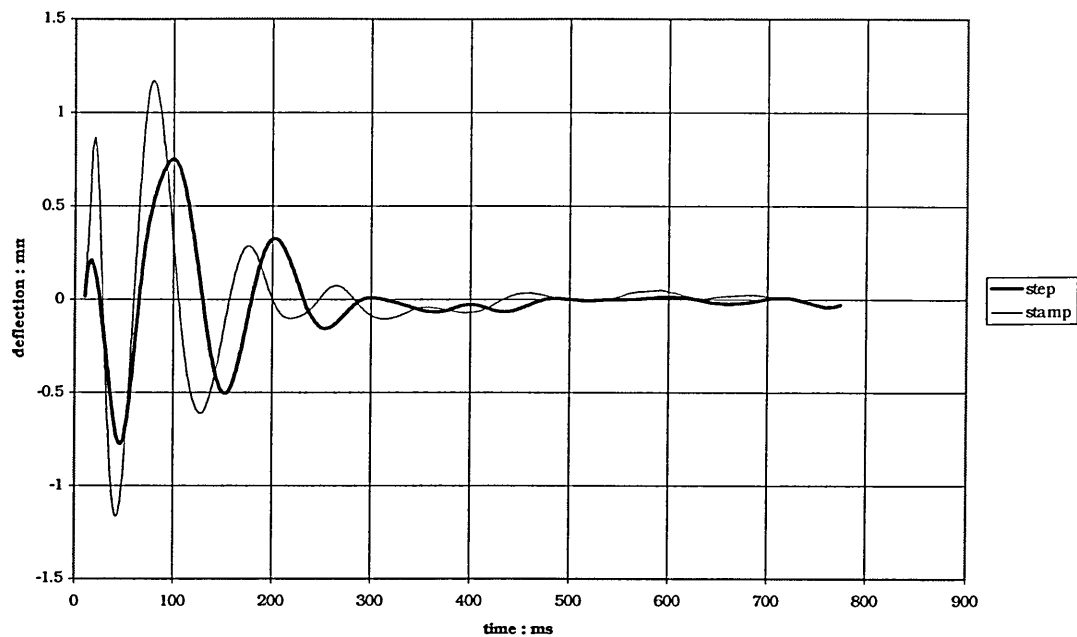


Figure 11.4; deflection of lightweight flooring with 78 kg/m³ polyurethane rebond resilient layer due to walking and stepping heavily.

11.7 Discussion

Stepping heavily on the mdf floating floor produced a maximum deflection corresponding to a strain on the resilient layer of around 22%. It was shown in Chapter 3 (Figure 3.4) that the rebond foam used as the resilient layer in this floating floor exhibits a linear relationship between static stress and strain up to strains of 40%. The foam is therefore operating in this linear region under both tapping machine loading and loading due to the supported surface being stepped upon. There would appear to be no problem with using the tapping machine to test these lightweight floating floors from the standpoint of the behaviour of the polyurethane foam “spring” comprising the resilient layer.

The question of whether the difference in the time that the tapping machine hammers spend in contact with the two surfaces affects the results so significantly that the tapping machine should not be used has still to be addressed however. Equation 11.1 was

derived by Lindblad in his research into the behaviour of soft coverings for floors. He shows that even with soft a covering on a concrete slab the tapping machine hammers will rebound unless the losses of the soft covering are “Not very big”. He states that for the hammers not to bounce the supporting slab must be very thin¹⁴.

It is known that when the tapping machine is used on soft coverings, e.g. carpet, the improvement in ΔL measured with the tapping machine may be greater than the improvement observed when the soft coverings are walked on¹⁶. This is partly due to the non linear behaviour of such materials and was, it would seem, one of the reasons for Lindblad’s interest in soft floor coverings which led to his research. When a tapping machine hammer strikes a relatively hard surface covering a softer material it cannot behave in the same manner as when striking a soft surface directly. The hammer will not deform or penetrate the surface in the same way and the area over which the impacting force is spread will remain much more constant.

In all the Figures in Chapter 9 showing measured L'_{nT} versus frequency, those values of L'_{nT} up to the resonance frequency for the system are little, if at all, different from the values for the bare concrete supporting slab. If they are different, L'_{nT} is usually made worse because of the effects of resonance. This does not suggest that the tapping machine hammer is putting less force into the system at these frequencies than was put into the bare floor. The mdf floating surface used in the systems under investigation in this research does not appear to behave in the same way as the chipboard floating floor examined by Gudmundsson. This chipboard floating floor had a mineral fibre resilient layer and rested on a concrete supporting floor¹⁵. Gudmundsson demonstrated that by correcting for ΔF at low frequencies, the correlation between measured and predicted values of ΔL was improved.

The density of flooring grade chipboard is around 720 kg/m^3 and c_L is approximately 2500 m/s . For 22 mm thick chipboard flooring, as used by Gudmundsson, then the driving point impedance (using Equation 8.21), will be roughly 2000 Ns/m , a little over 5.5 times greater than that of the mdf investigated in this research. The dynamic stiffness of the 50 mm thick mineral wool used in Gudmundsson’s experiment was around 11 MN/m^3 , calculated using the reported¹⁵ dynamic modulus of 0.55 MPa using¹⁷:

$$\text{dynamic stiffness} = \frac{\text{dynamic modulus}}{\text{thickness}} \quad \text{N/m}^3.$$

Equation 11.3

According to Gudmundsson's argument for whether or not the tapping machine hammers bounce (Equation 11.1) one would expect that the hammers would not bounce on the mdf either. The driving point impedance of the mdf (353 Ns/m) is lower than that of chipboard and the stiffness of the polyurethane foam (48 MN/m³) is greater than that of Gudmundsson's mineral wool. The measurements described earlier in this chapter show that this is not the case. The hammers do spend more time in contact with the surface of the mdf than the surface of the concrete but they clearly bounce. It would appear that further investigation is required in order to verify that Equation 11.1 can be legitimately used with lightweight floating floors. This result suggests that Equation 11.1 should only be used when the tapping machine is used on soft coverings i.e. the situation described by Lindblad leading to his derivation.

It is perhaps not surprising that the hammers should spend more time in contact with the surface of the mdf than with the surface of the concrete floor. The mdf is supported by the resilient layer which can be expected to deform slightly before recovering from hammer impacts. However, according to the specification in ISO 140-8³ the tapping machine hammers behave as they should in both situations (on the mdf and on the concrete). The Standard³ states that ; the time between impact and lift of the hammer shall be less than 80 ms. It does not specify the amount of time that the hammers should be in contact with the surface being tested.

It is clear that the extra time that the hammers spend in contact with the surface of the mdf will effect the shape of the force pulse applied to the floating surface and, therefore, to the supporting slab however. Gudmundsson compared the force input by the tapping machine hammers to different thicknesses of floating concrete slab and his chipboard floating floor. He showed that, depending on the hardness of the floor struck by the hammers, at a certain frequency the input force began to reduce. He called this the break frequency and demonstrated that for his chipboard floor this was around 550 Hz. Gudmundsson attributed the unexpectedly rapid reduction in force on the chipboard floating surface above 550 Hz to the fact that the break frequency and the cut off

frequency (f_{co}) of the chipboard occurred at roughly the same frequency. Recently, Scholl and Maysenholder¹⁸ demonstrated that the break frequency of timber floors is also around 550 Hz using mathematical modelling.

It has been demonstrated that the cut off frequency of the lightweight mdf floating surface investigated in this research is very low (112 Hz) compared with the chipboard floating surface investigated by Gudmundsson. It has also been shown that the third octave bands above 500 Hz are irrelevant for the sound insulation rating of these floors. There is no evidence that the break frequency of the mdf flooring lies below 500 Hz. The results from the tests described in Chapter 6 do not indicate an improvement in impact sound insulation below 250 Hz that might be attributed to reduced force input. According to Warnock's argument¹¹ then, there is no insurmountable problem in using the tapping machine to rate such floors. The necessary correction to the spectrum above f_{co} is known and can therefore be applied in order to improve the correlation with subjective impressions of their performance.

11.8 Conclusions

The literature reviewed in Sections 11.2 and 11.3 of this chapter suggested that the Standard tapping machine will continue to be used for some time to come. Its limitations are widely known but despite these, it provides a practical method of comparing and rating the impact sound insulation of floors. A considerable body of opinion supports its continued use.

Measurement of the displacement of the mdf surface of the floating flooring when it was walked upon showed that the resilient layer was not compressed beyond the linear region of the stress strain curves shown in Chapter 3. Under the load imposed by the tapping machine the resilient layer will be in the region where the linear relationship between stress and strain holds. The use of the tapping machine to measure the impact sound insulation of the lightweight mdf floating floors under investigation in this research is therefore justified.

It would appear that Gudmundsson may not be justified in using Lindblad's inequality to explain the apparent low frequency improvement in impact sound insulation of the

chipboard floating floors he investigated. Further investigation of this might be worthwhile.

11.9 References

- 1 Schultz T.J., *Impact noise testing and rating*, NBS-GCR-80-249, National Bureau of Standards, Washington DC, 1980.
- 2 McKell B., *The development of a screening test to determine the impact sound insulation of floors*, PhD thesis, Heriot-Watt University, Edinburgh, 1991.
- 3 EN ISO 140-8, 1998, *Acoustics - Measurement of sound insulation in buildings and of building elements, Part 8., Laboratory measurements of the reduction of transmitted impact noise by floor coverings on a heavyweight standard floor.*
- 4 Chrisler V.L., Schneider P., Transmission through wall and floor structures, *J. Research NBS*, 1929, 2, research paper 48, 541-559.
- 5 Kimura S, Inoue K, Practical calculation of floor impact sound by impedance method, *Applied Acoustics*, 1989, 26, 263-292.
- 6 Gerretsen E., A new system for rating impact sound insulation, *Applied Acoustics*, 1976, 9, 247-263.
- 7 Fothergill L.C., Carman T., Insulation - impact sound A comparison of methods for rating the insulation of floors against impact sound, *Building research and practice, The journal of CIB*, 1990, number 4.
- 8 Shi W., Johansson C., Sundback U., Assessment of the sound insulation of a wood joist construction due to different types of impact sources, *Applied Acoustics*, 1996, 48 No. 3, 195-203.
- 9 EN ISO 717-2, 1997, *Acoustics - Rating of sound insulation of buildings and of building elements, Part 2 impact sound insulation.*
- 10 Bodlung K., Alternative reference curves for evaluation of the impact sound insulation between dwellings, *Journal of Sound and Vibration*, 1985, 102, 3, 381-402.
- 11 Warnock A.C.C., Floor research at NRC Canada, *Proc Acoustic performance of medium-rise timber buildings*, Conference, December 3-4, 1998, Dublin, Ireland.
- 12 JIS 1418, *Japanese National Standard describing impact testing of floors.*
- 13 Shi W., Johansson C., Sundback U., An investigation of the characteristics of impact sound sources for impact sound measurement, *Applied Acoustics*, 1997, 51 No. 1, 85-108.

-
- 14 Lindblad S, Impact sound characteristics of resilient floor coverings, *Division of Building Technology, The Lund Institute of Technology, Sweden*, 1968, Bulletin 2.
 - 15 Gudmundsson S., Sound improvement of floating floors. A study of parameters, *und Institute of Technology, Department of Building Acoustics, Lund, Sweden*, 1984.
 - 16 Carman T.A., Fothergill L.C., Aubree D., Josse R., Villot M., A comparison of methods for rating the insulation of floors against impact sounds, BRE & CSTB, January 1988.
 - 17 PrEN 13163, 1998, *Thermal insulation products for buildings-Factory made products of expanded polystyrene-specification*.
 - 18 Scholl W., Maysenholder W., Impact sound insulation of timber floors: Interaction between source, floor coverings and load bearing floor, *Proc Acoustic performance of medium-rise timber buildings*, Conference, December 3-4, 1998, Dublin, Ireland.

SUMMARY AND CONCLUSIONS

12.1 Introduction

This chapter begins by restating the importance of the resilient layer to the impact sound insulation of floating floors. It points out that although there are accepted alternatives to the use of fibre quilts for isolation there is little published information on their dynamic properties. The reasons for the development of flooring systems comprising flexible polyurethane open cell foams as resilient layers are summarised and the special interest in the use of rebond foams to this thesis is justified.

The main findings of the laboratory tests and the field tests are summarised and the correlation between them is discussed. This allows the extent to which the objectives of this research programme have been met to be assessed. The discussion of the work undertaken leads to recommendations for further research.

12.2 Noise in buildings and floating floors

Complaints concerning unwanted noise in dwellings have risen significantly over the past twenty years and impact sound transmission through separating floors in dwellings has been shown to be particularly disturbing^{1,2,3,4}. The use of floating floors, where the walking surface is decoupled from the supporting structure, is an accepted method of reducing impact sound transmission⁵. In these systems the impact sound insulation of the floors is primarily governed by their resilient layers which, in the UK, usually comprise mineral or glass fibre quilts. Advances in polymer science since the early part of this century have led to the availability of other materials however and it is now accepted that both polystyrene and closed cell polyethylene can be used for impact sound insulation⁵.

The advantages offered by flexible polyurethane foams over the traditional fibre quilts were outlined in Chapter 1 but at the present time there is little information regarding

their suitability as isolating layers. Pritz⁶ could find no information on the dynamic Young's modulus and loss factor of polyurethane and polyethylene foams for use under floating floors and therefore repeated his earlier experiments carried out on fibre quilts to determine these parameters. Research into the use of flexible polyurethanes in floors has been conducted in Japan^{7,8,9} but only Mackenzie has proposed the use of open cell flexible polyurethane foams in floating floors.

The development of shallow profile floating floors comprising flexible open cell polyurethane foam was described in Chapter 1. It followed investigations by the Scottish Special Housing Association into the failure of fibre quilt resilient layers of floors installed in the 1970s. The failure of these quilts led to the search for alternative materials and the advantages offered by low density flexible open cell polyurethane foam led to its adoption. Not least of these was that thin layers, less than 10 mm, gave acceptable improvements in impact sound insulation. For the first time a system incorporating flexible open cell polyurethane foam as the resilient layer that could simply be placed on a supporting floor to improve its impact sound insulation whilst raising the existing floor level less than 20 mm was commercially available^{10,11}.

Searches of the literature, described in Chapter 2, confirmed that the use of open cell foam in floating floors is still novel and revealed that the characteristic behaviour under compression of virgin foam is well known. The literature also showed that, despite their growing availability, there was no published information regarding the static stress-strain characteristics of rebond foams, their dynamic behaviour or their airflow resistivity. Fatigue and compression set appear to be main concerns of industry.

The aim of this thesis was to investigate thin layers of flexible open cell polyurethane foam in order to identify the characteristics which made them most useful for use as resilient layers under lightweight shallow profile floating floors. It was intended to determine which of the Standard tests on the materials were most useful for this purpose and to identify a method for predicting the improvement in impact sound insulation offered by such floors. Although lightweight shallow profile floating floors were available there was no method for predicting whether using them would upgrade an existing floor sufficiently to comply with the Building Regulations Part E. A means of predicting this would be a useful contribution to the field.

12.3 Summary of main findings

Static tests were conducted on the different polyurethane foams primarily to assess their suitability for supporting floating floors. The materials' stress-strain characteristics under compression gave the required information and tests were conducted according to the method described in BS 4443¹². The tests confirmed that the virgin foams all exhibited the expected characteristic yield point under increasing compressive stress but showed that this yield point was absent with the rebond foams. The rebond foams showed constant static stiffness up to strains of at least 40% before beginning to become stiffer as the voids in the material were excluded and the cell walls began to interact with each other. With rebond foam therefore the sudden excessive deflections observed with virgin foams do not occur. This suggested that the unacceptable movement and possible fatigue along the tongued and grooved joints of shallow profile floating floors using virgin foam as the resilient layer might be avoided by using rebond foam.

The static tests also showed that most of the rebond foams were initially softer than the pre-yield virgin foams which suggested that they might also have lower dynamic stiffnesses than the virgin foams. If this proved to be the case rebond foams should offer better isolation against impact noise than low density virgin foams. The dynamic tests described in Chapter 4 confirmed that the dynamic stiffnesses of all but the most dense rebond foam were less than those of the pre-yield virgin foams.

In order to compare virgin and rebond foams having similar densities a 62 kg/m³ high resilience virgin foam was used for comparison as well as the 28 kg/m³ virgin foam. For a given thickness this material had a lower dynamic stiffness than the lower density foam but it was still higher than all but the highest density rebond foam examined. Static tests had shown that, of the 28 and 62 kg/m³ virgin foams, the lower density foam was stiffer before its yield point and so it might have been expected that a given thickness of the lower density foam would also have higher dynamic stiffness. This proved to be the case. With all the foams investigated, static stiffness served as a good indicator of the relative dynamic stiffness and there are indications that there may be a simple linear relationship between the two when measurements are conducted according to BS 4443 and BS EN 29052-1. However, more research is necessary to confirm this.

The relationship between the dynamic stiffness of a resilient layer under a floor and the dynamic stiffness of standard laboratory specimens made from the same material is defined in BS EN 29052-1¹³. The reason for any difference in the two values for dynamic stiffness is due to the fact that the air contained in foam specimens plays no part in the Standard Test¹³ whereas in a resilient layer under a floor, it may be highly significant. The relationship between the apparent dynamic stiffness of a laboratory specimen and the dynamic stiffness of a resilient layer under a floor is governed by the airflow resistivity of the material. The Standard states that if the airflow resistivity is too low then the Standard Method cannot be used to determine the dynamic stiffness of the resilient layer under a floor.

Measurements suggested that the airflow resistivity of open cell virgin foams is higher in the direction perpendicular to the foams' rise direction. With rebond foam there was no significant difference in the airflow resistivity in different directions. Any difference detected in airflow resistivity with direction was insufficient to make a difference in the calculation of resilient layer stiffness according to BS EN 29052-1 however. In general as the density of virgin open cell foams increases so does their airflow resistivity. It was therefore assumed by the manufacturers of the rebond foam that the airflow resistivity of the rebond foams would be higher than that of the low density virgin open cell foams produced. This proved not to be the case, the airflow resistivity of rebond foam was found to be to be unexpectedly low.

Investigations with a scanning electron microscope (SEM) showed that the rebond foams had far fewer remnants of cell wall membranes remaining than the virgin open cell foams. The shredding and mixing processes in the manufacture of rebond foam are likely to reduce the number of membranes found in the finished product. The number of remaining membranes could also be reduced when the virgin foam material was in use before its recovery for recycling. It is likely that the, much lower density, virgin foams have higher airflow resistivity due to the presence of the remaining membranes. Two of the rebond foams (64 kg/m^3 and 78 kg/m^3) had airflow resistivities so low that, according to BS EN 29052-1, the Standard could not be used to determine the dynamic stiffness of resilient layers comprising these materials. SEM micrographs of one of these rebond foams showed the material contained no significant membranes.

The results from the static and dynamic tests conducted suggested that rebond foam would be better to use than virgin foam as isolating layers in floating floors. No information on the performance of rebond foams could be found in the literature and therefore these materials in particular were investigated. The compressive stress-strain behaviour and relatively low dynamic stiffness of the 78 kg/m^3 rebond foam identified in this research led to its adoption in a, now, commercially available floating floor system. Field tests on the system showed that it combined good stability with impact sound insulation above the system resonance frequency when used on a concrete supporting floor leading to a significant reduction in $L'_{nT,w}$. The low airflow resistivity of the 78 kg/m^3 foam however meant that, according to the Standard¹³, there was no means of relating the specimen dynamic stiffness to that of resilient layers comprising this material under floating floors.

The field tests showed that flooring samples with similar thicknesses of the different densities of rebond foam and the virgin foam gave similar values for the weighted standardised impact sound level ($L'_{nT,w}$) when it was determined according to BS 5821 Part 2¹⁴. The measurements conducted with flooring samples having different thicknesses of the 78 kg/m^3 foam showed that $L'_{nT,w}$ decreased as the thickness of the resilient layer increased however. Since laboratory tests had shown that, for specimens of the same material, dynamic stiffness decreased as specimen thickness increased. It was felt that it should be possible to identify a relationship between specimen dynamic stiffness and these field results despite the low airflow resistivity of this 78 kg/m^3 rebond foam.

In order to relate the specimen dynamic stiffness to that of a resilient layer beneath a floating floor the effect of the air contained in the low airflow resistivity samples had to be included in the measurement of specimen dynamic stiffness. This was achieved by sealing the test system with petroleum jelly. The low mass of the mdf floating surface had still to be accounted for since the literature showed that, for such light weight floating surfaces, the mass of the Standard tapping machine hammers was significant above a certain cut off frequency¹⁵. This cut off frequency is determined by the driving point impedance of the mdf which is proportional to the longitudinal wave speed of sound in the material^{15,16}.

The longitudinal wave speed in the mdf was measured and found to be in good agreement with the value expected from comparison with the results from other research¹⁷. Once this had been done, the correction for the mass impedance of the hammers was made using Cremer's approach. The improvement in impact sound insulation was then calculated for each of the samples of flooring tested in the field using values of dynamic stiffness obtained from the sealed test system. Excellent correlation between the measured and predicted improvement in impact sound insulation was demonstrated.

The derivation of the Equation 8.19 for predicting the improvement in impact sound insulation offered by a floating floor assumes that the floating floor is infinite. In practical situations this is obviously not the case but for highly damped floating floors, e.g. asphalt floating floors, the equation holds¹⁸. The measurement of the driving point mobility of the lightweight floating flooring described in Chapter 10 showed that the behaviour of the lightweight floating floors of interest to this research will be dominated by the behaviour of the individual sections. Such floors can therefore be regarded as locally reacting and Equation 8.19, modified to account for the significance of the tapping machine hammers, can legitimately be used to predict the improvement in impact sound insulation when these systems are used on concrete supporting floors.

The usefulness of the tapping machine for rating the impact sound insulation of the lightweight floating floors studied was investigated in Chapter 11. It was concluded, from a review of the literature, that the ISO tapping machine can legitimately be used for measuring the impact sound insulation of floors with hard walking surfaces. The results from experiments described in this chapter confirmed that the use of the tapping machine on these lightweight floating floors is justified. The tapping machine behaves as specified¹⁹ and the measurements show that the resilient foam layer is not strained beyond its linear region (identified in Chapter 3) when stepped upon.

It can be concluded from the close correlation between the predicted and measured improvements in impact sound insulation that sealing the test system described in BS EN 29052-1 realistically includes the effect of the enclosed air in the test specimens. The dynamic stiffness of the sealed test system was compared with the stiffness given

by the sum of the unsealed system stiffness and the calculated air stiffness. The calculated air stiffness was obtained using the method described in BS EN 29052-1 which assumes isothermal compression of the resilient material. The literature showed that this was the most likely mechanism with open cell polyurethane foam also. The stiffness of the air in foams could therefore be calculated in the same way as with fibre quilts.

Lastly comment must be made on the Standard Method for the determination of the dynamic stiffness of resilient layers under floors, BS EN 29052-1. It has been found that open cell polyester foams having the same nominal density showed a variation from 20% to 30% in values of resonant frequency when loaded and tested under the same conditions²⁰. There is no Standard governing the amount of compression flooring grade polystyrene is subjected to before being supplied as a resilient layer. Such material from different sources is therefore also likely to have different static and dynamic Young's moduli depending on its source. Therefore, BS EN 29052-1 is likely to become more important in the future.

The development of new materials for use as resilient layers is also likely to make BS EN 29052-1 more important. If the dynamic stiffness of resilient materials were to be used as a specifier, rather than the density of specific types of material e.g. mineral fibre, it is likely to encourage innovation in the building industry. The work carried out in this research programme suggests that the Standard can be used more widely than previously thought. It has been demonstrated that the method can be used with resilient layers subjected to far lower imposed loads than 0.4 kPa by compensating for the tapping machine hammers. It has been shown that it is not necessary to bed the load plate onto flexible open cell polyurethane specimens. It has also been shown that, by sealing the test system, the dynamic stiffness of resilient layers with airflow resistivities less than 10 kPa.s/m² can be obtained even if the stiffness of the enclosed air is significant.

12.4 Final comments

Since the beginning of this project, research has continued to improve the correlation between the rating of floors and their subjective performance. Special attention has been paid to the of the low frequency sound insulation of building elements. For floors,

this has led to the introduction of the spectrum adaptation term C_I , defined in BS EN ISO 717-2 which was introduced 1997. This term was introduced because $L'_{nT,w}$ fails to account for level peaks at single (low) frequencies²¹. As was stated in Chapter 10, this meant that the difference in the low frequency impact sound insulation between massive concrete floors and some lightweight timber floors could be disguised by $L'_{nT,w}$.

The measurements of impact sound insulation conducted in this research were conducted using sections of lightweight floating floor on concrete supporting floors and the adaptation term (C_I) was insignificant for these. This would not necessarily be the case on timber floors however. This research clearly shows that the lightweight floating floors investigated add little to the impact sound insulation of supporting floors below the resonance frequency of the systems. On timber floors then, it is not necessarily the case that improvements in $L'_{nT,w}$ of the order of those observed with concrete supporting floors would be seen. If the adaptation term, C_I , were to be included in the impact sound insulation requirements in the Building Regulations then these lightweight floating floors would be unlikely to improve the impact sound insulation of poor floors at low frequencies sufficiently to make them acceptable.

12.5 Recommendations for further research

The prediction method for ΔL and $L'_{nT,w}$ described in this thesis has been shown to work extremely well for the small and large sections of flooring used in this research. It also worked well for a complete floating floor in the refurbished flat on a concrete supporting floor with much better acoustic properties than the other two used. Much more testing on full sized floors is required to validate the method. It would be useful to conduct the measurements under laboratory conditions where the amount of flanking transmission is more controlled.

The results of the field measurements described in Chapter 10 suggested that sealing the edges of single sections of flooring increased the damping of the mdf plate leading to performance very like that observed when larger sections of floating floor are tested. Further research into the effect of sealing the edges of small sections of floor prior to testing could make a useful contribution to the testing of novel flooring systems comprising interlocking small sections. If the same behaviour could be confirmed with other systems then testing new floating floors could be carried out more cheaply than at

present. It would also be useful to investigate the more widely used lightweight floating floor systems comprising fibre resilient layers and chipboard floating panels to test the applicability of the method with these.

In Germany, DIN 52214 was used to determine the dynamic stiffness of resilient layers before being superseded by EN 29052-1. The DIN Standard included the conditioning of materials under investigation by subjecting them to a pre-load of 50 kN/m^2 for 2 minutes before testing. It has been shown that this leads to incorrect estimates of dynamic stiffness²². The results presented in this thesis show that the conditioning cycles in the static tests result in a significant reduction in the stiffness of low density open cell virgin foam. A reduction was also observed with the rebond foams although it was not as large.

It is likely that pre-straining the test specimens prior to determining their dynamic stiffness would lead to an underestimation of the dynamic stiffness of resilient layers. This in turn would lead to an overestimation of the improvement in impact sound insulation. Investigation of the effect of pre-conditioning on the dynamic stiffness of recycled flexible open cell polyurethane foams would be useful. Combined with information regarding the materials' ability to recover from large strains such research could have implications for the specification of lightweight floating floor systems as well as their installation and handling. It is particularly important to determine the effect of pre-conditioning on polystyrene given the proposal to subject the material to massive pre-loads prior to determining its dynamic stiffness²³ according to the method described in BS EN 29052-1.

The field tests with systems having different types of polyurethane foam resilient layers of similar thickness (around 10 mm) revealed that all but one system gave the same value for $L'_{nT,w}$ after analysing the measurements taken in the receiving room. Four different rebond foams were used and one virgin foam. Three of the rebond foams had the same dynamic stiffness, within the limits of accuracy of the tests, but the other had a higher dynamic stiffness, around 30% higher, which was the same as that of the virgin foam. Despite this the virgin foam resilient layer gave the same value of $L'_{nT,w}$ as the three softest rebond foams although it performed least well at high frequencies.

In the field tests, the performance of the systems around their resonance frequency was shown to be the most significant in evaluation of $L'_{nT,w}$ since the measured, and predicted, L'_{nT} curve lies beneath the shifted reference curve at high frequencies. Comparison of the measurements of the damping in the laboratory test specimens with the field performance around the resonance frequency does not confirm any obvious relationship between the two although it would be expected that damping would be the most significant control mechanism in this frequency range. A study of the relative importance of material frame stiffness, air stiffness and damping in thin layers of rebond polyurethane foam beneath floating floors is required. Particular attention should be paid to the frequencies around the system resonance frequency.

Lastly, subjective investigations of the improvement in sound insulation offered by lightweight mdf floating floors would be informative. The cut off frequency, at which the force input by the hammers is reduced, is relatively low (around 112 Hz). There is also the reduction in force input by the tapping machine hammers above the break frequency to consider. It is likely that the break frequency would be sufficiently high that $L'_{nT,w}$ would be unaffected. The correction for the reduced input force above the cut off frequency is known and so the tapping machine can legitimately be used for rating lightweight mdf floating floors. However, it would be useful to confirm that the measured improvements in ΔL correspond with subjective impressions rather than being merely a function of the choice of impact sound source.

12.6 Concluding remarks

The author set out to review and to assess the usefulness of the Standard tests on flexible polyurethane foams for determining their usefulness as isolating layers under floating floors. The intention was to develop a method for predicting the likely improvement in impact sound insulation from placing lightweight shallow profile floating floor systems comprising flexible polyurethane foam on concrete supporting floors.

The determination of the compression stress-strain behaviour of the different foams showed which were likely to provide adequate support to floating floors and gave an indication of their relative dynamic stiffness. Most importantly the special suitability of rebond foams for use under floating floors was identified. The absence of a yield point

with these materials means that rapid and relatively large deflections when floors incorporating such materials are walked on should be avoided. The walking surface can be expected to be displaced slightly but since the foam stiffness remains constant up to 40% strain and is less affected by conditioning than lightweight virgin foams, the displacement is far less likely to be noticed by those walking on the floor.

BS EN 29052-1 states that it cannot be used for resilient layers subjected to an imposed load of less than 0.4 kN/m^2 by the floating surface. It has been shown that the Standard Method can be used with layers beneath lightweight floating surfaces by compensating for the mass impedance of the tapping machine hammers as described by Cremer¹⁵. The Standard can therefore be applied much more widely than previously thought. In addition it has been shown that by modifying the Method to include the effect of the air contained in the foam the apparent dynamic stiffness of the laboratory specimens can be directly related to the stiffness of a resilient layer under a floor. This extends the usefulness of the Method to polyurethane foam layers whose low airflow resistivity would previously have prohibited its use.

Data generated by the modified Method enabled the successful prediction of the improvement in the impact sound pressure levels in the receiving room over a range of 40 dB when specimens of lightweight floating floor were placed on the concrete supporting floor. In addition the prediction method has been shown to work for a large sections of floating floor and a complete floating floors on two different supporting floors. The treatment of the data developed in this thesis facilitates the prediction of $L'_{nT,w}$. A method for deciding whether using a particular polyurethane foam as a resilient layer in a lightweight floating floor will upgrade a concrete floor sufficiently to meet the requirements of the Building Regulations has been identified. The research also suggests that using denser rebond foams as the resilient layer will not have a significant adverse effect on $L'_{nT,w}$. This could be important for specifying resilient layers beneath floating floors where higher loadings are expected.

12.7 References

- 1 AVON, GLOUCESTERSHIRE AND SOMERSET ENVIRONMENTAL HEALTH MONITORING COMMITTEE, *Domestic noise - a guide for environmental health officers*, 1984.
- 2 BUILDING RESEARCH ESTABLISHMENT, *Sound insulation between dwellings*, BRE literature package, 1988e.
- 3 Chartered Surveyor Monthly, March, 1996.
- 4 RAW G.J., OSELAND N.A., Subjective response to noise through party walls in conversion flats, *Applied Acoustics*, 1991, Vol. 32, 215-231.
- 5 DEPARTMENT OF THE ENVIRONMENT AND THE WELSH OFFICE, The Building Regulations, *Resistance to the passage of sound, Approved Document E*, 1991.
- 6 PRITZ T., Dynamic young's modulus and loss factor of plastic foams for impact sound isolation, *J Sound and Vibration*, 1994, Vol. 178, 315-322.
- 7 SUEYOSHI S; SCHNIEWIND A.P., Dynamic behaviour of wood strip over elastic underlayment composite flooring subjected to light impact loads, *Wood Sci. Technol.*, 1991, Vol. 25, 309-318.
- 8 SUEYOSHI S; TONOSAKI M., Determination of localised dynamic behaviour of wood strip over foam rubber underlayment, composite flooring by random vibration, *Wood Sci. Technol.* , 1993, Vol. 27, 11-21.
- 9 SUEYOSHI S.; TONOSAKI M.; ORIBE M., Localised vibration of composite wood flooring fastened to a concrete slab, *Japan Wood Research Society*, 1995, Vol. 41, 31-36.
- 10 MACKENZIE R.K., European Patent Application No 949154618.6, *Floor construction involving shallow profile deck*, Filing Date 19 May 1994
- 11 MACKENZIE R.K., Upgrading of floors in refurbishment projects, *Proc. IOA*, 1993, Vol. 15, Part 15, 301-309.
- 12 BS 4443, 1988, British standard methods of test for flexible cellular materials, parts 1-7.
- 13 BS EN 29052-1, 1992, *Acoustics - Materials for Acoustical applications - Materials Used Under Floating Floors in Dwellings*.
- 14 BS 5821, 1984, *Rating the sound insulation in buildings and of building elements, Part 2, Method for rating the impact sound insulation*.

-
- 15 CREMER L., HECKL M., UNGAR E.E., *Structure-Borne Sound, 2nd ed.*, Publ. Springer-Verlag, 1988.
 - 16 VER I.L., Interaction of sound waves with solid structures, *Noise and Vibration Control Engineering*, (Ed) Beranek L.L., Ver I.L., 245-367, Publ. John Wiley and Sons Inc, 1992.
 - 17 HOPKINS C, 1996, Private Correspondence, BRE Acoustics Section.
 - 18 prEN 12354-2, 1997, *Draft Standard, Building acoustics, Estimation of acoustic performance of buildings from the performance of products, Part 2: Impact sound insulation between rooms.*
 - 19 BS EN ISO 140-8, 1998, *Acoustics – Measurement of sound insulation of buildings and of building elements, Laboratory measurements of the reduction of transmitted impact noise by floor coverings on a heavyweight standard floor.*
 - 20 CALCATERRA P.C., *Design guide for polyurethane foam isolation systems*, U.S. Naval Air Development Centre, 1965.
 - 21 BS EN ISO 717-2, 1997, *Acoustics - Rating of sound insulation in buildings and of building elements, Part 2, Impact sound insulation.*
 - 22 Metzen H.A., Effect of pre-load on the dynamic stiffness of impact insulation materials and on the predicted impact sound insulation, *Proc Internoise 96*, 1996, 1807-1810.
 - 23 PrEN 13163, 1998, *Thermal insulation products for buildings-Factory made products of expanded polystyrene-specification.*

APPENDIX A1

FIELD MEASUREMENT RESULTS

NOT PRESENTED IN THESIS

FIELD MEASUREMENT OF IMPACT SOUND INSULATION OF CONCRETE FLOOR BEFORE TREATMENT WITH MDF FLOATING FLOOR

See Figure 6.1

Flooring specimen: bare concrete floor
Date of measurement: 12/03/96
Area of test floor: 29.5 m²
Area of floating surface:
Receiving room volume: 278 m³

frequency: Hz	L' _{nT} : dB
100	46.5
125	46.8
160	51.5
200	53.6
250	52.8
315	52.8
400	55.8
500	57.2
630	58.8
800	60.9
1000	62.4
1250	65.5
1600	65.2
2000	65.8
2500	66.7
3150	65.9
L' _{nT,w}	72
Max. unfavourable result	-12.0
at frequency	3150 Hz

FIELD MEASUREMENT OF IMPACT SOUND INSULATION OF CONCRETE FLOOR AFTER TREATMENT WITH MDF FLOATING FLOOR

See Figure 6.1

Flooring specimen: concrete floor + mdf flooring system
Date of measurement: 12/03/96
Area of test floor: 29.5 m²
Area of floating surface: 15.1 m²
Receiving room volume: 278 m³

frequency: Hz	L' _{nT} : dB
100	46.9
125	46.3
160	50
200	49.1
250	50.3
315	47.3
400	39.9
500	37.9
630	38.2
800	35.4
1000	32.8
1250	30.4
1600	27.9
2000	28.9
2500	27.5
3150	28.1
L' _{nT,w}	42
Max. unfavourable result	-6.3
at frequency	250 Hz

FIELD MEASUREMENT OF IMPACT SOUND INSULATION OF CONCRETE FLOOR BEFORE TREATMENT WITH CHIPBOARD FLOATING FLOOR

See Figure 6.3

Flooring specimen: bare concrete floor
Date of measurement: 13/03/96
Area of test floor: 29.5 m²
Area of floating surface:
Receiving room volume: 278 m³

frequency: Hz	L'_{nT} : dB
100	42.2
125	46.3
160	52.4
200	54.3
250	56.1
315	55.3
400	55.2
500	54.4
630	56.8
800	58.1
1000	61.8
1250	65.1
1600	66.6
2000	65.1
2500	64.7
3150	63.2
L'_{nT,w}	71
Max. unfavourable result	-10.2
at frequency	3150 Hz

FIELD MEASUREMENT OF IMPACT SOUND INSULATION OF CONCRETE FLOOR AFTER TREATMENT WITH CHIPBOARD FLOATING FLOOR

See Figure 6.3

Flooring specimen: concrete floor + chipboard flooring system
Date of measurement: 13/03/96
Area of test floor: 29.5 m²
Area of floating surface: 14.4 m²
Receiving room volume: 278 m³

frequency: Hz	L' _{nT} : dB
100	42.0
125	46.0
160	51.9
200	53.5
250	46.2
315	40.3
400	39.2
500	36.2
630	34.7
800	35.0
1000	27.3
1250	26.0
1600	23.6
2000	20.5
2500	18.4
3150	16.1
L' _{nT,w}	40
Max. unfavourable result	-11.5
at frequency	200 Hz

**FIELD MEASUREMENT OF IMPACT SOUND INSULATION OF CONCRETE
SEPARATING FLOOR IN COUNCIL FLAT BEFORE TREATMENT WITH
SHALLOW PROFILE FLOATING FLOOR**

See Figures 8.21 and 8.32

Council Flat

Flooring specimen: bare concrete floor

Date of measurement: 17/05/95

Area of test floor: 13.6 m²

Area of floating surface: 13.6 m²

Receiving room volume: 32.6 m³

frequency: Hz	L'_{nT} : dB
100	60.7
125	58.7
160	65.3
200	66.4
250	68.5
315	67.3
400	70.0
500	68.2
630	67.7
800	65.8
1000	63.5
1250	62.0
1600	59.8
2000	57.4
2500	54.9
3150	52.1
L'_{nT,w}	66.0
Max. unfavourable result	-3.0
at frequency	400 Hz

**FIELD MEASUREMENT OF IMPACT SOUND INSULATION OF CONCRETE
SEPARATING FLOOR IN COUNCIL FLAT AFTER TREATMENT WITH
SHALLOW PROFILE FLOATING FLOOR**

See Figures 8.21 and 8.32

Council flat after refurbishment

Flooring specimen: concrete floor + mdf system with virgin foam layer

Date of measurement: 18/05/95

Area of test floor: 13.6 m²

Area of floating surface: 13.6 m³

Receiving room volume: 32.6 m³

frequency: Hz	L'_{nT} : dB
100	62.9
125	60.2
160	65.4
200	66.5
250	63.4
315	59.1
400	53.7
500	49.2
630	42.5
800	37.3
1000	32.7
1250	28.4
1600	26.4
2000	25.3
2500	22.4
3150	23.0
L'_{nT,w}	56.0
Max. unfavourable result	-7.5
at frequency	160 Hz

FIELD MEASUREMENT OF IMPACT SOUND INSULATION OF TIMBER

JOIST FLOOR

See Figures 6.2 and 6.4

Flooring specimen: timber joist floor

Date of measurement: 19/03/96

Area of test floor: 19.5 m²

Area of floating surface:

Receiving room volume: 57 m³

frequency: Hz	L' _{nT} : dB
100	75.2
125	77.2
160	75.7
200	74.4
250	74.9
315	71.7
400	67.0
500	63.7
630	60.6
800	58.6
1000	57.0
1250	54.2
1600	53.4
2000	52.8
2500	50.9
3150	47.3
L'_{nT,w}	68
Max. unfavourable result	-7.2
at frequency	125 Hz

**FIELD MEASUREMENT OF IMPACT SOUND INSULATION OF TIMBER
JOIST FLOOR AFTER ADDING FLOATING FLOOR**

See Figure 6.2

Flooring specimen: timber joist floor + mdf flooring system
Date of measurement: 21/03/96
Area of test floor: 19.5 m²
Area of floating surface: 19.5 m²
Receiving room volume: 57 m³

frequency: Hz	L' _{nT} : dB
100	74.1
125	74.9
160	70.2
200	68.3
250	65.9
315	61.7
400	56.8
500	50.9
630	45.6
800	43.7
1000	41.7
1250	39.3
1600	37.9
2000	37.9
2500	38.0
3150	37.4
L'_{nT,w}	63
Max. unfavourable result	-9.9
at frequency	125 Hz

**FIELD MEASUREMENT OF IMPACT SOUND INSULATION OF TIMBER
JOIST FLOOR AFTER ADDING FLOATING FLOOR**

See Figure 6.4

Flooring specimen: timber joist floor + chipboard flooring system
Date of measurement: 23/03/96
Area of test floor: 19.5 m²
Area of floating surface: 19.5 m²
Receiving room volume: 57 m³

frequency: Hz	L' _{nT} : dB
100	73.7
125	74.1
160	69.3
200	66.6
250	67.0
315	63.1
400	59.6
500	54.9
630	50.1
800	48.7
1000	45.3
1250	40.2
1600	37.2
2000	35.4
2500	34.6
3150	32.4
L' _{nT,w}	62
Max. unfavourable result	-10.1
at frequency	125 Hz

APPENDIX A2

THE MODIFIED METHOD FOR THE DYNAMIC STIFFNESS OF RESILIENT LAYERS

The test arrangement described in BS EN 29052-1 the Standard Method for the determination of dynamic stiffness for materials used under floating floors

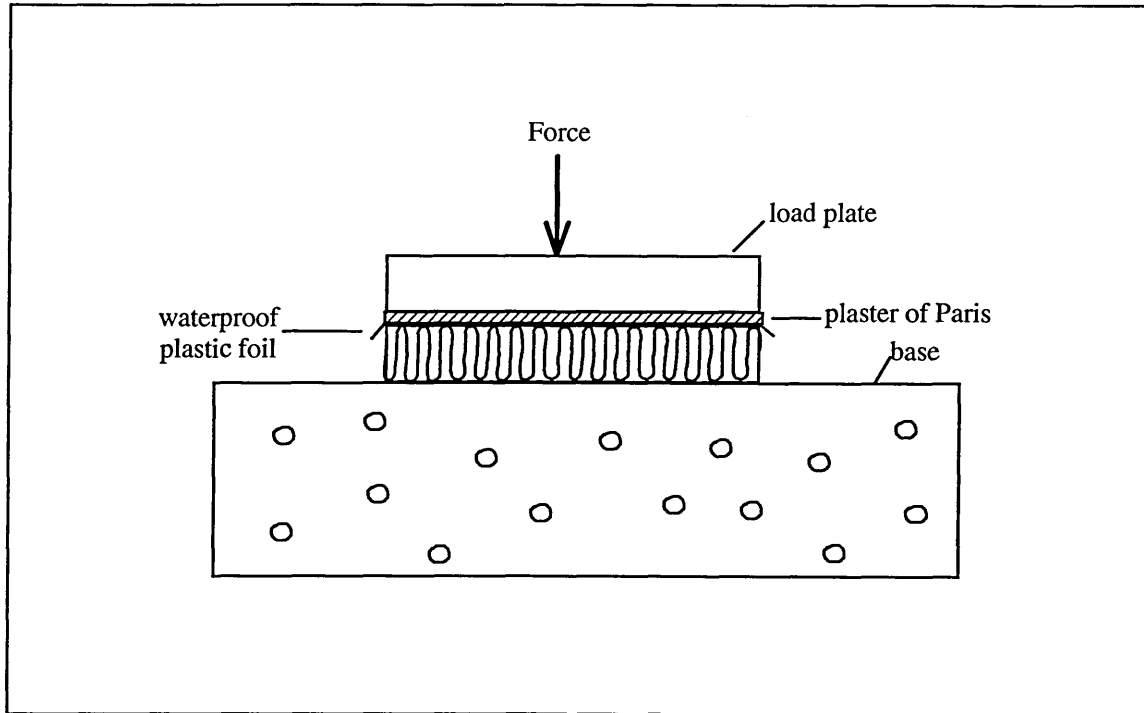


Figure A2.1: test arrangement in BS EN 29052-1, method 1a.

The test arrangement for open cell materials according to the Standard is illustrated in Figure A2.1. The top surface of the specimen is covered with waterproof plastic foil on which a thin paste of plaster of Paris and water is applied to a depth of at least 5 mm. The load plate $\{(200 \pm 3) \text{ mm} \times (200 \pm 3) \text{ mm}\}$ is bedded onto the plaster of Paris before it begins to set. The total mass supported by the specimen is $(8 \pm 0.5) \text{ kg}$.

When the plaster of Paris has dried the test can be started. An exciting force is applied to the load plate and the resonant frequency of the fundamental vertical vibration of the test system is obtained. A sinusoidal or white noise excitation signal is used. At least three specimens of the material are tested having been cut to the Standard size (200 mm x 200 mm). The inertia of the base is sufficiently large that its motion is insignificant compared with that of the load plate.

The modified test method for the determination of dynamic stiffness for flexible polyurethane open cell materials used under floating floors

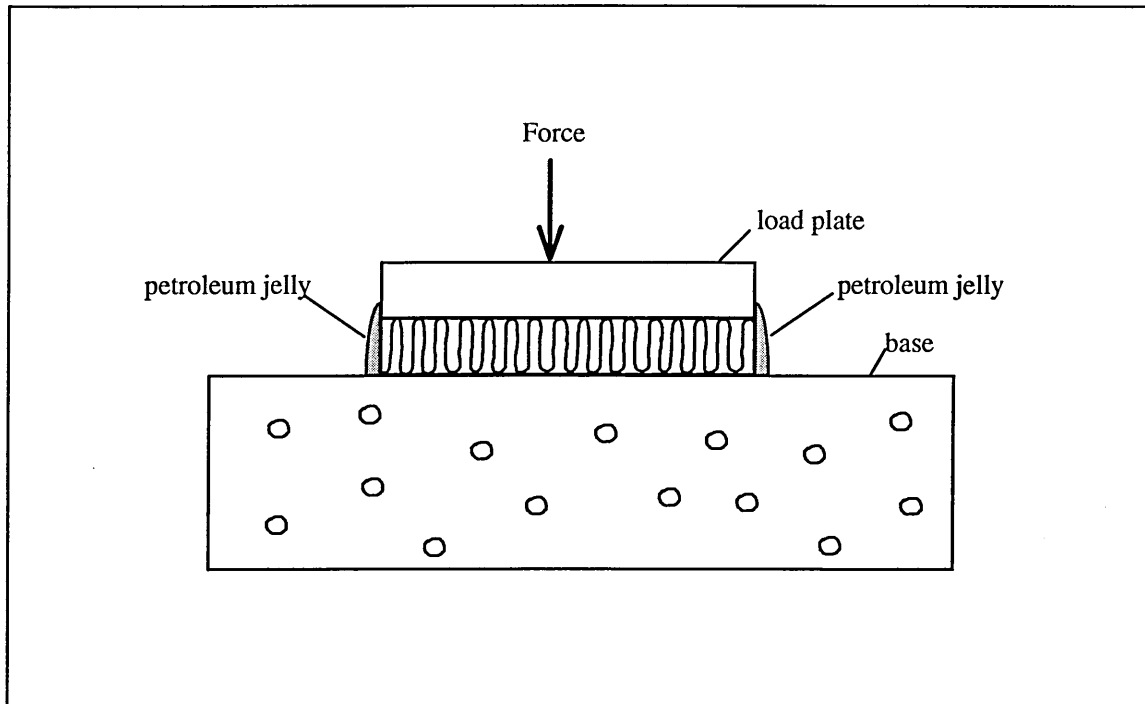


Figure A2.2: modified test arrangement

The modified test arrangement is illustrated in Figure A2.2. The load plate, specimen size and base are unchanged from those described in the Standard Method. The load plate has mass (8 ± 0.5) kg and dimensions $\{(200 \pm 0.5) \times (200 \pm 0.5) \text{ mm}\}$. The specimens are square with sides 200 mm and at least three are tested. There are two deviations from the Standard test arrangement. There is no plaster of Paris layer used and the sides of the test specimen are completely sealed with petroleum jelly.

Plaster of Paris

It was shown in Chapter 4 of this thesis that the plaster of Paris layer is unnecessary with polyurethane foam specimens. The plaster of Paris layer must be fully cured before testing can begin. This takes at least 24 hours which means that several load plates are necessary if more than one test is to be completed in a day.

Petroleum jelly

When closed cell specimens are tested using the method illustrated in Figure A2.1 the Standard states that the joint between the base and the specimen should be sealed with petroleum jelly. The modification to the Standard Method described here refers to open cell foams. The intention of the modification is to prevent the air contained in the specimens from moving laterally out of the specimens and therefore playing no part in the test.

In the modified test method the edges of the specimen are completely sealed with petroleum jelly. This keeps the air contained in the specimens within the test system which means that the stiffness per unit area of the specimen is the same as that of the material when used under a floating floor.

The test set-up is shown in Figure A2.2. The joints between the base and the specimen and the specimen and the load plate should be sealed in addition to the sides of the specimen. Special care is needed to ensure a good seal at the corners. When the system has been sealed its resonant frequency is determined as described in BS EN 29052-1. The apparent dynamic stiffness of the specimen is calculated as described in the Standard but this is now equal to the dynamic stiffness of the resilient layer.

APPENDIX A3

PUBLISHED WORK ARISING FROM

THIS RESEARCH

Proceedings of the Institute of Acoustics

DEVELOPMENTS IN THE APPLICATION OF FLEXIBLE OPEN-CELL POLYMER FOAMS FOR IMPACT SOUND REDUCTION IN FLOORS

R K Mackenzie (1) and R Hall (2)

(1) Napier University, Department of Building & Surveying, Colinton Road, Edinburgh

(2) Sheffield Hallam University, School of Construction, Pond Street, Sheffield

1. INTRODUCTION

It is now over eight years since the first flooring product incorporating a flexible open-cell (o-c) polymer foam layer was specified for use in buildings. The twin layer resilient batten, with closed cell and open cell foam strips laminated to a softwood timber bearer is now specified in over half of all new flats in Scotland. The use of open cell foam as a resilient layer now extends to a variety of products for both new build and refurbishment purposes.

Recent developments in the application of flexible open cell foam have improved both the stability of the walking surface and the low frequency impact sound attenuation. The use of higher density open cell foams has allowed a range of products capable of taking much higher imposed loads than before also to be introduced.

The use of multi-density reconstituted open cell foam provides a significantly different deflection characteristic compared with single density virgin foam. The research has also found that reconstituted foam has a lower natural frequency than equivalent virgin foam.

2. HISTORICAL REVIEW

The concept of the polymer only emerged as recently as 1920 following the work of Hermann Staudinger for which he was awarded the Nobel Prize. Manufactured polymeric materials such as vulcanised natural rubber, however, have been around since 1839 with the commercial development of thermoplastics commencing in 1870 following the innovative work of the Hyatt Brothers in using camphor as a plasticiser.

The first proprietary resilient flooring system did not appear until 1935 following a patent filed by Callum [1] with the first integral batten developed shortly thereafter in 1936 by Hofbauer [2]. These early inventions did not envisage the use of polymers as such, with cork being the preferred resilient material.

Whilst many of the commonly known homo-polymers were developed in the first half of the twentieth century it was not until 1952 that the first co-polymers were introduced, by Dow Chemical. Two such materials, closed cell polyethylene and polyurethane elastomers were introduced in the mid 1960's as resilient layers in buildings for use both under concrete screeds and as integral foam 'Durabella' battens [3]. The most recent developments came in the 1980's with the utilisation of low density open cell thermoplastic co-polymer elastomers such as polyether-urethane foam, both for integral battens or strips [4-7] and shallow profile resilient platform floor systems. [8-9].

3. FLEXIBLE CELLULAR POLYMERS IN FLOORS

The relative mechanical properties of cellular polymer foams can be best displayed in terms of their Stress vs Strain characteristic. At low compressive stress both types behave similarly, exhibiting linear elasticity due to cell wall bending. With increased stress open cell foam typically displays a non-linear elasticity characterised by a large increase in strain for minimal increase in stress due to the elastic buckling of the cell walls. This behaviour does not occur with closed cell foams which typically exhibit a continuing linear elasticity under stress due to a pneumatic resistance caused by the gas entrapped within the closed cell.

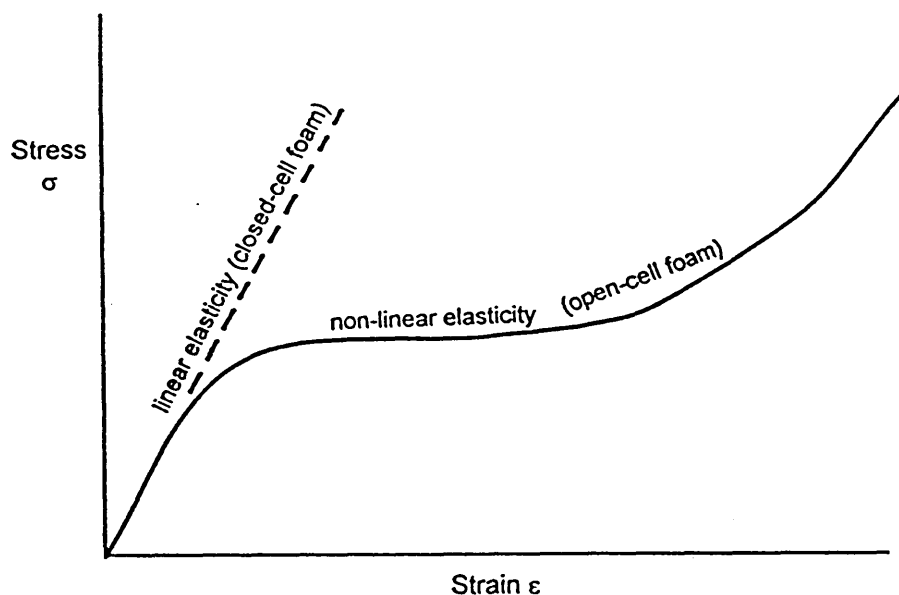


Figure 1. Characteristic Stress vs Strain Relationship of Flexible Cellular Foams

Research into the use of flexible open-cell polymer foams commenced in 1984 following investigations by the Scottish Special Housing Association into the failure of fibre quilt resilient layers used in the floors of dwellings constructed in the 1970's. Floor inspections revealed that many such quilts had disintegrated due to brittle fracture of the fibres compressed between the batten and the surface of the structural floor below. A further cause of failure occurred in kitchens and bathrooms as a result of water penetration. The research [10-11] which investigated the isolation efficiency of many different forms of polymer concluded that low density polyether-urethane open cell foam provided the most cost effective alternative to mineral and glass fibre quilts.

Proceedings of the Institute of Acoustics

DEVELOPMENTS IN THE APPLICATION OF FLEXIBLE OPEN-CELL POLYMER FOAMS

Subsequent research [12] investigated the relative level of impact sound reduction provided by both open and closed cell polymer foams.

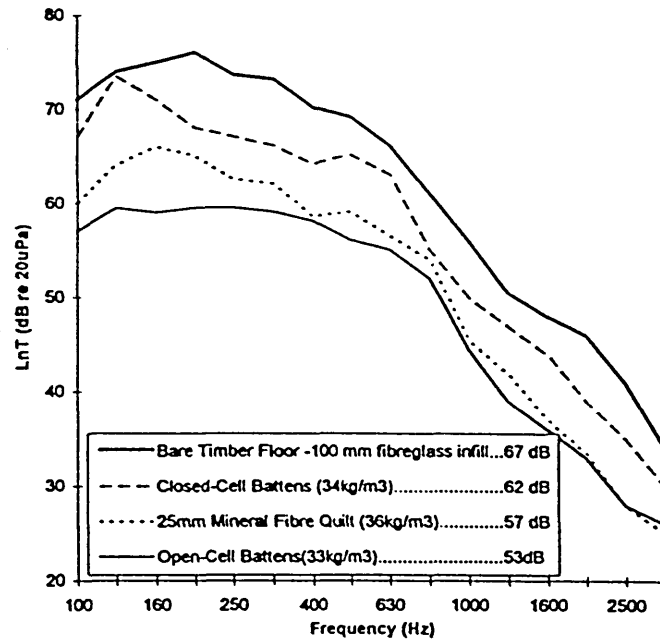


Figure 2 Impact Sound Performance of Different Resilient Layers in Ribbed Floor Constructions [12]

4. CURRENT POSITION

When considered in the context of the Building Regulations, the use of flexible open-cell polymer foam integral battens or strip as an alternative to mineral fibre has been broadly accepted by the building industry both in terms of impact sound performance and in terms of stability of the floating floor. The same cannot be said, however, in the case of platform or deck type systems. In terms of specified constructions within the Building Regulations, floor types 3A (new build) and floor treatment 5 (conversions) incorporating mineral fibre resilient layers provide a very marginal performance in terms of impact sound reduction [13]. The use of proprietary flooring systems incorporating polymer based elastomers to achieve the required resilience has not improved the situation and has given cause for concern in some cases [14]. The main problem lies not in the inherent properties of the polymer, but rather in the compromise required to be made in the design in order to meet industry's demand for shallow profile floors of less than 20 mm thickness, particularly for conversion work. [15] Whilst such shallow floors can produce improvements in impact sound reduction in concrete floors of between 18 dB (field) and 24 dB (laboratory) the corresponding result for a simple timber floor is typically 5 dB (field) and 10 dB (laboratory).

Proceedings of the Institute of Acoustics

DEVELOPMENTS IN THE APPLICATION OF FLEXIBLE OPEN-CELL POLYMER FOAMS

The figures below indicate the typical attenuation provided by shallow deck floors comprising of 9 mm Medium Density Fibreboard (MDF) bonded to 8 mm thick open cell virgin foam.

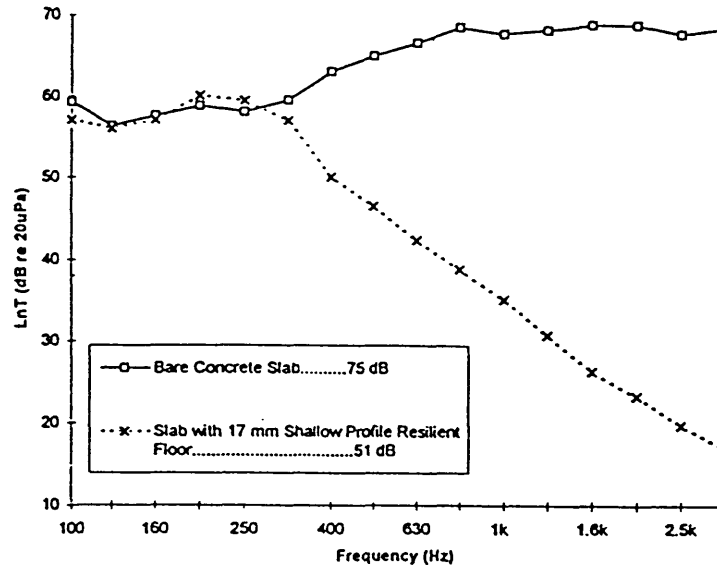


Figure 3. Typical Attenuation Provided by a Shallow Deck Resilient Flooring System (MDF+ Virgin Open Cell Foam) applied to a Concrete Floor

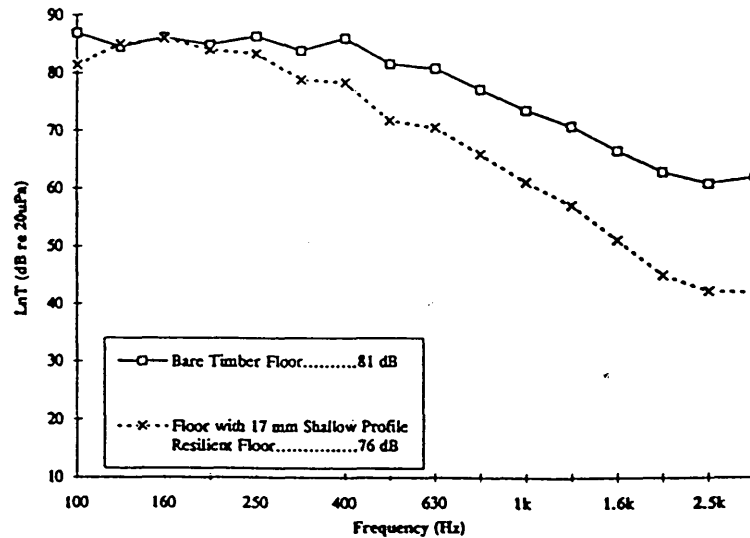


Figure 4. Typical Attenuation Provided by a Shallow Deck Resilient Flooring System (MDF+ Virgin Open Cell Foam) applied to a Timber Floor

Proceedings of the Institute of Acoustics

DEVELOPMENTS IN THE APPLICATION OF FLEXIBLE OPEN-CELL POLYMER FOAMS

The problem with shallow profile floors has always been associated with the transmission loss in the range 100 Hz - 200 Hz. The only practical solution to resolving this problem with virgin open cell foam has been to increase the thickness of the foam thereby lowering the natural frequency.

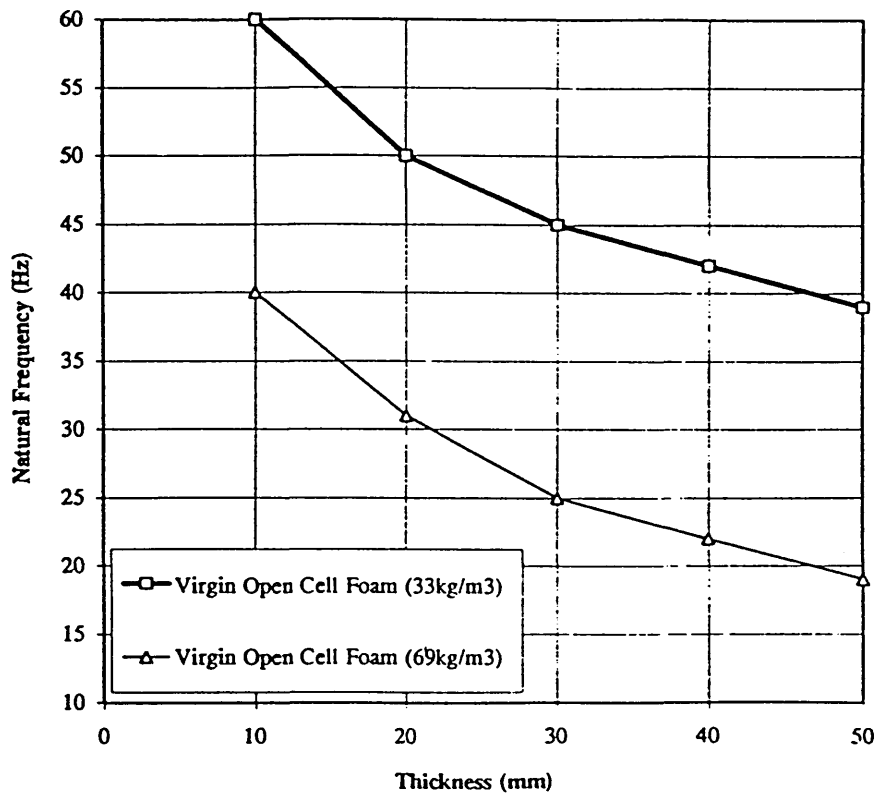


Figure 5. Natural frequency versus thickness for Virgin Open Cell Foam

Increasing the thickness of virgin o-c foams introduces a different problem, that of stability of the walking surface. This situation is not unusual in resilient floors and affects mineral fibre floors in a similar way requiring the eventual choice to be a compromise between satisfactory impact sound insulation and stability of the floor

Proceedings of the Institute of Acoustics

DEVELOPMENTS IN THE APPLICATION OF FLEXIBLE OPEN-CELL POLYMER FOAMS

5. MULTI DENSITY RECONSTITUTED FOAM - PHYSICAL PROPERTIES

In order to find a solution for the problem referred to above, recent research [16] has investigated the acoustic and dynamical behaviour of different foams and has found particularly encouraging results from the use of reconstituted polyether o-c foam. Such foams have been found to exhibit lower natural frequencies than equivalent virgin o-c foams.

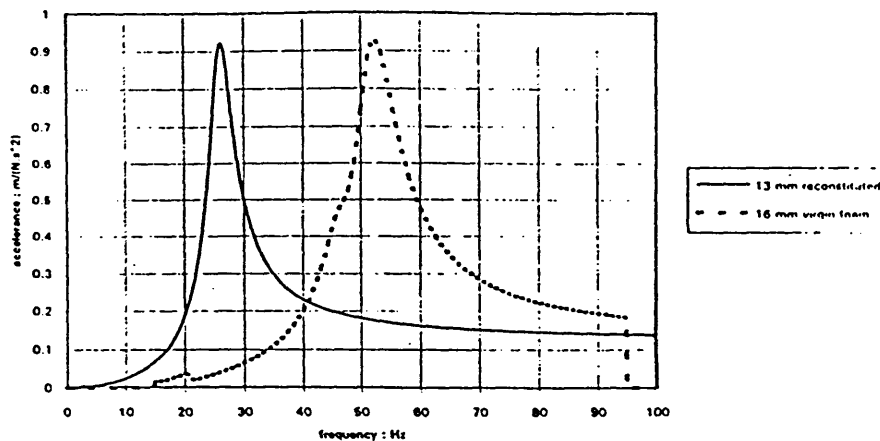


Figure 6. Natural Frequencies of Reconstituted and Virgin Open Cell Foams

It has also been found that reconstituted open cell foams have an almost linear compressive stress-strain relationship up to about 40% strain without the marked yield point observed with virgin o-c foam. The absence of cell wall buckling provides a noticeably more stable walking surface, which is not significantly affected by increased thickness.

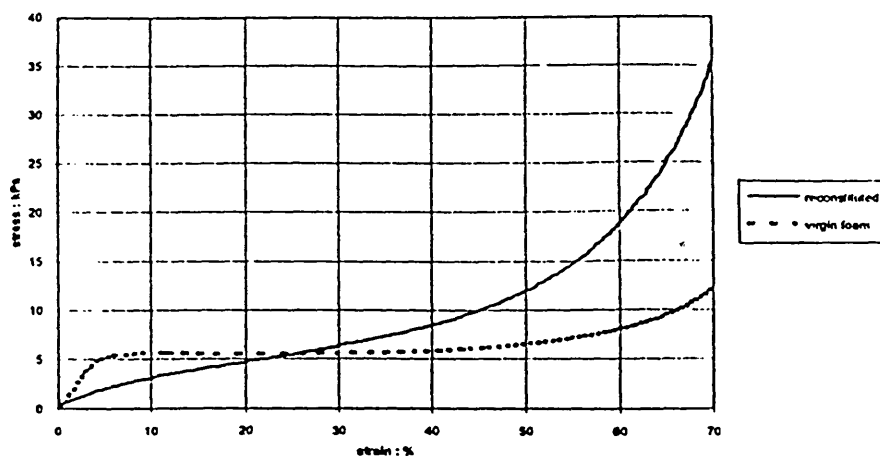


Figure 7. Relative Stress vs Strain Curves for Reconstituted o-c Foam and o-c Virgin Foam

Proceedings of the Institute of Acoustics

DEVELOPMENTS IN THE APPLICATION OF FLEXIBLE OPEN-CELL POLYMER FOAMS

6. MULTI DENSITY RECONSTITUTED FOAM - ACOUSTIC RESULTS

Comparative laboratory tests have shown a significant improvement in low frequency performance by use of multi density o-c foam. The relative performance of two shallow profile panels, one with 8 mm o-c single density virgin foam and one with 8 mm o-c multi density reconstituted foam is shown below.

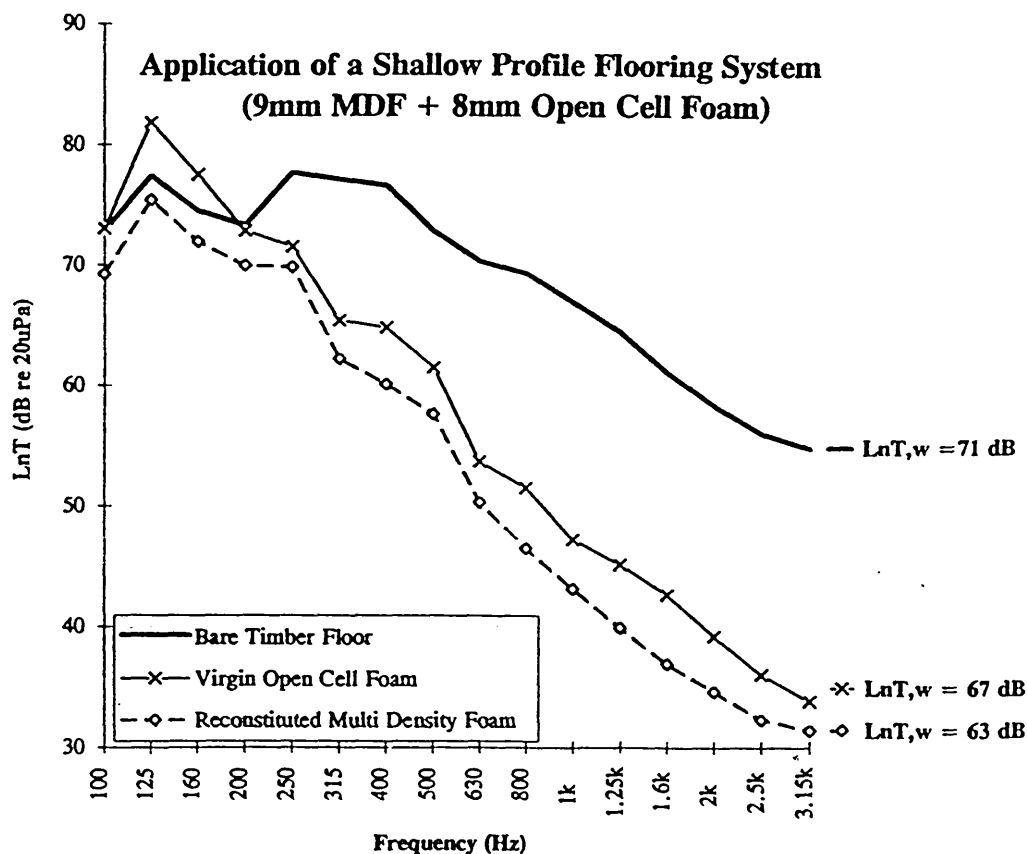


Figure 8. Relative Performance of Shallow Profile (9 mm MDF + 8 mm Foam) Panels

Proceedings of the Institute of Acoustics

DEVELOPMENTS IN THE APPLICATION OF FLEXIBLE OPEN-CELL POLYMER FOAMS

A particular observation from the research was the significant improvement in low frequency performance produced by increasing the thickness of the reconstituted foam from 8 mm to 10 mm. This provided a 2 dB reduction in $L_{nT,w}$ value, a reduction which cannot be explained by the change in natural frequency. The most likely reason would appear to be due to the presence of 8 mm cube shaped pieces of high density (192 kg/m³) foam dispersed throughout the reconstituted foam sheet. In the case of 8 mm foam, these cubed shaped pieces effectively act as stiff couplings between the MDF and the structural floor surface. With 10 mm foam the presence of 8 mm cubes does not appear to create coupling to the same degree.

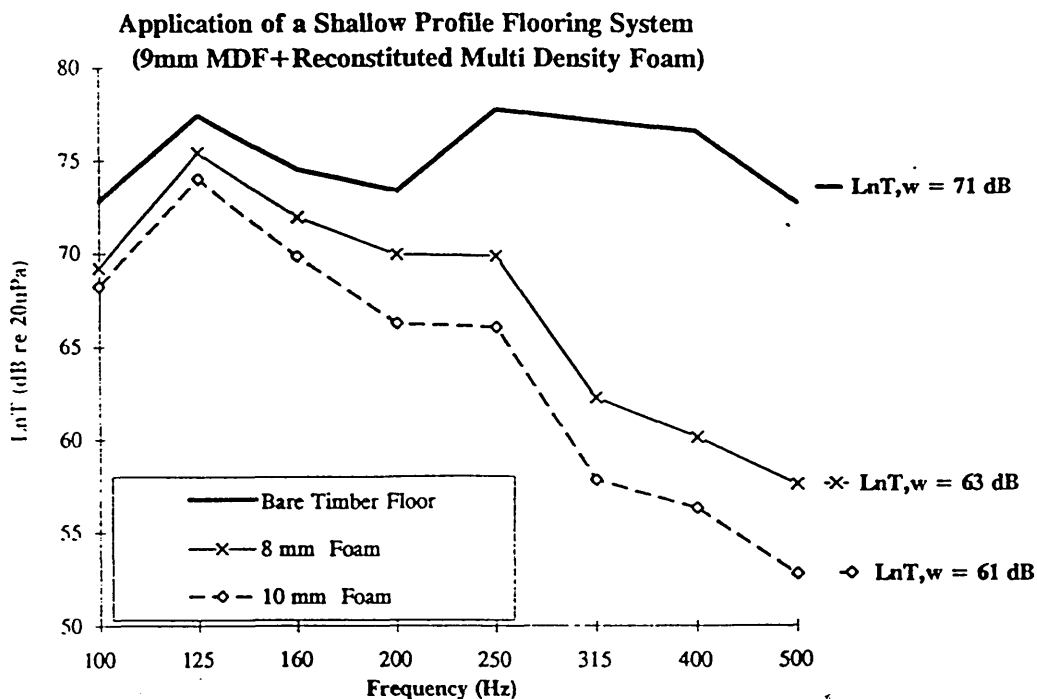


Figure 9. Relative Performance of Shallow Profile Resilient Panels with 8 mm and 10 mm Reconstituted Foam.

Proceedings of the Institute of Acoustics

DEVELOPMENTS IN THE APPLICATION OF FLEXIBLE OPEN-CELL POLYMER FOAMS

The effect of increasing the density of the reconstituted foam provides correspondingly increased stability, but with only a small reduction in acoustic performance. This provides significant scope for the use of reconstituted foam in commercial applications with high imposed loading.

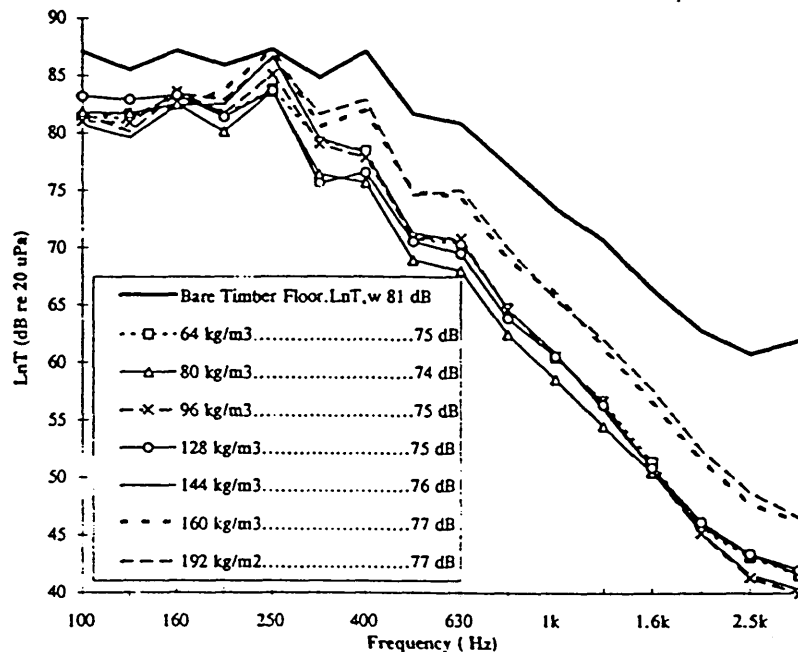


Figure 10. Relative Performance of Shallow Profile Resilient Floors with different Densities of Reconstituted Foam.

The application of high density foam extends to its use in integral foam battens in areas of high imposed loading, such as kitchens or offices where closed cell battens fail to provide adequate impact sound attenuation.

7. CONCLUSION

A number of the problems associated with open cell foam in shallow profile resilient floors have been overcome by the use of multi-density reconstituted o-c foam. Impact sound insulation has been improved at the important low frequency region and the walking stability of the floor has been significantly improved.

8. ACKNOWLEDGEMENT

The authors wish to acknowledge the collaboration of the Proctor Group, Blairgowrie during this research programme.

Proceedings of the Institute of Acoustics

DEVELOPMENTS IN THE APPLICATION OF FLEXIBLE OPEN-CELL POLYMER FOAMS

REFERENCES

- [1] CULLUM, D J, UK Patent No 14468. "Improvements in the Construction of Floors" Filing Date 17 May 1935.
- [2] HOFBAUER, G, German Patent No 714399. "Schall and Warmedammende Verbindung von im Abstand Voneinander Angeordneten Bauteilen". Filing Date 17 December 1935.
- [3] DURABELLA LTD, UK Patent No 1309231. "Improvements in and relating to vibration inhibition in building construction". Filing Date 9 December 1968.
- [4] MACKENZIE, R K, UK Patent No 2192913. "Sound Attenuating floor construction using an open-cell foam strip". Filing Date 24 June 1986.
- [5] MACKENZIE, R K, UK Patent No 2196356. "Sound Attenuating Floor Construction using a laminated open and closed cell foam strips". Filing Date 25 June 1986.
- [6] MACKENZIE, R K, UK Patent No 2214537. "Improvements in Sound Attenuating Floor Construction". Filing Date 25 January 1988.
- [7] MACKENZIE, R K, European Patent No 0536161. "Floor Construction involving resilient strip". Filing Date 23 May 1991.
- [8] MACKENZIE, R K, UK Patent No 2259131. "Sound Deadening in Floor Construction". Filing Date 21 August 1992.
- [9] MACKENZIE, R K, European Patent Appl. No 949154618.6: "Floor Construction involving shallow profile deck". Filing Date 19 May 1994.
- [10] MACKENZIE, R K, Improvement of Sound Insulation of Timber Floors: A Study of the Relative Significance of Mass, Resonance and Resilience in the System, Proc IOA, Vol 8, 79-89, 1986.
- [11] MACKENZIE, R K, The Development of a Sound Absorbing Flooring System, Proc IOA, Vol 8, 169-174, 1986.
- [12] MACKENZIE, R K, The Sound Insulation of Flooring Systems incorporating Resilient Foam Strips, Proc IOA, Vol 10, 53-61, 1988.
- [13] FOTHERGILL, L C & ROYLE, P "The Sound Insulation of Timber Platform Floating Floors in the Laboratory and Field" J Applied Acoustics 33 (1991) 249-261.
- [14] GRIMWOOD, C & FOTHERGILL, L C. "Sound Insulation between conversions - Feedback on the Operation of the New Requirements" Building Control, March 1995.
- [15] MACKENZIE, R K, "Upgrading of Floors in Refurbishment Projects Proc IOA, Vol 15, 301-308, 1993.
- [16] HALL, R & MACKENZIE, R K. "Reconstituted versus Virgin Open Cell Foams in Floating Floors". J BUILDING ACOUSTICS 2 (2), (1995) 449-61.

Reconstituted Versus Virgin Open Cell Foams in Floating Floors

by

Robin Hall and Robin K. Mackenzie

Reprinted from

**Journal of
Building Acoustics**

VOLUME 2 NUMBER 2 1995

MULTI-SCIENCE PUBLISHING CO. LTD.
107 High Street, Brentwood, Essex CM14 4RX, United Kingdom

Reconstituted Versus Virgin Open Cell Foams in Floating Floors

Robin Hall¹ and Robin K Mackenzie²

¹*School of Construction, Sheffield Hallam University*

²*Department of Building and Surveying, Napier University, Edinburgh*

(Received 1 February 1996, and in revised form 28 February 1996)

ABSTRACT

Sound reducing flooring systems using flexible polymer foams as a decoupling resilient layer are increasingly being used in both new build and refurbishment. Such foams have been investigated and results suggest that reconstituted polyether foam from waste products may offer some advantages over the low density open cell (l.d.o.c.) foams currently used in some systems. It has been shown that reconstituted open cell (o.c.) foams have an almost linear compressive stress-strain relationship up to about 40% strain without the marked yield point observed with virgin o.c. foams. Stress strain characteristics for reconstituted o.c. and virgin l.d.o.c. foams compared in this study indicate that, for stresses below the yield point for the virgin foam, greater strain is observed in reconstituted foam. When tested according to BSEN 29052-1, systems comprising reconstituted foam exhibited lower natural frequencies than those with the lower density virgin foam.

1. INTRODUCTION

The purpose of this study is to investigate the behaviour of flexible polymer foams of the type used as a decoupling layer under floors and specifically to compare the performance of virgin foams with that of reconstituted foam. Polymer foams offer several advantages over mineral fibre slabs traditionally used in floating floors. They are more pleasant to handle, often have better long term performance¹ and, more important for refurbishment where there may be restrictions due to ceiling height, can be used in thinner layers. Low density open cell (l.d.o.c.) virgin foams are currently used in several commercially available sound reducing flooring systems. A range of reconstituted and virgin foams was tested and some comparative data are shown. To illustrate the differences in behaviour between the two types, 78 kg/m³ (o.c.) reconstituted polyether foam was compared with 69 kg/m³ and 28 kg/m³ virgin (o.c.) polyether foams.

2. BACKGROUND

The foams tested in this programme were characterised by their stress-strain behaviour (static tests) and by the resonant frequency (f_r) of a standard system as specified in BSEN 29052-1 (dynamic tests)². The system for the dynamic tests is illustrated in Figure 1 and comprises a 25 mm thick steel load plate and transducers, of total mass 7.53 kg,

supported by the foam sample under test. The samples were of varying thickness but their load bearing surfaces had the same dimensions as the top and bottom surfaces of the load plate (200 mm x 200 mm). In static tests the stress strain data obtained under compression give an indication of the load bearing capacity of the materials. The resonant frequency of systems comprising foam as a resilient decoupling layer should give an indication of the isolation offered by a particular material.

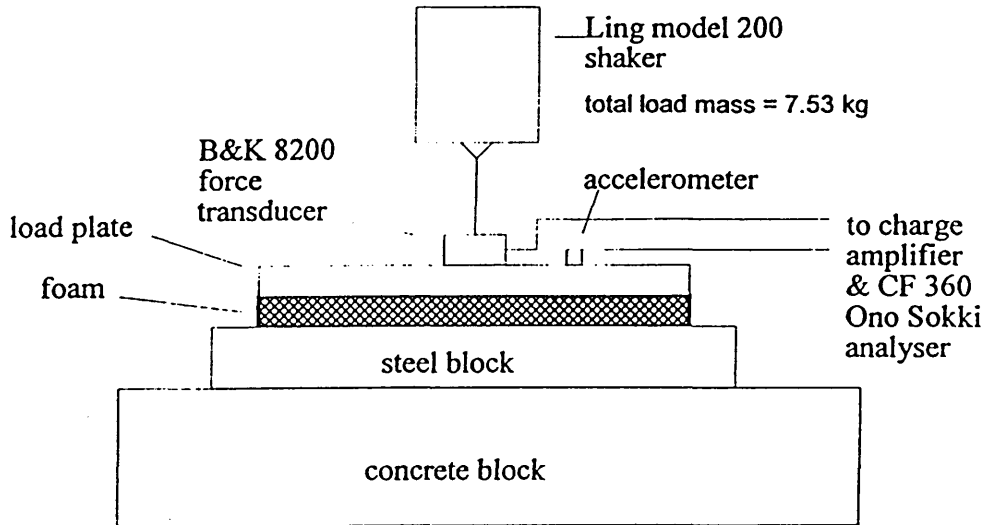


Figure 1. Resonant frequency apparatus.

For an undamped single degree of freedom system the transmissibility (T) is given by:

$$T = \frac{1}{\left| 1 - \left(\frac{f_f}{f_n} \right)^2 \right|} \quad (1)$$

where: f_f = forcing frequency
 f_n = the natural frequency of the system

Useful isolation is provided when $f_f > \sqrt{2}f_n$ and to maximise the frequency range of this useful isolation the natural frequency for the system should be as low as possible. The curve in Figure 1 is modified when damping is taken into account but the principle remains the same, the lower the natural frequency the greater the range of isolation. This simple single degree of freedom model is often useful since it states that natural frequency for a system depends only on static deflection and is given by:

$$f_n = \frac{1}{2\pi} \sqrt{\frac{g}{\Delta}} \quad (2)$$

where: g is acceleration due to gravity
 Δ is the static deflection.

Hence a large static deflection means a low natural frequency and good isolation.

In real situations when dealing with linear resilient isolators, simply measuring static deflection and using Equation 2 often gives a very good indication of natural frequency and isolation. This is not necessarily the case, however, with polymer foam materials since these are highly non linear, especially at high strains.

3. TESTING METHOD

Static and dynamic tests were carried out on samples of foam. Dynamic tests, according to BSEN 29052-1, are used to determine the dynamic stiffness of materials used under floating floors but, for materials with low airflow resistivity, this method may not be appropriate. To assess the suitability of this method for the materials investigated, airflow resistivities were measured according to BSEN 29053³. All tests were carried out at $(20 \pm 2)^\circ\text{C}$ and $(55 \pm 7)\%$ relative humidity.

3.1 Static Tests

Stress-strain data were obtained for three samples of each foam according to BS4443-14 using a Hounsfield H10KR testing machine under computer control. Foam samples were compressed to 70% of their original thickness at a rate of 100 mm/min and then the load removed at the same rate. This cycle was immediately repeated a further three times and on the fourth and final loading stroke the stress strain data were recorded. The preferred sample size (50 mm thick with load bearing surface 100 mm x 100 mm) was used in all cases. To illustrate the effect of the three conditioning cycles, data from the initial loading stroke for virgin and reconstituted foam samples of identical size were also recorded.

3.2 Dynamic Tests

According to the BSEN 29052-1 the resonant frequency (f_r) for the dynamic test system is defined by Equation 3:

$$f_r = \frac{1}{2\pi} \sqrt{\frac{s_t}{m_t}} \text{ Hz} \quad (3)$$

where: s_t the system dynamic stiffness per unit area
 m_t is the total mass per unit area supported by the sample under test.

The apparent stiffness (s_t) of the sample is then obtained by determining the resonant frequency of the system and transposing Equation 3. The resonant frequency for each of the test systems was determined by monitoring the input force and output acceleration as the system was excited by a slow sine wave sweep produced by the analyser.

The resonant frequency was taken to be that at which peak acceleration response

occurred⁵ but phase difference between input and output signals was also recorded for corroboration. A departure from the standard method of testing was that the load plate was not bedded onto the foam samples with a layer of plaster of Paris as specified. This layer is used to ensure that the whole of the sample surface is excited. Preliminary tests on foam with smooth surfaces, with and without plaster of Paris, showed that the plaster layer had no significant effect on the resonant frequency of systems. Reconstituted foams have rougher surfaces than virgin foams so the need for the layer with these foams was investigated in greater detail.

Experiments on 12.4 mm thick reconstituted foam with a density of 66 kg/m³ were carried out. Resonant frequencies were obtained for systems with and without plaster of Paris. Tests were then conducted without the plaster layer but with an equivalent mass (570g) added to the load plate. The same sample was used for all three experiments. Finally, systems with 78 kg/m³ reconstituted and 28 kg/m³ virgin foam glued to 9 mm medium density fibre board (m.d.f.) were tested. The samples used were (200 mm x 200 mm) in area and were excited, as in the standard test, by slowly sweeping a sine wave over the desired frequency range. This was done on an 18 mm chipboard box (500 mm x 500 mm x 330 mm) and the acceleration transfer function measured over a frequency range from 2 Hz up to 2000 Hz using a B&K 4393 accelerometer on the sample and a B&K 4370 accelerometer on the box. Later the tests were repeated measuring the transfer function at third octave intervals up to 3150 Hz. A slow sine wave sweep was preferred to random noise excitation because it gave a better signal to noise ratio especially at low frequency.

4. RESULTS

The results of the static tests are shown in Figures 2-7 while those obtained from the dynamic tests are shown in Figures 8-15. Figure 2 shows stress strain curves from the final loading stroke for four different densities of reconstituted foam. All exhibit almost linear behaviour up to strains of at least 40% after which the curves rise more steeply but higher levels of stress for given strains are obtained as foam density increases. Results from tests on three different types of virgin foam are shown in Figure 3. The foams have a yield point at a stress between 2 and 5 kPa followed by a more rapid increase in strain up to around 50% strain. Beyond this point, stress begins to increase rapidly as with the reconstituted foams. Results from the virgin foams again suggest that stress levels for given strains are higher in the denser foams.

Figures 4, 5 and 6 show the initial loading and final unloading strokes as well as the final loading stroke for reconstituted and virgin foam samples of the same size having densities of 78 kg/m³, 28 kg/m³ and 69 kg/m³ respectively. It can be seen that the l.d.o.c. virgin foam is affected much more by the conditioning cycles in the test than the more dense foams. Its yield stress on the final loading stroke, at around 2 kPa, is less than half that on the first stroke (over 5 kPa) and the slope of the graph after the yield point is modified to a greater extent than that of the denser virgin foam. When the yield stress is exceeded, on the first stroke, the 28 kg/m³ virgin foam continues to compress up to a strain of around 35% without any increase in stress but on the final stroke the loading curve has a positive gradient after the yield point. With the two higher density foams the

conditioning cycles had little effect on the shape of the loading curves although it can be seen that load bearing ability is reduced and neither foam recovers to its original thickness before the final loading stroke starts since these curves do not begin at the origin. Comparison of Figures 4 and 6 also shows that on both first and final loading strokes a given stress results in a greater strain in the reconstituted foam than the virgin foam for strains up to 60%. Between 60% and 70% strain the situation is reversed and at 70% strain the reconstituted foam has the higher level of stress.

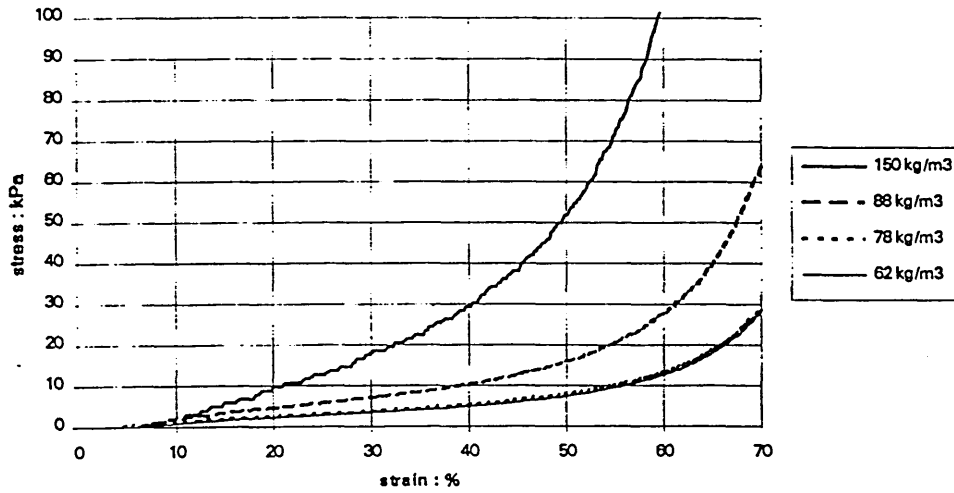


Figure 2. Final loading curves for reconstituted open cell foams.

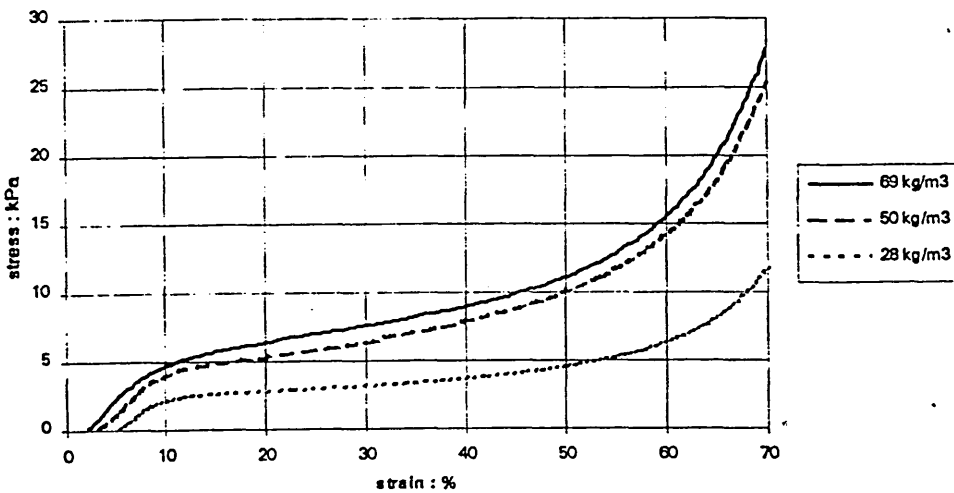


Figure 3. Final loading curves for open cell polyether foams.

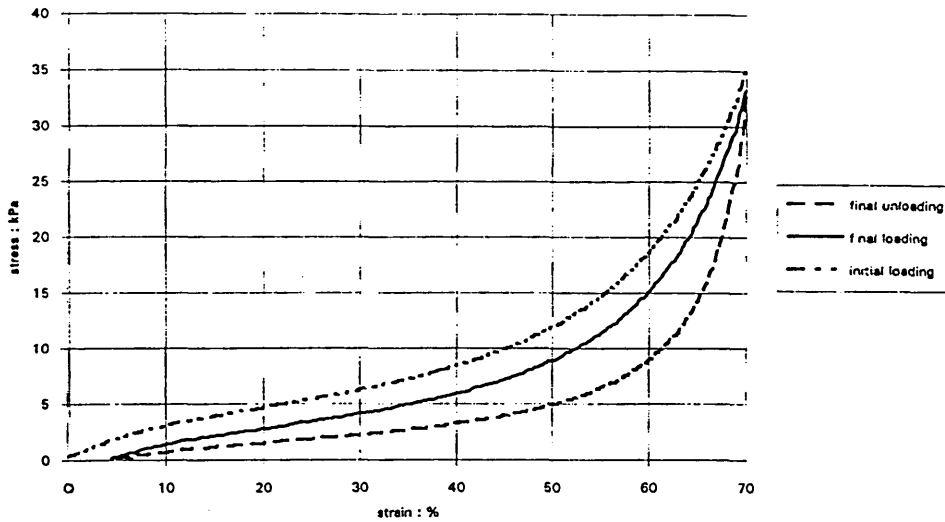


Figure 4. Initial loading, final loading and unloading curves for reconstituted o.c. foam (78 kg/m^3).

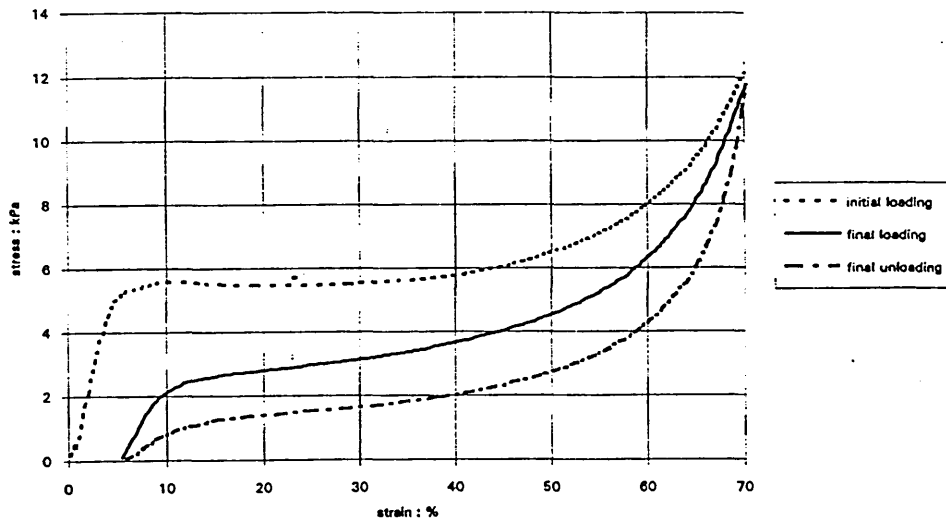


Figure 5. Initial loading, final loading and unloading curves for virgin o.c. foam (28 kg/m^3).

Table 1 shows the energy used in the deforming cycles of Figures 4, 5 and 6. The areas under the first and final loading curves represent the energy absorbed per unit volume by the materials on these cycles⁶. The area under the final unloading curve represents the energy stored in the foam and available to return it to its original shape after the final loading stroke. Thus subtracting this value from the energy absorbed on the final stroke gives the energy dissipated on the final cycle. It can be seen that the 69 kg/m^3 virgin foam

absorbs most energy on both first and final compression strokes and also stores most energy on the final cycle. The reconstituted foam dissipates most energy over the final cycle and absorbs more energy than the 28 kg/m³ virgin foam on the first and final compression strokes as well as storing more energy than the lower density virgin foam after the final loading stroke.

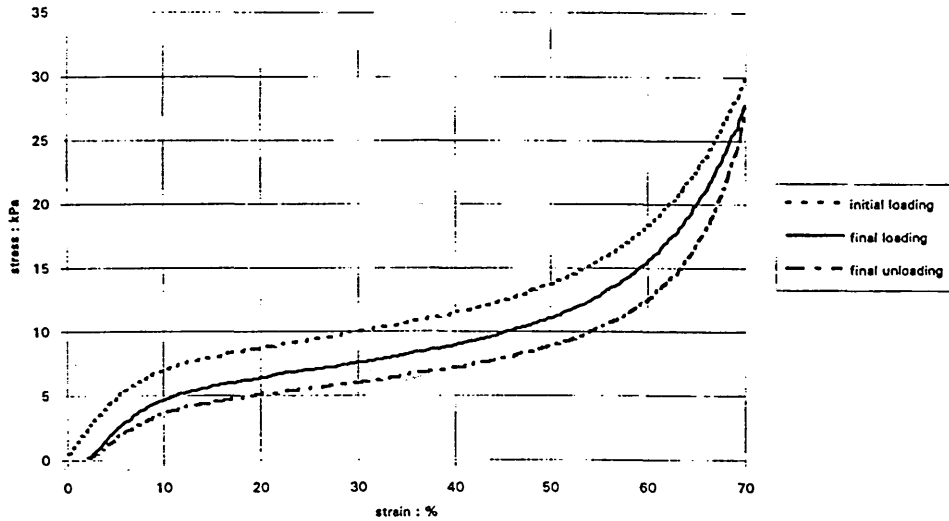


Figure 6. Initial loading, final loading and unloading curves for virgin o.c. foam (69 kg/m³).

Table 1
Energy involved in loading and unloading cycles

	Energy absorbed per unit volume on first loading stroke kJ/m ³	Energy absorbed per unit volume on final loading stroke kJ/m ³	Energy stored per unit volume after final loading stroke kJ/m ³	Energy dissipated per unit volume on last cycle kJ/m ³
reconstituted foam 78 kg/m ³	6.9	5.2	3.3	1.9
virgin foam 28 kg/m ³	4.4	2.7	1.7	1.0
virgin foam 69 kg/m ³	8.3	6.6	5.4	1.2

Figure 7 shows data from final loading curves from identically sized samples of two reconstituted and two virgin foams. The enlarged scale shows the differences in

compression characteristics up to 40% strain more clearly. It is evident that the behaviour of the reconstituted foams is linear over this strain range with neither foam exhibiting the yield point which is clearly evident with both virgin foams. It is also noted that for the 69 kg/m³ virgin foam, once the yield point is passed, its curve has a similar gradient to those of the reconstituted foams.

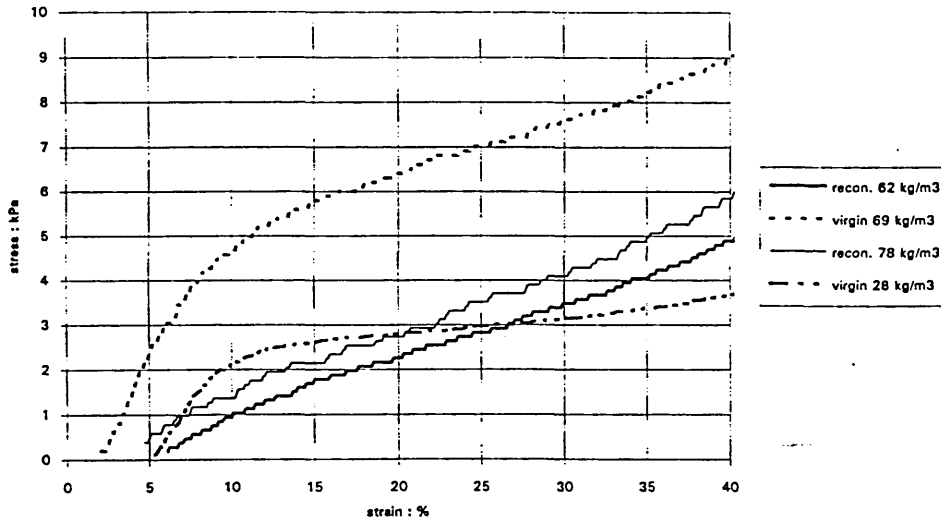


Figure 7. Comparison of final loading strokes for reconstituted and virgin open cell foams.

Figures 8a to 9b show transfer functions (accelerance) in input-output phase differences over a range of frequencies up to a maximum of 100 Hz for the test system with four different samples of the same virgin foam (28 kg/m³). The curves have similar shapes but it can be seen that the thicker foam samples have lower resonant frequencies, 52 Hz in Figure 8, 62 Hz and 65 Hz in Figure 9. In all cases maximum acceleration response occurred at the frequency at which input-output phase difference was 90°. Figures 10a and 10b show results for the test system with a layer of 78 kg/m³ reconstituted foam. These show that the resonant frequency for the system using this material is around 26 Hz, half that with the thicker virgin foam and nearly 40 Hz lower than with the thinner virgin foam. Figures 11a and 11b were produced using data from a test on the 69 kg/m³ virgin foam and show that this system had a resonant frequency of 39 Hz.

The effect of sample thickness on resonant frequency for reconstituted foam is illustrated in Figure 12 which shows resonant frequencies for the test system with four different thicknesses of foams having densities ranging from 62 to 150 kg/m³. It can be seen that, for all foams, the increases in sample thickness lead to a decrease in resonant frequency. The graph also shows, apart from the overlapping curves of the two least dense foams, increases in density for reconstituted foam are accompanied by increases in resonant frequency. Resonant frequencies for different thicknesses of 69 kg/m³ virgin foam are also shown on this graph for comparison. Again resonant frequency falls as

sample thickness is increased but these frequencies are higher, for a given thickness, than all but the most dense reconstituted foam.

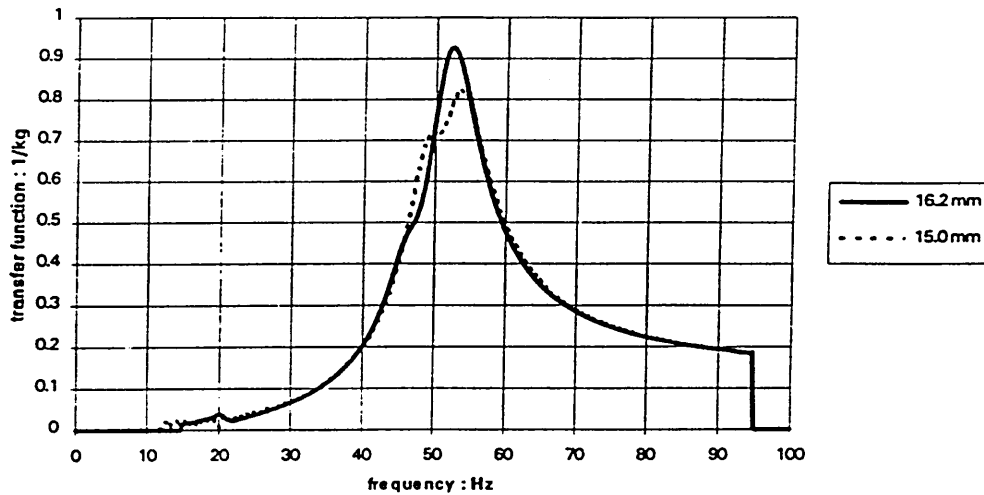


Figure 8a. Transfer function for virgin open cell foam (28 kg/m³).

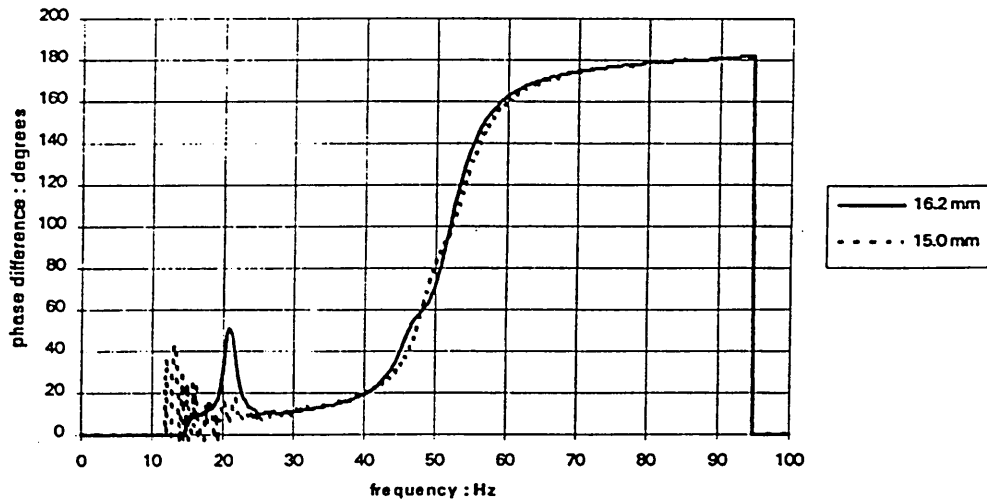


Figure 8b. Input-output phase difference for virgin open cell foam (28 kg/m³).

Figure 13 illustrates differences in the transfer function of two identically sized samples of medium density fibre board samples, over the range 2 Hz to 2000 Hz, to which different types of foam (28 kg/m³ virgin and 78 kg/m³ reconstituted) were glued. It can be seen that, in general, the transfer function for the system with reconstituted foam is smaller than that of the system with virgin foam. This is particularly the case for

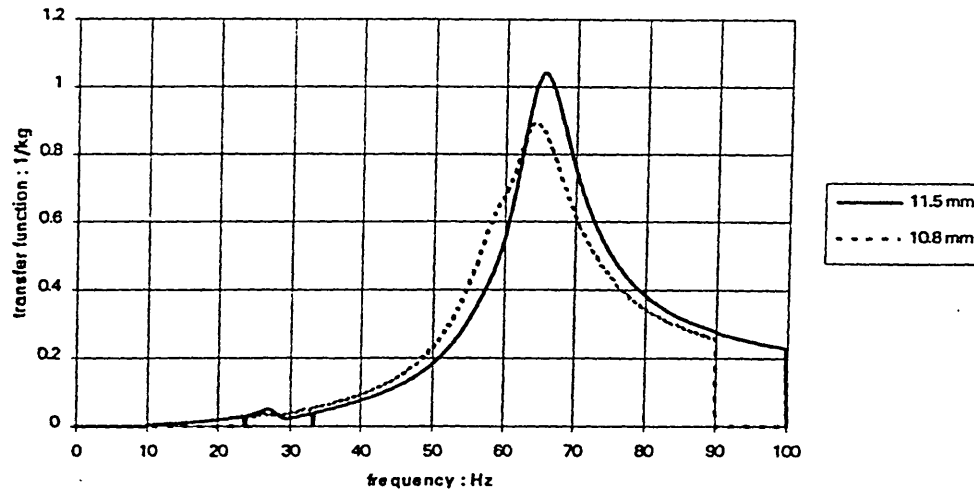


Figure 9a. Transfer function for virgin open cell foam (28 kg/m^3).

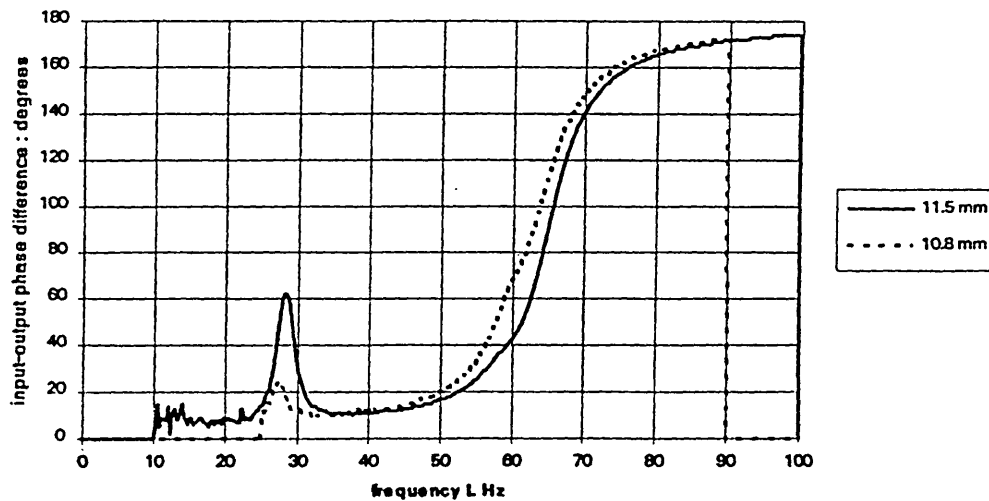


Figure 9b. Input-output phase difference for virgin open cell foam (28 kg/m^3).

frequencies greater than 1100 Hz but also true within the range 315 Hz to 630 Hz as illustrated in Figure 14 which shows the two transfer functions in third octave intervals up to 3150 Hz. The transfer function for the system with reconstituted foam is only greater than that of the other in three of the third octave intervals.

Finally Figure 15 shows the effect of the plaster of Paris layer on tests according to BSEN 29052-1. It can be seen that the frequency of the initial peak is unchanged in all three tests at 28 Hz and that 90° phase difference between input and output also occurs at this same frequency for all three systems.

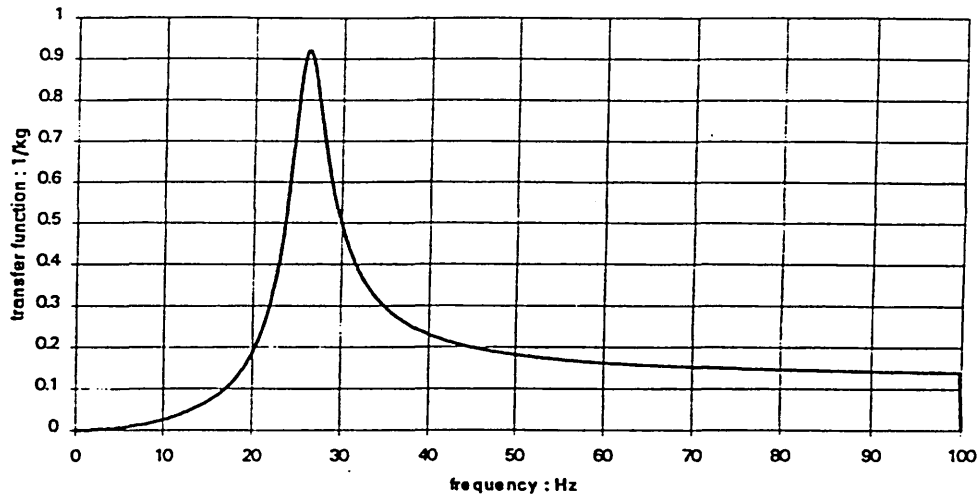


Figure 10a. Transfer function for 13.2 mm thick reconstituted o.c. foam (78 kg/m³).

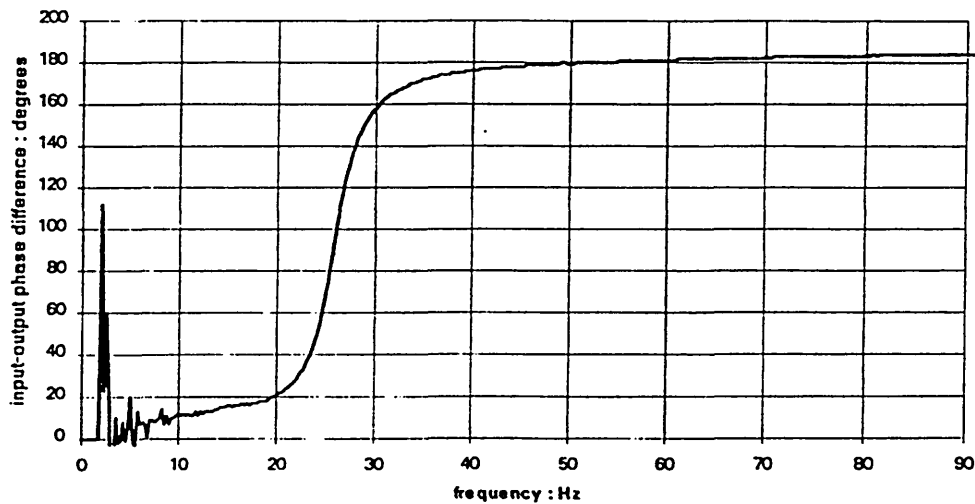


Figure 10b. Input-output phase difference for 13.2 mm thick reconstituted o.c. foam (78 kg/m³).

5. DISCUSSION

Some flooring systems incorporating l.d.o.c. virgin foam exhibit discernible movement under foot as they are walked on which poses potential problems of fatigue along joints in tongued and grooved systems. These relatively large and rapid deflections can be explained by the behaviour of the foam under compression. Virgin foams characteristically exhibit an almost linear relationship between stress and strain up to a particular yield stress after which there is a rapid increase in strain for little increase in stress^{6,7}. This behaviour is most pronounced on the first compression stroke shown in

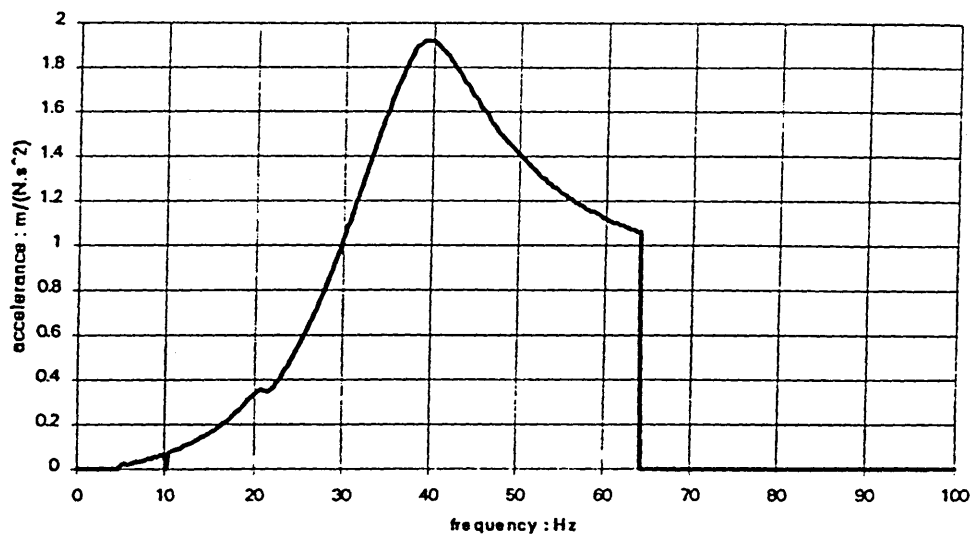


Figure 11a. Transfer function for 10 mm thick virgin o.c. foam (69 kg/m^3).

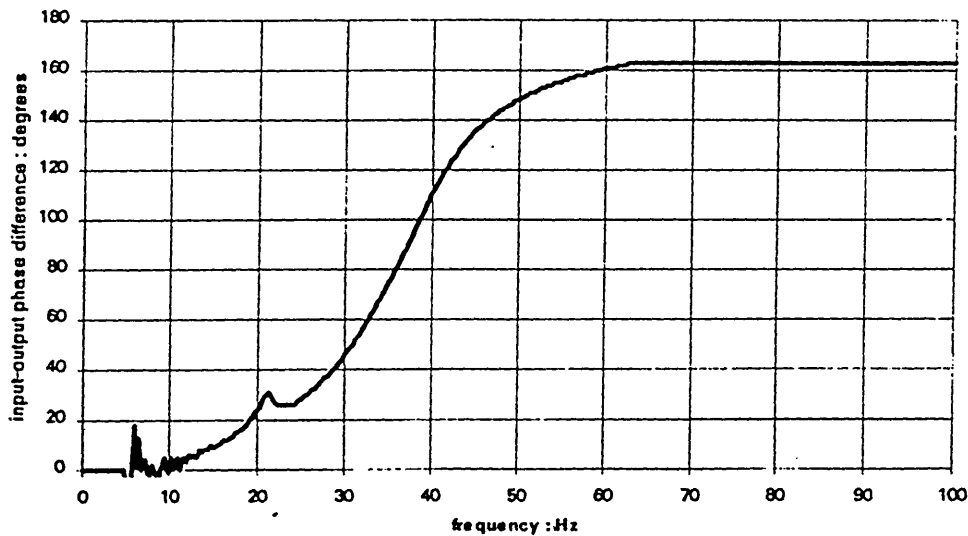


Figure 11b. Input-output phase difference for 10 mm thick virgin o.c. foam (69 kg/m^3).

Figure 5 although all curves in Figure 3, for virgin foam, show a clearly defined yield point. The reconstituted foams tested do not behave in this way. Figure 2 shows a virtually linear relationship between stress and strain on the fourth compression stroke up to at least 40% strain and that as density increases, strain is reduced for a given stress. Figures 4, 5 and 6 show that conditioning cycles in the test method have a much more significant effect on the lowest density (virgin) foam than on the two denser foams. With these, comparison of first and final loading strokes in Figures 4 and 6 shows that the

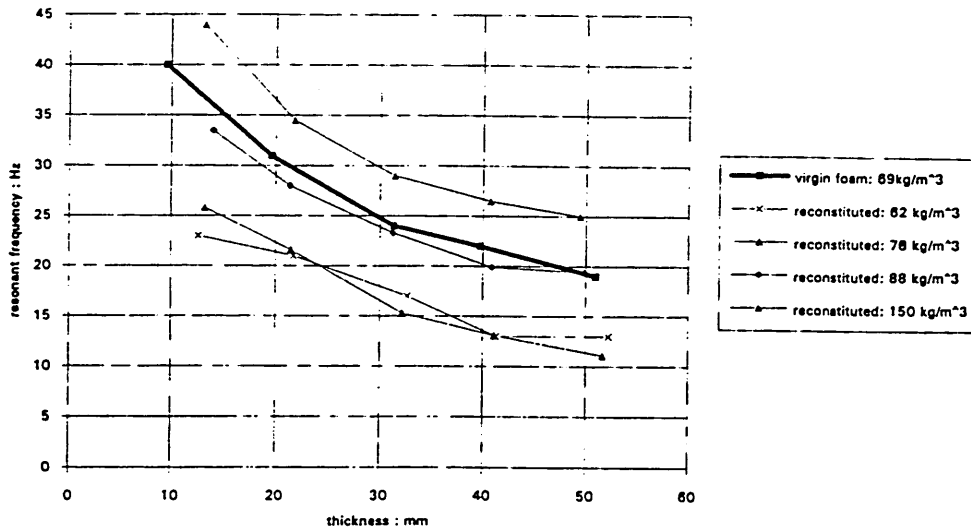


Figure 12. Variation of test system natural frequency with different sample thicknesses.

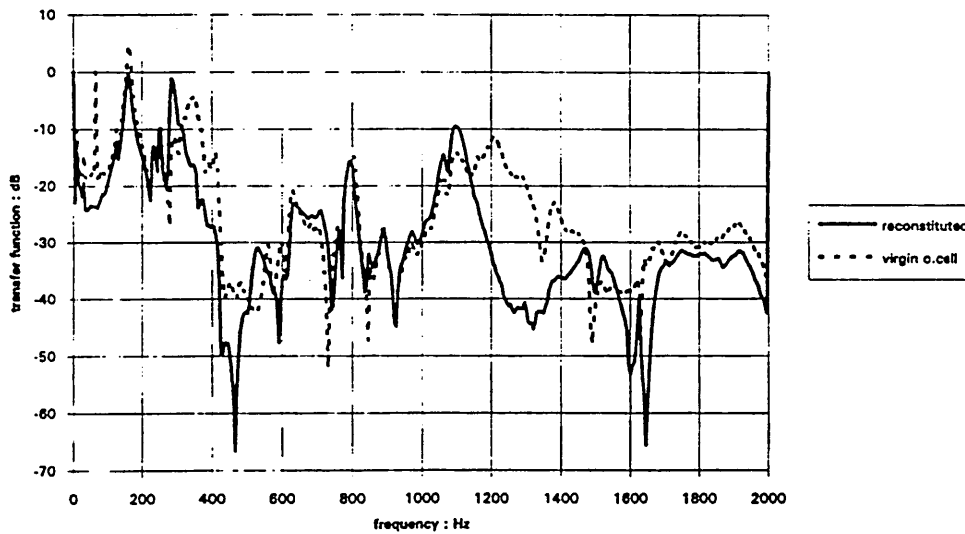


Figure 13. Acceleration transfer function for virgin and reconstituted foams glued to medium density fibre board.

conditioning caused some softening but had little effect on the shape of the final loading curves. The difference in behaviour shown by the foams is important. A floor comprising 28 kg/m³ virgin foam will yield at much lower strains after conditioning and this is likely to be noticeable to those walking on it. With the reconstituted foam the difference in behaviour before and after conditioning is likely to be imperceptible since there is no yield point and the gradients of the first and final curves are virtually the same.

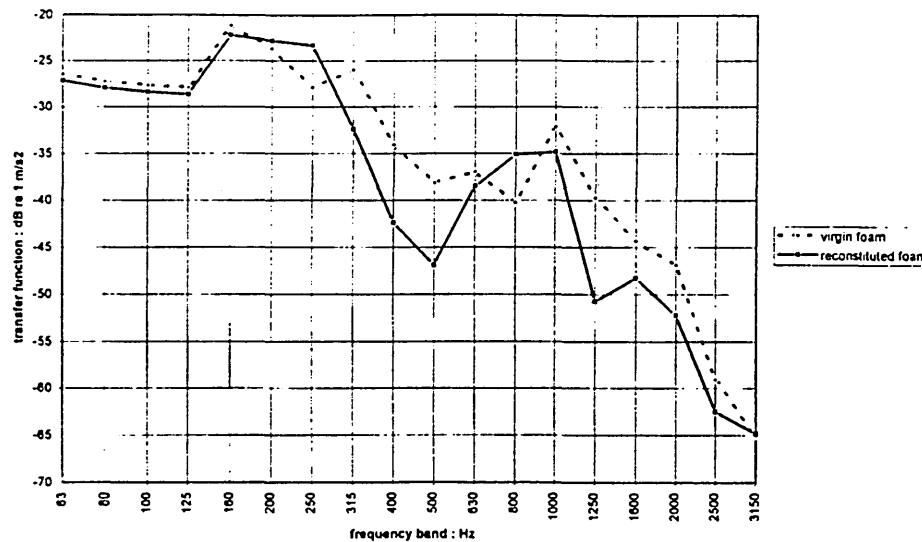


Figure 14. Acceleration transfer function for virgin and reconstituted foams glued to medium density fibre board (third octave frequency bands).

The areas under the curves in Figures 4, 5 and 6 were obtained by integration and Table 1 shows the energy involved in the cycles illustrated. It can be seen that more energy is absorbed on both first and final compression strokes and stored on the final stroke with the reconstituted foam than with the lower density virgin foam. The reconstituted foam dissipated most energy over the final loading and unloading cycle. The higher density virgin foam absorbed more energy in compression and also stored more energy over the last cycle than any other foam tested. The difference in compressive behaviour up to 40% strain is shown more clearly in Figure 7. With reconstituted foam the behaviour in compression is clearly linear over this range whilst both virgin foams exhibit a yield point. The higher density virgin foam clearly requires a greater stress to produce a given strain than any of the other foams. It should be noted, however, that the 78 kg/m^3 and 62 kg/m^3 reconstituted foams exhibit greater strain than the much lower density virgin foam for stresses below 2.7 kPa and 3 kPa respectively.

Both static and dynamic stiffness are inversely proportional to sample thickness so it is to be expected that f_r should fall as sample thickness increases. Figures 8 and 9 illustrate that this is the case with l.d.o.c. virgin open cell foam and Figure 12 confirms the relationship for reconstituted foams tested and the higher density virgin foam.

When Figures 8 and 9 are compared with Figure 10 it can be seen that the system with the denser reconstituted foam has a much lower resonant frequency. Although results for only one test with, 13.2 mm thick foam, are shown in Figure 10, repeatability of other tests and the sets of curves shown in Figure 12 suggest that, generally, systems with reconstituted foam are likely to have lower natural frequencies than those with lower density virgin open cell foams of the same thickness. Figure 12 also suggests that there is little point in foam layers being greater than 50 mm thick in order to achieve a low

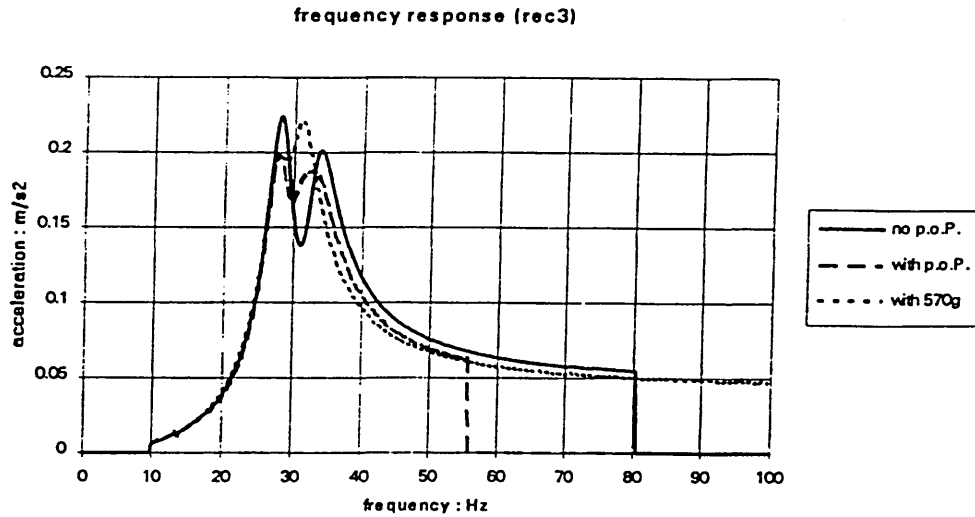


Figure 15a. Acceleration response for reconditioned foam, with and without plaster of Paris.

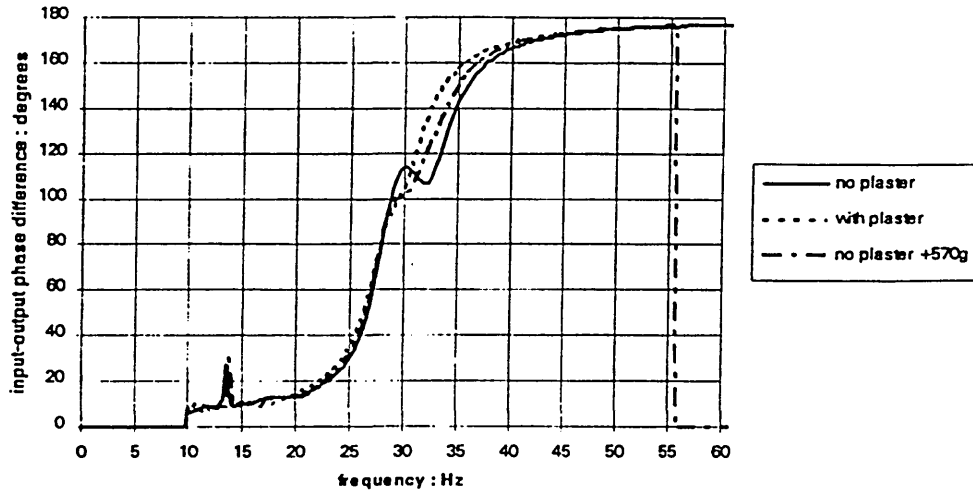


Figure 15b. Input-output difference for reconditioned foam, with and without plaster of Paris.

resonant frequency. The transfer function for the system with 69 kg/m³ virgin foam is shown in Figure 11a. The value of the transfer function at the resonance frequency is considerably higher than those for systems tested with other foams and this was the case with all thicknesses of this material. The width of the peak also suggests that the system is more damped with this foam than with the others tested.

That systems tested with reconstituted foam consistently had lower resonant frequencies than those with the l.d.o.c. virgin foam might be explained by the relative behaviour of the materials at small strains. The load plate used in the dynamic tests

imposed a stress of 1.8 kPa on the foam samples which is less than the yield stress for the l.d.o.c. virgin foam (see Figure 5). Experimental data from which Figures 4 and 5 were produced suggest that this stress causes a strain of around 4% in the 78 kg/m³ reconstituted foam and around 1.5% in the l.d.o.c. virgin foam. Their stress strain behaviour suggests that for such small strains these foams are likely to behave much more like linear materials than they do at large strains. If this is the case then it would be expected that if greater deflections due to the load plate were to be observed in reconstituted foam than in virgin foam, then lower natural frequencies would result in systems comprising reconstituted foam. Using these predicted strains in the foams above to estimate static deflection caused by the load plate in dynamic tests and substituting these in equation 2 gave values for f_r of 33 Hz and 22 Hz for 15 mm virgin foam and 13.2 mm reconstituted foam respectively. Comparing these values with those obtained from Figures 8 and 10 suggests that using likely static strain to predict resonant frequency for a system is of little practical use if it comprises virgin foam. The predicted f_r for reconstituted foam is much closer to the experimentally measured value and suggests that the small strain properties of these foams may be worth further investigation. It should be noted however that stress strain curves were produced using samples 50 mm thick and tests in this programme have demonstrated that sample thickness affects these data.

Earlier dynamic tests in this programme on different virgin foams showed that if static stress due to loading was increased, thereby increasing static deflection, then resonant frequency for the system decreased whilst yield stress was not exceeded. However, when the load stress was sufficiently large to cause a static deflection greater than around 5 mm in a 12.5 mm thick l.d.o.c. virgin foam layer, resonant frequency started to rise. Resonant frequencies of systems with virgin foams have been shown to increase when subjected to large strains in excess of around 40%. This appears to be due to an increase in the real part of their complex modulus at high strains⁷ resulting in increased stiffness. Increases in stiffness are likely to result in lower isolation and therefore lower noise reduction since natural frequency is proportional to the square root of stiffness. It is therefore likely that isolating properties of cellular materials are diminished under these circumstances and that large static strains should be avoided in floors incorporating cellular plastic materials although this has not so far been tested in this programme.

BSEN 29052-1 states that if materials tested have airflow resistivities of less than 10 kPa.s/m² and that the stiffness of the air enclosed is significant when compared with that of the test system, then this method cannot be used to determine dynamic stiffness of floors comprising such materials. Airflow resistance measurements, according to BSEN 29053 method A, showed this to be the case for the 78 kg/m³ and 62 kg/m³ reconstituted foams (8.9 kPa.s/m² and 6.2 kPa.s/m² respectively). For the 28 kg/m³ virgin foam airflow resistivity was found to be 16 kPa.s/m² which according to BSEN 29052 means a correction factor due to the stiffness of enclosed air must be added to the test sample dynamic stiffness in order to give the dynamic stiffness of a floor comprising this foam. For 15 mm thick 28 kg/m³ virgin foam a resonant frequency of 53 Hz gives a dynamic stiffness of 21 MN/m³ for the sample. A correction for air stiffness of 7.4 MN/m³ must be added to give the dynamic stiffness of this material when used under a floating floor. It could be argued that a test method where a correction factor greater than 33% of an

experimentally determined value is needed is not the best one to use but the test does give comparative information on the resonant frequencies of test systems and is therefore deemed to be useful for this programme.

Figures 13 and 14 show results from the acceleration transmissibility tests. It can be seen that the method is sufficiently sensitive to detect differences between the two systems and it is felt that they support the hypothesis that reconstituted foam is likely to provide better isolation than l.d.o.c. virgin foam.

Finally, the plaster of Paris layer specified in the standard testing method has an insignificant effect on the results as illustrated in Figure 15. It is therefore felt that not using the plaster of Paris layer is justified in these dynamic tests.

6. CONCLUDING REMARKS

Static and dynamic tests conducted so far both suggest that reconstituted foam may be better to use than lower density virgin open cell foam in floors. Static tests illustrate the better load bearing potential of reconstituted foam and its stress strain characteristics suggest that large rapid strains associated with stresses exceeding the yield point of virgin foam may be avoided. Dynamic tests have shown that using reconstituted foam in a system gives a lower natural frequency than using virgin foam. That this in turn means better isolation is supported by transmissibility tests so far completed.

Airflow resistivity means that BSEN 29052-1 cannot be used for determining the dynamic stiffness of resilient layers under floors if they comprise some of the reconstituted foams compared in this study. It is therefore important to develop alternative small scale tests for use with these materials to assist with the prediction of the dynamic performance of floating floors.

It remains to carry out impact tests on full scale floors. Researchers in Japan have studied the localised dynamic behaviour of wood strip samples over foam layers⁸ and have identified a correlation between dynamic stiffness and shock absorbing performance of composite resilient flooring systems subject to light impact loads⁹ and it is felt that a similar approach should be adopted to develop the present programme. Transfer functions and resonant frequencies of samples of flooring systems will therefore be investigated and results compared with field tests on complete floors.

It is known that l.d.o.c. foams become stiffer when subject to large strains. It is therefore intended to investigate the effect of strain on dynamic stiffness on these and reconstituted foams. The effect of strain on transmissibility of flooring samples will also be investigated.

ACKNOWLEDGEMENTS

Acknowledgement is made for the support by The Royal Society and the EPSRC during the initial part of this research programme.

The authors would also like to acknowledge the contribution of Dr. H. Bougdah of Sheffield Hallam University during the preparation of this report and Messrs. Rowland Murphy and Ian Colley of Vitafoam (Middleton) for providing materials used in the tests.

REFERENCES

1. R.K. Mackenzie, 1986, Development of a sound absorbing flooring system, *Proc. I.O.A.*, Vol. 8, 53-61.
2. BSEN 29052-1: 1992, *Acoustics – Determination of dynamic stiffness – Materials used under floating floors in dwellings.*
3. BSEN 29053:1993, *Acoustics – Materials for acoustical applications – Determination of airflow resistance.*
4. BS 4443 Part 1:1988, *Flexible cellular materials – Method 5a – Determination of compression stress-strain characteristics.*
5. C.M. Harris, 1988, *Shock and Vibration Handbook*, 3rd ed., Publ. McGraw-Hill.
6. L.J. Gibson and M.F. Ashby, 1988, *Cellular Solids – Structure and Properties*, Publ. Pergamon Press.
7. N.C. Hilyard and A. Cunningham, 1994, *Low Density Cellular Plastics – Physical Basis of Behaviour*, Publ. Chapman and Hall.
8. S. Sueyoshi, and M. Tonosaki, 1993, Determination of localised dynamic behaviour of wood strip over foam rubber underlayment, composite flooring by random vibration, *Wood Science and technology*, Vol. 27, 11-21.
9. S. Sueyoshi, M. Tonosaki and Y. Oribe, 1995, Localised vibration of wood flooring fastened to a concrete slab, *Wood Science and technology*, Vol. 41, 31-36.

Proceedings of the Institute of Acoustics

THE USE OF LOW DENSITY POLYMER FOAMS AS RESILIENT LAYERS IN FLOORS

Robin K Mackenzie, Robin Hall

Sheffield Hallam University, School of Construction, Pond Street, Sheffield S1 1WB

1. INTRODUCTION

Recent developments in the manufacturing techniques associated with flexible cellular foams have opened up new possibilities in the design of products incorporating these new materials. Research at Sheffield Hallam University during the past twenty years by Hilyard et al (1) has helped to characterise the mechanical properties of cellular foams. New research is being carried out to facilitate the evaluation of the dynamic properties of cellular foams both independently and as part of complete flooring systems. Reference is made to the use of low density cellular foam in the manufacture of resilient flooring products with particular reference to laminated and co-planar applications of open and closed cell foams.

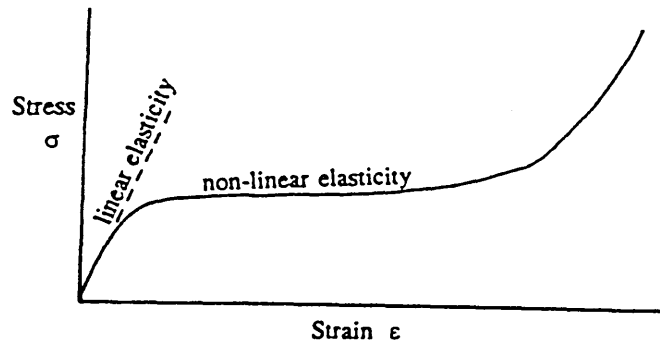
2. BACKGROUND

Current standard test procedures (2) for the evaluation and characterisation of cellular foams used as resilient layers in buildings are limited in their scope and do not apply to complete floor systems. Most standard tests on cellular elastomer foams relate to their use as packaging or cushioning material in vehicles or furniture. A review of current testing procedures for elastomer foams is currently underway in order to establish their usefulness in predicting the dynamic performance of resilient floors. As part of this research foams are being categorised using mechanical methods developed at SHU in earlier investigations (3).

Gibson and Ashby (4) treat cellular solids as class of material with elastomer foams being just one particular form. They have modelled the behaviour of such foams by considering each individual cell in the foam to be made up of interconnected beams. Equations describing the behaviour of beams coupled with scaling laws have then been used to describe the behaviour of the bulk foam. Consideration of this approach led to the recognition that current research in the Department of Applied Physics at SHU into osteoporosis might well be relevant to this study. The commonality is that cancellous bone, like foam, is a form of cellular material and any technique which can classify bone might well be used to classify cellular foam indeed any form of cellular material encountered in buildings. Recent work undertaken now suggests that this is indeed a possibility.

Deformation mechanisms in foams

When compressed, elastomer foams usually exhibit the stress / strain relationship illustrated in fig. 1.



Initially, at low strain, linear elasticity (cell wall bending) followed by a "plateau" (elastic buckling of cell walls) where strain increases rapidly for small increases in stress and finally a steep rise in stress with strain as the matrix polymer is itself compressed following collapse of cells in the foam. Foams can be of open or closed cell form and the use of both is described in flooring systems later in this document.

Gibson and Ashby (4) propose that cell wall bending and buckling are of fundamental importance in describing the behaviour of foams and this is supported by the observations of the authors. Their characterisation of the mechanical behaviour of isotropic elastomer foams is briefly described below.

Linear elasticity

Two moduli are needed to describe linear behaviour in isotropic foams (more if the foam is anisotropic). Of primary importance are Young's Modulus (E^*), Shear Modulus (G^*) and Poisson's ratio (ν^*). The moduli are expressed in terms of cell wall (base polymer) modulus (E_s) and the foam's relative density (ρ^*/ρ_s).

(N.B. the superscript "*" refers to the foam and the subscript "s" refers to the base polymer).

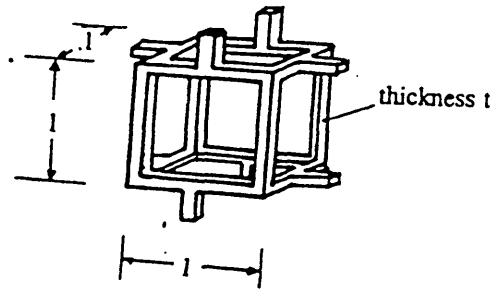
Open cell foam

Figure 2 illustrates cell wall bending for an open cell foam.



Proceedings of the Institute of Acoustics

Figure 3 shows the cell model used to estimate the moduli. This is similar to the approach of Gent and Thomas (4) but here each cell is joined to another by a strut in the middle of one of its beams.



Relative density of the cell (ρ^*/ρ_s) and second moment of area (I) are related by:

$$\frac{\rho^*}{\rho_s} \propto \left(\frac{t}{l}\right)^2 \quad (1)$$

and

$$I \propto t^4 \quad (2)$$

For a beam of length (l) and thickness (t) loaded at its mid point, Timoshenko (6) gives the deflection (δ) as:

$$\delta \propto \left(\frac{Fl^3}{E_s I}\right) \quad (3)$$

and

$$F \propto \sigma l^2$$

$$\varepsilon \propto \frac{\delta}{l}$$

Hence Young's Modulus for the foam becomes:

$$E^* = \frac{\sigma}{\varepsilon} = (\text{constant}) \left(\frac{E_s I}{l^3}\right) \quad (4)$$

and from (1) & (2):

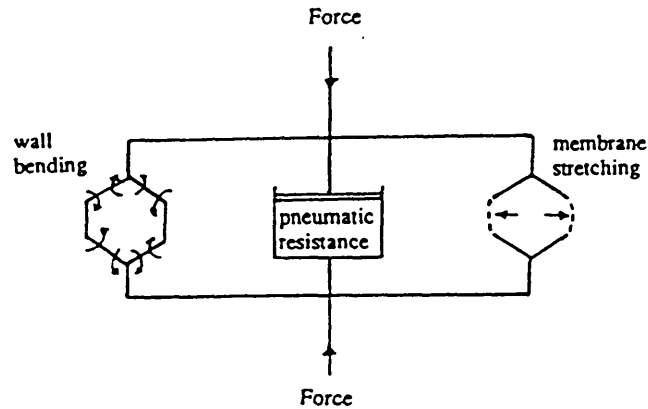
$$\frac{E^*}{E_s} = C_1 \left(\frac{\rho^*}{\rho_s}\right)^2 \quad (5)$$

C_1 contains all the constants of proportionality.

Proceedings of the Institute of Acoustics

Closed cell foams

Closed cell foams are more complicated than open cell foams. The effects of material in the faces and fluid contained in the cell must be considered as well as the contribution of the cell edges. The situation is illustrated below in Figure 4.



Non-linear elastic behaviour

With elastomer foams, the initial linear rise of stress with strain is followed by non-linear elastic deformation. Elastic because the strain is recoverable. In open cell foams there is a long plateau as strain increases rapidly with little or no increase in stress. With closed cell foams there is an increase of stress with strain caused by gas enclosed in the cells and the cell walls themselves.

Open cell foams

The non-linear deformation of these foams is controlled by the elastic buckling of the cell edges. Buckling takes place at stress = σ_{el} illustrated in figure 1.

Euler's formula gives the critical buckling load as:

$$F_{crit} = \frac{n^2 \pi^2 E_s I}{l^2} \quad (6)$$

As before:

l = beam length; E_s = Young's modulus; I = 2nd moment of area. n^2 describes the degree of constraint at the ends of columns. The stress (σ_{el}^*) at which buckling occurs is obtained from:

$$\sigma_{el}^* \propto \frac{F_{crit}}{l^2} \propto \frac{E_s I}{l^4} \quad (7)$$

From equations 1 & 2:

$$\frac{\sigma_{el}^*}{E_s} = C_2 \left(\frac{\rho^*}{\rho_s} \right)^2 \quad (8)$$

C_2 contains all the constants of proportionality.

Proceedings of the Institute of Acoustics

Closed cell foams

With closed cell foams elastic buckling is modified by the gas contained in the cells and probably by the cell faces as they fold over themselves. As cell walls buckle then the pressure of the gas can be expected to increase which suggests an explanation of post buckling behaviour. These foams exhibit an increase in the gradient of stress / strain graphs.

Critical buckling stress is given by:

$$\frac{\sigma_{cl}^*}{E_s} = (\text{constant}) \left(\frac{\rho^*}{\rho_s} \right)^2 + \frac{p_0 - p_{at}}{E_s} \quad (9)$$

where p_0 and p_{at} are original and atmospheric pressure respectively. The constant has been shown to be approximately 0.05.

For manufactured foams $p_0 = p_{at}$ so enclosed gas in cells does not affect the onset of buckling but as compression increases p_0 is modified to p' where:

$$p' \approx \frac{p_0 \epsilon}{1 - \epsilon - \left(\frac{\rho^*}{\rho_s} \right)} \quad (10)$$

The post collapse stress / strain behaviour is therefore described by:

$$\frac{\sigma^*}{E_s} = 0.05 \left(\frac{\rho^*}{\rho_s} \right)^2 + \frac{p' \epsilon}{E_s \left(1 - \epsilon - \left\{ \frac{\rho^*}{\rho_s} \right\} \right)} \quad (11)$$

It has been demonstrated (4) that by removing the second term on the right hand side of equation 11, the stress / strain curves of closed cell foams give a curve which matches the behaviour of open cell foams.

Densification

Equation 11 fits experimental data less and less as foam density increases. Also as compressive strain increases, a point is reached where the cell walls are jammed together following near total cell collapse. It has been shown (3) that this takes place when:

$$\epsilon_D = 1 - 1.4 \left(\frac{\rho^*}{\rho_s} \right) \quad (12)$$

Following densification the stress - strain curve rises with a gradient tending to E_s .

3 RESILIENT LAYERS FOR BUILDING USE

The advantages of open cell polymer foams for use as resilient layers has already been described in earlier publications (7-12). The characteristic difference between closed cell and open cell foam under an applied load is found in their relative static deflections. A closed cell foam strip, 12mm thick, under normal domestic loading, is unlikely to deflect by more than 1mm compared to a figure of 6mm obtained with open cell foam of similar thickness.

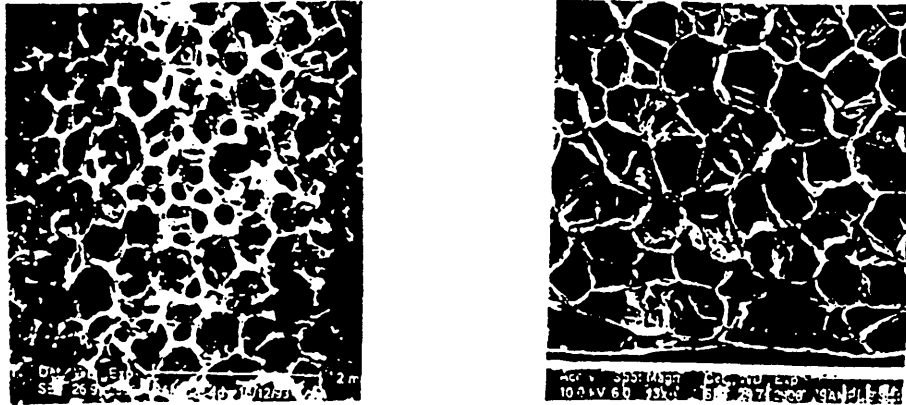


Figure 5 - Micrographs showing the different cellular structure of open cell (left) and closed cell (right) polymer foam.

Closer examination of the movement of open cell flexible foams under dynamic loading has indicated that it is the cellular structure which dictates the rate of deflection whereas it is the polymer material itself which determines its resilience or ability to return to its original state.

The main problem with rock (i.e. mineral wool) or glass fibre quilts is that they comprise of strands of brittle material (i.e. glass state) which achieve resilience by means of interweaving in free form or by resin bonding. Over a period of time these fibres break and in low density foam are frequently ground to dust.

Open cell polymer flexible foams do not exhibit such brittle fracture because of the elastic behaviour of the soft co-polymer. The only problem which can arise, therefore, is due to a breakdown in the chemical bond or a change of chemical state. Under normal domestic loading, bond breakdown is extremely unlikely and virtually impossible where cross-linking has been carried out. A change of state is, however, a possibility, with some materials more susceptible than others. Natural rubber will oxidise and after a period of time lose its resilience. This, however, is a slow process in an underfloor location where catalysts such as UV light are absent. The polyester-urethane co-polymer is essentially unstable and through being hydrolytic will, in a damp or humid environment, gradually lose its compressive strength giving rise to creep. In terms of dynamic behaviour, chemical stability and cost, polyether based polyurethane open cell foam is the most suitable material.

Proceedings of the Institute of Acoustics

Applications in Floating Floors

Laminations of open-cell and closed-cell foam strips have been utilised in the design of resilient timber battens or strips.(13,14) The micrograph below shows the compression under normal domestic loading of a 10mm open cell strip laminated to a 10mm closed cell strip.

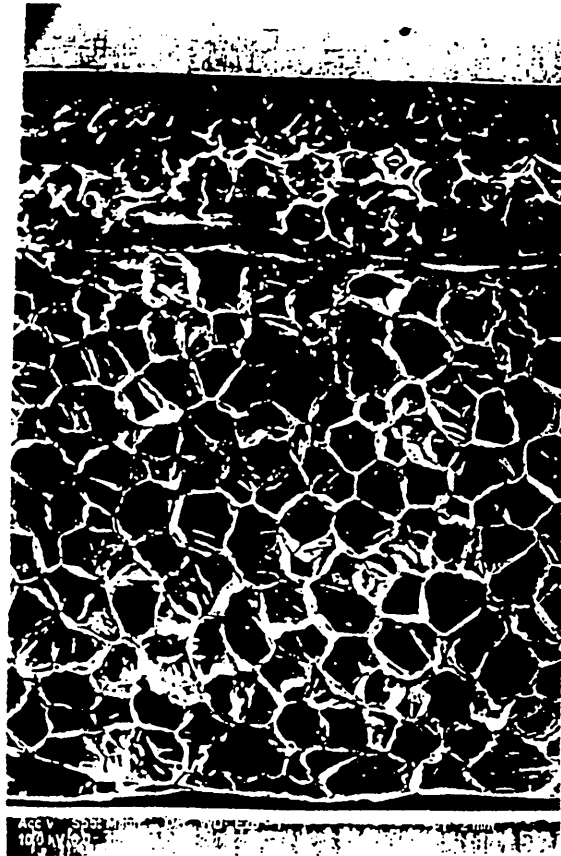


Figure 6 - Compression of the Profloor Dynamic Strip under normal domestic loading. Courtesy: Proctor Group

The 12mm thick open cell foam deflects by up to 6mm under normal domestic loading to provide a suitable isolation efficiency against impact sound. Further deflection is resisted by a combination of the elastomer in the open cell foam together with the pneumatic resistance provided by the entrapped air within the closed cell strip. The elastic behaviour under normal domestic loading, $<4\text{kPa}$, is clearly shown in the plateau in Figure 7, between 2mm and 6mm deflection.

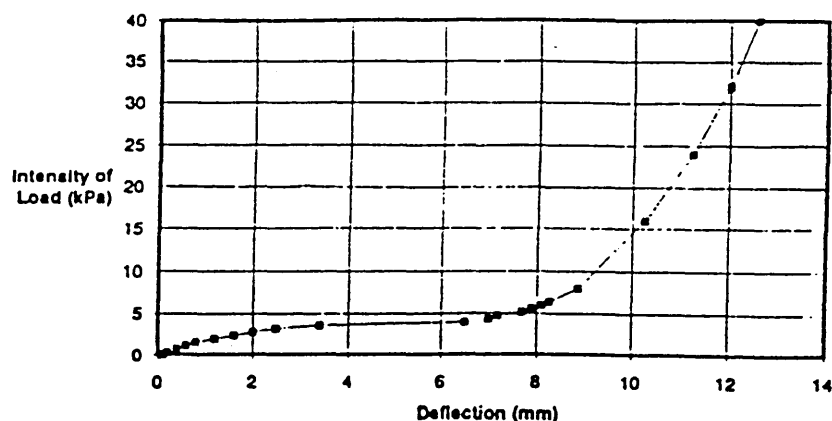


Figure 7 - Deflection of Laminated Cellular Foam Strip

A natural extension of the technology involved in the laminated foam strip was to produce a flooring system for use in the upgrading of timber and concrete floors in refurbishment projects. Designs have been produced involving the use of open cell polyurethane foam as the resilient layer.(15) Such decks have limited airborne attenuation properties and additional treatment (16) is desirable in order to provide a balanced upgrade in terms of both airborne and impact sound reduction.

The question of stability of very thin boards is a major problem especially with high compliance resilient layers. This has been overcome in the design by incorporating a closed cell peripheral foam, 50mm wide, around two adjacent sides of each board so that each joint is supported by a low deflection strip as shown in Figure 8

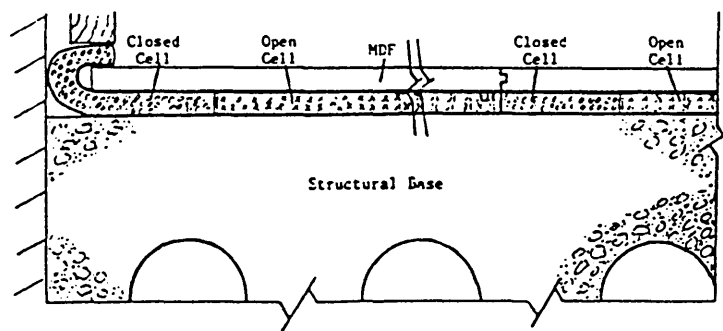


Figure 8 - Section through Shallow Profile Platform Floor

A shallow profile floor has been designed with both excellent walking stability and acoustic performance, giving an 18 dB weighted impact sound improvement as calculated in accordance with Annex A of B.S. 5821:1984

Proceedings of the Institute of Acoustics

4. A BROAD BAND ULTRASONIC FOAM ANALYSER (BUFA)

A BUFA system was developed at SHU by Langton and Deakin (3) in order to extend work being carried out on a contact system for broad band ultrasonic analysis of bone. The structural similarities between foam and cancellous bone were noted and the results of the investigation, although by no means conclusive, suggest that the possibility exists for developing an ultrasonic technique for foam characterisation.

A foam sample was placed between a high frequency speaker and a microphone and the speaker swept through a range of 15 kHz to 40 kHz. The amplitude of the transmitted signal was recorded using a spectrum analyser for different frequencies in the range. These signal amplitudes were then compared with those obtained with no sample present between speaker and microphone which were used as a reference. Subtracting this reference spectrum from that obtained with the foam in place gave the signal attenuation due to the foam. It was found (for all the samples used) that the attenuation characteristic obtained was linear over a portion of its spectrum and the gradient of this linear portion was taken to be the broad band attenuation index (BUAI) for the foam. Reproducibility of the BUAI for foams was found to be better than 4%.

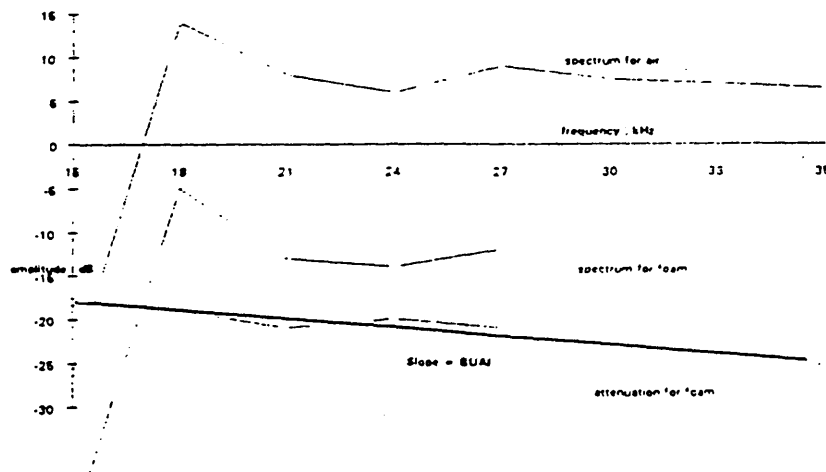


Figure 9 - Illustration of BUAI calculation

Proceedings of the Institute of Acoustics

When compared with data from earlier studies on foam (17) it was found that there was a linear relationship between BUAI and Young's Modulus at small strains. Further tests showed a linear relationship between force at 70% compression and BUAI. Typical results obtained are shown below.

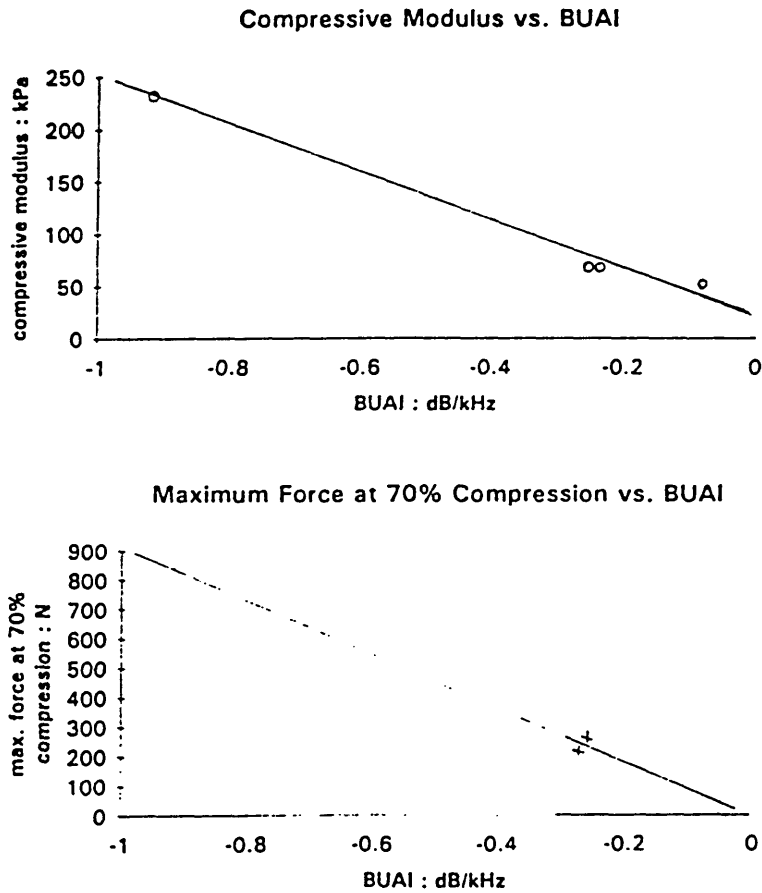


Figure 10
- Relationship between Compression and BUAI

CONCLUSION

Mechanical tests on foams will be conducted in order to classify them and determine their dynamic behaviour. Research has found that treating elastomer foams as one form of cellular material leads to interesting possibilities for investigating their classification and behaviour. An example is the use of equation solving software to calculate stress-strain relationships of layered arrays of of elastomer foam (18).

Proceedings of the Institute of Acoustics

ACKNOWLEDGEMENTS

This work was financed under a Royal Society/Science and Engineering Research Council Industrial Fellowship in collaboration with A. Proctor Developments, part of the A Proctor Group, Blairgowrie, Perthshire.

REFERENCES

- 1 Hilyard, N C (ed) (1982) *Mechanics of Cellular Plastics*, Applied Sciences Publ. London
- 2 Determination of Dynamic Stiffness, ISO 9052-1, 1989.
- 3 Langton, C M et al. A Contact Method for the Assessment of Ultrasonic Velocity and Broadband Attenuation in Cortical and Cancellous Bone, *Clin. Phys. Physiol. Meas.* Vol. 11, 1990.
- 4 Gibson, L J & Ashby, M F. (1988) *Cellular Solids*, Pergamon Press
- 5 Gent, A N and Thomas A G, *RubberChem Tech.*, 36, 597, 1963
- 6 Timoshenko, S P and Goodier, J N (1970) *Theory of Elasticity*, 3rd Edition, McGraw Hill
- 7 Mackenzie, R K. The Development of a Sound Absorbing Flooring System, *Proc I.O.A.* 169-174 (8) 1986
- 8 Mackenzie, R K. The Sound Insulation of Flooring Systems Incorporating Resilient Foam Strips, *Proc. I.O.A.* 53-61 (10) 1988
- 9 Mackenzie, R K. Sound Attenuating Floor Construction Incorporating a Polyether Foam Resilient Strip, U.K. Patent No 2196356, publication date 2 April 1991
- 10 Mackenzie, R K. Sound Attenuating Floor Construction Incorporating a Laminated Foam Resilient Strip, U.K. Patent No. 2192913, publication date 3 April 1991
- 11 Mackenzie, R K. Sound Attenuating Floor Construction, U.K. Patent No. 2214537, publication date 29 April 1992
- 12 Mackenzie, R K. Upgrading of Floors in Refurbishment Projects, *Proc I.O.A.* 301 - 308 (15) 1993
- 13 Mackenzie, R K. Sound Attenuating Laminated Strip, U.K. Patent Application, No 9012368.8, filing date 2 June 1990.
- 14 Mackenzie, R K. Sound Deadening in Panels and Like Building Structural Parts, U.K Patent Application No. 2259131, filing date 21 August 1992
- 15 Mackenzie, R K. Floor Construction (Buildings), U.K Patent Application No 9310312.5, filing date 19 May 1993
- 16 Mackenzie, R K. Improvement of Sound Insulation of Timber Floors : A Study of the Relative Significance of Mass, Resonance and Resilience in the System, *Proc. I.O.A.* 79-89 (8) 1986
- 17 Collier, P. The Design and Performance of Non Linear Vibration Isolating Materials, PhD Thesis 1985.
- 18 Peleg, M. Calculation of the Compressive Stress-Strain Relationships of Layered Arrays of Cellular Solids Using Equation Solving Computer Software, *Journal of Cellular Plastics*, Volume 29, 1993.
- 19 Langton C.M., Deakin, A J. Characterisation of Composite Materials Using Broadband Ultrasonic Attenuation, SHU internal report, 1992

Impact Sound Insulation of Floors

Using

Recycled Polyurethane Foam

(Proceedings Clima 2000)

Impact Sound Insulation of Floors Using Recycled Polyurethane Foam

Hocine Bougdah
Robin Hall

School of Construction, Sheffield Hallam University, Pond street, Sheffield S1 1WB, UK.

SUMMARY

Noise is the most common cause of complaint to environmental health officers in England and impact noise through ceilings has been identified as being particularly disturbing to occupants of dwellings. Floating floors incorporating a resilient layer are an accepted method of reducing impact noise and traditionally rockwool or mineral fibre quilts have been used. Flexible polyurethane open cell foams are now used in some systems in thinner layers than mineral fibre quilts and are more pleasant to handle. These have been the subject of research at Sheffield Hallam University and laboratory investigations of their static and dynamic properties suggested that reconstituted open cell foam produced from scrap polyurethane might offer advantages over virgin open cell foam which is used in some floating floor systems. This paper briefly describes the laboratory tests carried out on open cell polyurethane foams and presents results from the first field tests on flooring systems comprising reconstituted foam now available in the market.

1 INTRODUCTION

Environmental health officers in England receive more complaints concerning unwanted noise than about any other single issue. The 1993/94 annual report by the Chartered Institute of Environmental Health found an increase of 10.5% in the number of complaints about noise over the previous year [1]. In conversion flats the most disturbing noise was found to be impact noise from dwellings above [2] and one accepted method of reducing impact noise through ceilings is to install a "floating floor" in the room above where the walking surface is laid on a resilient layer thus decoupling it from the rest of the structure [3]. Floating floors in dwellings most commonly use mineral fibre slabs as a resilient layer although closed cell foams such as flooring grade polystyrene are also used.

Despite their initial good acoustic performance, as floors comprising mineral fibres are walked on their brittle fibres rub together and this action can, in the long term, result in the loss of resilience. These materials are unpleasant to handle and their fibres can pose a potential health risk should they become airborne. Polyurethane foams do not pose such problems and lightweight floating floors comprising low density flexible virgin open cell polyurethane foams as the resilient layer have been developed [4]. The behaviour of these foams is the subject of research at Sheffield Hallam University, UK.

This research programme is concerned with investigating the static and dynamic performance of polyurethane foams used under floors and the development of useful laboratory tests for predicting the acoustic performance of flooring systems comprising these materials. As a result of this work, reconstituted polyurethane foam was identified as having characteristics which suggested that it would be particularly useful as a resilient layer in low profile floating floors. This in turn led to a programme of laboratory and field tests for a manufacturer wishing to produce such flooring systems. As a result of this research work, floating floors comprising reconstituted foam have now been launched on the market.

This paper presents some results from laboratory tests on open cell polyurethane foams and samples of flooring systems incorporating them. It describes how these tests were used to develop flooring systems incorporating reconstituted foam and illustrates the improvements obtained from these systems on wooden and concrete floors.

2 BACKGROUND

Acoustically, the main problem with all resilient layers is that if they are sufficiently stiff to give a floor the required stability they are less capable of providing a high degree of acoustic isolation and a balance has to be struck between mechanical and acoustic properties [5]. Tests to determine the compressive behaviour of virgin and reconstituted foams were carried out according to BS 4443 [6] and typical results are shown in Figure 1.

For the virgin foam, there is a clearly defined yield point around a stress of about 5kPa after which the foam suffers a rapid increase in strain up to nearly 40% without any increase in stress. This behaviour is typical of low density virgin open cell polyurethane foams [7,8] and once the yield stress for such a foam used in a floating floor is exceeded a rapid deflection will be perceived by anyone walking across it.

The compressive stress-strain characteristics for all the reconstituted foams investigated have differed from those of virgin foams in that they do not exhibit a clearly defined yield point. Indeed all have shown a virtually linear increase in stress with strain up to around 40%. This suggested that floors comprising these materials as a resilient layer might not exhibit the sort of deflection typical of virgin foams and that using reconstituted foam was worthy of further investigation.

Reconstituted foam was also considered attractive because it is produced from a waste product and should therefore offer the potential for energy saving. The scrap foam used in its production is derived from both the production of virgin slabstock foams and from recycled foam from furniture and other applications. According to the Polyurethane Foam Association, despite efforts to minimise waste in the production of polyurethane foam, up to 30% can become scrap after cutting and shaping foam for different applications [9]. By recycling the scrap a useful material is produced from what might otherwise be a potentially expensive disposal problem and the cost of foam used in end product manufacturing can be reduced. In the USA recycling scrap polyurethane foam is a substantial part of the industry and carpet underlay, for example,

is often produced from recycled foam. In the UK recycling is not so developed although some companies see the potential of utilising scrap foam and are seeking to develop their existing recycling facilities in order to improve efficiency and quality control of the production process.

3 DYNAMIC BEHAVIOUR OF FOAMS

The only standard identified for the assessment of the dynamic properties of materials used as resilient layers in floating floors is BSEN 29052-1 [10]. This standard determines the dynamic stiffness of the materials by identifying the resonant frequency of a standard system comprising a sample of the test material. This method was adopted in the test programme with one slight departure from the recommended test set up [11] and virgin and reconstituted foams with densities ranging from 21 to 65 kg/m³ and 62 to 230 kg/m³ respectively were tested.

Systems with low natural frequencies usually give useful vibration isolation over a greater range of frequency and it was found that reconstituted foams having density of less than 80 kg/m³ gave the standard test system a lower natural frequency than any of the virgin foams tested. It was felt that results from these tests, together with their stress-strain characteristics, suggested that reconstituted foam might offer advantages over virgin foam for use in low profile floating floor systems.

The publication of the results from this first series of laboratory tests has led to outside interest in the project being expressed from industry. An industrial partner joined the programme with a view to develop and produce sound reducing flooring systems. Reconstituted foam was decided upon as the resilient layer but the best density and thickness of the material had to be decided upon. Static and dynamic tests similar to those described previously were carried out and an example of data from the dynamic tests is shown in Figure 2.

In the above test the load plate required by BS EN 29052-1 was placed on sections of flooring cut to the specified size and the natural frequencies of the systems were obtained. It can be seen that the 8mm thick layer gave the system a lower natural frequency and that this might mean better vibration isolation. This was supported by results from vibration transmissibility tests. As a result of the laboratory tests, reconstituted foam of density 78 kg/m³ was selected for use in the flooring products and 8mm was chosen for the thickness of the foam layer for systems comprising 9mm medium density fibre board and 18mm chipboard. These systems were then produced and tested in the field.

4 FIELD TESTS

A series of field tests according to BS 2750 part 7 were carried out [12] in order to assess the acoustic performance of the different systems. Investigations were carried out on wooden and concrete floors which were rated according to BS 5821 [13] before and after refurbishment with the different floating floor systems. Examples of such floors are illustrated in Figures 3 and 4. The tests on wooden floors were conducted in a large stone fronted house about a hundred years old which is typical of the sort of property often converted into separate dwellings. Two different floors were tested, one on the first floor of the house and the other on the second floor which had absorbent material placed between the joists when it was upgraded. Results from these tests are shown in Figures 5 to 8. Results from tests on a hollow beam concrete floor on the premises at Sheffield Hallam University are given in Figures 9 and 10.

Figures 5 and 6 show test results for the timber floor. An improvement in the Weighted Standardised Impact Sound Pressure Level ($L'_{nT,w}$) of 5 dB was obtained by simply placing the tongued and grooved interlocking medium density fibre board -MDF- and foam system on the existing floor. The MDF system was then replaced by a chipboard system which when tested produced a slightly better performance, 6 dB, which is probably to be expected due to the extra mass added by chipboard compared to medium density fibre board. After the attic floor had been tested the floorboards were lifted and 150mm of rockwool absorbent of density 24 kg/m^3 was laid between the joists which were irregularly spaced with centres between 400 and 480mm. Many of the old floorboards were damaged when lifted and so these were replaced by 22mm thick standard chipboard flooring on which the resilient flooring systems were placed. The results from these tests are illustrated in Figures 7 and 8 showing improvements in $L'_{nT,w}$ of 10 and 8 dB for the chipboard and medium density fibre board systems respectively. Improvements in the performance of the hollow beam concrete floor were 31 and 30 dB for the chipboard and medium density fibre board systems respectively.

5 DISCUSSION

Before its refurbishment the first wooden floor tested in the old house failed to meet the required impact noise insulation rating³ value for floors in conversion flats ($L'_{nT,w} = 65 \text{ dB}$). The chipboard and medium density fibre board systems reduced the $L'_{nT,w}$ values to 62 dB and 63 dB respectively which would be acceptable in England, Wales and Northern Ireland for floors separating flats in converted houses and would also make a discernible difference to occupants of the room below. In the case of the medium density fibre board system this improvement was achieved without raising the upstairs floor level by more than 17mm. When used in conjunction with a new supporting surface and absorbent material between the joists the improvements with the floating floor systems were more significant, $L'_{nT,w}$ of 55 dB and 57 dB for chipboard and medium density fibre board respectively, which are comfortably within the requirements for refurbished dwellings in England.

The improvements observed with these systems on the hollow beam concrete floor are much larger than those seen on the wooden floors tested. For non-acousticians it may seem surprising that improvements in the single figure $L'_{nT,w}$ value should vary so

much for the same system on different floors. The systems appear to work better on concrete floors than on wooden floors but the apparent difference in performance is due to the nature of the original floor and the standard method of rating floors laid down in BS 5821. It can be seen that the untreated hollow block concrete floor transmitted higher frequencies much better than either of the wooden floors. These higher frequencies are more easily attenuated by the lightweight resilient floating floors systems and it is this along with the rating method which explains the greater improvements in $L'_{nT,w}$.

Other research has suggested that reconstituted foams may give improved performance at low frequencies [14] which is potentially significant because it is in this frequency range that systems comprising thin layers of flexible open cell foam perform least well. Research work in the USA [15] suggests that the performance of timber floors can be made worse by the addition of a resilient walking surface by increasing the amplitude of vibration at their fundamental natural frequency (usually less than 100 Hz). If it is the case that using reconstituted foam as a resilient layer does not create this adverse effect then a positive contribution to sound control in multiple occupation dwellings will have been made. This remains to be fully investigated however.

The research programme at Sheffield Hallam University has identified reconstituted foam as a useful material in floating floor systems but a laboratory test capable of predicting the performance of floors incorporating such material has yet to be developed. Tests according to BSEN 29052-1 have been useful in comparing the performance of different foam layers and those giving systems lower natural frequencies appear to give better vibration isolation in laboratory tests. However, BSEN 29052-1 states that this test is unsuitable for determining the dynamic stiffness of materials with airflow resistivities of less than 10 kPa s/m^2 where the stiffness due to the enclosed air is significant. This is the case for the reconstituted foams identified as being most useful for use in floors in this study. Furthermore this standard is not applicable for floors which impose a static load of less than 0.4 kPa on the resilient layer. The surface density of 22mm chipboard is around 16 kg/m^2 which means an imposed load of about 0.2 kPa without furniture and fittings which again means that the standard is inappropriate for these flooring systems.

Nothing has been found in the literature regarding tests for predicting the performance of flooring systems comprising low airflow resistivity reconstituted foam although work has been done on systems incorporating closed cell foam by researchers in Japan [16,17]. Future work will concentrate on developing laboratory tests for predicting the likely benefit of using floating floor systems incorporating low airflow resistivity polyurethane foams by seeking correlation with field tests. With more lightweight, low profile sound reducing flooring systems coming into the market it is felt that the development of such tests would be a major contribution to the field.

6 CONCLUSIONS

Flexible open cell polyurethane foams offer advantages over traditional materials used in floating floors. Laboratory tests on virgin and reconstituted open cell polyurethane foam suggest that the latter is more suited for use as the resilient layer in floating floor systems. Field tests on floating floors comprising this foam have shown significant improvements in impact noise insulation in refurbishment projects. These improvements have been obtained without raising floor levels as much as when using systems comprising mineral fibre. In addition, the floors do not exhibit the sorts of deflections observed when the yield point of virgin foam is exceeded.

In addition to its performance, the wider adoption of the use of reconstituted foam should assist in keeping down the cost of virgin slabstock foam as well as alleviating a potentially expensive disposal problem.

A standard test for assessing the usefulness of these materials as resilient layers in floating floors needs to be developed.

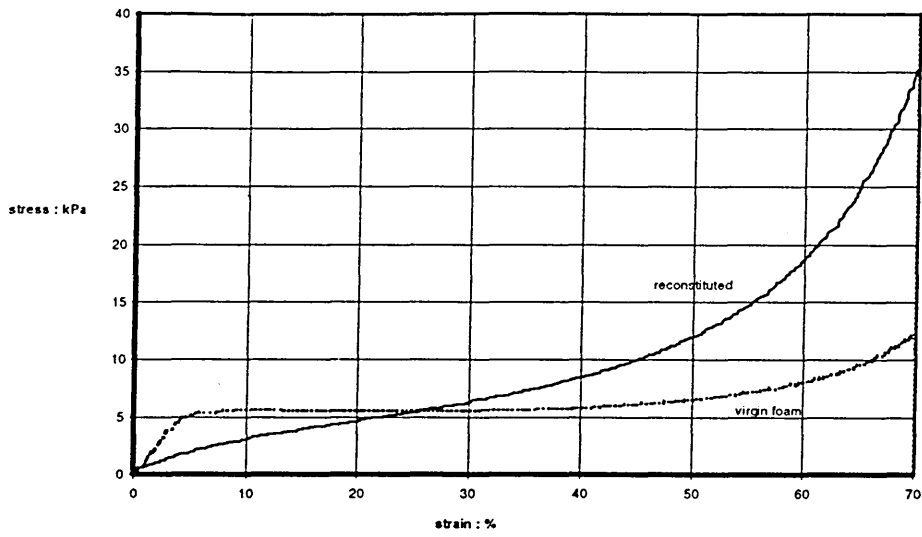


Figure 1: Stress strain curves from the first compression stroke on the foam

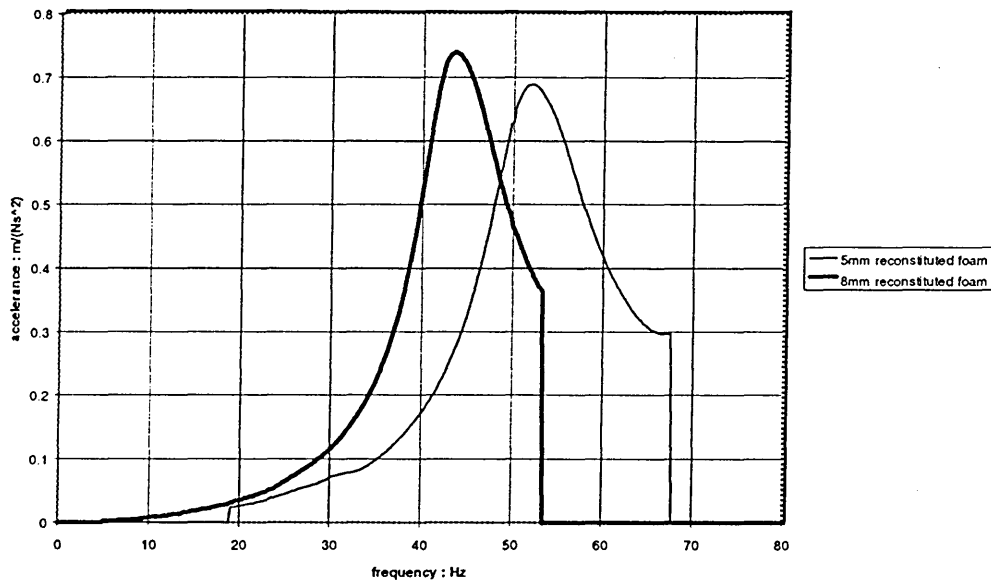
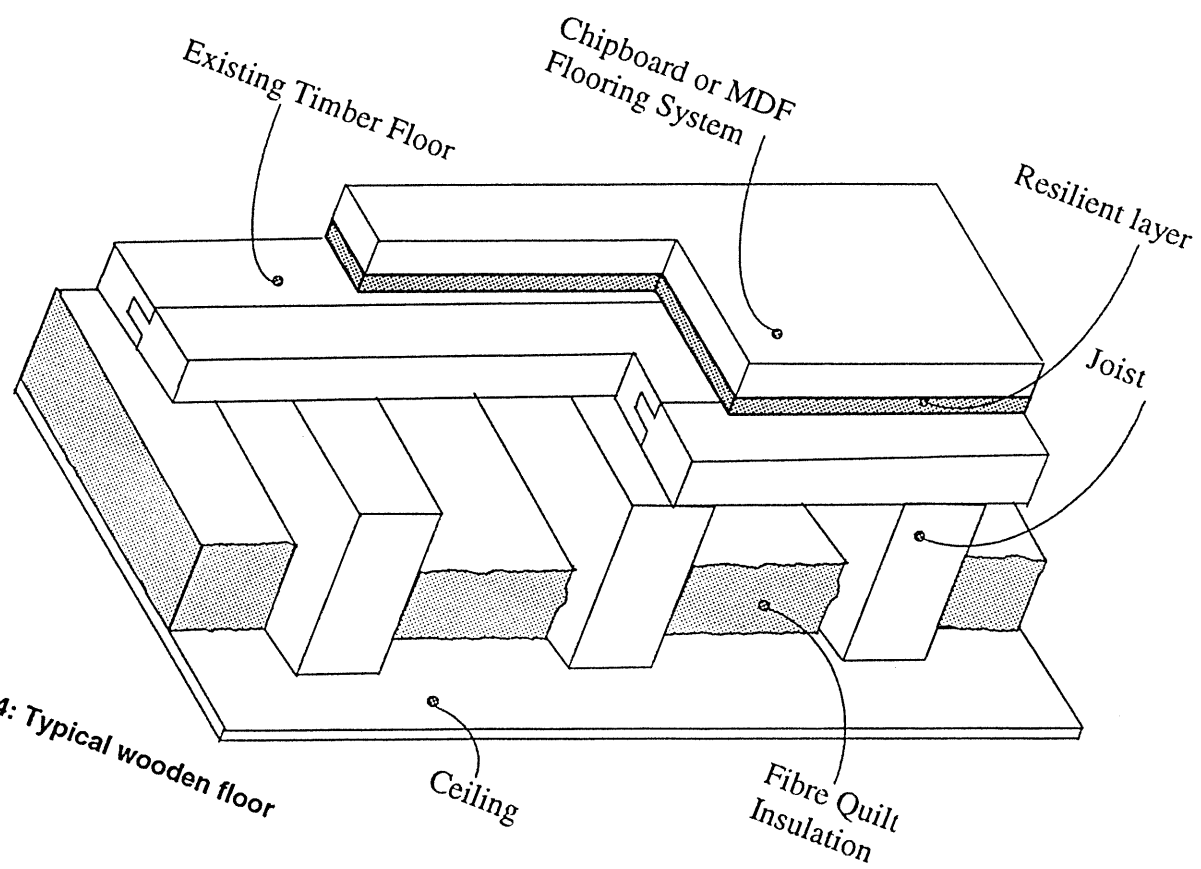
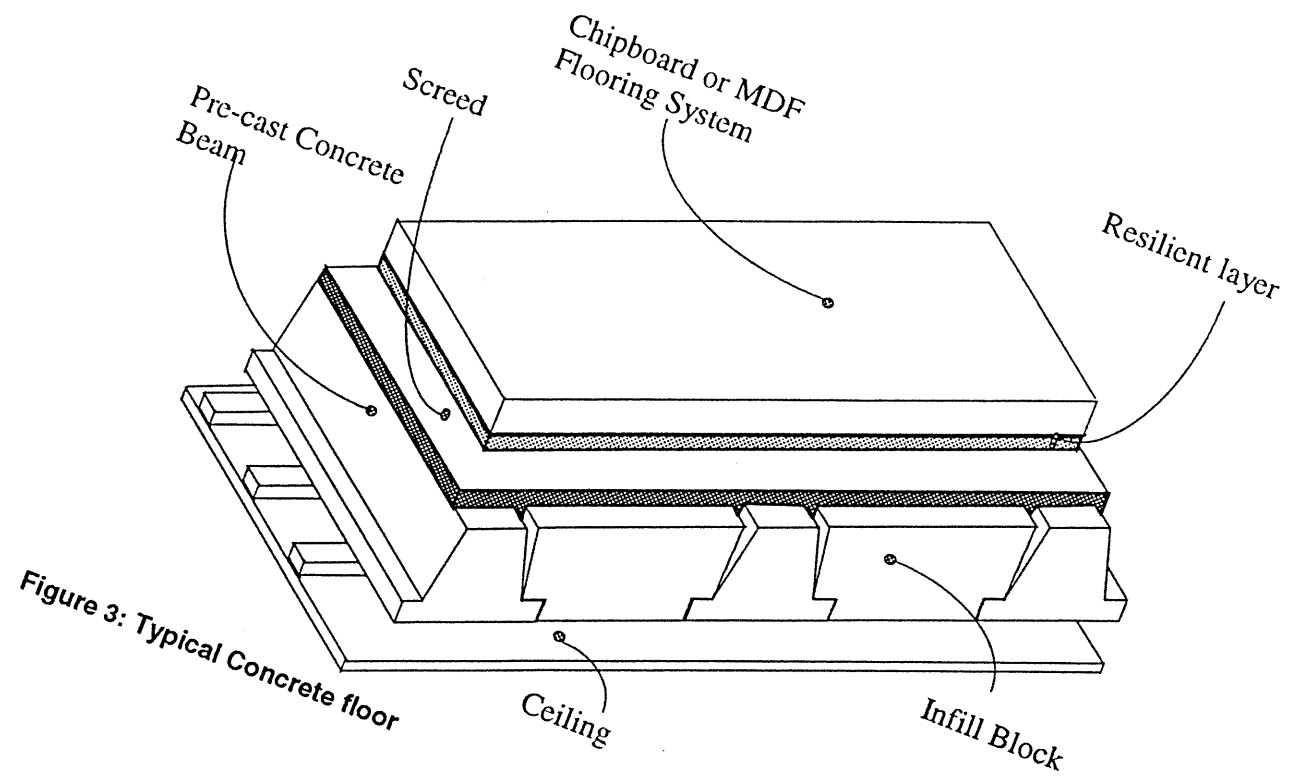


Figure 2: Results from dynamic testing on two thicknesses of 78 kg/m³ reconstituted foam



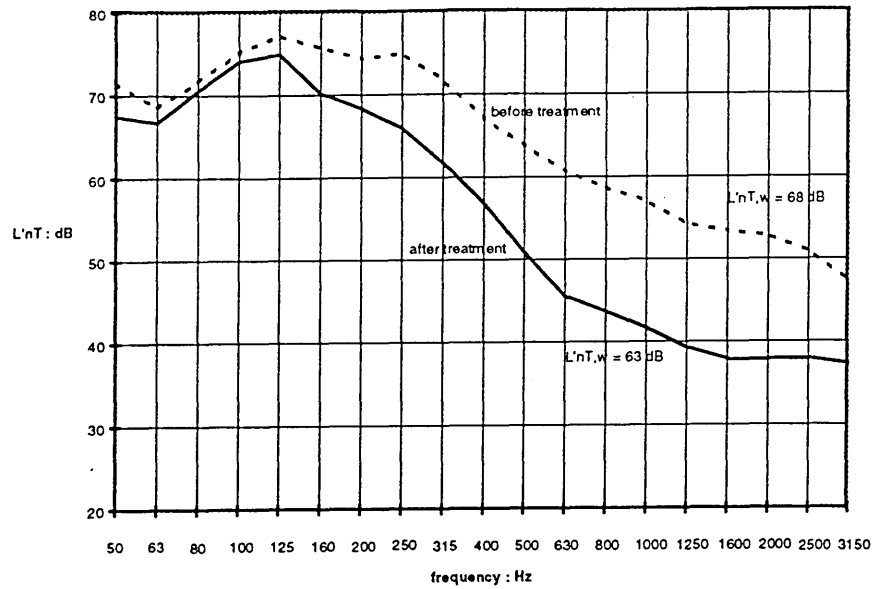


Figure 5: Wooden floor with MDF sound reducing flooring system.

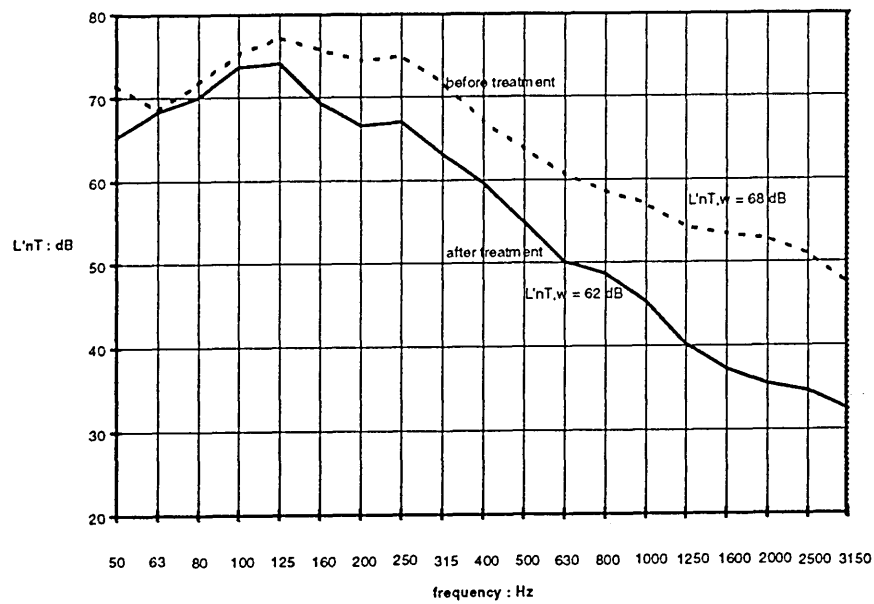


Figure 6: Wooden floor with chipboard sound reducing flooring system

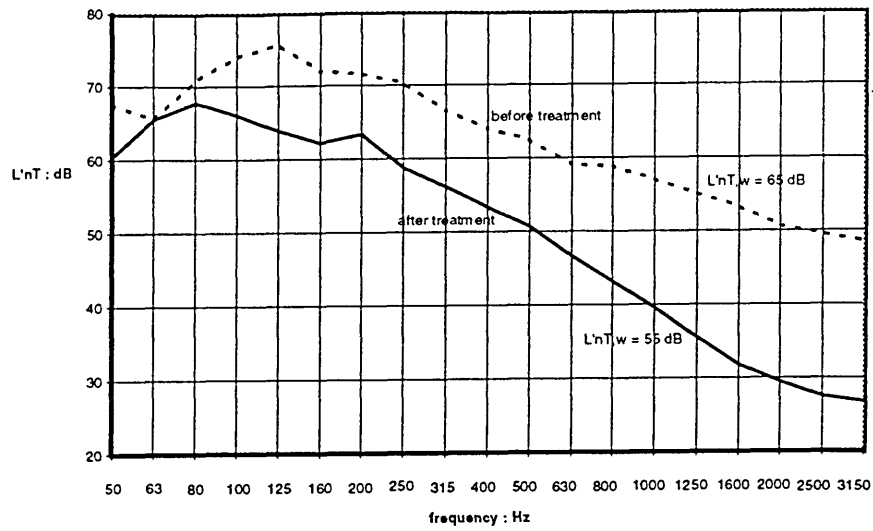


Figure 7: Wooden floor with chipboard system and absorbent material in the cavity.

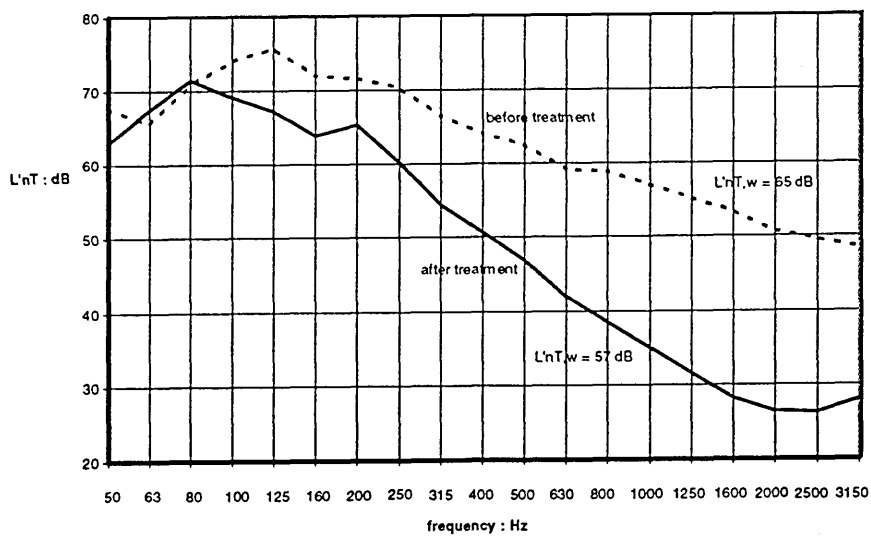


Figure 8: Wooden floor with MDF system and absorbent material in the cavity.

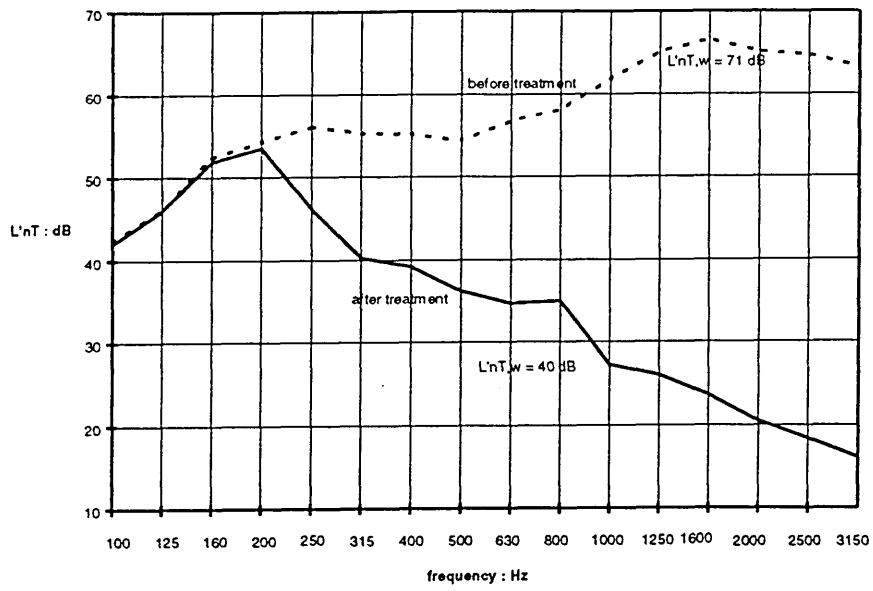


Figure 9: Concrete floor with chipboard and reconstituted foam

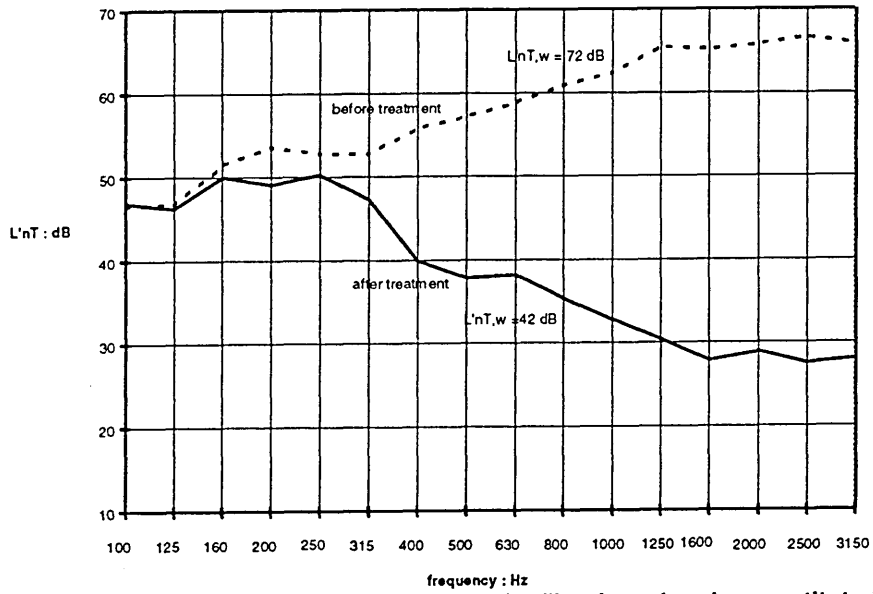


Figure 10: Concrete floor with medium density fibre board and reconstituted foam

7 REFERENCES

- 1 The Royal Institute of Chartered Surveyors, Noise Pollution Tackled by President's EQ initiative, *Chartered Surveyor Monthly*, March 1996, Vol 5, N° 6, 10-11.
- 2 Raw G.J., Oseland N.A., 1991, Subjective Response to Noise Through Party Walls in Conversion Flats, *Applied Acoustics*, Vol 32, 215-231.
- 3 Department of the Environment and the Welsh Office, *The Building Regulations 1991, Resistance to the Passage of Sound*, Approved Document E.
- 4 Mackenzie R.K., 1986, Development of a Sound Absorbing Flooring System, *Proc. IOA*, Vol 8, 53-61.
- 5 Macneil J., 1992, Making the Peace, *Building*, 13 March.
- 6 BS4443 Parts 1 - 7, 1988, *Flexible Cellular Materials*.
- 7 Gibson L.J.; Ashby M.F., 1988, *Cellular Solids*, Pergamon, Oxford.
- 8 Hilyard N.C., Hysteresis Loss and Energy Loss in Flexible Polyurethane Foams, *Low Density Cellular Plastics-Physical Basis of Behaviour*, Ed. Hilyard N.C. & Cunningham A., 226-268, Chapman and Hall, London.
- 9 <http://www.pfa.org/intouch/ntouch41.txt>
- 10 BSEN 29052-1, 1992, *Acoustics - Materials for Acoustical applications - Materials Used Under Floating Floors in Dwellings*.
- 11 Hall R.; Mackenzie R.K., 1995, Reconstituted Versus Virgin Open Cell Foams in Floating Floors, *Building Acoustics*, Vol 2, 419-436.
- 12 BS 2750, 1980, *Measurement of Sound Insulation in Buildings and Building Elements, Part 7, Field Measurements of Impact Sound Insulation of Floors*.
- 13 BS 5821, 1984, *Rating the Sound Insulation in Buildings and of Building Elements, Part 2, Method for Rating the Impact Sound Insulation*.
- 14 Mackenzie R.K.; Hall R., 1996, Developments in the Application of Flexible Open-Cell Polymer Foams for Impact Sound Reduction in Floors, *Proc. IOA*, Vol 18 Part3, 29-38.
- 15 Blazier W.E.; DuPree R.B., 1994, Investigation of Low_Frequency Footfall Noise in Wood-Frame, Multifamily Building Construction, *J. Acoust. Soc. Am*, Vol 96, 1521-1532.
- 16 Sueyoshi S.; Tonosaki T., 1993, Determination of Localised Dynamic Behaviour of Wood Strip Over Foam Rubber Underlayment, *Composite Flooring by Random Vibration*, *Wood Sci. Technol.*, Vol 27, 11-21.
- 17 Sueyoshi S.; Tonosaki T.; Oribe Y., 1995, Localised Vibration of Composite Wood Flooring Fastened to a Concrete Slab, *Japan Wood Research Society*, Vol 41, 31-36.

A Method for Predicting $L'_{nT,w}$ for Lightweight Floating Floors Comprising
Low Density Flexible Polyurethane Foam on Concrete Supporting Floors

by

Robin Hall, Hocine Bougdah and Robin K. Mackenzie

Reprinted from

Journal of
Building Acoustics

VOLUME 3 NUMBER 2 1996

MULTI-SCIENCE PUBLISHING CO. LTD.
107 High Street, Brentwood, Essex CM14 4RX, United Kingdom

A Method for Predicting $L'_{nT,w}$ for Lightweight Floating Floors Comprising Low Density Flexible Polyurethane Foam on Concrete Supporting Floors

Robin Hall¹, Hocine Bougdah¹ and Robin K. Mackenzie²

¹*School of Construction, Sheffield Hallam University;* ²*Department of Building and Surveying, Napier University, Edinburgh*

(Received 25 February 1997 and accepted in revised form 30 June 1997)

ABSTRACT

Lightweight floating floors of medium density fibreboard supported by a resilient layer of flexible polyurethane foam are increasingly being used in both new build and refurbishment projects. BS EN 29052-1 describes the Standard Method for determining the dynamic stiffness of resilient layers used under floating floors: this states that the Standard does not apply for loadings of less than 0.4 kPa, which is higher than the static load imposed by medium density fibreboard. The Standard also states that it does not apply to materials whose airflow resistivity is less than 10 kPa.s/m² if the dynamic stiffness of the air enclosed in the material is not negligible compared with the apparent dynamic stiffness of the test specimen. Despite these restrictions it was found that, when sections of flooring were tested in the field, the Standard Method provided data which allowed the prediction of the improvement in impact sound insulation over a range of 40 dB and also the prediction of the weighted standardised impact noise level according to BS 5821, 1984, Part 2. This was achieved by taking account of the stiffness of the air in laboratory samples and the effect of the mass impedance of the hammers on the standard tapping machine used in field tests.

1. INTRODUCTION

One of the factors affecting the performance of lightweight floating floors is the dynamic stiffness of the resilient supporting layer. The Standard Method for determining the dynamic stiffness of resilient layers used under floating floors is BSEN 29052-1¹ which states that the method described therein is unsuitable for assessing resilient materials with airflow resistivities less than 10 kPa.s/m² if the stiffness of the air contained in the material is significant. It also states that the method is unsuitable for resilient layers when their floating slabs impose a static load less than 0.4 kPa. The lightweight floating floors of interest in this research programme all impose static loads considerably less than 0.4 kPa on their resilient layers and some of these layers have airflow resistivities less than 10 kPa.s/m². This paper describes an attempt to correlate laboratory tests on flexible polyurethane foams with field tests on flooring systems in which they are used. It also suggests a method of predicting the Weighted Standardised Impact Sound Level ($L'_{nT,w}$) when such floors are laid on concrete supporting floors.

2. BACKGROUND

The types of floating floor investigated comprise a shallow profile (9 mm thick) walking surface of medium density fibreboard (mdf) glued to supporting layers of different flexible polyurethane foam. Such floors offer advantages over systems comprising mineral wool quilts, especially in refurbishment projects where it is necessary to minimise increases in floor level², and several different systems are now available commercially. Despite their increasing use, the only Standard Method¹ identified for determining the dynamic stiffness of resilient materials used under floating surfaces excludes such layers under these floors because of the specified requirements of imposed static load. The method of BSEN 29052-1 was, however, deemed to be the most useful to investigate the dynamic properties of the foam layers used since it does enable measurement of the dynamic stiffness of the foam sample.

The Standard has been proven to be a good indicator of the performance of floating floors comprising concrete screeds laid on mineral wool where, according to Cremer *et al.*,³ the improvement in impact noise insulation, ΔL , as defined by Gosele⁴, due to the floating layer is given by:

$$\Delta L = 40 \log \left(\frac{f}{f_0} \right) \text{dB} \quad (1)$$

where⁵:

$$f_0 = \frac{1}{2\pi} \sqrt{\frac{s'}{m'}} \text{ Hz} \quad (2)$$

and:

s' = the dynamic stiffness of the layer (including the trapped air) supporting the floating slab (N/m^3);

m' = the surface density of the floating slab (kg/m^2).

Multiplying by a factor of 30 instead of 40 has been found to give better correlation with field measurements for such floors⁶ since these are lightly damped and reflected waves in the floating slab are significant. No evidence has been found of the usefulness of BS EN 29052-1 in predicting the improvement in ΔL for floors with shallow profile lightweight floating slabs however.

Cremer *et al.*³ explain that, with lightweight floating floors such as those made from mdf, since their driving point impedance is much lower than for concrete floating slabs the mass impedance of the tapping machine hammers is significant above a certain cut off frequency (f_{co}) given by:

$$f_{co} = \frac{Z}{2\pi m_0} \text{ Hz} \quad (3)$$

where:

m_0 = the mass of the hammer (0.5 kg);

Z = the driving point impedance of the floating floor given by:

$$Z = 2.3 c_L \rho h^2 \text{ N.s/m} \quad (4)$$

where:

c_L = the longitudinal wave speed in the floating floor (m/s);

h = the thickness of the floating floor (m);

ρ = the density of the floating floor (kg/m^3).

Equation 1 is modified to take account of this and becomes³:

$$\Delta L = 40 \log \left(\frac{f}{f_0} \right) + 10 \log \left[1 + \left(\frac{f}{f_{co}} \right)^2 \right] \text{ dB} \quad (5)$$

The agreement between predicted and measured values of ΔL given in reference 3 is good up to around 1000 Hz. At higher frequencies, predicted and measured values diverge but these higher frequencies are usually much less significant than those below 1000 Hz for concrete floors with floating layers when the method for rating the impact sound insulation of floors is used⁷.

Equation 5 predicts that ΔL will become increasingly negative at frequencies below f_0 . The continuing decrease in impact insulation at these low frequencies bears no relation to reality although it is often observed that there is a worsening of impact noise insulation at the resonant frequency of the floating floor^{5,8}. There is unlikely to be any significant improvement in ΔL at frequencies below f_0 however³ and so in this approach for the prediction of $L'_{nT,w}$, ΔL is equated to zero when it becomes negative.

The series of tests described in this paper was undertaken to see if any correlation could be found between field tests on sections of flooring and laboratory measurements of dynamic stiffness by making use of Equation 4. It also attempted to include the effect of the air trapped in the layer in the laboratory tests.

3. TESTING METHOD

Field tests were carried out using single panels of different floors which were tested on a concrete floor of area 29.5 m^2 above a room with a volume of 85.4 m^3 . Measurements were made of the Standardised Impact Sound Level (L'_{nT}) using the method described in BS 2750 Part 7⁹. Since small ($1.13 \text{ m} \times 0.52 \text{ m}$) sections of flooring were used, only one (central) position was marked and used for the tapping machine. Impact sound levels were averaged over 48 s for the bare floor and 32 s for the floating floor sections in the room below the floor using a rotating boom and a building acoustics analyser. Two series of measurements were made and the L'_{nT} values for the bare floor taken at the beginning of each series. Included for comparison are measurements using 8 tapping

machine positions on a different concrete floor with a section of floating floor (3.6 m × 4.2 m).

Laboratory tests of the dynamic stiffness of the resilient layers were carried out according to the method of BSEN 29052-1 with the modification described in an earlier publication¹⁰. Three samples of foam were cut from each of the sections of flooring tested in the field and for each of these the natural frequency of the test system was recorded. The samples were tested as usual and then tested with their edges sealed with petroleum jelly to prevent the enclosed air moving laterally out of the sample. By doing this it was hoped to include the effect of the enclosed air in the measurement of natural frequency.

4. RESULTS

The values for natural frequency and dynamic stiffness shown in Table 1 are the averages of three samples of each type of foam. All were of reconstituted polyurethane scrap except the 28 kg/m³ foam (results shown in bold) which is a virgin polyurethane foam. Tests according to BS EN 29053¹¹ have shown that the reconstituted foams having densities of 64 kg/m³ and 80 kg/m³ have airflow resistivities less than 10 kPa.s/m².

Table 1
Results from laboratory tests.

Density of foam: kg/m ³	Thickness of foam: mm	f_n without petroleum jelly: Hz	f_n with petroleum jelly: Hz	Sample dynamic stiffness without petroleum jelly: MN/m ³	Sample dynamic stiffness with petroleum jelly: MN/m ³	Material dynamic stiffness including calculated air stiffness: MN/m ³
64	10	45.5	65.6	15.4	31.9	26.5
96	11.5	43	61	13.7	27.7	23.4
128	9	61.5	82	28.1	50.0	40.4
144	11	43.5	65	14.1	31.4	24.1
28	8	62.5	76	29.0	42.9	42.9
80	8	43.5	73	14.1	39.6	28.0
80	12	29.5	54	6.5	21.7	15.8
80	14	30	51.5	6.7	19.7	14.6
80	16	26	46	5.0	15.7	11.9

Figures 1 and 2 show the measured and predicted ΔL for two densities of foam. From these generated data the predicted values for L'_{nT} for the curves shown in Figures 3 and 4 were produced by subtracting the predicted values for ΔL from the measured L'_{nT} values for the bare floor. Other curves showing the predicted values for L'_{nT} used to estimate $L'_{nT,w}$

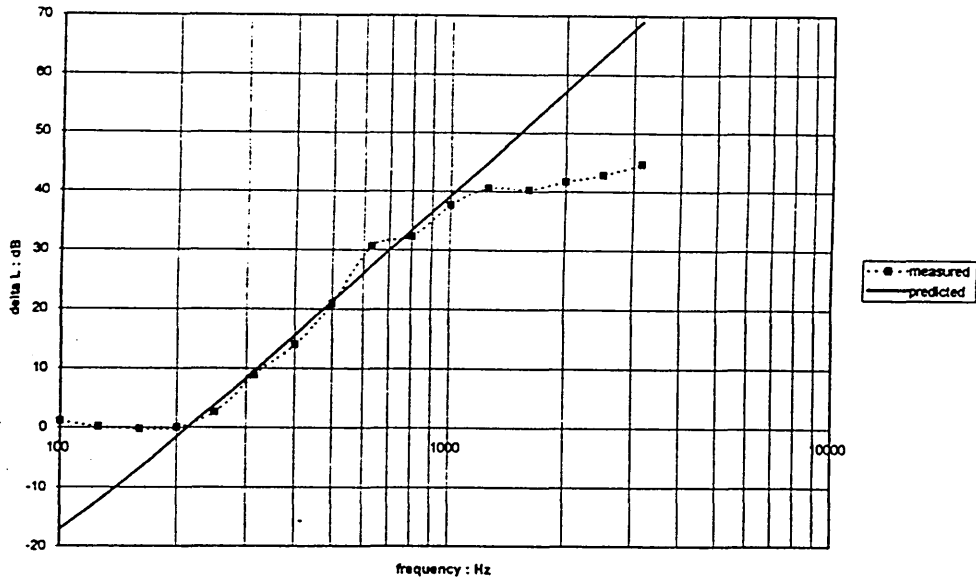


Figure 1. Measured and calculated values of ΔL for a 64 kg/m^3 reconstituted foam resilient layer. The stiffness of the resilient layer was obtained from tests according to BSEN 29052-1 with the edges sealed.

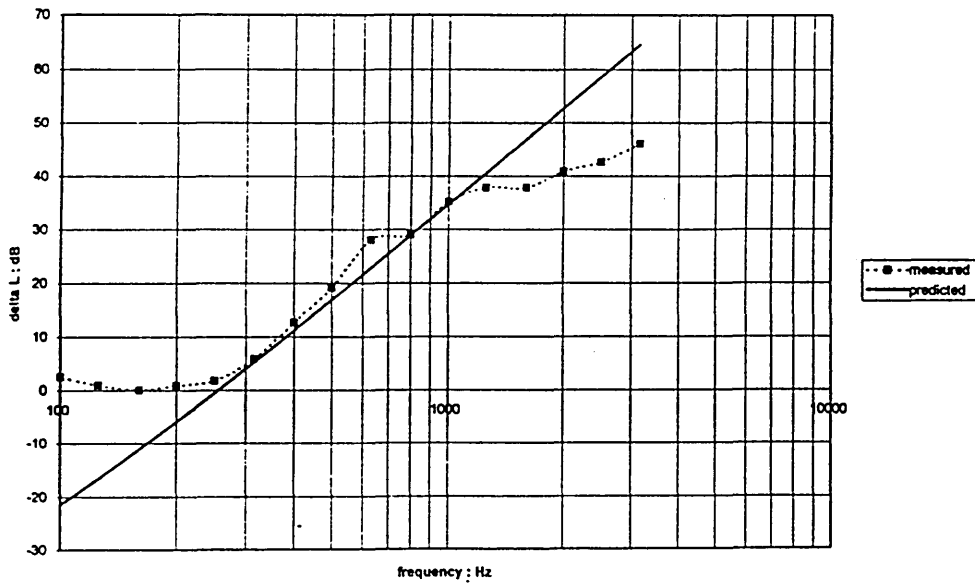


Figure 2. Measured and calculated values of ΔL for a 28 kg/m^3 virgin foam resilient layer. The stiffness of the resilient layer was obtained from tests according to BS EN 29052-1 by adding the air stiffness to the sample stiffness.

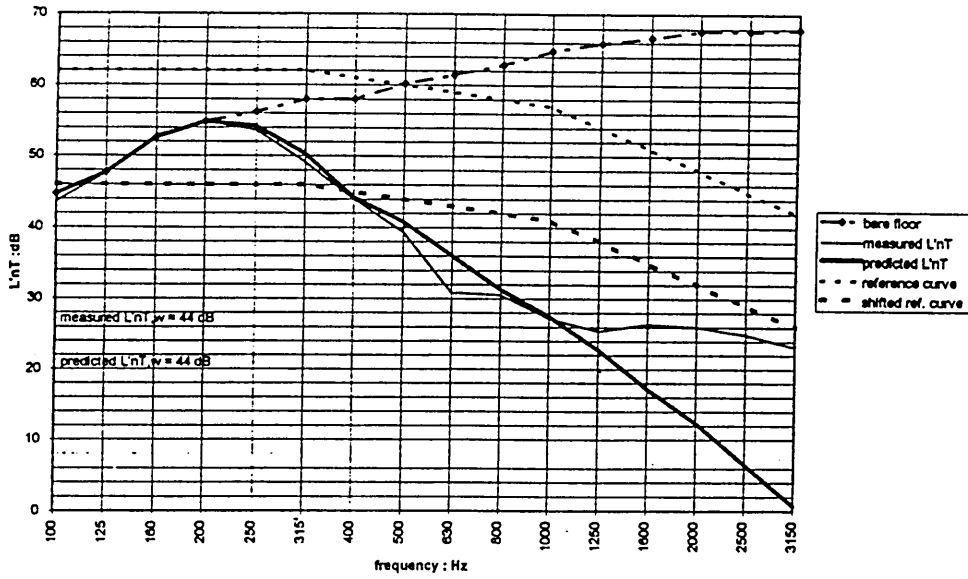


Figure 3. Predicted and measured values for L'_{nT} and $L'_{nT,w}$ from the data shown in Figure 1.

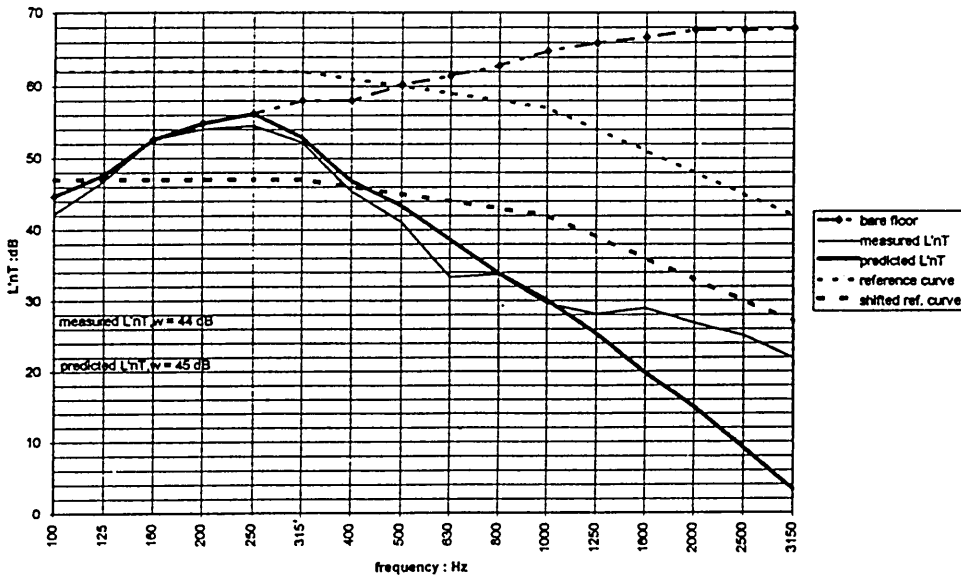


Figure 4. Predicted and measured values for L'_{nT} and $L'_{nT,w}$ from the data shown in Figure 2.

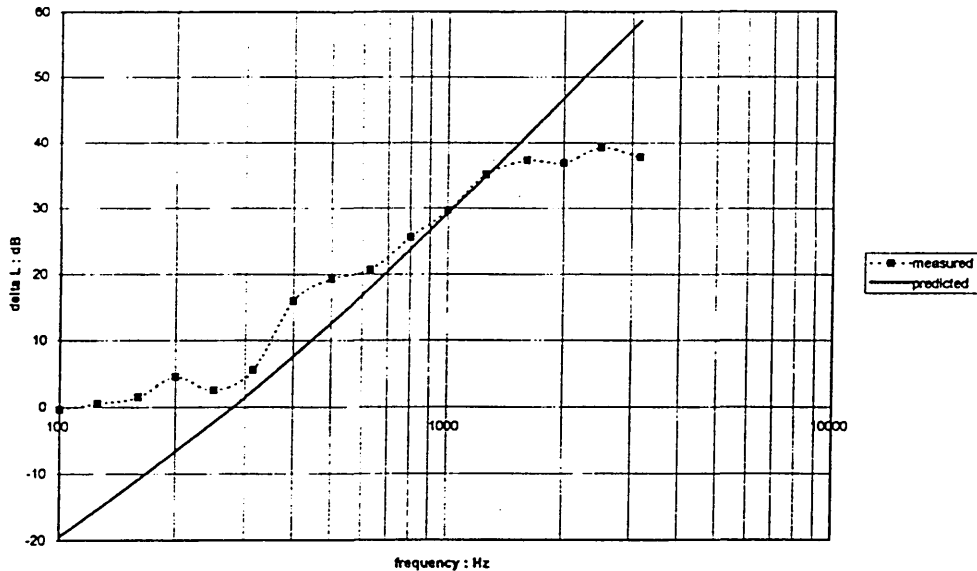


Figure 5. Measured and calculated values of ΔL for a 15 m² section of flooring comprising mdf with an 80 kg/m³ reconstituted foam resilient layer.

are shown in the appendix for the case of 80 kg/m³ foam. Those marked (V) were produced from tests with the edges of the sample sealed.

Table 2 contains the predicted and measured values of $L'_{nT,w}$ for all the systems tested along with those for the second concrete floor on which the larger area of floating floor was tested (these latter values are shown in bold italic). The comparison between predicted and measured values of ΔL for the second floor are shown in Figure 5.

The $L'_{nT,w}$ value for the first floor was found to be 73 dB. The second concrete floor had an $L'_{nT,w}$ value of 71 dB.

The density of the mdf used was 790 kg/m³ for all the samples except that with the virgin foam which was 720 kg/m³. The longitudinal wave speed in the mdf was measured at 2500 m/s giving $f_{co} = 117$ Hz for the 790 kg/m³ mdf and $f_{co} = 107$ Hz for the 720 kg/m³ mdf.

5. DISCUSSION

The cut off frequency (f_{co}), above which the mass impedance of the tapping machine hammers becomes significant, is proportional to the driving point impedance of the mdf floating floor given by Equation 4. The measured value for c_L of 2500 m/s is in agreement with the results of measurements on mdf by other researchers¹². Since the mass of the tapping machine hammers is known and it is a simple matter to determine the dimensions of the flooring sections it is assumed that the value for f_{co} used in the estimate of ΔL will not prove controversial. The values for f_{co} of 117 Hz and 107 Hz also appear to be of the correct order when compared with the 223 Hz for the 12 mm thick wooden floor used in Cremer's example.

Table 2
Measured and predicted $L'_{nT,w}$ values.

Density of foam: kg/m ³	Thickness of foam mm	$L'_{nT,w}$ (without petroleum jelly): dB	$L'_{nT,w}$ (with petroleum jelly): dB	Measured $L'_{nT,w}$: dB
64	10	43	44	44
96	11.5	43	43	44
128	9	45	46	45
144	11	43	44	44
28	8	45	45	44
80	8	42	43	44
80	12	42	43	43
80	14	41	43	42
80	16	40	41	41
80	8	43	44	42

The calculated values for the dynamic stiffness of the air contained in the foam layers were obtained using the approximation described in BSEN 29052-1 which assumes a porosity for the material of 0.9. In all cases these appear to be reasonable estimates since the porosities of the materials differ little from 0.9, where¹³:

$$\text{porosity} = 1 - \frac{\text{foam density}}{\text{base polymer density}}$$

and there were no significantly large variations in atmospheric pressure.

It can be seen from Table 1 that, apart from with the virgin foam, the values for dynamic stiffness derived from tests in which the edges of the samples were sealed are larger than those where the calculated air stiffness is added to the sample stiffness and that for all the foams the dynamic stiffness of the air is significant. It is noteworthy that for the virgin foam, the two values for stiffness including the contribution of the enclosed air are identical. This was both the thinnest and the stiffest sample in the laboratory tests but at present the authors can offer no explanation for why there should be such perfect agreement here and nowhere else. Further tests with and without petroleum jelly sealing the sample edges were carried out on different thicknesses (15 and 16 mm) of the same virgin foam and a 20 kg/m³ (12.5 mm thick) virgin foam without achieving the same correlation. Since all the values in Table 1 are the average results from three tests it is unlikely that this is the only case where the petroleum jelly contributed significantly to the sample stiffness.

The values for dynamic stiffness, including air stiffness, were used in Equation 2 to calculate the values for f_0 which, in turn, were substituted into Equation 5 to predict the improvement in impact noise insulation. The examples illustrated in Figures 1 and 2 show good agreement with the measured values over the 40 dB range up to 1000 Hz that Cremer

et al. reported so it is not surprising that Figures 3 and 4 also show good correlation between measured and predicted data up to this frequency. The poorest fit with measured data came from the 15 m² section of floating floor on the second concrete floor as can be seen from Figure 5 yet even here the predicted data gave a good estimation of the $L'_{nT,w}$ value as can be seen from Table 2 (bold italic). All the other values of $L'_{nT,w}$ in Table 2, show good agreement with measured values with only two deviating from the measured value by more than 1 dB. According to BS 5821 Part 2, $L'_{nT,w}$ is found by moving the reference curve towards the curve of measured L'_{nT} values in steps of 1 dB. $L'_{nT,w}$ is then subject to a potential uncertainty of (± 1) dB which means that all but two of the predicted $L'_{nT,w}$ values lie within the limits of accuracy of the procedure.

It could be argued that the reason for the good correlation has more to do with the insensitivity of the rating method than anything else. Certainly it is not claimed that this approach describes the performance of the floating floors investigated. It does not account for reduced impact noise insulation around the resonance frequency for the floor and bears no similarity at frequencies above 1000 Hz. It does, however, provide sufficiently good agreement with data over the most significant frequency range to predict the $L'_{nT,w}$ values for the different types of flooring in the series of tests. The largest deviations between predicted and measured results occur at frequencies where the predicted L'_{nT} values lie beneath the shifted rating curve. Whilst this is the case, unrealistic L'_{nT} values are insignificant in the prediction of $L'_{nT,w}$.

From the results obtained so far it cannot be determined whether sealing the sample with petroleum jelly gives more realistic results than adding the calculated air stiffness to the sample stiffness. The question of air stiffness in flexible open cell polyurethane foams is worthy of further research however. Johansson and Agren¹⁴ state that, for a floating floor, the resilient layer should not be less than 25 mm or the air stiffness will dominate. This does not appear to be the case with these polyurethane foams. The values of stiffness for the different thicknesses of the 80 kg/m³ reconstituted foam in Table 1 suggest that the relative contributions of the frame material and the enclosed air to the total stiffness remain roughly constant as can be seen in Table 3.

It is perhaps worth noting, however, that $L'_{nT,w}$ differs little with the different types of flooring. This may mean that the weighted standardised impact sound pressure level might

Table 3
Relative contribution of frame material stiffness to the stiffness including air stiffness of different 80 kg/m³ reconstituted foam samples.

Thickness: mm	Ratio; (with petroleum jelly) <u>sample stiffness</u> sample + air stiffness	Ratio; (using calculated air stiffness) <u>sample stiffness</u> sample + air stiffness
8	0.36	0.50
12	0.30	0.41
14	0.34	0.46
16	0.32	0.42

not be made significantly worse if a material with better load bearing ability (i.e., stiffer) were to be chosen for a given situation.

6. CONCLUSION

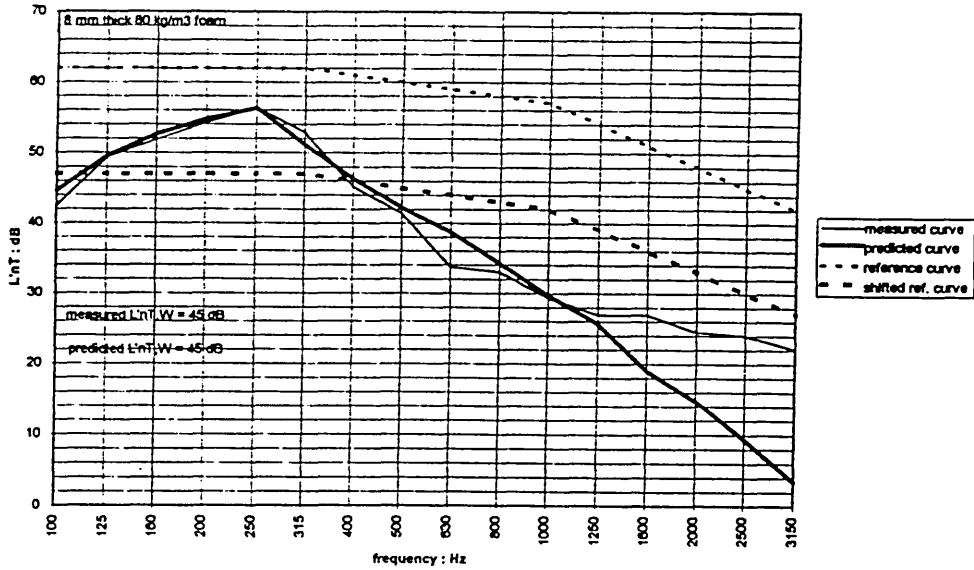
Despite the low load imposed by the mdf on the resilient layers and despite the fact that both the 64 and 80 kg/m³ foams have airflow resistivities less than 10 kPa.s/m², the results from tests according to BS EN 29052-1 have proved useful in predicting the $L'_{nt,w}$ value for the different types of floating floor systems investigated. Should this prove to be the case in other situations it will be possible to estimate whether applying a particular lightweight floating floor comprising a flexible polyurethane resilient layer to an existing concrete floor will meet the requirements of the Building Regulations Part E.

This series of tests suggests that the Standard Method described in BS EN 29052-1 can be used to determine the dynamic stiffness per unit area of flexible polyurethane foam layers under lightweight floating floors which impose a static load less than 0.4 kPa on the layers. The results suggest that this is the case even when the foam has an airflow resistivity less than 10 kPa.s/m² and the dynamic stiffness per unit area of the air enclosed in the material is significant when compared with the apparent dynamic stiffness per unit area of the test specimens.

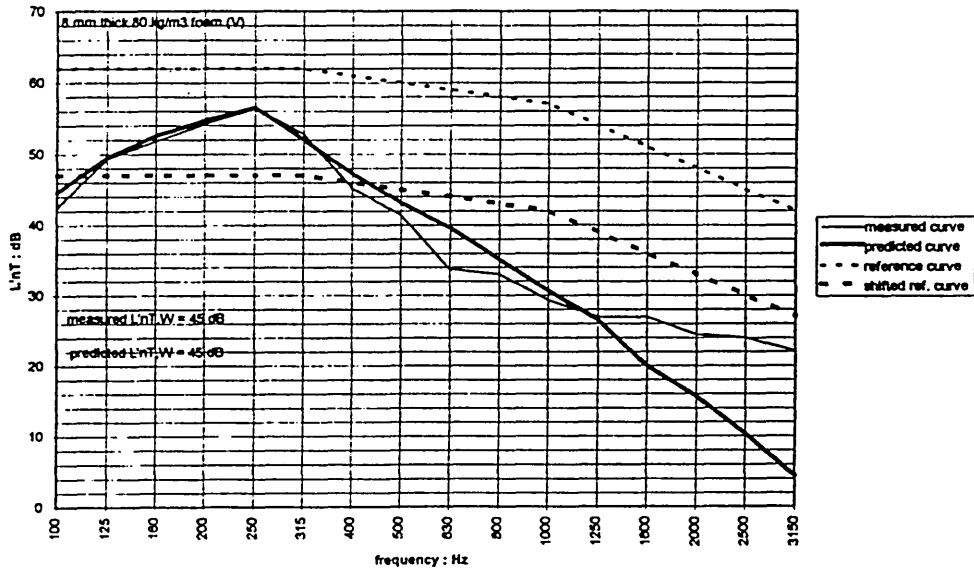
REFERENCES

1. BS EN 29052-1: 1992. *Acoustics – Determination of dynamic stiffness – Materials used under floating floors in dwellings.*
2. Mackenzie, R.K. (1986). Development of a sound absorbing flooring system, *Proc. I.O.A.*, Vol. 8, 53–61.
3. Cremer, L., Heckle, M. and Ungar, E.E. (1988). *Structure-Borne Sound*, 2nd ed., Publ. Springer-Verlag.
4. Gosele, K. (1949). *Gesundheitsing.* 70, 66.
5. Ver, I.L. (1992). *Interaction of Sound Waves with Solid Structures, Noise and Vibration Control Engineering.* 245–367, Publ. John Wiley and Sons Inc.
6. EN 12354-2, 1997. Draft Standard, *Building Acoustics, Estimation of acoustic performance of buildings from the performance of products, Part 2: Impact sound insulation between rooms.*
7. BS 5821, 1984. *Rating the sound insulation in buildings and of building elements, Part 2. Method for rating the impact sound insulation.*
8. Blazier, W.E. and Dupree, R.B. (1994). Investigation of low frequency footfall noise in wood-frame multifamily building construction, *J. Acoust. Soc. Am.* 96(3), 1521–1532.
9. BS 2750, 1980. *Measurement of sound insulation in buildings and of building elements, Part 7. Field measurements of impact sound insulation of floors.*
10. Hall, R. and Mackenzie, R.K. (1995). Reconstituted versus virgin open cell foams in floating floors. *Building Acoustics*, Vol. 2, Number 2, 419–436.
11. BS EN 29053. 1993. *Acoustics – Materials for acoustical applications – Determination of airflow resistance.*
12. Hopkins, C. (1997). BRE Acoustics Section, private communication.
13. Gibson, L.J. and Ashby, M.F. (1988). *Cellular Solids – Structure and Properties*, Publ. Pergamon Press.
14. Johansson, C. and Angren, A. (1994). Development of a lightweight wooden joist floor, *Applied Acoustics*, 43, 67–79.

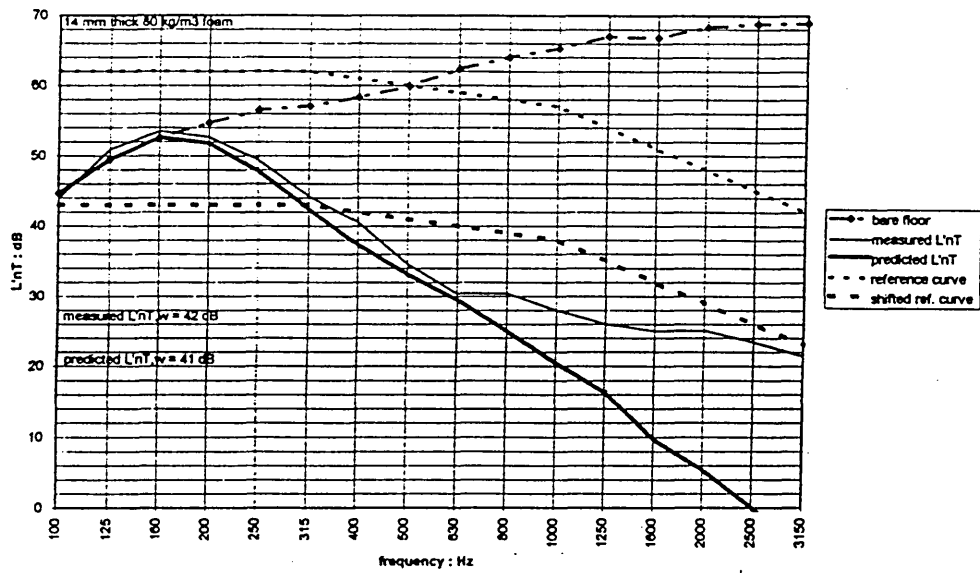
APPENDIX – PREDICTED VALUES FOR L'_{nT}



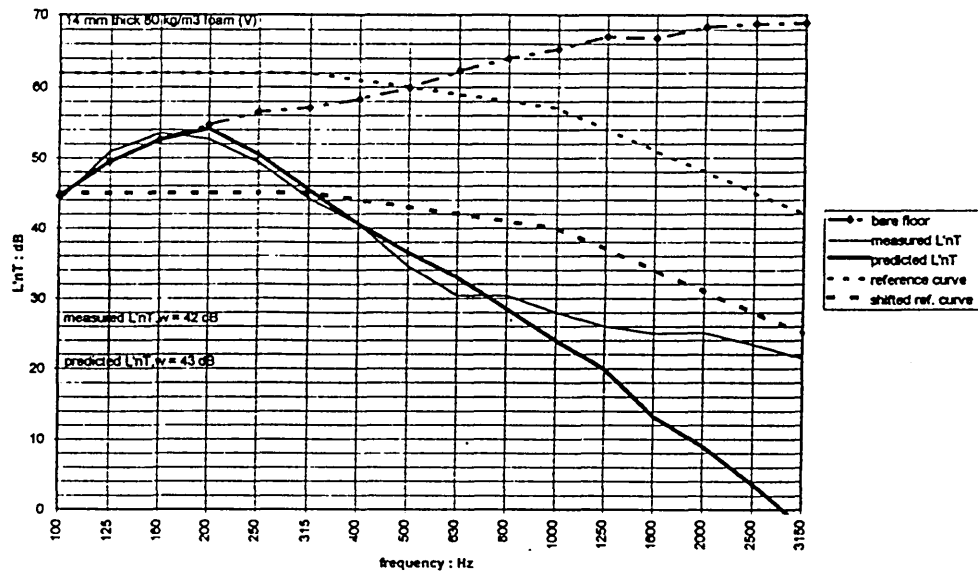
A1. For 8 mm, 80 kg/m³ foam.



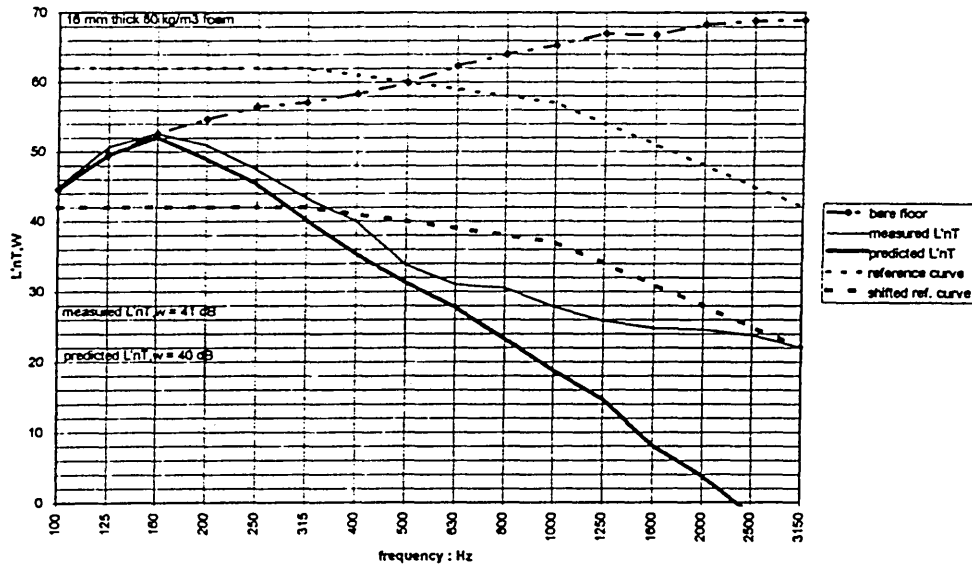
A2. With sealed edges.



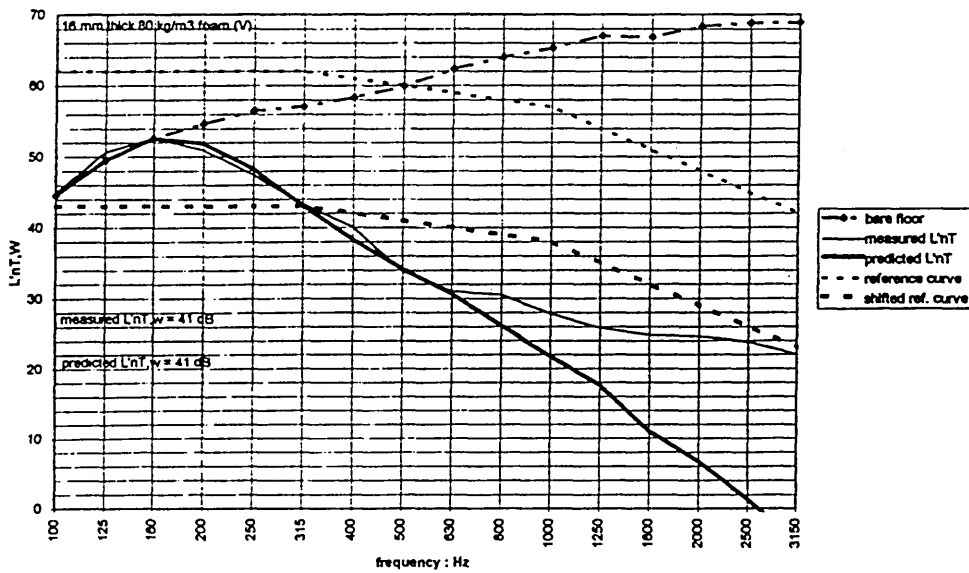
A3. 14 mm, 80 kg/m³ foam.



A4. With sealed edges.



A5. 15 mm. 80 kg/m³ foam.



A6. With sealed edges.